



ICES
CIEM

International Council for
the Exploration of the Sea

Conseil International pour
l'Exploration de la Mer

ICES COOPERATIVE RESEARCH REPORT
RAPPORT DES RECHERCHES COLLECTIVES

NO. 313 SPECIAL ISSUE
AUGUST 2012

**ICES Phytoplankton and Microbial
Plankton Status Report 2009/2010**





ICES
CIEM

International Council for
the Exploration of the Sea
Conseil International pour
l'Exploration de la Mer

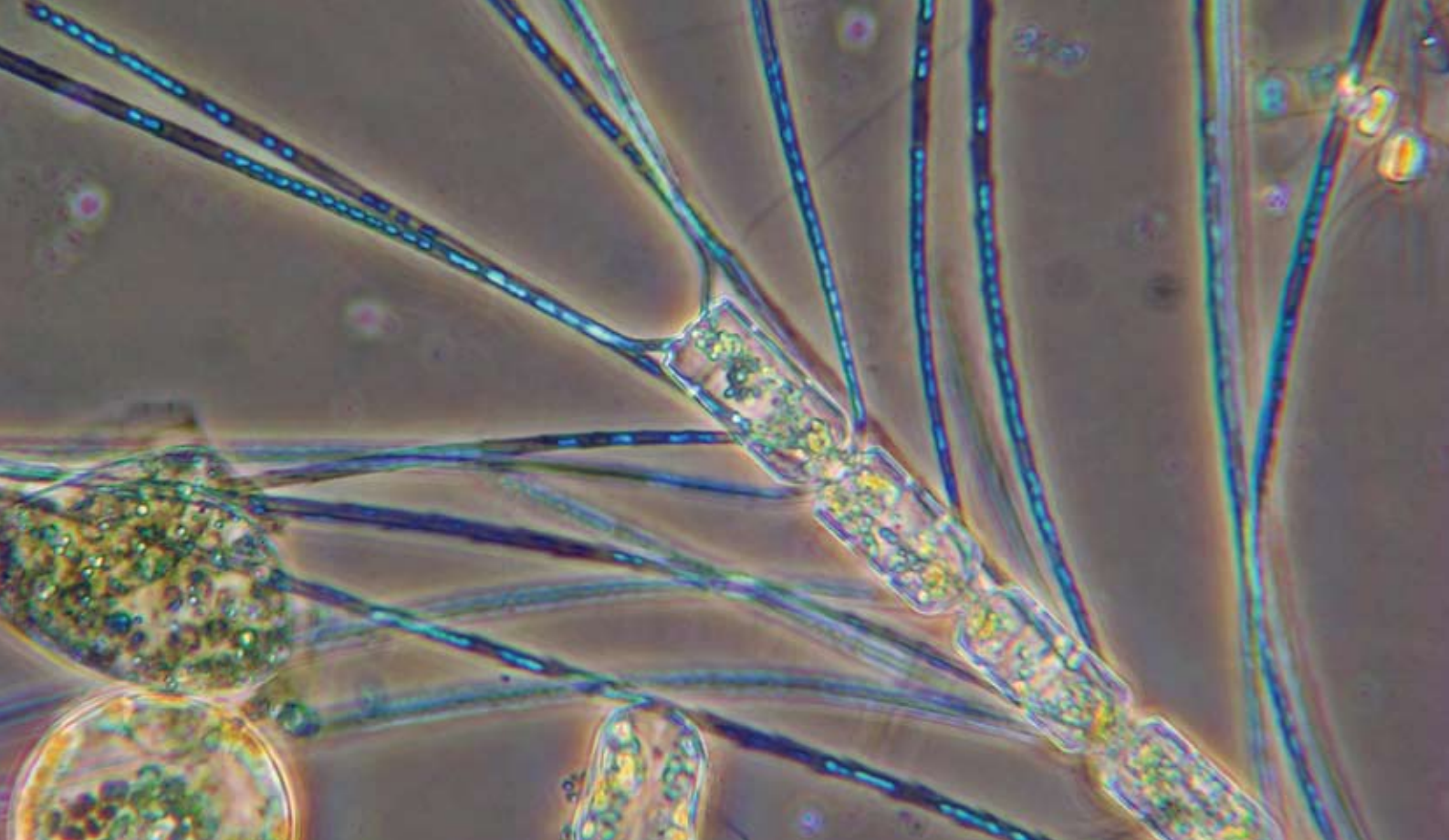
ICES Cooperative Research Report
Rapport des Recherches Collectives

No. 313 Special Issue
August 2012

ICES Phytoplankton and Microbial Plankton Status Report 2009/2010

Editors

Todd D. O'Brien , William K. W. Li, and Xosé Anxelu G. Morán



International Council for the Exploration of the Sea
Conseil International pour l'Exploration de la Mer

H. C. Andersens Boulevard 44–46
 DK-1553 Copenhagen V
 Denmark
 Telephone (+45) 33 38 67 00
 Telefax (+45) 33 93 42 15
 www.ices.dk
 info@ices.dk

Recommended format for purposes of citation:

O'Brien, T. D., Li, W. K. W., and Morán, X. A. G. (Eds). 2012.

ICES Phytoplankton and Microbial Plankton Status Report 2009/2010.

ICES Cooperative Research Report No. 313. 196 pp. <https://doi.org/10.17895/ices.pub.5407>

Series Editor: Emory D. Anderson

For permission to reproduce material from this publication, please apply to the General Secretary.

This document is a report of an Expert Group under the auspices of the International Council for the Exploration of the Sea and does not necessarily represent the view of the Council.

SBN XXXXXXXXXX 978-87-7482-320-9

ISSN 2707-7144

© 2012 International Council for the Exploration of the Sea

Above.

Chaetoceros concavicornis
 (Bacillariophyceae)

Photo credit: Fisheries and
 Oceans Canada.

Cover image.

A selection of diatoms
 (Bacillariophyceae) collected
 from the Plymouth L4 time-
 series site.

Photo: Claire Widdicombe,
 Plymouth Marine Laboratory.

CONTENTS

1	Introduction	4
2	Time-series data analysis and visualization	8
2.1	Time-series data analysis	8
2.1.1	Representation of "absence" and zero-value measurements	11
2.2	Time-series data visualization: standard figures	13
2.2.1	Environmental summary plot	13
2.2.2	Multiple-variable comparison plot	13
2.3	Time-series supplemental data	15
2.3.1	Sea surface temperature data: HadISST	15
2.3.2	Sea surface chlorophyll data: GlobColour	17
2.3.3	Sea surface wind data: ICOADS	18
3	Phytoplankton and microbial plankton of the Northwest Atlantic Shelf	20
4	Phytoplankton and microbial plankton of the Labrador Sea	32
5	Phytoplankton and microbial plankton of the Baltic Sea	38
6	Phytoplankton and microbial plankton of the North Sea and English Channel	70
7	Phytoplankton and microbial plankton of the Northeast Atlantic Shelf	92
8	Phytoplankton and microbial plankton of the Bay of Biscay and western Iberian Shelf	114
9	Phytoplankton and microbial plankton of the Mediterranean Sea	136
10	Phytoplankton of the North Atlantic Basin	154
11	Spatio-temporal atlas of the North Atlantic	168
12	References	180
13	List of contributors	196

1. INTRODUCTION

William K. W. Li, Xosé Anxelu G. Morán, and Todd D. O'Brien

The ICES Science Plan adopts an ecosystem approach to management that is built on scientific capacity to understand ecosystem functioning. To understand, one should first know; to know, one should first observe. To understand well and to know much, one should observe far and wide and for long and always. This, in a manner of speaking, is the rationale for multidecadal oceanic ecological datasets and their application in marine ecology and biogeochemistry (Ducklow *et al.*, 2009) as well as in marine policy and management (Edwards *et al.*, 2010).

The ICES Status Report on Climate Change in the North Atlantic (Reid and Valdés, 2011) is a review of the scientific literature, including a consideration of long-term physical variability (Holliday *et al.*, 2011), chlorophyll and primary production (Bode *et al.*, 2011a), and an overview of trends in plankton communities (Licandro *et al.*, 2011). The knowledge base underlying this literature continually expands through status reports on oceanic hydrography from the Working Group on Oceanic Hydrography (WGOH) (Hughes *et al.*, 2011) and on zooplankton ecology from the Working Group on Zooplankton Ecology (WGZE) (O'Brien *et al.*, 2011). The Working Group on Phytoplankton and Microbial Ecology (WGPME) emerged from the Planning Group on Phytoplankton and Microbial Ecology (PGPYME) in response to an ICES need for linkage between hydrography and zooplankton. An interim status report was presented earlier (Li *et al.*, 2011a). In this first full report, the ecological status of phytoplankton and microbial plankton of the North Atlantic and adjacent seas is presented by reference to seven geographical regions containing 61 monitoring locations (Figures 1.1 and 1.3), and to 40 standard areas of the Continuous Plankton Recorder survey (Figure 1.2). Coverage stretches from the subpolar waters of the Labrador Sea to the subtropical waters of southwestern Iberia, and extends into the Mediterranean Sea.

In the North Atlantic and connected seas, as elsewhere in the world's oceans, microbes are extremely numerous, with abundance exceeding, by orders of magnitude, those of any other planktonic group ($>10^7$ microbes ml^{-1}). Not only do microbes constitute the largest reservoir of biomass involved in energy and material transfer, but also the largest reservoir of genetic information involved in supplying functional players to the ecological theatre. Microbial plankton are ribosome-encoding organisms from all three domains of cellular life (Bacteria, Archaea, Eukarya) as well as capsid-encoding organisms (viruses). Cellular microbes obtain energy from light (phototrophy) or chemicals (chemotrophy), electrons from water (lithotrophy) or organic carbon (organotrophy), and carbon from inorganic (autotrophy) or organic (heterotrophy) compounds, with the possibility of mixed modes of nutrition (mixotrophy). In oxygenated waters of the euphotic zone, primary production (virtually entirely microbial) is carried out by phytoplankton, which are photolithoautotrophs, comprising a huge diversity of algae of domain Eukarya and cyanobacteria of domain Bacteria. Microbial secondary production is carried out by chemoorganoheterotrophs belonging to the domain Bacteria.

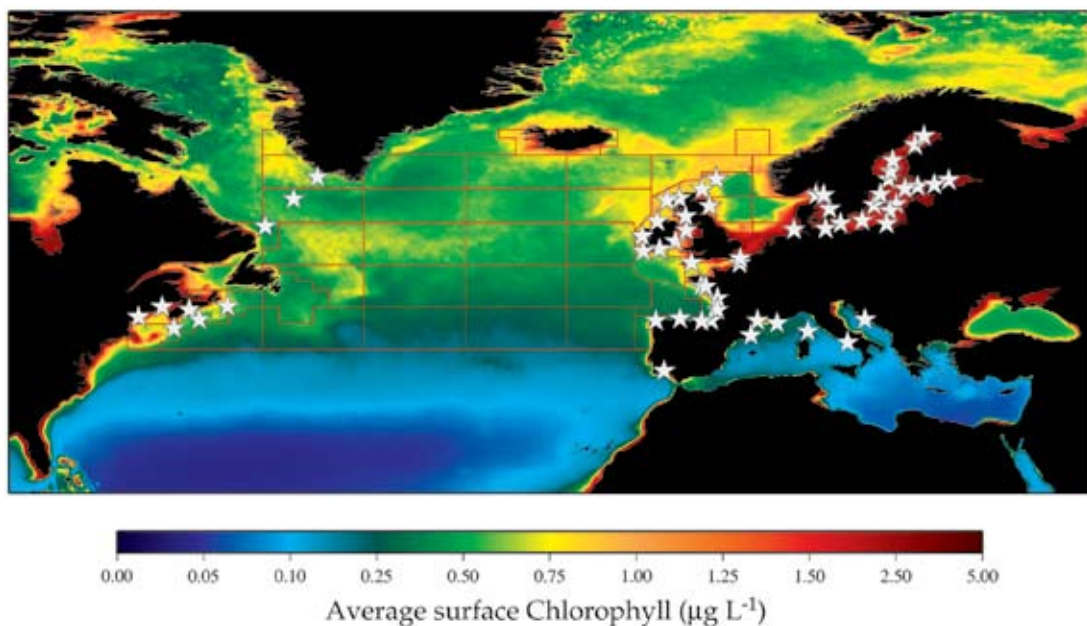


Figure 1.1
Phytoplankton and microbial plankton monitoring sites within the ICES Area plotted on a map of average chlorophyll concentration. Only programmes summarized in this report are indicated on this map (white stars). The red boxes outline CPR standard areas (see Figure 1.2 and Section 10).



Figure 1.2
Map of CPR standard areas in the North Atlantic (see Section 10 for details). Grey dots and lines indicate CPR sampling tracks.

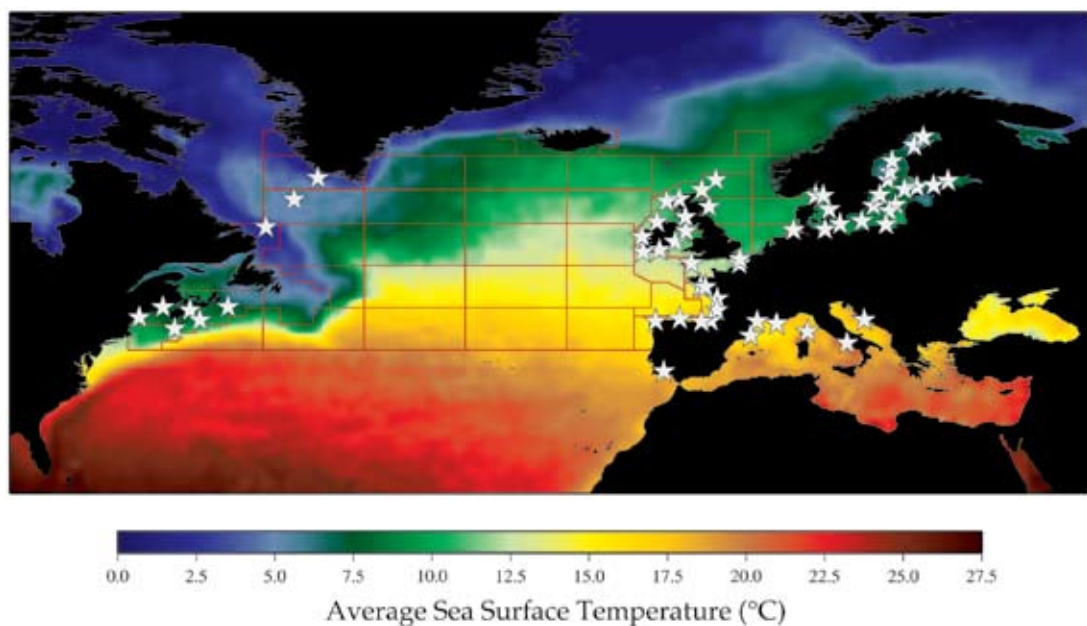
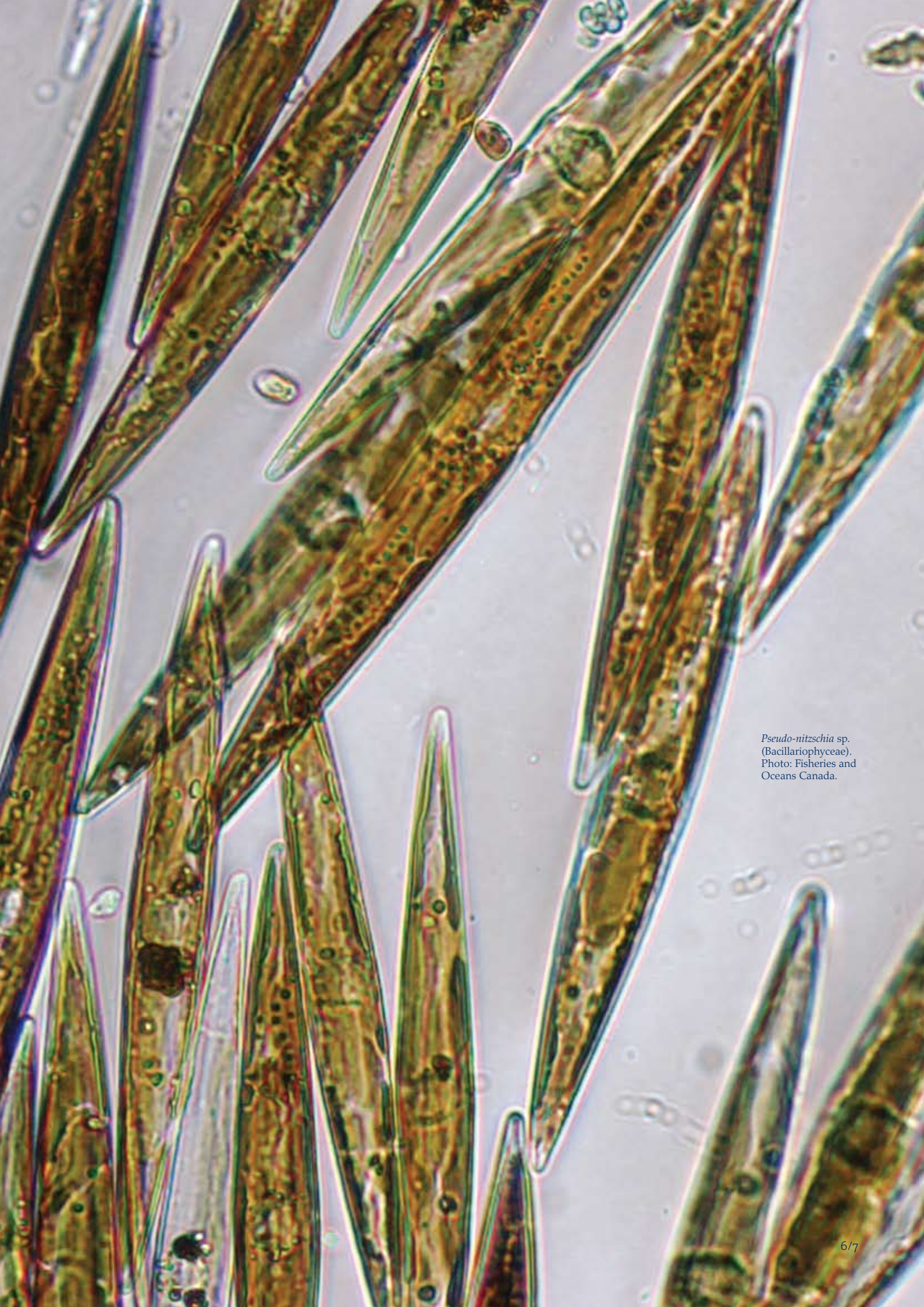


Figure 1.3
Phytoplankton and microbial plankton monitoring sites within the ICES Area plotted on a map of average sea surface temperature. Only programmes summarized in this report are indicated on this map (white stars). The red boxes outline CPR standard areas (see Figure 1.2 and Section 10).

Towards an understanding of ecosystem functioning, it is useful to classify plankton according to commonly shared adaptive features, such as physiological or morphological traits, which lead in combination to predictable ecosystem functions. In this report, eight such provisional microbial plankton types (Le Quéré *et al.*, 2005) are represented in lesser or greater detail at the collection of North Atlantic sampling sites. For example, picoheterotrophs include bacteria; picoautotrophs include picocyanobacteria (*Synechococcus*, *Prochlorococcus*) and picoeukaryotic algae; nitrogen fixers include some filamentous cyanobacteria; calcifiers include coccolithophores; dimethylsulphide producers include some dinoflagellates and some prymnesiophytes, notably *Emiliania huxleyi* and *Phaeocystis* sp.; silicifiers include many diatoms; mixed phytoplankton include many algae that do not tend to form blooms; and protozooplankton include heterotrophic flagellates and ciliates.

In this report, we also include information, where available, on aspects of the physical and chemical environments that are known to influence structure and function of microbial communities. For example, water temperature, salinity, wind, and nutrients are necessary to inform rule-based models of ecological response to external forcing. On one such habitat templet (Southwood, 1988), namely the quadrangular nutrient–turbulence model (Longhurst, 2007), seasonal diatom blooms might be mapped to the quadrant of high nutrients and high turbulence. Red tides and other dinoflagellate blooms of shallow seas might be mapped to the quadrant of high nutrients and low turbulence. A vigorous microbial loop might be mapped to the quadrant of low nutrients and low turbulence. It is a question whether such event-scale and seasonal-scale forcings can be discerned as we consider the annualized responses in the multiyear time-series, or whether succession and other longer-term modes of variability need to be invoked. The monitoring of phytoplankton and marine microbes is an important activity that supports science priorities in the management of North Atlantic ecosystems. This report would not be possible without the dedicated work and contributions of scientists, technicians, managers, administrators, institutes, agencies, and governments associated with ocean monitoring programmes.



Pseudo-nitzschia sp.
(Bacillariophyceae).
Photo: Fisheries and
Oceans Canada.

2. TIME-SERIES DATA ANALYSIS AND VISUALIZATION

Todd D. O'Brien

The Coastal and Oceanic Plankton Ecology, Production, and Observation Database (COPEPOD; <http://www.st.nmfs.noaa.gov/copepod/>) is a global database of plankton survey data, time-series, and plankton data products hosted by the National Marine Fisheries Service (NMFS) of the National Oceanic and Atmospheric Administration (NOAA). Through eight years of scientific collaboration and data-analysis support for plankton working groups such as the ICES Working Group on Zooplankton Ecology (WGZE) and now the ICES Working Group on Phytoplankton and Microbial Ecology (WGPME), COPEPOD has developed a collection of plankton-tailored, time-series analysis and visualization tools, including those used in the creation of this report. These tools in turn became COPEPOD's Interactive Time-series Explorer (COPEPODITE, <http://www.st.nmfs.noaa.gov/nauplius/copepodite/>), a free, online time-series processing and visualization toolkit which can be used to generate figures and analyses similar to those used in this report (and much more). COPEPODITE also features an interactive metabase that provides information on and contact points for hundreds of phytoplankton and zooplankton time-series and monitoring programmes from around the world. This metabase also acts as an access point to all of the sites used in this report as well as those from the concurrent ICES Zooplankton Status Report.

This section describes the time-series data-analysis methods (Section 2.1), the standard data-visualization figures used throughout this report (Section 2.2), and the supplemental data sources (e.g. sea surface temperature, chlorophyll, and wind speed) included in the standard analyses of each monitoring site (Section 2.3).

2.1 Time-series data analysis

The time-series analysis methods (and visualizations) used in this report were developed in cooperation with the SCOR Global Comparisons of Zooplankton Time-series working group (WG125), the ICES Working Group on Zooplankton Ecology (WGZE), and the ICES Working Group on Phytoplankton and Microbial Ecology (WGPME). The analyses used for this report use only a small subset of the entire collection of visualizations and analytical approaches created for these working groups. For simplicity, the subset of analysis and figures used for this report is referred to hereafter as “the WGPME time-series analysis”.

The WGPME time-series analysis is used to compare interannual trends across a variety of plankton and other hydrographic variables, each with different measurement units and sampling frequencies (e.g. to compare interannual trends in the “number of dinoflagellates per litre of water, sampled once a month” with the “average concentration of chlorophyll *a* in the 0–5 m surface waters, sampled weekly”). The WGPME analysis method uses a unitless ratio (or “anomaly”) to look at changes in data values over time relative to the long-term average (or “climatology”) of those data.

Each zooplankton time-series $P(t)$ is represented as a series of log-scale anomalies $p'(t)$ relative to the long-term average \bar{P} of those data:

$$p'(t) = \log_{10}[P(t)] - \log_{10}[\bar{P}] = \log_{10}[P(t)/\bar{P}]$$

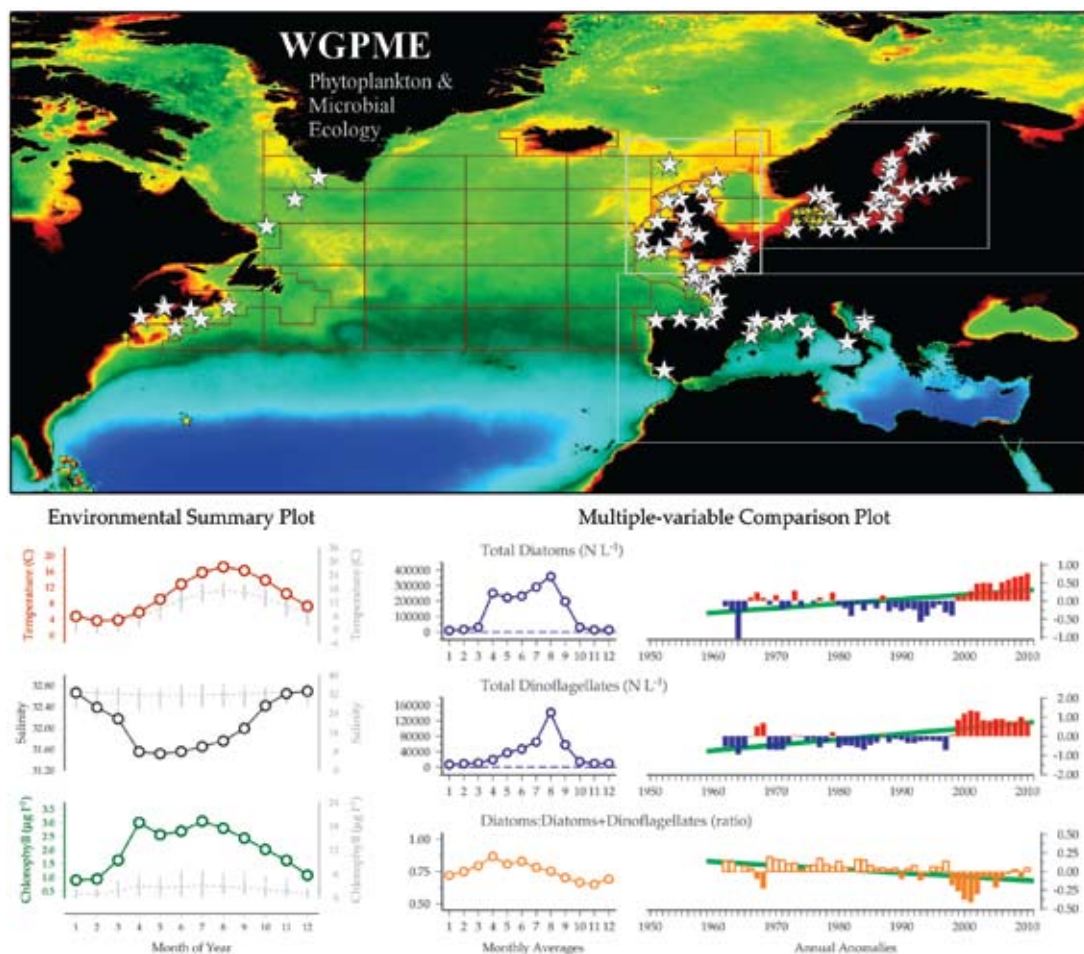


Figure 2.1
Examples of the interactive mapping and visualization tools used for the creation of this report are available online at <http://WGPME.net>.

If a dataset series at a given site is collected consistently and uniformly for the duration of a monitoring programme, the sampling bias (b) is represented in the equation as follows:

$$p'(t) = \log_{10}[b \times P(t)] - \log_{10}[b \times \bar{P}] = \log_{10}[bP(t)/b\bar{P}]$$

As the sampling bias (b) is present in both the numerator and denominator of the equation, it is cancelled out during the calculation. Likewise, the measurement units of the values are also cancelled out, creating a unitless ratio (the anomaly):

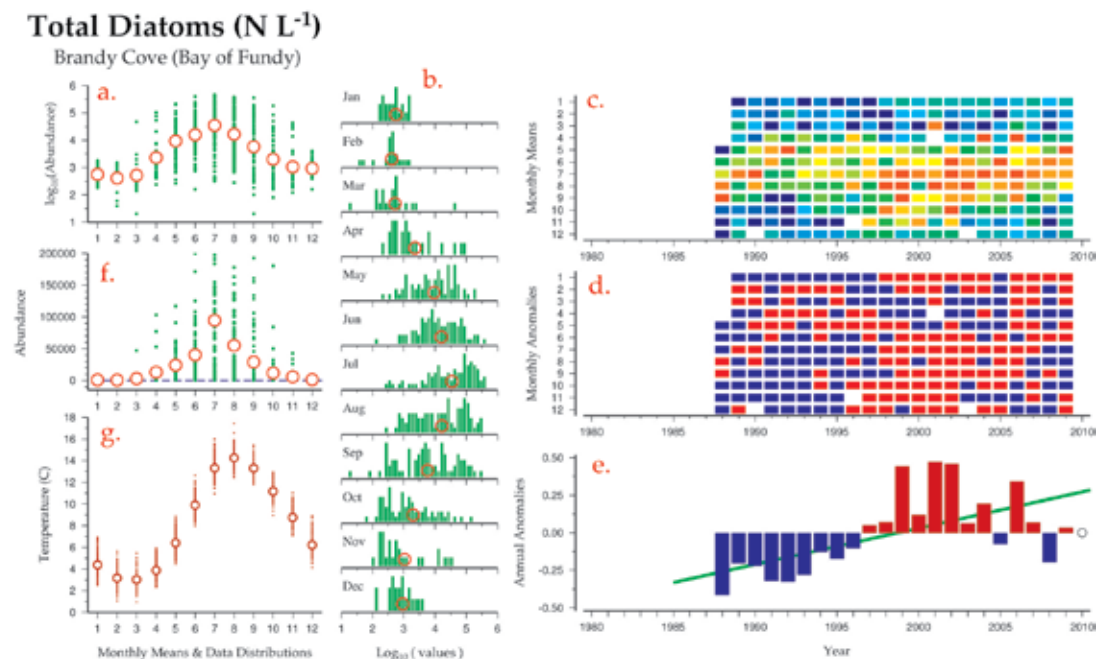
$$p'(t) = \log_{10}[b \times P(t)] - \log_{10}[b \times \bar{P}] = \log_{10}[bP(t)/b\bar{P}] = \log_{10}[P(t)/\bar{P}]$$

By using unitless anomalies, WGPME can make comparisons in the form “dinoflagellate abundances doubled during the same time interval that chlorophyll a concentrations decreased by half”. These comparisons can be made within a single site as well as between sites.

The WGPME analysis examines interannual variability and long-term trends by looking at changes in average annual values throughout a time-series. In most regions of the North Atlantic, plankton have a strong seasonal cycle, with periods of high (often in spring) and low (often in winter or late summer) abundance or biomass. As a result of this strong seasonal cycle, calculation of a simple annual average of plankton from low-frequency or irregular sampling (e.g. once per season, once per year) can be greatly influenced by when the sampling occurs (e.g. during, before, or after these seasonal peaks). This problem is further compounded by missing months or gaps between sampling years. The WGPME analysis addresses this problem by using the technique of Mackas *et al.* (2001), in which the annual anomaly value is calculated as the average of individual monthly anomalies within each given year. As this effectively removes the seasonal signal from the annual calculations, this method reduces many of the issues caused by using low-frequency and/or irregular monthly sampling to calculate annual means and anomalies.

Figure 2.2

A collection of standard WGPME time-series visualization figures illustrating the steps and components used in the WGPME analysis for creating annual anomalies of total diatom abundance from the Brandy Cove time series (Bay of Fundy, Site #2, see Section 3.2 for more information on this site).



The WGPME time-series analysis involves a series of calculation steps (Figure 2.2):

1) The incoming time-series data (i.e. total diatom abundance sampled twice a month) are binned into monthly means by year over the entire dataset. During this step, plankton, chlorophyll, and nutrient values are \log_{10} transformed, whereas temperature and salinity values are not. The distributions of values in each month of each year of the time-series are plotted as the green dots in Figure 2.2a and their value frequency is shown in the green bars in Figure 2.2b subpanel. The month-by-year mean values are also shown in the temporal matrix of Figure 2.2c, where colours represent value range categories and white spaces indicate months or years with no data or sampling. Together, these three subplots provide the investigator with a detailed overview of their data's distribution, variability, and temporal coverage.

2) The long-term average for each month, also known as its climatology, is then calculated. These monthly climatology values are represented by the open red circles in Figure 2a,b.

3) Each month's climatology value is then subtracted from each month-by-year value (e.g. the matrix cells in Figure 2.2c) in order to calculate month-by-

year monthly anomaly values for the time-series. In the monthly anomaly matrix (Figure 2.2d), months with value greater than that month's climatology (i.e. a positive anomaly) are indicated with a red cell, whereas months with a value less than that month's climatology (i.e. a negative anomaly) are indicated with a blue cell. Months with no data (no sampling) are left blank (white).

4) Annual anomalies for all of the years in the time-series (Figure 2.2e) are calculated (per Mackas *et al.*, 2001) as the average of all of the monthly anomalies (Figure 2.2c) present within that year. In this figure, annual anomaly values greater than zero are indicated with red, whereas annual anomaly values less than zero are indicated with blue. An open circle drawn on the anomaly zero line (e.g. 2010 in Figure 2.2e) indicates that data were not available that entire year. This symbol for "no-data years" is used to distinguish them from near-zero value anomalies (which plot as a very thin line in this figure).

5) In Figure 2.2e, the green line drawn behind the anomaly bars represents the linear regression of the annual anomalies vs. year. The color and form of this line indicate the statistical significance of this trend (e.g. solid green is $p < 0.01$, dashed green is $p < 0.05$, thin grey is $p > 0.05$).

6) Figures 2.2f and 2.2g are not used in the anomaly calculation, but provide useful information to the investigator. The left middle subpanel (Figure 2.2f) shows the distribution of raw (non-log-transformed) values and their climatological monthly means (green dots and open red circles). This plot allows the investigator to see the true value range of the values presented. The left lower subpanel (Figure 2.2g) shows the distribution and climatological monthly means of water temperatures at the sampling site. Water temperatures can influence the seasonal cycle of the plankton as it may affect the plankton both directly (e.g. metabolic rates) and indirectly (e.g. water column stratification and subsequent nutrient limitation).

Figure 2.2 summarizes the seasonal and interannual trends of diatoms at Brandy Cove as follows: Diatoms at Brandy Cove have a seasonal maximum in summer (July) and a seasonal minimum in winter (December–February; Figure 2.2a,f). Over the sampling period 1988–2009, annual average abundance estimates were below the long-term average prior to 1997 (Figure 2.2e, blue or negative annual anomalies) and have generally been above the long-term average during 1997–2007 (Figure 2.2e, red or positive annual anomalies). Focusing on Figure 2.2c,d,e, the positive annual anomalies during 1997–2004 (Figure 2.2e) coincide with years in which the seasonal maximum occurred later in the year (Figure 2.2c, patch of red mid-summer cells) and whose higher abundance values carried into summer, autumn, and winter (Figure 2.2d, positive anomalies, red cells, remaining red into autumn and winter unlike pre-1996 years). Overall abundance has been increasing since sampling began in 1988 (Figure 2.2e, $p < 0.01$, solid green line).

2.1.1 Representation of “absence” and zero-value measurements

Some plankton groups and species have a temporary seasonal presence within a monitoring site and may completely disappear during parts of the year. At the Brandy Cove monitoring site (see Figure 2.2), diatom abundance can become quite low in winter (but remain above zero), whereas dinoflagellates can become completely absent during December–March. The dinoflagellate data at this site have zero values that indicate “looked for and found absent”. Including these zero values in the time-series analysis is a challenge, however, as the WGPME method log-transforms these data, and $\log(0)$ is an illegal math operation.

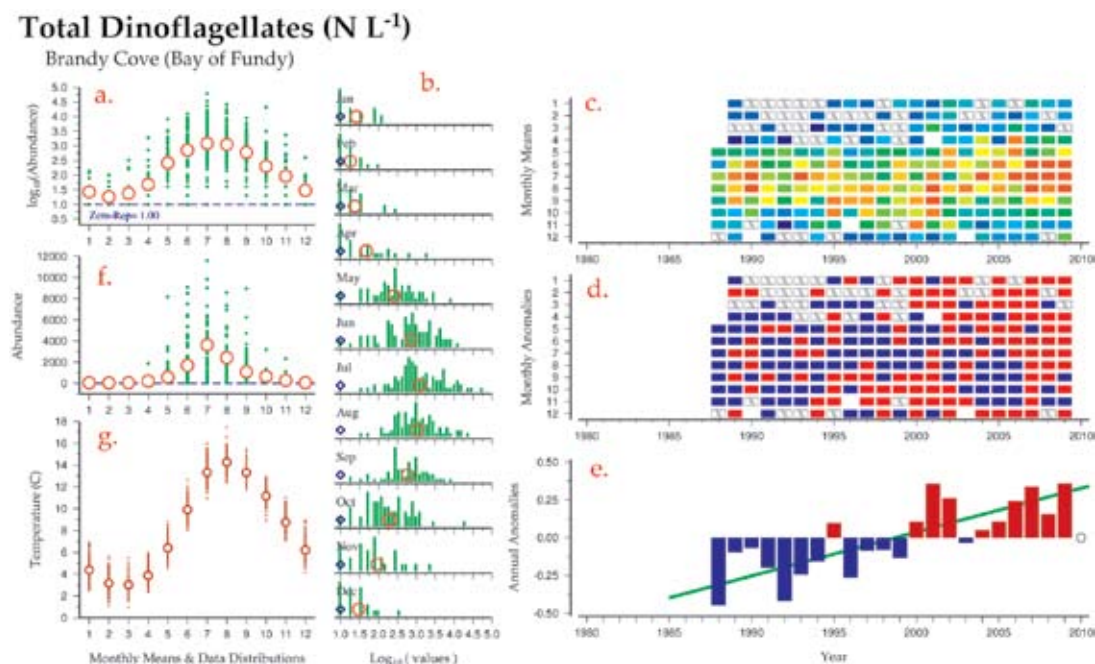
One commonly used log/zero-handling solution is to add a 1 to all of the values before log-transforming them, often referred to as “ $\log(x+1)$ ”. The problem with this solution is that the “ $x+1$ ” offset numerically affects smaller value range data (e.g. counts of a rare species with non-zero values ranging from 1 to 20 per unit) at a different magnitude than it numerically affects larger value range data (e.g. counts of an entire group of blooming species with non-zero values ranging from 1000 to 20 000). In the latter case, the zero value (“ $x+1 = 0+1 = 1$ ”) is 1/1000th of the otherwise lowest recorded value, and using it will have a greater impact on the calculation of the climatological means and anomalies than that same “ $x+1$ ” offset will have on the smaller range example. An alternate and improved version of the “ $x+1$ ” method is, therefore, to add a value offset that is based on the value range of the data itself (“ $x+0.01$ ”, “ $x+100$ ”), but adding even a small offset still has a non-linear effect on all of the other (non-zero) values in the dataset.

The WGPME zero-handling method does not add any offset. Instead, it replaces any incoming zero value with a fixed “zero-representation value” (Zero-rep), which is equal to one half of the lowest non-zero value seen in the entire data stream for that variable (regardless of year or month). The Zero-rep would be 0.5 for data ranging from 1 to 20, and 500 for data ranging from 1000 to 20 000. The Zero-rep method works with both small and large range value sets, without introducing non-linear biases or offsets. This method requires knowing the value range of the data before processing it, calculating the Zero-rep, and then replacing any zero values with this Zero-rep value. Although this may be difficult to do by hand, especially with hundreds of variables, it is automatically done by the COPEPODITE toolkit during the data preparation process. When the “Zero-rep” function is active for a plankton

variable, the standard figures shown in Figure 2.2 include some additional elements. In the standard figure collection for dinoflagellates at Brandy Cove (Figure 2.3), the “Zero-rep” value is indicated as a blue dashed line in Figure 2.3a,f and as a blue diamond in Figure 2.3b. When dinoflagellates are absent for an entire month, the month-by-year mean matrix cell for that month is represented with an “[X]”. In Figure 2.3c, this symbol differentiates December 1995 (an “[X]” cell, a month in which no dinoflagellates were found in the samples) from November 1996 and December 2003 (both blank/white cells, months in which no sampling was done). In the monthly anomaly matrix (Figure 2.3d), any monthly anomaly based only on this Zero-rep value is indicated with an “[X]” cell. Although this cell could also be represented with a dark blue cell (as a negative anomaly), the “[X]” indicates the complete absence within that month and distinguishes this from a very low value month. These monthly anomalies still participate in the calculation of the annual anomaly averaging calculation like any other value.

Figure 2.3 summarizes the seasonal and interannual trends of dinoflagellates at Brandy Cove as follows. Dinoflagellates at Brandy Cove have a seasonal maximum in summer (July) and a seasonal minimum in winter (December–February) (Figure 2.3a,f). Dinoflagellates are periodically absent during December–March, most notably in the years 1990–1994 (Figure 2.3c,d). Over the 1988–2009 sampling period, average annual abundance estimates were generally below the long-term average prior to 2000 (Figure 2.3e, blue or negative annual anomalies) and have generally been above the long-term average after 2000 (Figure 2.3e, red or positive annual anomalies). The positive annual anomalies during 2000–2009 coincide with years in which the dinoflagellates remained present throughout most of winter (Figure 2.3c) and had subsequent higher abundance estimates throughout the rest of the year (Figure 2.3d). Overall dinoflagellate abundance has been increasing since sampling began in 1988 (Figure 2.2f, $p < 0.01$, solid green line).

Figure 2.3
A collection of standard WGPME time-series visualization figures illustrating the steps and components used in the WGPME analysis for creating annual anomalies of total dinoflagellate abundance from the Brandy Cove time-series (Bay of Fundy, Site #2, see Section 3.2 for more information on this site).



2.2 Time-series data visualization: standard figures

With more than 1000 different variables in the full WGPME time-series collection (e.g. taxonomic groups and species abundance and biomass estimates, surface, at-depth, or integrated temperature, salinity, nutrients, and pigments, wind speed, river inflow, and Secchi depth), one of the biggest challenges in creating this report was to find a way of quickly representing these data in a standard visual format within the report itself. From a plankton perspective, these figures need to quickly report seasonal variability, interannual changes, and the presence (or absence) of any long-term trends or patterns. Each time-series monitoring site summary in this report begins with an environmental summary plot (Section 2.2.1) and a multiple-variable comparison plot (Section 2.2.2).

2.2.1 Environmental summary plot

The environmental summary plot (see examples in Figure 2.4) shows the seasonal cycle of three key hydrographic variables (average monthly values of surface temperature, salinity, and chlorophyll) at each monitoring site. Each figure in this plot shows the average monthly values plotted on dual y -axes that show both the localized value range (left, coloured symbols and y -axis) and a broad value range that is shared across all sites in this report (right, grey symbols and y -axis). In Figure 2.4, the

left axis subplot and black symbols highlight the similar salinity seasonal cycles found at both sites (with higher values in winter and lower values in summer), whereas the right axis subplot and grey symbols highlight the large differences in average salinity between the sites (around 32 at Helgoland Roads, but only 7–9 at Arkona Basin). This dual axis was adopted because using only the left axis did not always convey these broad differences found between sites, and using only the common right axis removed much of the seasonal signal (such as the flat grey lines seen in the salinities of Figure 2.4).

2.2.2 Multiple-variable comparison plot

The multiple-variable comparison plot (Figure 2.5) presents a seasonal and interannual comparison of select cosampled variables sampled within a monitoring site. The figures in this plot are created by combing figures “f” and “e” from the WGPME standard figures discussed in Section 2.1 (see also Figures 2.2f,e and 2.3f,e). The colour of the annual anomalies will not always be blue and red. Although annual anomalies of plankton abundance and biomass variables are blue and red, annual anomalies for chlorophyll and pigment variables are green, annual anomalies for temperature variables are dark red, annual anomalies for salinity and density variables are black, and annual anomalies for nutrients, ratios, meteorological values, and anything else is orange (see Figure 2.5 for examples).

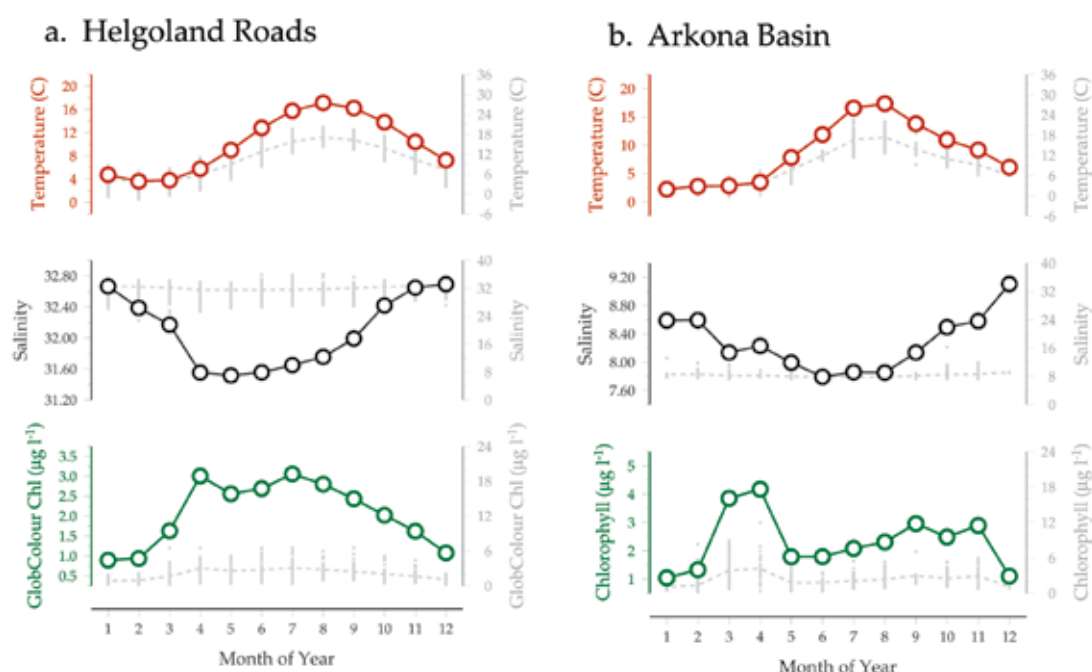


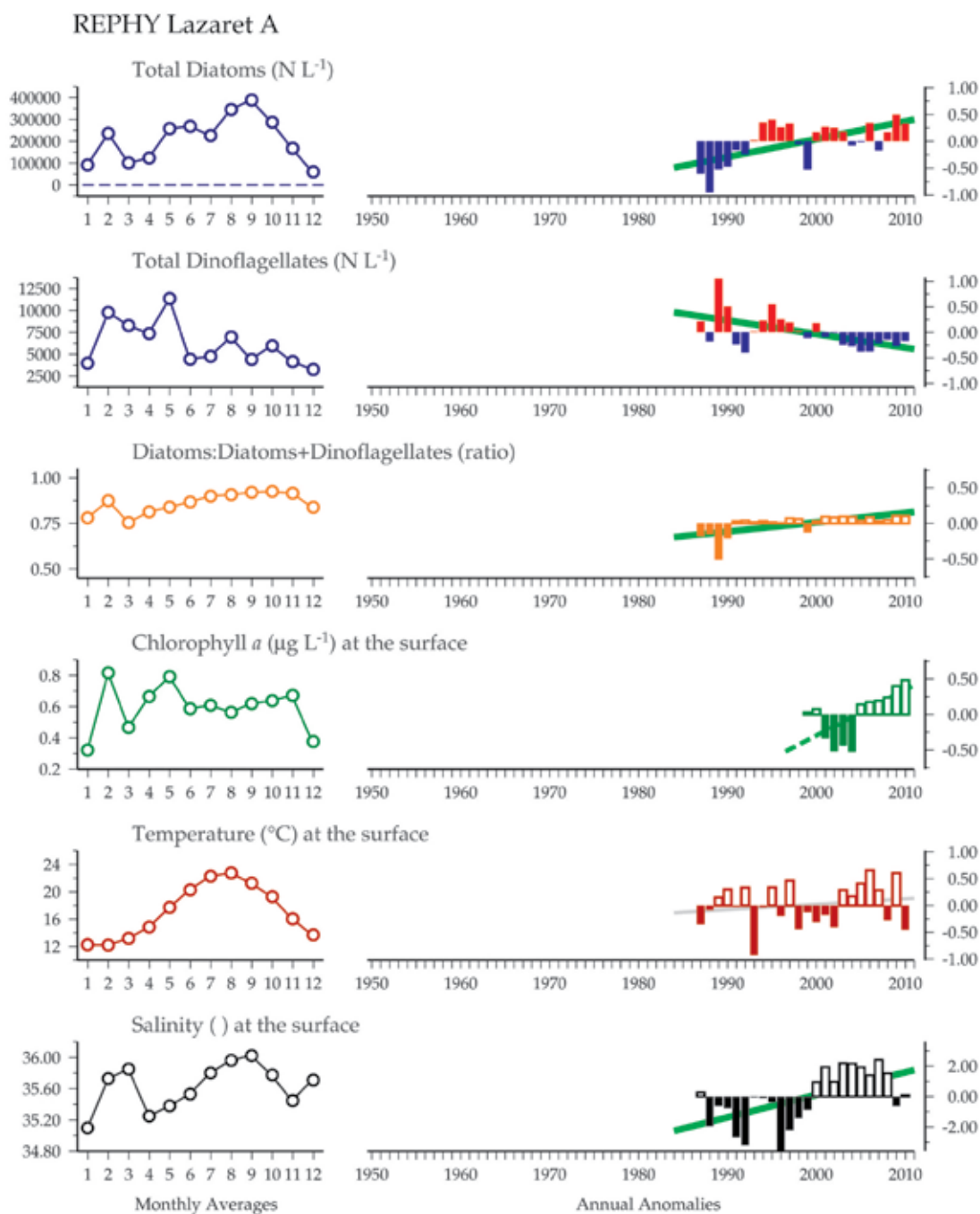
Figure 2.4
Examples of two environmental summary plots (see Section 2.2.1) showing average month-to-month water temperature, salinity, and chlorophyll at the Helgoland Roads (Site 30, Section 6.1) and Arkona Basin (Site 25, Section 5.5) monitoring sites.

As described in Section 2.1, the left column of figures summarize the seasonal cycle of each variable, whereas the right column of figures summarize the interannual patterns and trends of each variable. In Figure 2.5, diatoms at REPHY Lazaret A are increasing, whereas dinoflagellates are decreasing. Both trends are significant ($p < 0.01$), but opposite in direction. The dashed green line in the chlorophyll *a* figure indicates significance of only $p < 0.05$. The grey trend line in the temperature figure indicates the trend is non-significant ($p > 0.05$).

Only a select number of variables and plots are shown for each time-series site to reduce the size of the printed version of this publication. Most of the multiple-variable comparison plots in this report, therefore, display less than ten variables, whereas many of the time-series sites have 20 or more variables. The WGPME time-series site (<http://WGPME-net/time-series>) contains the missing variables and additional visualization figures (like Figure 2.2 and 2.3) that were not shown in this report.

Figure 2.5

Example of a multiple-variable comparison plot (see Section 2.2.2) showing the seasonal and interannual properties of select cosampled variables at the REPHY Lazaret A monitoring site (Site #57, Section 9.3). The green lines drawn in the right figures represent the linear regression of the annual anomalies vs. year. The color and form of these lines indicate the statistical significance of the trend (e.g. solid green is $p < 0.01$, dashed green is $p < 0.05$). The grey line (temperature) indicates a non-significant trend.



2.3 Time-series supplemental data

Water temperature is an excellent indicator of the physical environment in which plankton are living because it affects plankton both directly (i.e. through physiology and growth rates) and indirectly (i.e. through water-column stratification and related nutrient availability). Similarly, chlorophyll concentration is an excellent indicator of the average phytoplankton community biomass. Although most sites already had *in situ* temperature and chlorophyll data available, a handful of sites did not. In these cases, the supplemental data sources (summarized in this section) were used to fill in these missing variables. Further, to provide a collection-wide set of uniform-method temperature and chlorophyll data, WGPME included these supplemental time-series data (in addition to all available *in situ* data) with each site. These supplemental datasets are summarized below.

2.3.1 Sea surface temperature data: HadISST

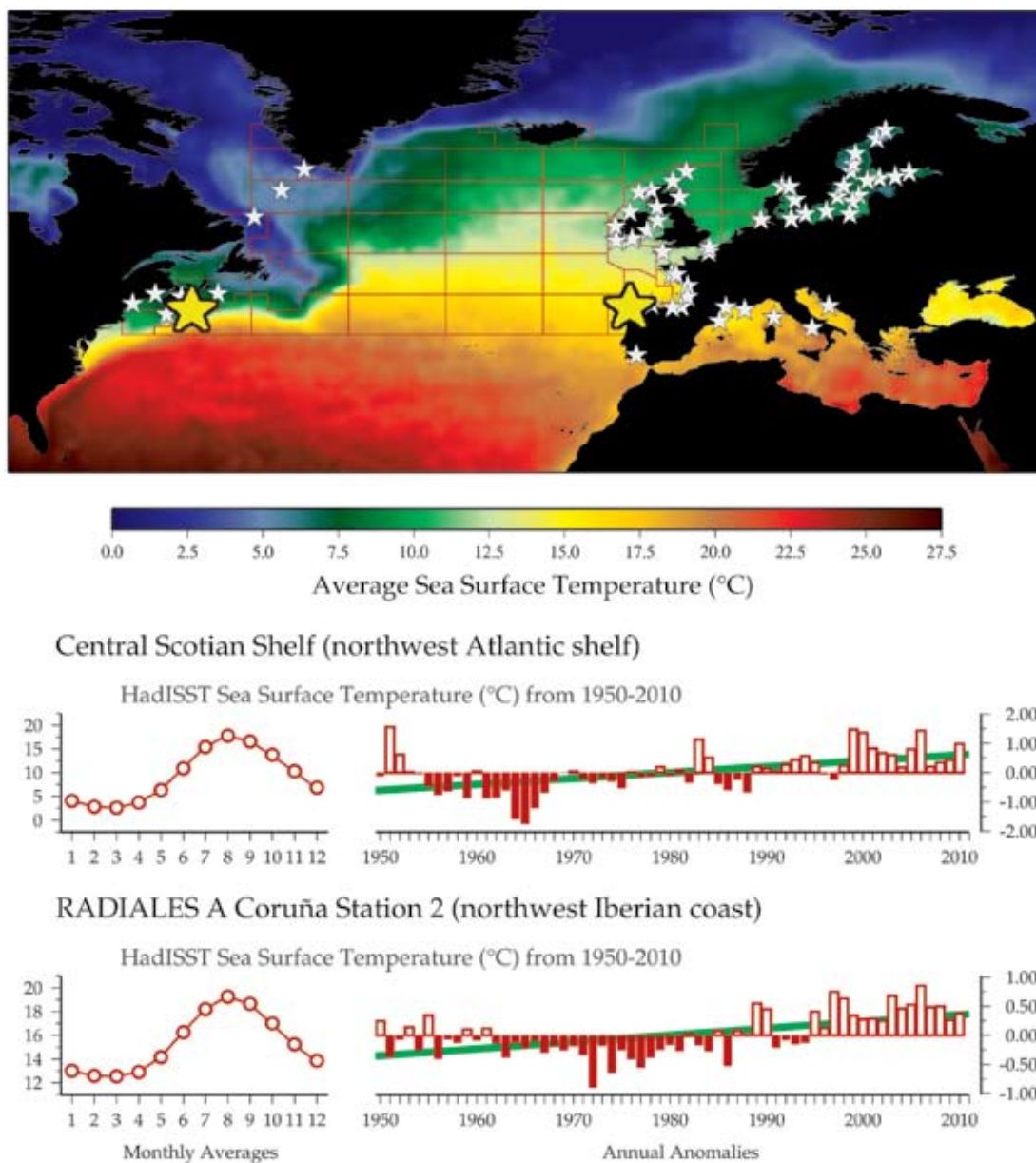
In order to provide a common, long-term dataset of water temperatures for every site in the North Atlantic study area, the Hadley Centre Global Sea Ice Coverage and Sea Surface Temperature (HadISST, version 1.1) dataset, produced by the UK Met Office, was used to add standard temperature data to each site (Figure 2.6). The HadISST is a global dataset of monthly SST values from 1900 to the present. This product combines historical *in situ* ship and buoy SST data with more recent bias-adjusted satellite SST and statistical reconstruction (in data-sparse periods and/or regions) to create a continuous global time-series at 1° spatial resolution (roughly 100 km × 100 km). The HadISST data are not intended to represent the exact temperatures in which plankton was sampled, but they do provide a 110-year average of the general water temperatures in and around the sampling area. These additional data become important as, in many regions of the North Atlantic, temperatures have been increasing over the last 60–110 years (Figure 2.6, lower panel), and the plankton growing in those regions may be experiencing the warmest water temperatures seen in the last 50 or 100 years.

For each plankton time-series, the immediately overlaying HadISST 1° grid cell was selected. For single-location sampling sites, this 1° cell included a ~100 km × 100 km area in and around the sampling site. For transects and region-based surveys (e.g. Iceland, Norway, Gulf of Maine), the centre point of the transect or region was used to select a single 1° cell to represent the general conditions of the entire sampling area (comparisons with multicell averages revealed no substantial differences). Once a 1° cell was selected, all HadISST temperature data were extracted from that cell for the period 1900–2010 and used to calculate annual anomalies.

The HadISST v. 1.1 dataset is available online at <http://badc.nerc.ac.uk/data/hadisst/>.

Figure 2.6

Map of HadISST sea surface temperature (see Section 2.3.1) overlaid with phytoplankton time-series site locations (white and yellow stars) and CPR standard areas (red boxes). The lower sub-panel shows examples of seasonal and interannual properties (see Section 2.2.2) of HadISST sea surface temperatures from the Central Scotian Shelf (left yellow star, Site #5, Section 3.4) and RADIALES A Coruña station 2 (right yellow star, Site #53, Section 8.5).



2.3.2 Sea surface chlorophyll data: GlobColour

To provide a common, long-term dataset of chlorophyll for every site in the North Atlantic study area, the GlobColour Project chlorophyll merged level-3 ocean colour data product (GlobColour) was used to add standard chlorophyll data to each site (Figure 2.7). This data product is a global dataset of monthly satellite chlorophyll data from 1998 to the present. Although the original

product is available at a resolution of 4.63 km, it was binned into a 1° spatial resolution (roughly 100 km × 100 km) in order to be compatible with the HadISST dataset. The GlobColour dataserries were assigned to corresponding 1° boxes using the same method outlined for the HadISST dataserries (see Section 2.3.1).

The GlobColour Project chlorophyll concentration merged level-3 data product (GlobColour) is available online at <http://www.globcolour.info/>.

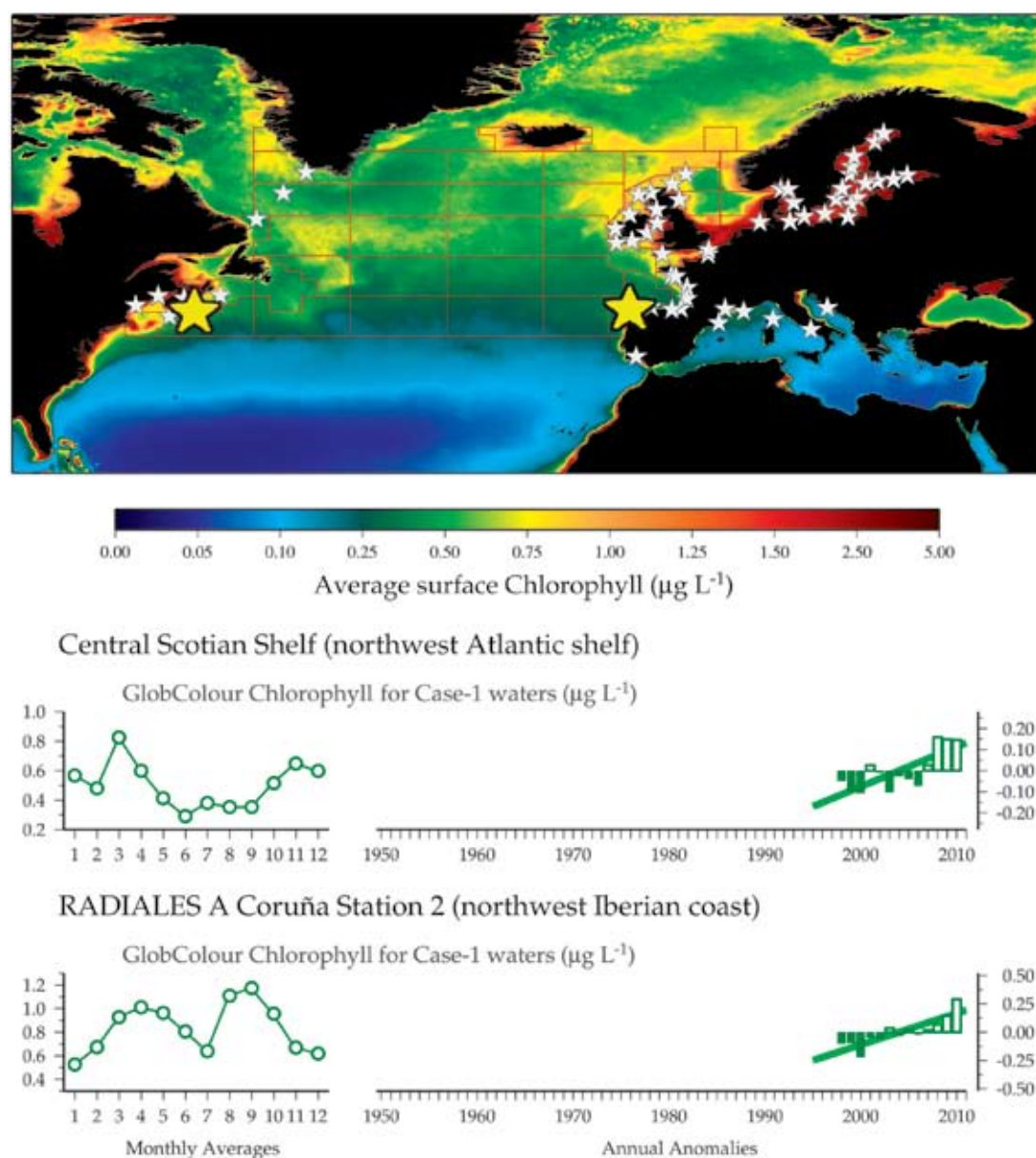


Figure 2.7
Map of GlobColour sea surface chlorophyll concentrations (see Section 2.3.2) overlaid with phytoplankton time-series site locations (white and yellow stars) and CPR standard areas (red boxes). The lower subpanel shows examples of seasonal and interannual properties (see Section 2.2.2) of sea surface chlorophyll concentrations from the Central Scotian Shelf (left yellow star, Site #5, Section 3.4) and RADIALES A Coruña station 2 (right yellow star, Site #53, Section 8.5).

2.3.3 Sea surface wind data: ICOADS

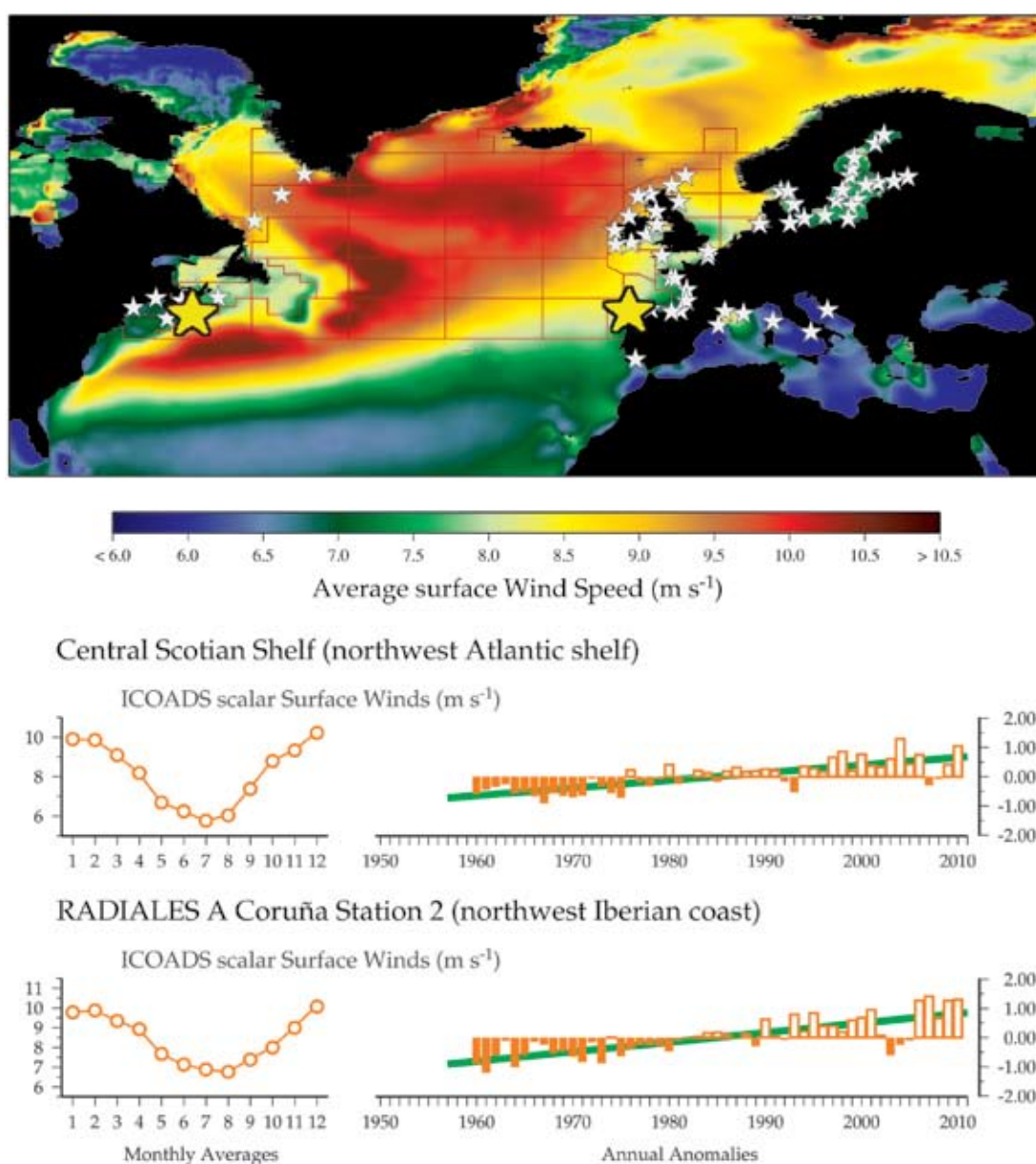
Temperature and wind both play an important role in determining the level of mixing or stratification in the marine environment, which, in turn, can determine the availability of nutrients and influence plankton production. A recent study by Hinder *et al.* (2012), using scalar wind speed data from the International Comprehensive Ocean–Atmosphere Data Set (ICOADS), found a strong relationship between Continuous Plankton Recorder (CPR) diatom and dinoflagellate abundance, surface wind speed, and surface water temperatures. This

study also noted strong, long-term increasing or decreasing trends in many regions of the North Atlantic (see Figure 2.8).

ICOADS (scalar) surface wind speed data were added as a supplemental variable to each of the monitoring sites in this study. The ICOADS wind dataserries were assigned to corresponding 1° boxes using the same method outlined for the HadISST dataserries (see Section 2.3.1).

The ICOADS data are available online at (<http://icoads.noaa.gov/>).

Figure 2.8
Map of ICOADS surface wind speed (see Section 2.3.3) overlaid with phytoplankton time-series site locations (white and yellow stars) and CPR standard areas (red boxes). The lower subpanel shows examples of seasonal and interannual properties (see Section 2.2.2) of ICOADS surface wind speed from the Central Scotian Shelf (left yellow star, Site #5, Section 3.4) and RADIALES A Coruña station 2 (right yellow star, Site #53, Section 8.5).





Deploying a Niskin bottle and Conductivity-Temperature-Depth (CTD) instrument package at the AZTI Station D2 time-series site. Photo: Marta Revilla, AZTI-Tecnalia.

3. PHYTOPLANKTON AND MICROBIAL PLANKTON OF THE NORTHWEST ATLANTIC SHELF

William K. W. Li, Nicole Poulton, Michael Sieracki, Jennifer Martin, and Murielle LeGresley

The Northwest Atlantic Shelf is the continental shelf extending from Newfoundland to Cape Hatteras, which includes the Gulf of St Lawrence, the Nova Scotian Shelf, the Bay of Fundy, the Gulf of Maine, Georges Bank, the southern New England Shelf, and the Mid-Atlantic Bight. The physical oceanography of this area has been described in detail (Loder *et al.*, 1998; Townsend *et al.*, 2006). The shelf area is generally broad and topographically complex, but well connected to deep slope waters through the Laurentian Channel running into the Gulf of St Lawrence and the Northeast Channel running into the Gulf of Maine. Surface circulation is a general southwest flow, but there is clockwise movement around banks and anticlockwise movement around basins. Subpolar water of low temperature and low salinity is transported here from the Labrador and Newfoundland shelves. At the Cabot Strait, there is a bifurcation of flow that supplies the Nova Scotian current on the inner Scotian Shelf, and a shelf-break flow along the western side of the Laurentian Channel and the outer Scotian Shelf. Hydrographic conditions are strongly seasonal, being influenced by ocean-atmosphere heat exchange, freshwater run-off, precipitation, melting of sea ice, and exchange with offshore slope waters.

Strong gradients of temperature and salinity exist horizontally and vertically on the shelf, as these properties are modified by diffusion, mixing, currents, and shelf topography (Hughes *et al.*, 2011).

The seasonal cycles of pelagic production and consumption in this region have been well described by Longhurst (2007), with particular attention paid to the Scotian Shelf, the Bay of Fundy, the Gulf of St Lawrence, the Gulf of Maine, and Georges Bank. Across this region, as in oceans elsewhere, microbial diversity spans three domains (Archaea, Bacteria, Eukarya) and also includes viruses. Viruses are largely cyanophages and bacteriophages. Bacteria comprise the dominant SAR11 phylotype cluster, and other abundant phylotypes such as SAR86-like cluster, SAR116-like cluster, *Roseobacter*, Rhodospirillaceae, Acidomicrobidae, Flavobacteriales, *Cytophaga*, and unclassified Alphaproteobacteria and Gammaproteobacteria clusters. Phototrophic prokaryotes include cyanobacteria that contain chlorophyll (mainly *Synechococcus*), aerobic anoxygenic phototrophs that contain bacteriochlorophyll, and bacteria that contain proteorhodopsin. Eukaryotic microalgae include Bacillariophyceae (diatoms), Dinophyceae (dinoflagellates), Prymnesiophyceae, Prasinophyceae, Trebouxiophyceae, Cryptophyceae, Dictyochophyceae, Chrysophyceae,

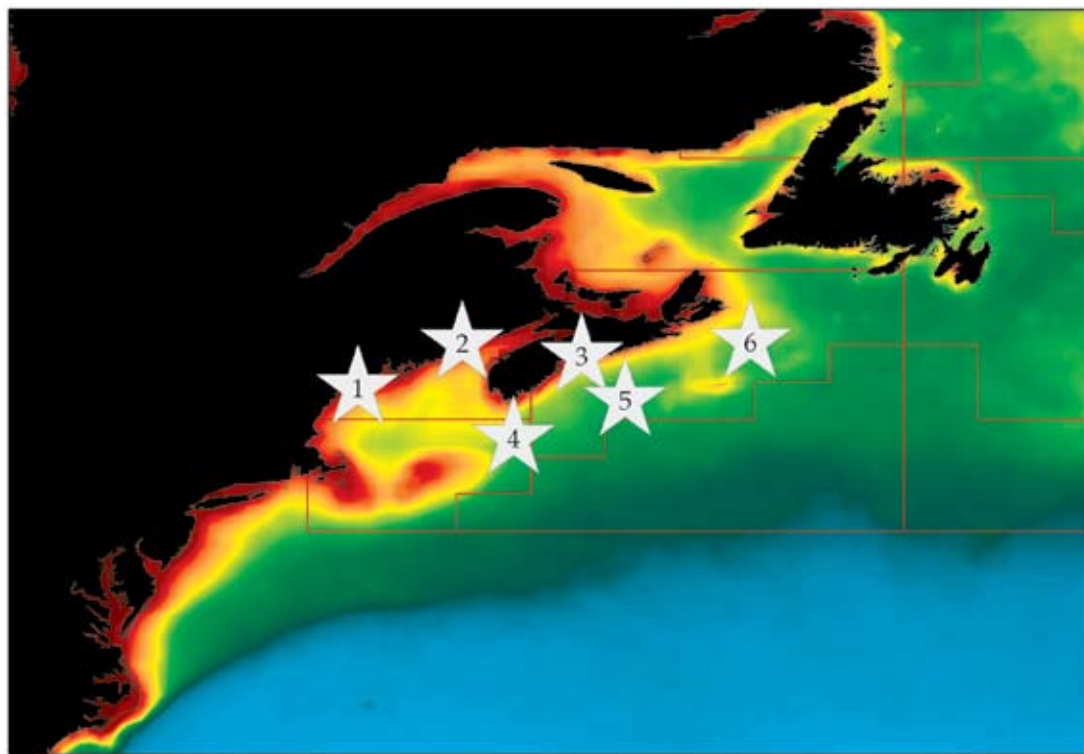


Figure 3.1
Locations of the Northwest Atlantic Shelf plankton monitoring areas (Sites 1–6) plotted on a map of average chlorophyll concentration.

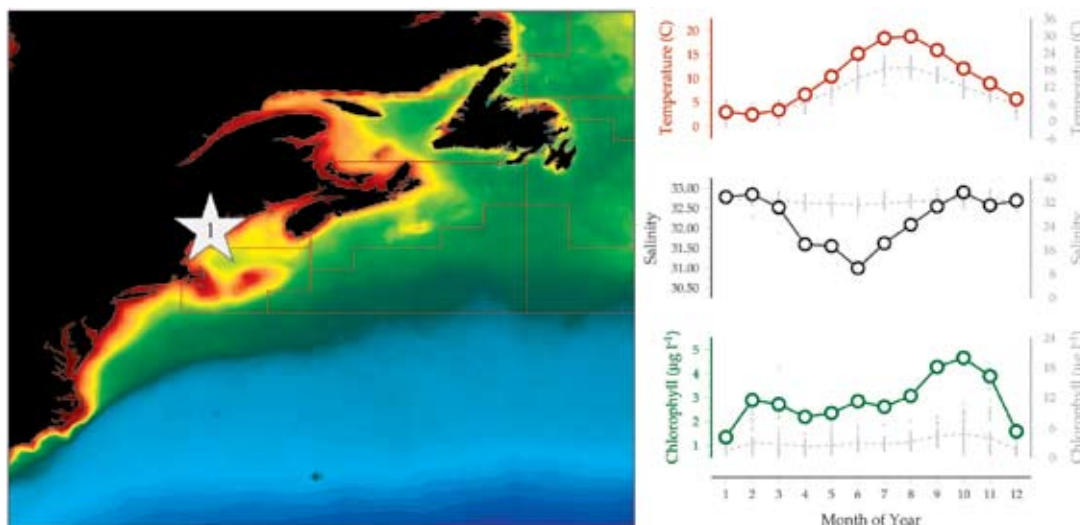
Eustigmatophyceae, Pelagophyceae, Synurophyceae, and Xanthophyceae. Heterotrophic eukaryotic protists include Dinophyceae, Alveolata, Apicomplexa, amoeboid organisms, Labrynthulida, and heterotrophic marine stramenopiles (MAST). Ciliates include *Strombidium*, *Lohmaniella*, *Tontonia*, *Strobilidium*, *Strombidinopsis*, and the mixotrophs *Laboea strobila* and *Myrionecta rubrum* (Li *et al.*, 2011b).

Although there are large seasonal changes in sea surface temperature and thermal stratification, it is the inflows of low temperature and low salinity waters that appear to drive interannual variability in water-column stability and mixed-layer depth, causing interannual changes in phytoplankton dynamics and phenology (Martin *et al.*, 2006; Ji *et al.*, 2007; Song *et al.*, 2010). Increased water-column stability alleviates light limitation, but exacerbates nutrient limitation. Although these counter-effects largely offset each other on an annual basis, changes in higher trophic level production may be sensitive to phenological considerations of primary production, such as the timing of spring and autumn phytoplankton blooms (Song *et al.*, 2011). Nearshore locations such as Bedford Basin, Passamaquoddy Bay, and Booth Bay are influenced by local land–sea interactions that modify the regional pattern, but a persistent common seasonality can, nevertheless, be discerned in phytoplankton groups across the region as a whole.

3.1 Booth Bay, Maine (Site 1)

Nicole Poulton and Michael Sieracki

Figure 3.1.1
Location of the Booth Bay, Maine plankton monitoring area (Site 1), plotted on a map of average chlorophyll concentration, and its corresponding environmental summary plot (see Section 2.2.1).



Booth Bay is a small mesotidal embayment located along midcoast Maine in New England, near the town of West Boothbay Harbor, with no direct major river input. Circulation is dominated by strong semi-diurnal tidal mixing with offshore Gulf of Maine coastal waters. The monitoring site was initiated from a floating dock in 2000 located near the State of Maine's Department of Marine Resources. The purpose of the study is to monitor long-term physical and chemical changes, and phytoplankton population dynamics. Weekly observations at high tide of phytoplankton, bacteria, and eukaryotic heterotrophs are made using flow cytometry. Temperature, salinity (refractometer measurements), and size-fractionated chlorophyll *a* (< 3, 3–20, and >20 µm) are also determined. Flow cytometric taxonomic groups are defined and enumerated (*Synechococcus*, cryptophytes, and total phytoplankton < 20 µm). Bacteria are detected and enumerated using PicoGreen, a DNA stain (Invitrogen; Veldhuis *et al.*, 1997). Heterotrophic and mixotrophic eukaryotes (microflagellates and small ciliates) are detected using the food vacuole stain Lysotracker Green (Invitrogen; Rose *et al.*, 2004). Microplankton taxonomic distribution (15–300 µm) and abundance are collected using an imaging cytometer, FlowCAM (Sieracki *et al.*, 1998). As of 2012, samples for nutrient analysis and zooplankton (vertical net tows) are also collected.

Seasonal and interannual trends (Figure 3.1.2)

Strong seasonal patterns emerge with all of the plankton populations and chlorophyll *a* that correlate with changes in temperature and the onset of spring and autumn phytoplankton. This site experiences a strong seasonal cycle in temperature, ranging from 1 to 20°C. Cryptophytes and *Synechococcus* bloom on an annual basis within a narrower period of time, usually July and September, respectively. Bacteria often increase following the spring bloom and then increase again as water temperature increases. Larger microphytoplankton (not shown) are imaged by the FlowCAM, capturing the onset of the spring and autumn blooms. The spring bloom is dominated by diatoms, typically *Thalassiosira*, *Chaetoceros*, and *Skeletonema*, and the autumn bloom is a more diverse mix of diatoms and dinoflagellates, usually *Prorocentrum*.

Over the 10-year period, different trends were observed among the plankton. *Synechococcus*, total phytoplankton (< 20 µm), heterotrophic and mixotrophic eukaryotes all increase, with the largest positive anomalies observed from 2009 to 2010. Since 2000, positive trends are observed in sea surface temperature and chlorophyll *a*, whereas negative trends are observed in salinity and bacteria. These data provide a basis for future modelling of planktonic organisms capable of quickly tracking changing environmental conditions.

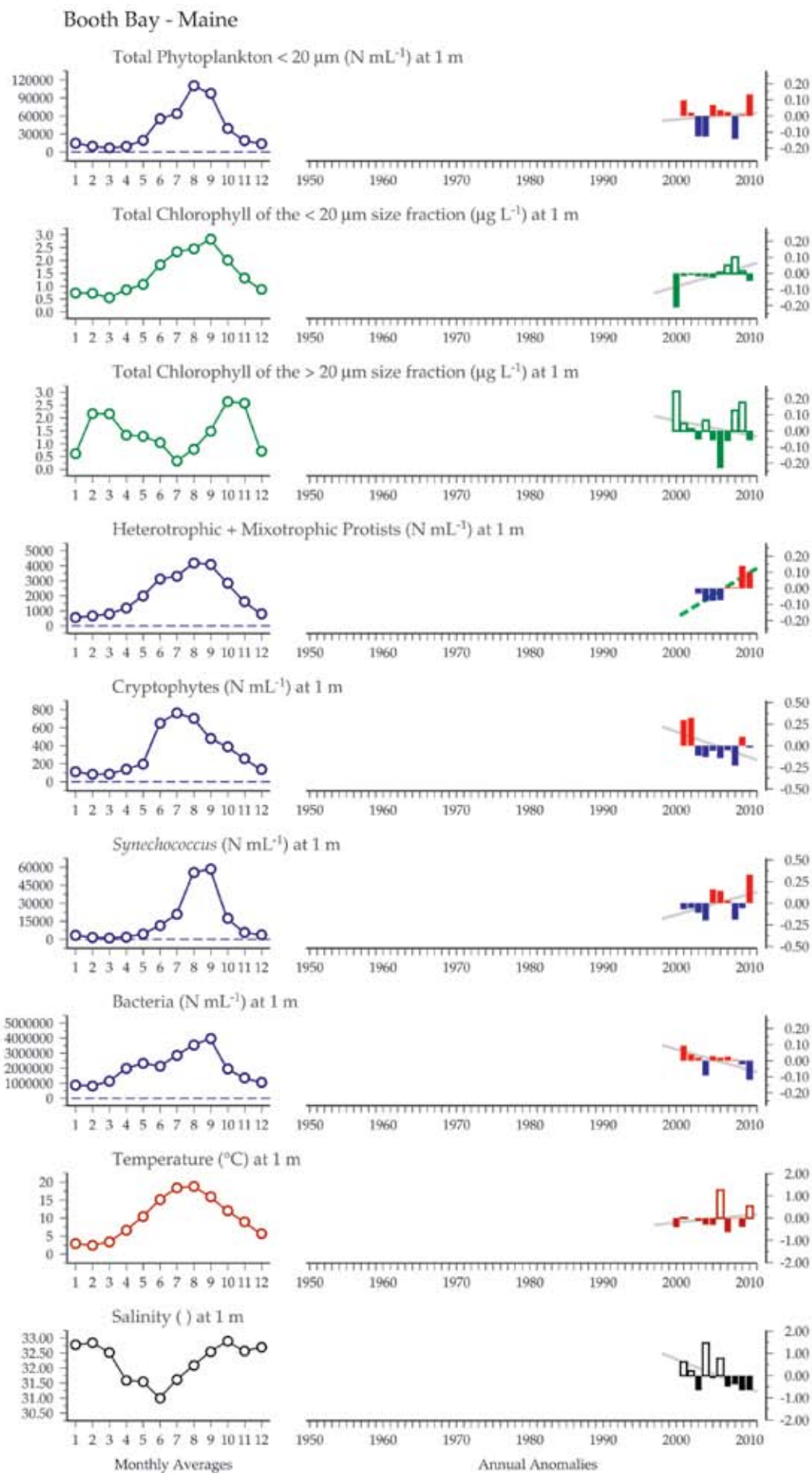
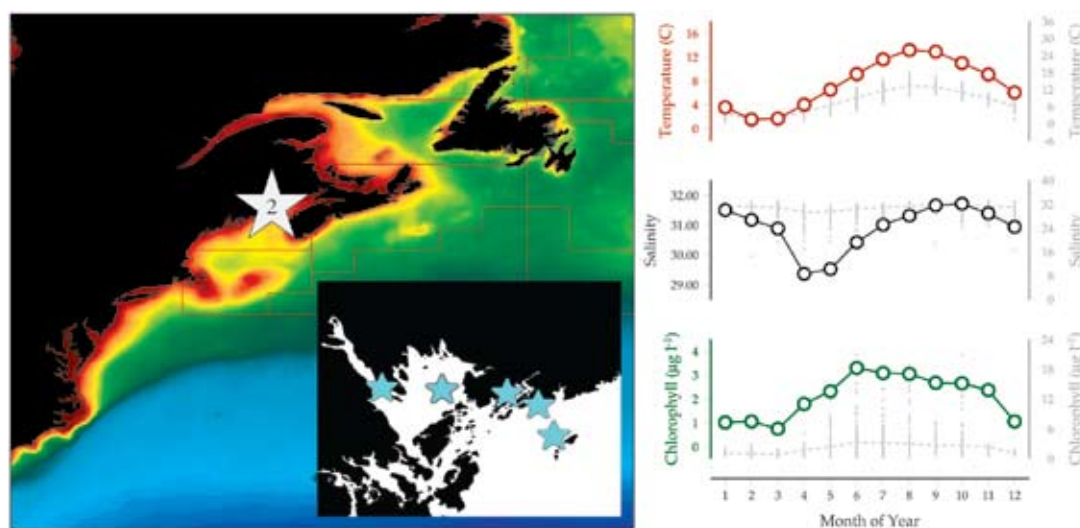


Figure 3.1.2
Multiple-variable comparison plot (see Section 2.2.2) showing the seasonal and interannual properties of select cosampled variables at the Booth Bay, Maine plankton monitoring site. Additional variables from this site are available online at <http://wgpme.net/time-series>.

3.2 Bay of Fundy (Site 2)

Jennifer Martin and Murielle LeGresley

Figure 3.2.1
Location of the Bay of Fundy plankton monitoring area (Site 2), plotted on a map of average chlorophyll concentration, and its corresponding environmental summary plot (see Section 2.2.1). The map inset shows the location of the five individual monitoring sites within the Bay of Fundy.



Phytoplankton sampling has been ongoing since the late 1980s at four locations in the Bay of Fundy, southwest New Brunswick, and eastern Canada. The Brandy Cove site is a brackish site influenced by the Saint Croix River estuary, the Lime Kiln Bay site is located in the Letang estuary where a number of aquaculture sites are located, the Deadmans Harbour site is an open bay with offshore influence, and the Wolves Islands site is an offshore indicator site for phytoplankton blooms that are initiated offshore and can be advected inshore. An extra sampling site was added in mid-Passamaquoddy Bay in 1998 following observations of frequent brick-red patches of water caused by *Mesodinium rubrum*. For this review, data were pooled from the four longest running sites (excluding Passamaquoddy Bay) to create a single figure and result set. Figures and results from each of the individual sites are available online at <http://WGPME.net/time-series>.

Sampling was conducted aboard the research vessel CCGS "Pandalus III" until 2010, when the vessel was decommissioned, and now the CCGS "Viola M. Davidson" is the sampling platform. Weekly samples are collected from late April to the end of October. Sampling is conducted biweekly in the month of November and monthly during all other months. A Seabird Model 25 CTD profiler is used to collect vertical profiles of temperature, salinity, and fluorescence at each site. Phytoplankton and nutrient samples are collected at the surface by bucket from all five stations, and additional depths of 10, 25, and 50 m at the Wolves Islands station with a Niskin bottle. During summer, a 10 m vertical plankton haul is made with a 20 µm mesh net, 0.3 m in diameter. A subsample is preserved

with formalin:acetic acid (1:1 by volume) for further phytoplankton identification and scanning electron microscopy (SEM). Live phytoplankton samples are immediately iced for the return trip to the laboratory. Samples for nitrate+nitrite (referred to as nitrate), nitrite, ammonia, phosphate, and silicate are frozen immediately and later measured using a Technicon Autoanalyzer II as described by Strain and Clement (1996). Water samples (250 ml) are immediately preserved with 5 ml formalin:acetic acid. Later, 50 ml subsamples are settled in Zeiss counting chambers for 16 h. All phytoplankton greater than 5 µm are identified and enumerated (as cells l⁻¹) with the Utermöhl technique using a Nikon inverted microscope (Sournia, 1978). Species have been grouped by dinoflagellates, diatom, and "other", which include ciliates and smaller zooplankton. Samples and data are recorded according to date, location, and depth; as well, an independent identification number is assigned at the time of collection. Information is entered, maintained, and accessed in a database. Individual net haul results and individual depth profiles from the Seabird profiler are stored separately. Results from the earlier years of the monitoring programme have been published previously (Wildish *et al.*, 1988, 1990; Martin *et al.*, 1995, 1999, 2001, 2006).

Seasonal and interannual trends (Figure 3.2.2)

Temperature and salinity both have strong seasonal patterns. The highest temperatures are in August–September, whereas the lowest are in February–March. The lower salinities in April and May are influenced by the ice and snow melt and

subsequent river run-off. Although salinity appears to be decreasing slightly, the trend is inconclusive and not significant. Strong seasonal patterns are also apparent in the total phytoplankton community and the diatom and dinoflagellate components, with peak abundance in July for dinoflagellates and August for diatoms. Total numbers of diatoms, dinoflagellates, and "other" organisms have been increasing significantly ($p < 0.01$) since 1988. The ratio of diatoms:diatoms+dinoflagellates appears to be decreasing slightly, but the trend is not significant. In many years, the spring/early summer

dominance of diatoms reduces as dinoflagellate abundance increases. In general, the nutrient data show typical seasonal cycles for inshore temperate waters. Nitrate, phosphate, and silicate (not shown in this report) are highest in winter, are depleted by the spring bloom, and replenish by vertical mixing that accompanies the breakdown of stratification in late autumn. However, there are some features of these distributions that are specific to the Bay of Fundy, and there are differences between the different monitoring stations.

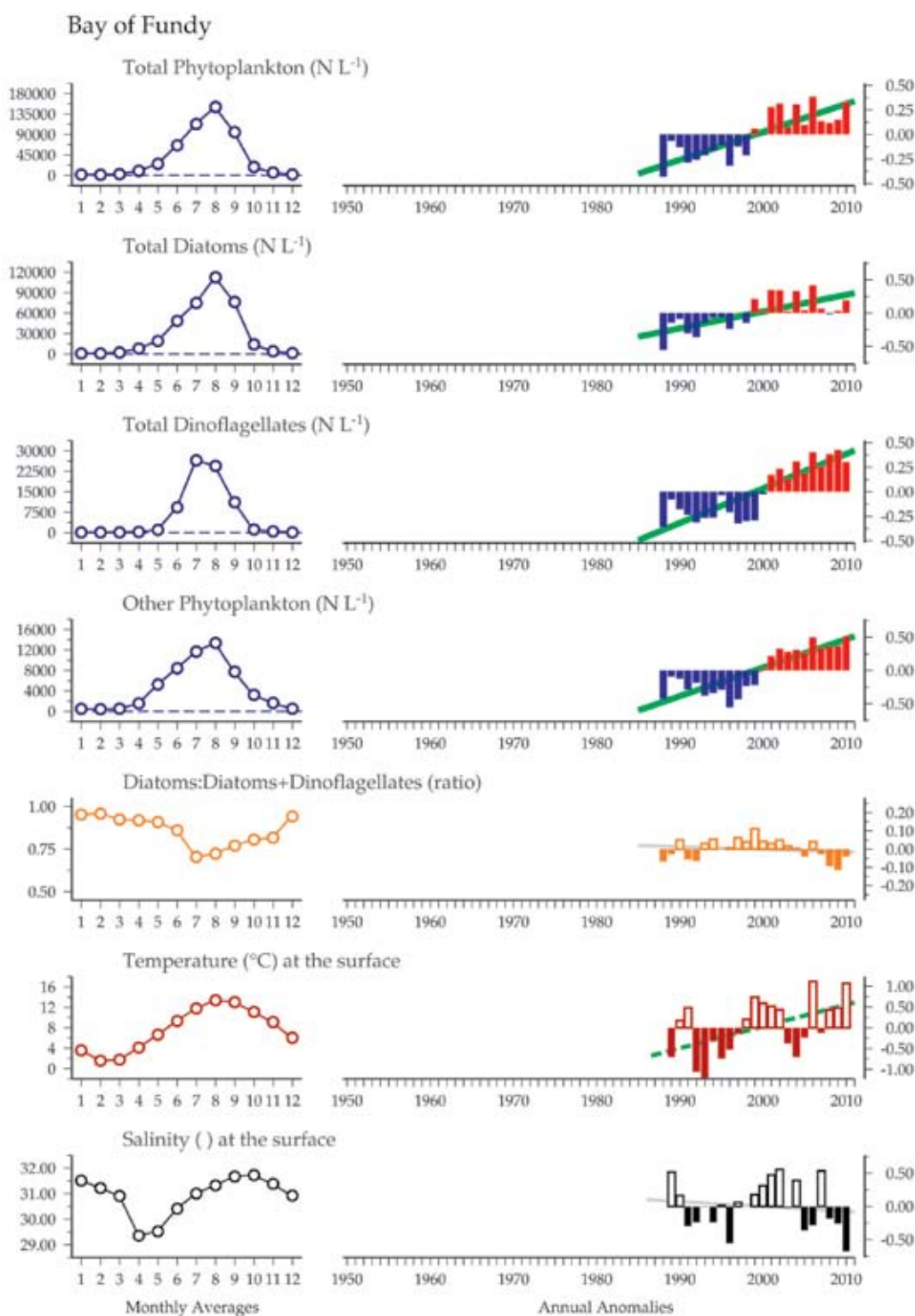
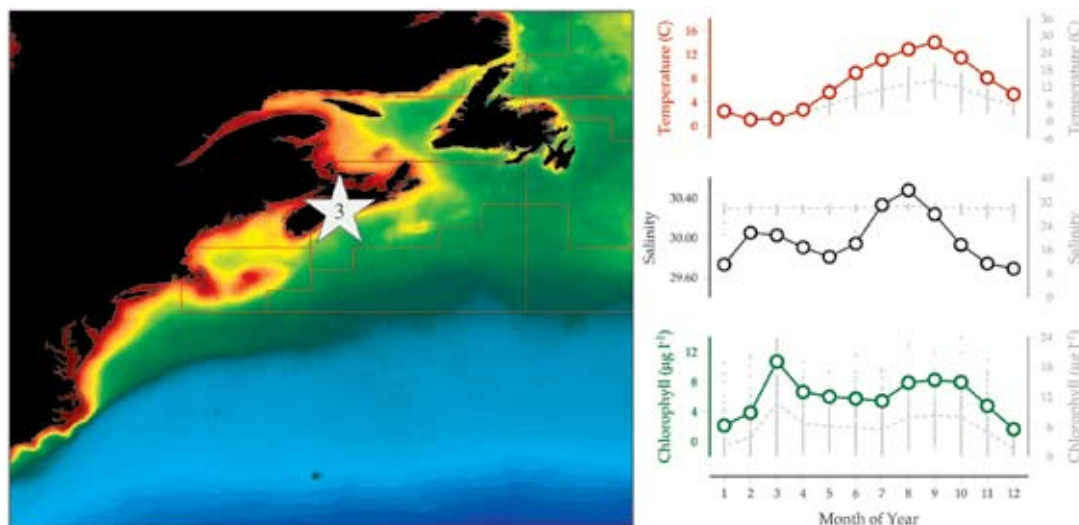


Figure 3.2.2
Multiple-variable comparison plot (see Section 2.2.2) showing the seasonal and interannual properties of select cosampled variables at the Bay of Fundy plankton monitoring site. Additional variables from this site are available online at <http://wgpmc.net/time-series>.

3.3 Bedford Basin (Site 3)

William K. W. Li

Figure 3.3.1
Location of the Bedford Basin plankton monitoring area (Site 3), plotted on a map of average chlorophyll concentration, and its corresponding environmental summary plot (see Section 2.2.1).



Bedford Basin is a small embayment forming the inner portion of Halifax Harbour, encircled by the largest urban population centre in eastern Canada. Bedford Basin is an estuary with a maximum depth of 71 m and a connection to the adjoining harbour through a narrow and shallow sill. The Basin receives freshwater from the Sackville River at an annual average inflow of $5 \text{ m}^3 \text{ s}^{-1}$. Additional run-off enters the Basin from a large watershed. The mean circulation is a two-layer structure where lower density surface water (salinity 29–31) flows outwards to the open Atlantic, and deeper saline water (salinity 31–32) flows into the Basin over the sill. The mean tidal range is 1.5 m, the ratio of tidal to freshwater volume is 109:1, and the flushing time is 261 h.

The Compass Buoy station (44°41'37"N 63°38'25"W) in Bedford Basin may be considered the inshore terminus of the Halifax Line of the Atlantic Zone Monitoring Programme (AZMP) conducted by Fisheries and Oceans Canada. Since 1992, weekly measurements have been made of selected properties by CTD profiling and Niskin sampling to characterize the physical, chemical, biological, and optical environments of the water column (Li and Dickie, 2001). Phytoplankton are characterized by chlorophyll *a* concentration measured by *in vitro* fluorescence, by cell abundance in size classes measured by flow cytometry, and by accessory pigment concentration measured by high-performance liquid chromatography. Bacterial abundance is measured by flow cytometry after cells have been stained with SYBR Green I, a

nucleic acid-binding fluorochrome. In this report, the values for samples collected at 1, 5, and 10 m are averaged to represent the state of surface waters in the Basin.

Seasonal and interannual trends (Figure 3.3.2)

Seasonal vertical stratification of the water column is determined primarily by temperature, but multiyear change in the seasonally adjusted annual average stratification is related to salinity, which is correlated *inter alia* with local precipitation and river discharge. At the multiyear time-scale, stratification anomalies explain significant amounts of variability in the anomalies of total phytoplankton biomass (chlorophyll *a*), especially that contributed by diatoms (fucoxanthin), but not the biomass of picophytoplankton (*Synechococcus* and picoeukaryotic algae). Instead, the multiyear response of these small phytoplankton appears directly related to variations in temperature (Li and Harrison, 2008).

On a four-decade time-scale (1970s–2000s), sea surface temperature, nitrate, ammonium, phosphate, chlorophyll *a*, and particulate organic matter have all increased (Figure 3.3.2; Li *et al.*, 2010). On a shorter two-decade time-scale, over which flow cytometry measurements are available, the picophytoplankton have also increased.

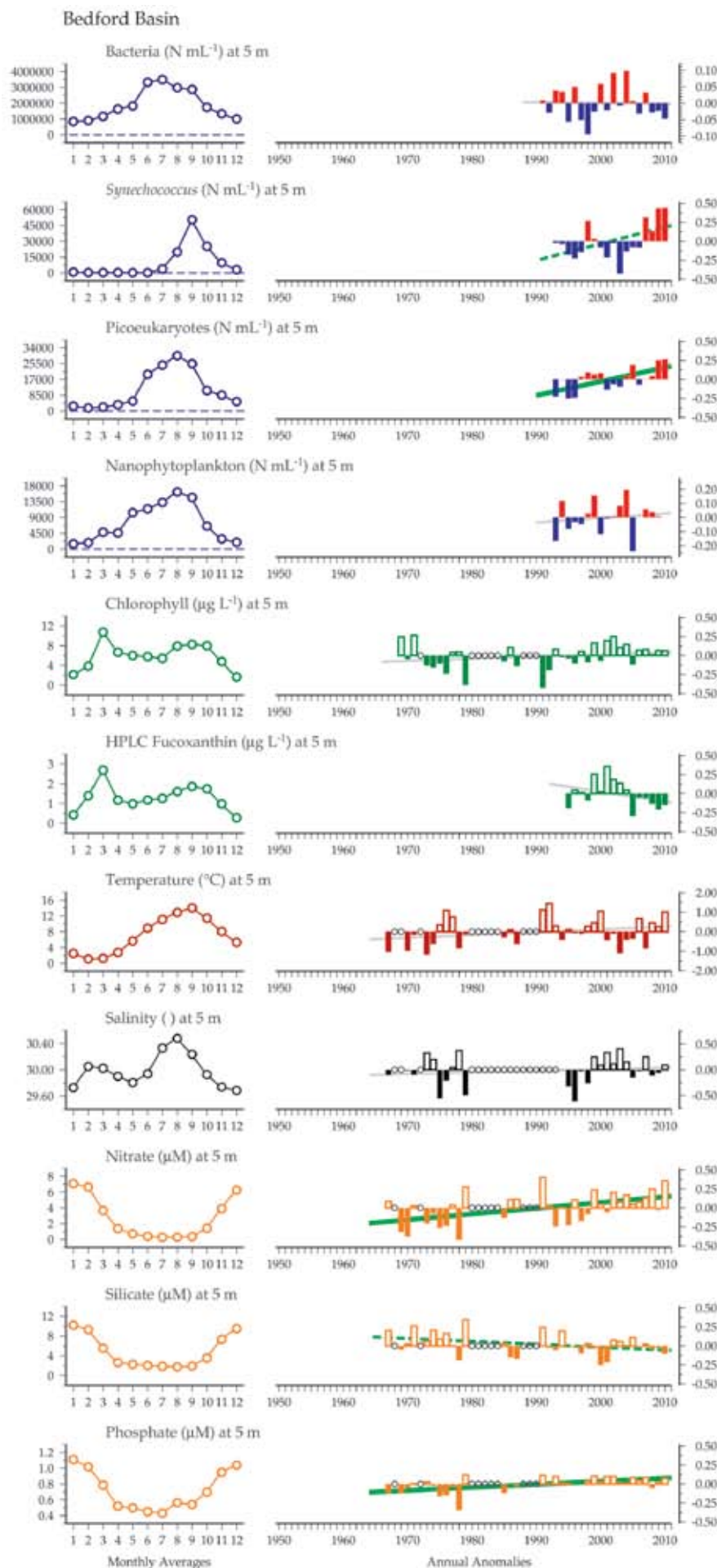
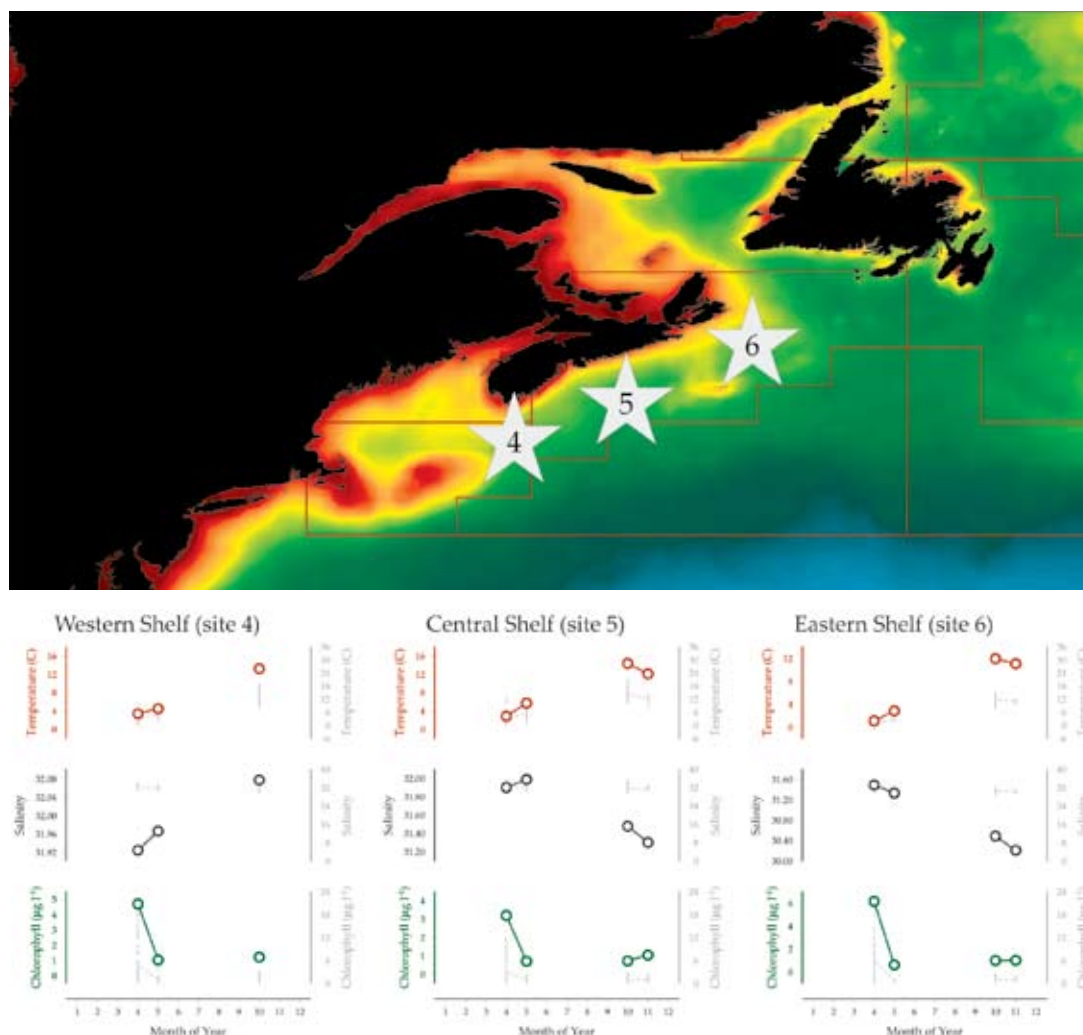


Figure 3.3.2
Multiple-variable comparison plot (see Section 2.2.2) showing the seasonal and interannual properties of select cosampled variables at the Bedford Basin plankton monitoring site. Additional variables from this site are available online at <http://wgpmc.net/time-series>.

3.4 Scotian Shelf (Sites 4–6)

William K. W. Li

Figure 3.4.1
Location of the Scotian Shelf plankton monitoring areas (Sites 4–6), plotted on a map of average chlorophyll concentration, and their corresponding environmental summary plots (see Section 2.2.1).



The Atlantic Zone Monitoring Programme (AZMP) is a multifaceted, multiplatform oceanographic observation programme in the Northwest Atlantic Shelf conducted by Fisheries and Oceans Canada, with the aim of increasing capacity to understand, describe, and forecast the state of the ocean environment and marine ecosystem (Therriault *et al.*, 1998). The main objectives of AZMP are twofold: (1) to collect and analyse biological, chemical, and physical data to characterize and understand the causes of oceanic variability at the seasonal, interannual, and decadal scales; and (2) to provide the multidisciplinary datasets that can be used to establish relationships among the biological, chemical, and physical variability. Regular reports of the optical, chemical, and biological oceanographic conditions on the Scotian Shelf are made to the Canadian Science Advisory Secretariat (Harrison *et al.*, 2009).

Three different oceanographic regimes of the Scotian Shelf are sampled: (1) at the western end of the shelf, where tidal mixing fundamentally alters water-mass structure (Browns Bank Line BBL); (2) at the central shelf, where slope water plays a greater, if not dominant, role (Halifax Line HL); and (3) at the eastern end of the shelf (Louisbourg Line LL), where St Lawrence water dominates, but slope water is exerting a significant influence. Methods and protocols for sampling and analyses are documented in Mitchell *et al.* (2002). In this report, regional averages are computed across seven primary stations that lie across the shelf along these three lines, namely BBL1 to BBL7, HL1 to HL7, and LL1 to LL7. Phytoplankton are characterized by chlorophyll *a* concentration measured by *in vitro* fluorescence, and by cell abundance in size classes measured by flow cytometry. Bacterial abundance is measured by flow cytometry after cells have been

stained with SYBR Green I, a nucleic acid-binding fluorochrome. The values for samples collected in the upper 100 m are averaged to represent the state of upper ocean waters.

Seasonal and interannual trends (Figure 3.4.2)

Across the entire Scotian Shelf, there is strong seasonality in climatic factors and in phytoplankton development. Most notably, the average abundance of picophytoplankton (represented by *Synechococcus* and picoeukaryotes) is approximately 2 orders of magnitude higher in autumn, when it is warm, than in spring, when it is cold. Generally, it appears that there has been an increase in picophytoplankton abundance and a decrease in nanophytoplankton abundance over the years of observation.

In searching for broader patterns, an assessment is made of multiyear change in nutrients, phytoplankton, and zooplankton on the Scotian Shelf by examination of normalized, seasonally adjusted, annual anomalies of aggregate indices. These indices are based on near-surface and deep nitrate inventories, on chlorophyll inventories, the magnitude, timing, and duration of the spring chlorophyll bloom, and on the abundance of zooplankton *Calanus finmarchicus*, *Pseudocalanus* spp., total copepods, and total non-copepods. To date, covariance has been weak among the aggregate indices over the years, even when large swings in anomalies have been observed (Harrison *et al.*, 2009). Thus, at the annual time-scale, mechanistic linkages from the physical-chemical environment of temperature, salinity, stratification, and nutrients to the biological communities of phytoplankton and zooplankton are obscured by complexity and indeterminacy of ecosystem trajectories.

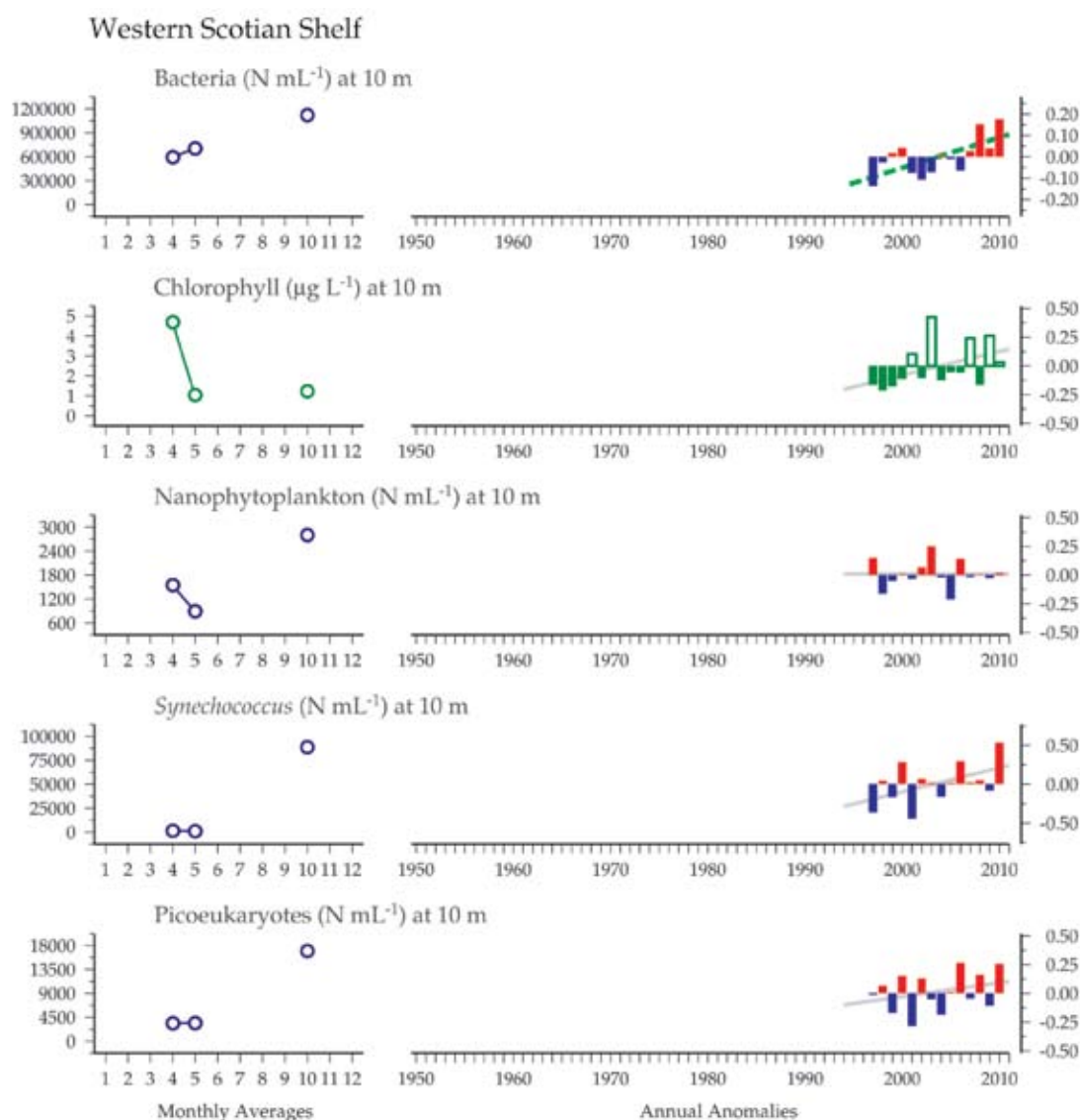
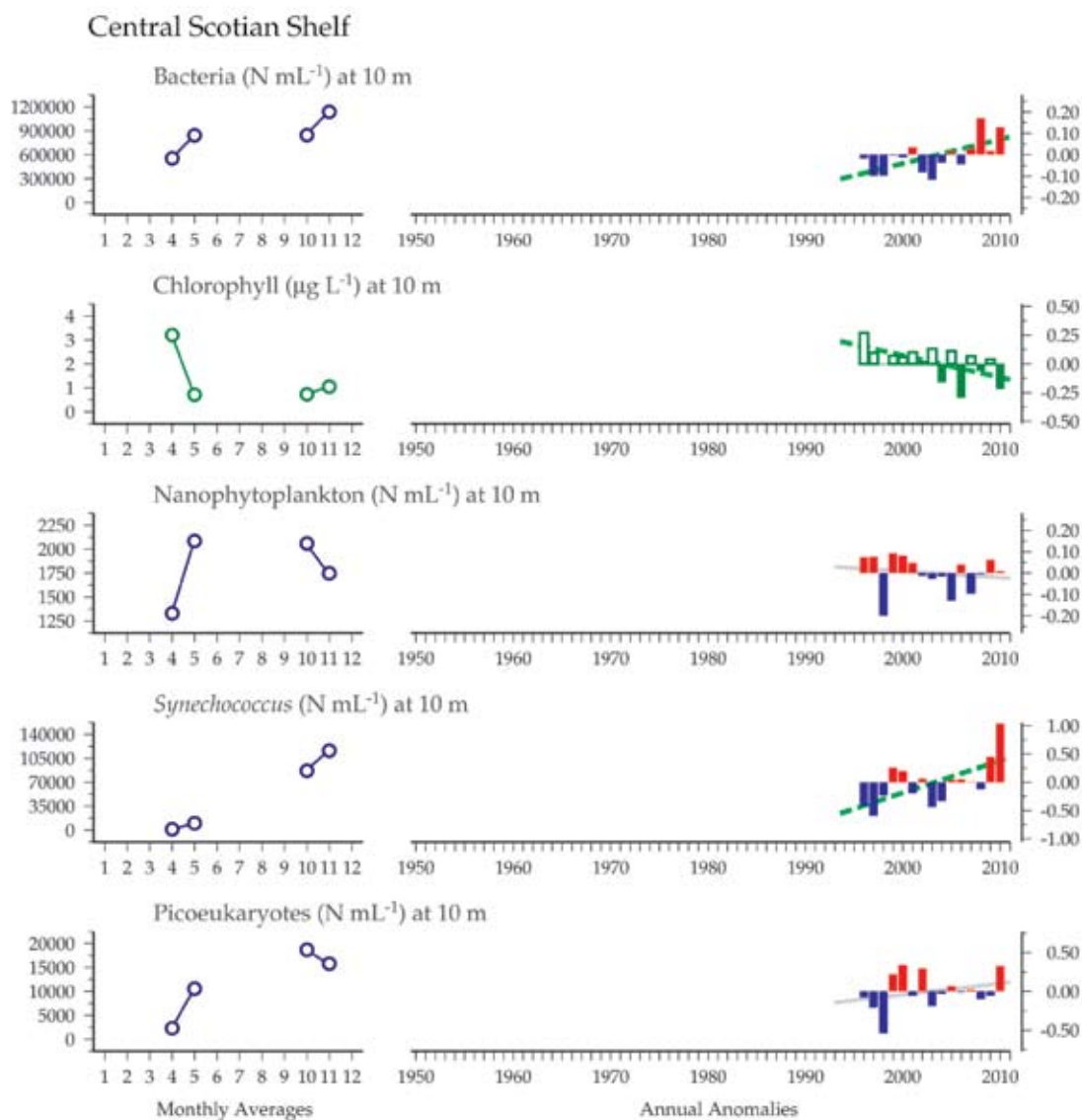


Figure 3.4.2
Multiple-variable comparison plot (see Section 2.2.2) showing the seasonal and interannual properties of select cosampled variables at the Western Scotian Shelf plankton monitoring site. Additional variables from this site are available online at <http://hogpme.net/time-series>.

Figure 3.4.3

Multiple-variable comparison plot (see Section 2.2.2) showing the seasonal and interannual properties of select cosampled variables at the Central Scotian Shelf plankton monitoring site. Additional variables from this site are available online at <http://wgpme.net/time-series>.



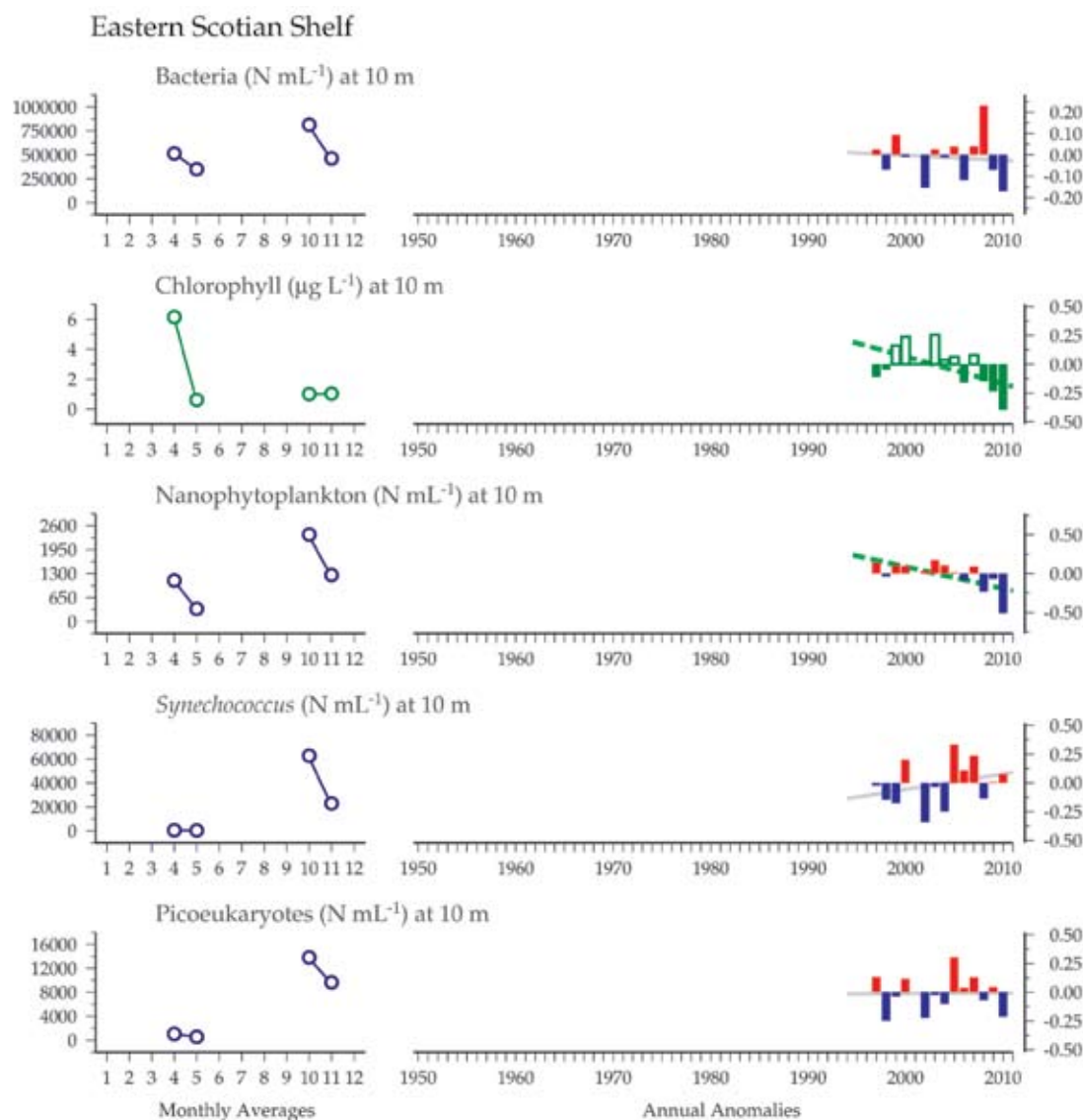


Figure 3.4.4
Multiple-variable comparison plot (see Section 2.2.2) showing the seasonal and interannual properties of select cosampled variables at the Eastern Scotian Shelf plankton monitoring site. Additional variables from this site are available online at <http://wgpme.net/time-series>.

4. PHYTOPLANKTON AND MICROBIAL PLANKTON OF THE LABRADOR SEA

William K. W. Li

The Labrador Sea is located between Greenland and the Labrador coast of eastern Canada. The physical oceanography of this area is described in reports of the Working Group on Oceanic Hydrography (WGOH; Hughes *et al.*, 2011). The broad Labrador Shelf and the narrow Greenland Shelf are both influenced by cold, low-salinity waters of Arctic origin: from the north on the Labrador Shelf via the inshore branch of the Labrador Current, and from the south on the Greenland Shelf, via the West Greenland Current, which is formed as the East Greenland Current turns around the tip of Greenland. Warm, saline Atlantic waters flow north into the Labrador Sea on the Greenland side and become colder and fresher as they circulate. There are strong boundary currents beyond the shelf break, which include inputs of Arctic water from the north along the Labrador slope in the offshore branch of the Labrador Current, and of Atlantic water from the south into the eastern region of the Labrador Sea in the Irminger Current. The central basin exceeds 3500 m at its deepest point and is composed of a mixture of waters of Atlantic and Arctic origin.

The Labrador Sea is one of the few areas in the global ocean where intermediate-depth water masses are formed through convective sinking of dense surface waters. This convection transports

cold, dense water to the lower limb of the ocean's Meridional Overturning Circulation. The depth of convection varies from year to year and is strongly influenced by atmospheric forcing, as manifested by the North Atlantic Oscillation (NAO) index. In years when the NAO index is high, there are strong winds from the northwest in late winter, leading to low air temperatures, convection to depths of 1000 m or more, and reduced water temperatures. Conversely, in years when the NAO is low, the winds are not as strong, and air and water temperatures are also warmer.

Changes in Labrador Sea hydrographic conditions on interannual time-scales depend on the variable influences of heat loss to the atmosphere, heat and salt gain from Atlantic waters, and freshwater gain from Arctic outflow, melting sea ice, precipitation, and run-off. Conditions have generally been milder since the mid-1990s. The upper layers of the Labrador Sea have become warmer and more saline as heat losses to the atmosphere have decreased and Atlantic waters have become increasingly dominant (Hughes *et al.*, 2011). The Labrador Sea has a major influence on oceanographic and ecosystem conditions on the Atlantic Canadian continental shelf system, for which it is an upstream source.

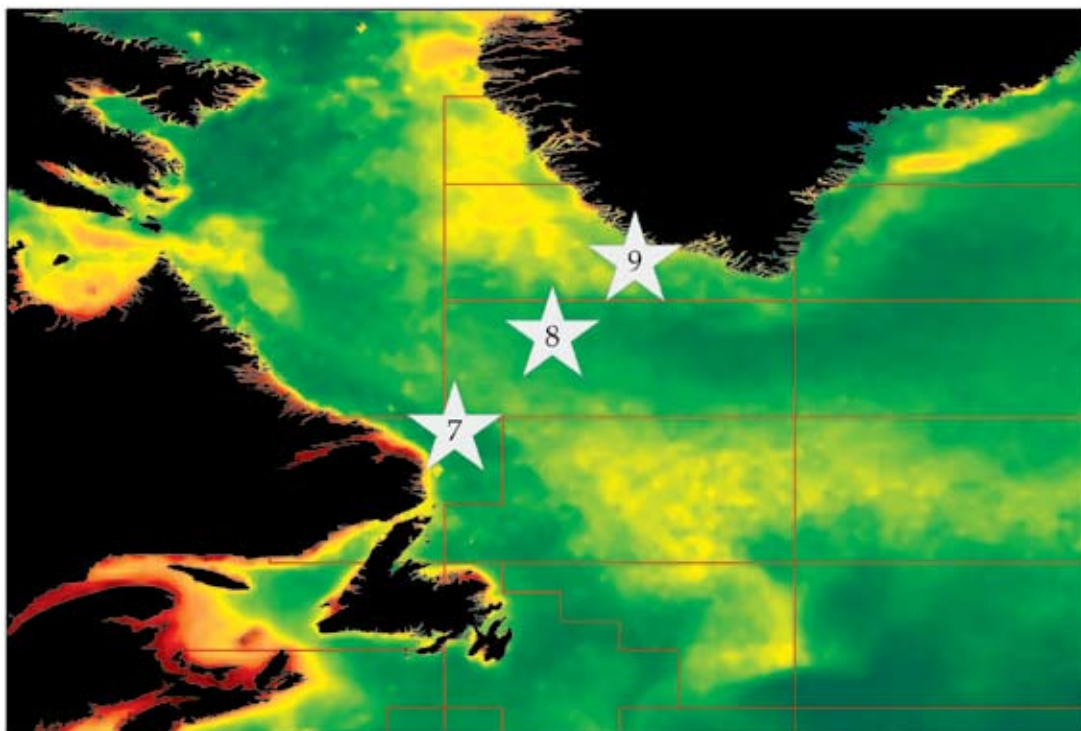


Figure 4.1
Locations of the Labrador Sea plankton monitoring areas (Sites 7–9) plotted on a map of average chlorophyll concentration.

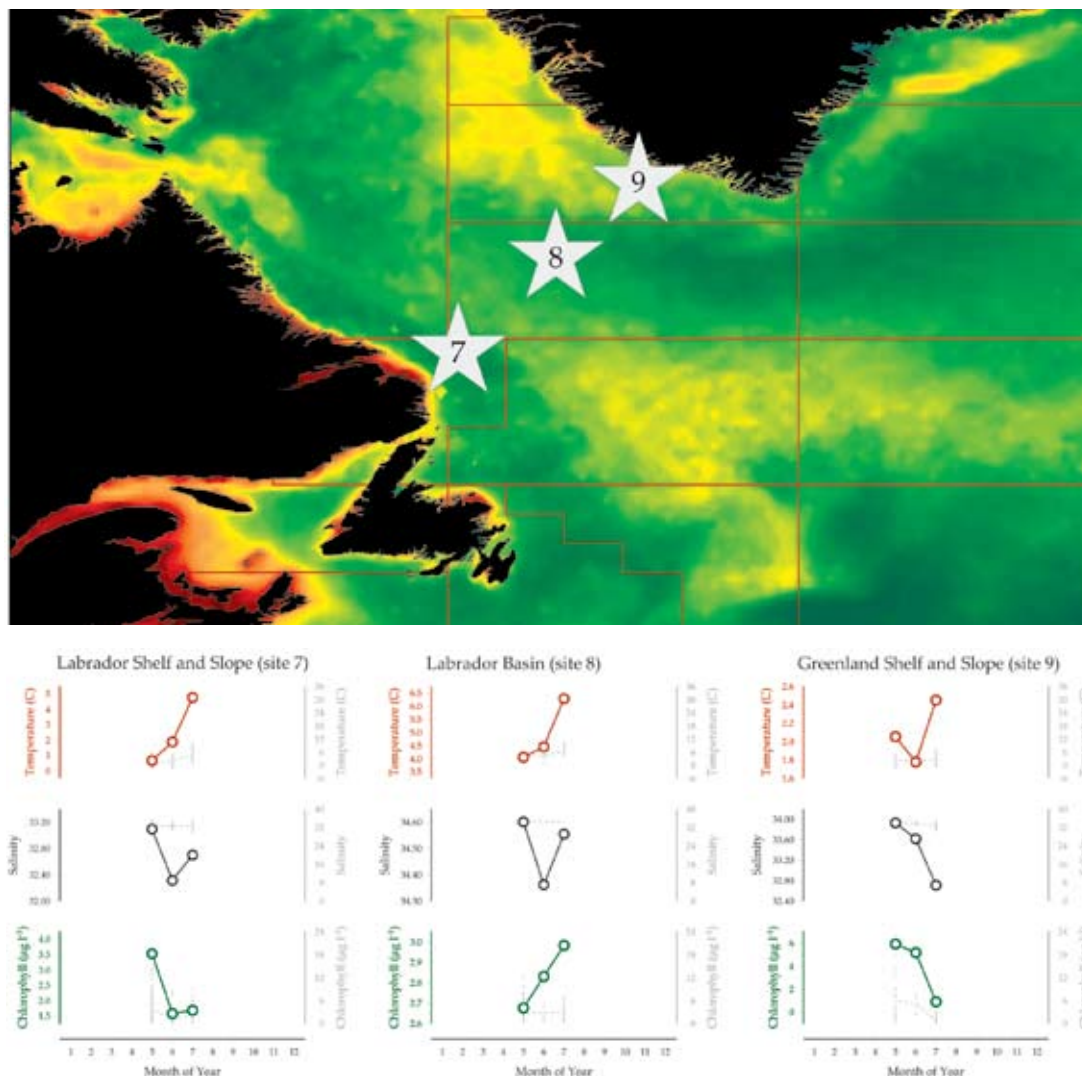
The ecology of phytoplankton in the Labrador Sea has been described elsewhere (Harrison and Li, 2007; Harrison *et al.*, 2012). Mixing of near-surface waters and stratification have an influence on both the light environment and nutrient availability for phytoplankton growth. Convective mixing occurs in winter, well before seasonal light conditions favour phytoplankton growth in spring. However, the extent of vertical mixing determines nutrient reserves available for growth, thus setting a limit on the magnitude and duration of the spring bloom. As incident radiation increases in spring, both ice melt and/or surface water warming establish a stratified mixed layer that provides the light conditions needed to initiate the spring bloom. Here, ice retreat precedes surface water warming and, therefore, density stratification may result in spring blooms that precede those in waters where thermal stratification dominates the mixing dynamics.

The phytoplankton are a mixture of the major taxonomic groups common to boreal and temperate waters. The major bloom-formers are the prymnesiophyte *Phaeocystis* and the diatoms dominated by centric forms such as *Chaetoceros* and *Thalassiosira*, along with pennate forms such as *Fragilariopsis*, *Navicula*, and *Pseudonitzschia*. Dinoflagellates such as *Ceratium* and the heterotrophic genus *Protoperidinium*, as well as chrysophyte flagellates are more common under post-spring bloom conditions. Although microphytoplankton account for a large proportion of photosynthetic biomass, it is the picophytoplankton and nanophytoplankton which constitute the numerical dominants of the photosynthetic community. The picocyanobacterium *Synechococcus* seems to have a strong affinity with Atlantic-source water. The numerical dominant in the entire region appears to be the picoeukaryotic prasinophyte *Micromonas*, which is thought to form the baseline community that persists throughout all seasons.

4.1 Labrador Sea monitoring (Sites 7–9)

William K. W. Li

Figure 4.1.1
Locations of the Labrador Sea plankton monitoring areas (Sites 7–9), plotted on a map of average chlorophyll concentration, and their corresponding environmental summary plots (see Section 2.2.1).



The Labrador Sea Monitoring Programme is an oceanographic observation programme conducted by Fisheries and Oceans Canada, primarily in spring or early summer on the Atlantic Repeat Hydrography Line 7 West (AR7W) designated in the 1990–2002 World Ocean Circulation Experiment (WOCE). AR7W extends from Hamilton Bank on the Labrador Shelf, continues across the central Labrador Basin, and ends at Cape Desolation on the Greenland Shelf. Systematic measurements of physical (temperature, salinity), chemical (nutrients), and biological (bacteria, phytoplankton, zooplankton) properties have been made at least once every year since 1994 on 28 nominal stations along the AR7W transect. In some years, the Labrador Shelf is still covered with pack ice in late May, which prevents sampling at some or all of the stations there. Farther

east, the section is ice-free, except for a few icebergs on or near the Greenland Shelf, which can also interfere with sampling at some stations. Annual reporting of observations is made to the Canadian Science Advisory Secretariat in the context of the Atlantic Zone Off-Shelf Monitoring Programme (Greenan *et al.*, 2010).

From the standpoint of phytoplankton, light conditions and nutrient availability that determine seasonal growth cycles and community structure are strongly influenced by the regional characteristics of circulation (mixing and transport) imposed by the complex of water masses making up the Labrador Sea system. As well, seasonal sea ice dynamics of the Labrador and Greenland continental shelves have a major effect on light conditions and water-

column stability, the latter affecting nutrient supply to the upper mixed layer, which influences phytoplankton growth (Harrison and Li, 2007).

In this report, regional averages are computed within three defined areas that differ in water-mass characteristics. These are the Labrador Shelf/Slope (Site 7, based on AR7W stations L3-01 to L3-10), the Labrador Basin (Site 8, based on AR7W stations L3-11 to L3-23), and the Greenland Shelf/Slope (Site 9, based on AR7W stations L3-24 to L3-28). Phytoplankton are characterized by chlorophyll *a* concentration measured by *in vitro* fluorescence, and by cell abundance in size classes measured by flow cytometry. Bacterial abundance is measured by flow cytometry after cells have been stained with SYBR Green I, a nucleic acid-binding fluorochrome. The average value for samples collected in the upper 100 m represents the state of upper ocean waters.

Seasonal and interannual trends (Figures 4.1.2 – 4.1.4)

Over the length of the observation period since 1994, SST has increased in all regions of the Labrador Sea. However, the direction of microbial change, if any, seems to be region-specific. Thus, in the Greenland Shelf/Slope region at the eastern end of AR7W, a weak increase seems to be occurring in chlorophyll, picophytoplankton, nanophytoplankton, and bacteria. Conversely, in the Labrador Shelf/Slope region at the western end of AR7W, the direction of multiyear change in microbes appears (weakly) to be in the opposite (negative) sense. As a pivot between increases in the east and decreases in the west, the microbial populations in the central Labrador Basin region show no directional multiyear change. In other words, it seems that any change, or lack thereof, is coherent between the phytoplankton and bacteria (Li *et al.*, 2006).

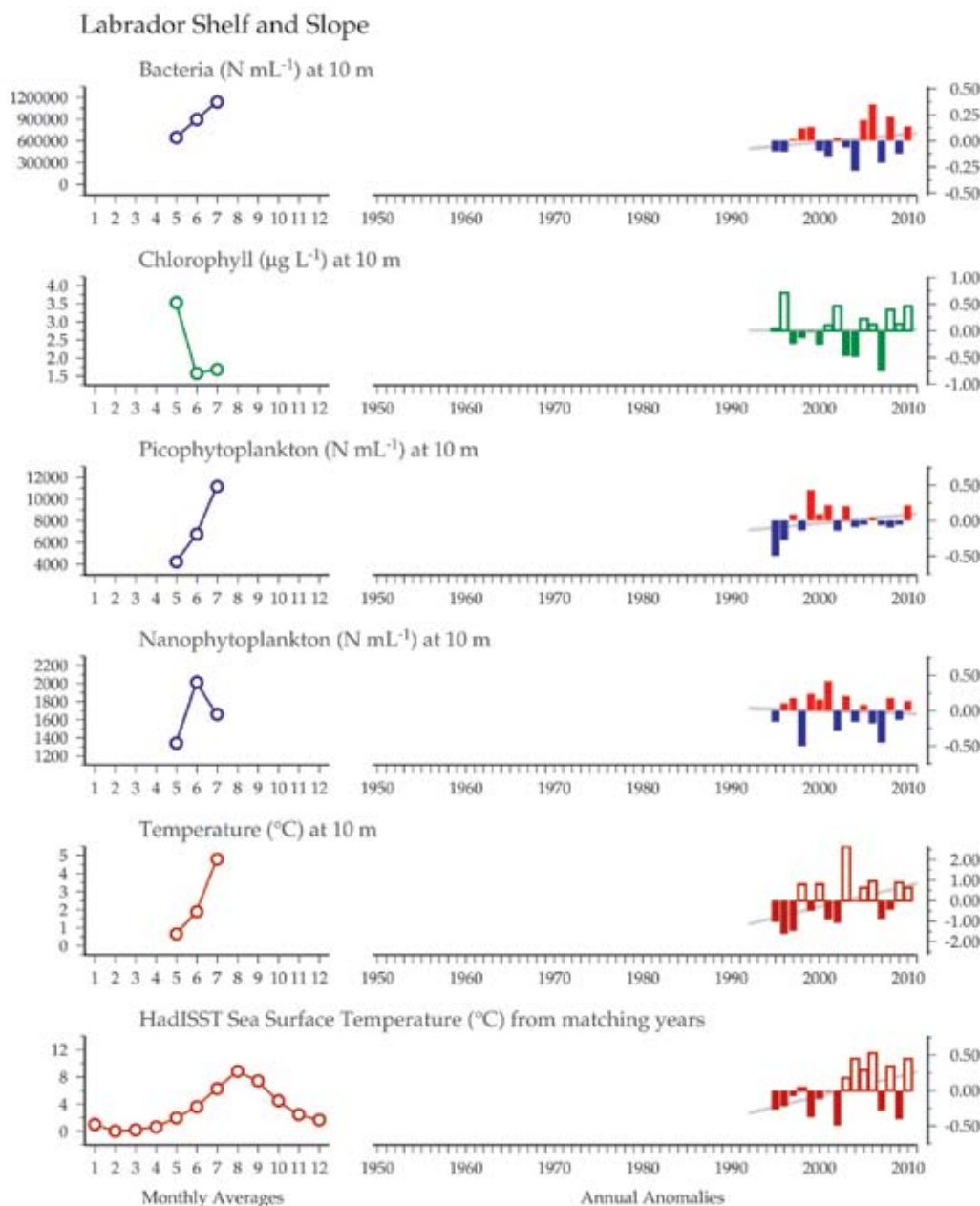
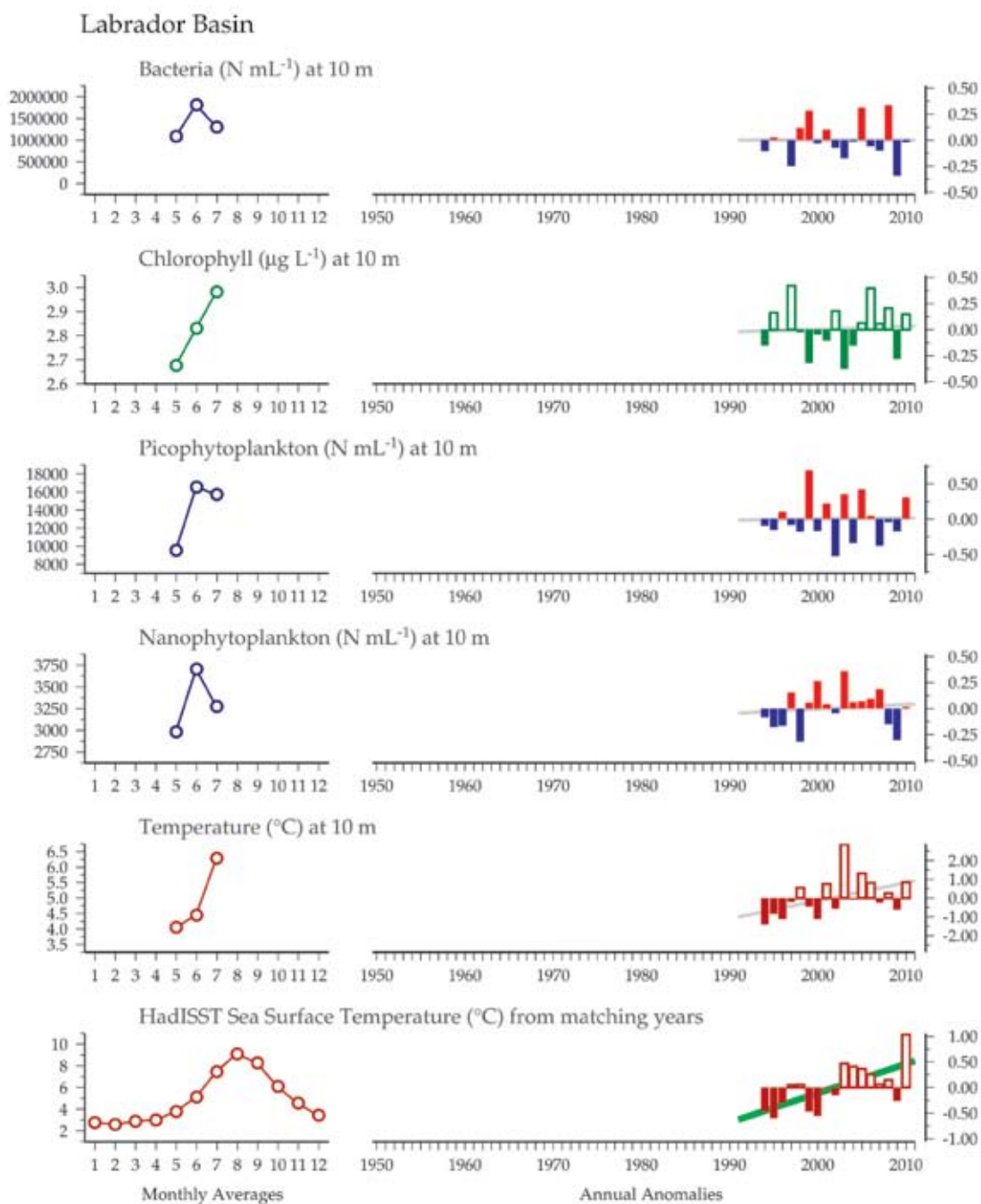


Figure 4.1.2
Multiple-variable comparison plot (see Section 2.2.2) showing the seasonal and interannual properties of select cosampled variables at the Labrador Shelf and Slope plankton monitoring site. Additional variables from this site are available online at <http://wgpmc.net/time-series>.

Figure 4.1.3

Multiple-variable comparison plot (see Section 2.2.2) showing the seasonal and interannual properties of select cosampled variables at the Labrador Basin plankton monitoring site. Additional variables from this site are available online at <http://wgpme.net/time-series>.



Greenland Shelf and Slope

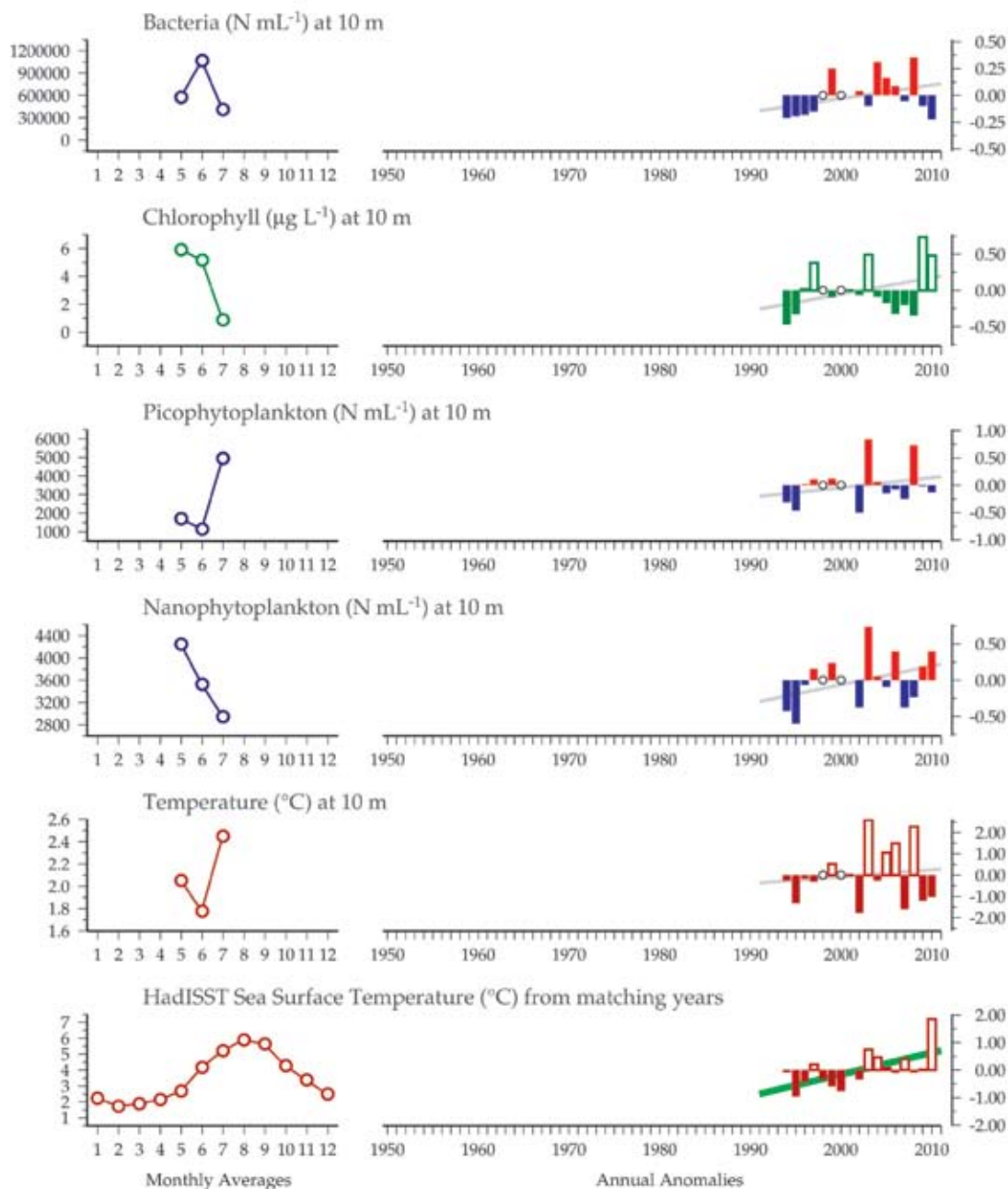


Figure 4.1.4
Multiple-variable comparison plot (see Section 2.2.2) showing the seasonal and interannual properties of select cosampled variables at the Greenland Shelf and Slope plankton monitoring site. Additional variables from this site are available online at <http://wgpmc.net/time-series>.

5. PHYTOPLANKTON AND MICROBIAL PLANKTON OF THE BALTIC SEA

Norbert Wasmund, Sirpa Lehtinen, Anetta Ameryk, Günther Nausch, and Marie Johansen

The Baltic Sea is a classic example of a shallow intracontinental shelf sea, with a mean depth of 52 m. It is connected to the North Sea only by the shallow and narrow Danish Straits, which limit water exchange between these regions. The Kattegat, Sound (Øresund), and Belt Sea (Great Belt, Little Belt, Kiel Bight, and Mecklenburg Bight) represent the transitional area between the North Sea and the Baltic Proper. The Baltic Proper stretches from Darss Sill to the entrances to the gulfs of Riga, Finland, and Bothnia, and comprises different basins that are stratified by a permanent halocline (at depth of 60–80 m in the deepest basins) and a summer thermocline (at 10–30 m depth). Owing to a limited exchange with the North Sea, the Baltic Sea is a brackish sea with not only a vertical, but also a horizontal, salinity gradient. The salinity of surface water decreases to the east and north. A detailed survey of the state and evolution of the Baltic Sea is given by Feistel *et al.* (2008).

Large rivers import nutrients from the densely populated and intensively cultivated catchment area (Bergström and Carlsson, 1994), resulting in an increase in phytoplankton biomass, primary production, and turbidity in the euphotic zone and oxygen deficit in deep-water layers (Elmgren and Larsson, 2001; Rönnerberg and Bonsdorff, 2004). The riparian countries recognized the increasing environmental problems and agreed to establish the Baltic Marine Environment Protection Commission

(Helsinki Commission, HELCOM) in 1974. One of its aims was to investigate long-term trends in trophic conditions by the Baltic Monitoring Programme (BMP, later the COMBINE programme), which has been conducted since 1979 according to a coordinated sampling schedule and binding methodology. The data collected by the riparian countries in the frame of the HELCOM monitoring are stored in the ICES databank and form the basis for this analysis.

Already in previous periods, the data have been analysed for trends by the HELCOM community, for example in periodic assessments (e.g. HELCOM, 2002) or in thematic assessments (e.g. on climate change or eutrophication; see HELCOM, 2007, 2009). Specific papers on trends in phytoplankton had to take into account differences between the subareas of the Baltic Sea. In fact, trends in the different regions may even be opposite. For example, trends in chlorophyll *a* concentrations were found to decrease in Mecklenburg Bight, but increase in the Baltic Proper in spring from 1979 to 2005 (Wasmund and Siegel, 2008). Wasmund *et al.* (1998) discovered a strong decrease in diatom biomass in spring blooms in the southern Baltic Proper, but not in Mecklenburg Bight. This sudden diatom decrease at the end of the 1980s was later identified as a regime shift by Alheit *et al.* (2005). The decrease in spring diatoms is compensated by an increase in dinoflagellates (Wasmund and Uhlig, 2003).

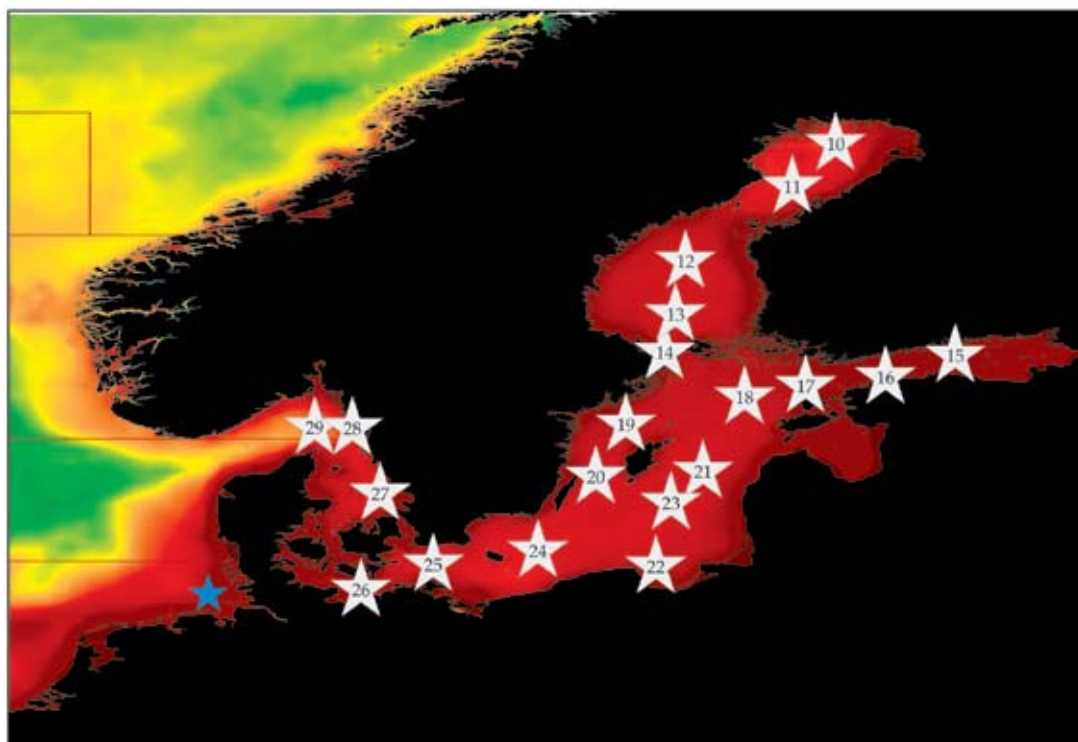


Figure 5.1
Locations of the Baltic Sea plankton monitoring areas (Sites 10–29) plotted on a map of average chlorophyll concentration. Blue stars indicate locations of sites described in the adjacent North Sea and English Channel region (see Section 6).

The diatoms and dinoflagellates demonstrated alternating oscillations: strong spring blooms of diatoms occurred in the 1980s and since 2000, but those of dinoflagellates in the 1990s (Wasmund *et al.*, 2011).

Suikkanen *et al.* (2007) analysed especially the summer phytoplankton communities in the northern Baltic Proper and the Gulf of Finland. They found increasing chrysophyte and chlorophyte biomass in both areas, increasing dinoflagellates in the northern Baltic Proper, and increasing cyanobacteria in the Gulf of Finland, together with an increase in chlorophyll concentrations, temperature, and winter DIN (dissolved inorganic nitrogen) concentrations.

A complex trend analyses with monitoring data of the whole Baltic Sea was performed by Klais *et al.* (2011). They found high variability in the spring bloom biomass, with peaks in the Gulf of Finland, Gulf of Riga, Pomeranian Bight, and the Danish coast of the Kattegat. Dinoflagellates dominate in the northern Baltic Proper, but diatoms in coastal areas and in the western Baltic. In the relatively short period considered (1995–2004), dinoflagellates decreased primarily in the Bornholm Sea and the Gulf of Riga, but increased in the Gulf of Finland and Bothnian Bay.

The analysis presented here generally agrees with these previous analyses. Its data basis is, however, more complete than in the older papers, because it involves all data available from the specific sea areas and is not restricted to selected shorter periods (as in Klais *et al.*, 2011) or selected seasons (as in Suikkanen *et al.*, 2007). In contrast to the earlier study of Suikkanen *et al.* (2007), for example, cyanophytes and chlorophytes did not increase in the Gulf of Finland or in the northern Baltic Proper in the analysis in this report.

Since the start of the monitoring programme in 1979, the biomass in many phytoplankton groups has increased. Changes in many smaller groups are statistically significant, but the ecological importance of these groups is rather low owing to their small biomass. From the ecologically important groups, the dinoflagellates are increasing, whereas the diatoms are decreasing, especially if spring data are considered, and the diatoms:diatoms+dinoflagellate ratio during the spring bloom period is also decreasing. The sudden decrease at the end of the 1980s, known from the literature, is clearly visible, primarily in the Bornholm Sea and the Eastern Gotland Basin. The diatoms:diatoms+dinoflagellates ratio may be an important indicator of changes in the ecosystem, which may have high relevance for the food chain.

The autotrophic ciliate *Mesodinium rubrum* establishes itself as a third ecologically important group. It is strongly increasing in all seasons, especially in the 1990s, but part of this shift may be an artefact because some contributors may have included this ciliate in the phytoplankton only after the early 1990s. However, the sudden increase of the prymnesiophyte *Chrysochromulina polylepis* since the end of 2007 is well documented. The only major group that is decreasing is cyanobacteria. Only the summer period, when they form blooms, is relevant to this consideration. The decrease in cyanobacteria is especially prominent in July and/or August in the Arkona Sea and Bornholm Sea.

A general increase in temperature was detected in all sea areas, but was not significant in the Eastern Gotland Basin. The concentrations of dissolved inorganic nitrogen ($\text{DIN} = \text{NO}_2 + \text{NO}_3 + \text{NH}_4$) are decreasing in the long-term dataseries in all open sea areas. This is interesting because nitrogen is considered to be the limiting nutrient in the Baltic Proper, but its decrease has no clear effect on the phytoplankton biomass. The lack of correlations between DIN and chlorophyll concentrations is surprising and needs to be investigated.

5.1 Northern Baltic Sea (Sites 10–21)

Sirpa Lehtinen

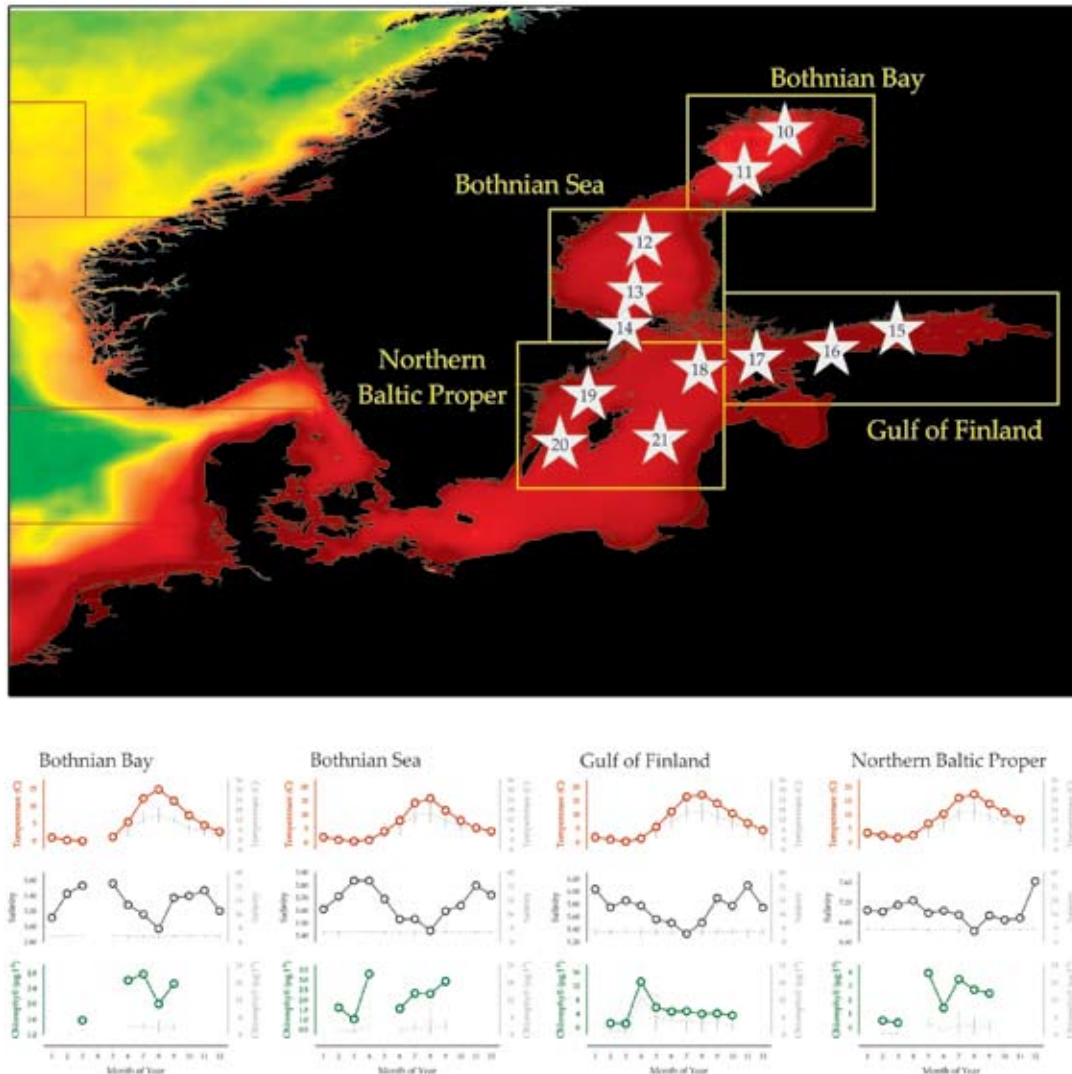


Figure 5.1.1

Location of Finnish Environmental Institute (SYKE) phytoplankton monitoring stations in the northern Baltic Sea (Sites 10–21), and their corresponding environmental summary plots (see Section 2.2.1). The yellow boxes and labels indicate the four subareas described in the report text.

The Northern Baltic Sea consists of four subareas: Bothnian Bay, Bothnian Sea, the Gulf of Finland, and the northern Baltic Proper (Figure 5.1.1). In the frame of the international COMBINE-monitoring programme of the Helsinki Commission (HELCOM), the Marine Research Centre of the Finnish Environment Institute (SYKE) samples phytoplankton yearly in August at twelve open-water stations (Sites 10–21) and in numerous coastal stations (not considered in this report). This sampling has been carried out since 1979, with the data available in the main ICES database. Sampling, processing, and analysis of the samples have been carried out according to the compulsory

manual and the HELCOM PEG (Phytoplankton Expert Group) taxa and biovolume list (Olenina *et al.*, 2006; HELCOM, 2010). For the purposes of this report, the twelve open-water stations have been combined into four geographical subareas: Bothnian Bay, Bothnian Sea, Gulf of Finland, and northern Baltic Proper. Additional time-series results for the individual sites, as well as additional SYKE coastal monitoring sites, are available online at <http://wgpme.net/time-series>.

5.1.1 Bothnian Bay (Sites 10–11)

The Bothnian Bay is the most northern part of the Baltic Sea, characterized by low salinity (ca. 2.9–3.5), the strong influence of river waters, and the long duration of ice cover (over 150 d). In addition, Bothnian Bay is the only predominantly phosphorus-limited Baltic Sea subregion, most notably during summer (Tamminen and Andersen, 2007). The maximum bottom depth is 148 m, with a mean depth of 40 m. The open-water sampling stations in the Bothnian Bay are F2 (Site 10, 65°23'N 23°27'E) and BO3 (Site 11, 64°18'N 22°21'E).

Seasonal and interannual trends (Figure 5.1.2)

Diatoms, especially *Chaetoceros wighamii*, dominate during the spring bloom, but dinoflagellates, like *Peridiniella catenata*, are also important. During summer, cryptophytes and chlorophytes are numerous. In autumn, there is usually another diatom peak. In the Bothnian Bay, the diazotrophic cyanobacteria is not as common as in other parts of the Baltic Sea; one reason for this is probably the predominant phosphorus limitation.

Since the start of the monitoring programme in 1979, salinity has decreased, whereas silicate has increased. Temperature and chlorophyll *a* have a slightly rising trend, but neither is statistically significant. Diatoms, dinoflagellates, cryptophytes, euglenophytes, and heterotrophs have all decreased significantly in the Bothnian Bay since sampling began in the mid-1980s.

5.1.2 Bothnian Sea (Sites 12–14)

Surface salinity in the Bothnian Sea is ca. 5.4–5.9. The maximum depth of the Bothnian Sea is 293 m, with a mean depth of 60 m. The open-sea sampling stations in the Bothnian Sea are US5B (Site 12, 62°35'N 19°60'E), SR5 (Site 13, 61°05'N 19°35'E), and F64 (Site 14, 60°11'N 19°08'E).

Seasonal and interannual trends (Figure 5.1.3)

The phytoplankton community in the Bothnian Sea is usually nitrogen-limited during summer, as it is in all of the other more southern areas of the Baltic Sea. Species such as the mixotrophic haptophyte *Chrysochromulina* spp. and cyanobacteria *Aphanizomenon* sp. and *Nodularia spumigena* are important during summer (Andersson *et al.*, 1996). Other important species are the diatom *Thalassiosira*

baltica and dinoflagellate *Peridiniella catenata* in spring, and photosynthetic ciliate *Mesodinium rubrum* after the spring bloom.

Since the start of the monitoring programme in 1979, temperature and chlorophyll *a* have increased, whereas salinity and silicate have decreased. Diatoms, dinoflagellates, cryptophytes, and heterotrophs have decreased significantly, whereas chrysophytes and the endosymbiotic ciliate *Mesodinium rubrum* (not shown) have increased.

5.1.3 Gulf of Finland (Sites 15–17)

The surface salinity in the Gulf of Finland is ca. 5.4–6.1. The maximum depth of the Gulf of Finland is 121 m. The open-sea sampling stations in the Gulf of Finland are LL3a (Site 15, 60°04'N 26°20'E), LL7 (Site 16, 59°51'N 24°49'E), and LL12 (Site 17, 59°29'N 22°54'E).

Seasonal and interannual trends (Figure 5.1.4)

The phytoplankton community structure is complex and shifting, owing to unstable mixing conditions in the Gulf of Finland. Dinoflagellates *Scrippsiella* sp., *Biecheleria baltica*, and *Gymnodinium corollarium* are important spring-bloom species. Late-summer communities in the Gulf of Finland are characterized by cyanobacterial blooms. Nitrogen limitation and low nitrogen-to-phosphorus ratio are supposed to promote the cyanobacterial blooms because diazotrophic cyanobacteria are able to fix nitrogen from the atmosphere. In addition to filamentous cyanobacteria, colonial cyanobacteria and cryptophytes as well as other small flagellates are numerous in the summer communities of the Gulf of Finland.

Since the start of the monitoring programme in 1979, temperature and chlorophyll *a* have increased, whereas salinity and silicate have decreased (Figure 5.1.4). Dinoflagellates have decreased in August, although their biomass and proportion in the spring bloom have increased (Klais *et al.*, 2011). Cryptophytes, euglenophytes, and heterotrophs have also decreased. Suikkanen *et al.* (2007) found that late-summer cyanobacterial biomass increased in the Gulf of Finland from the late 1970s to the beginning of the 2000s. In this August-only analysis, this cyanobacteria increase was not evident in the Gulf of Finland or in the northern Baltic Proper in the 2000s (Figure 5.1.5), possibly owing to differences in time-span or time-series analysis methods.

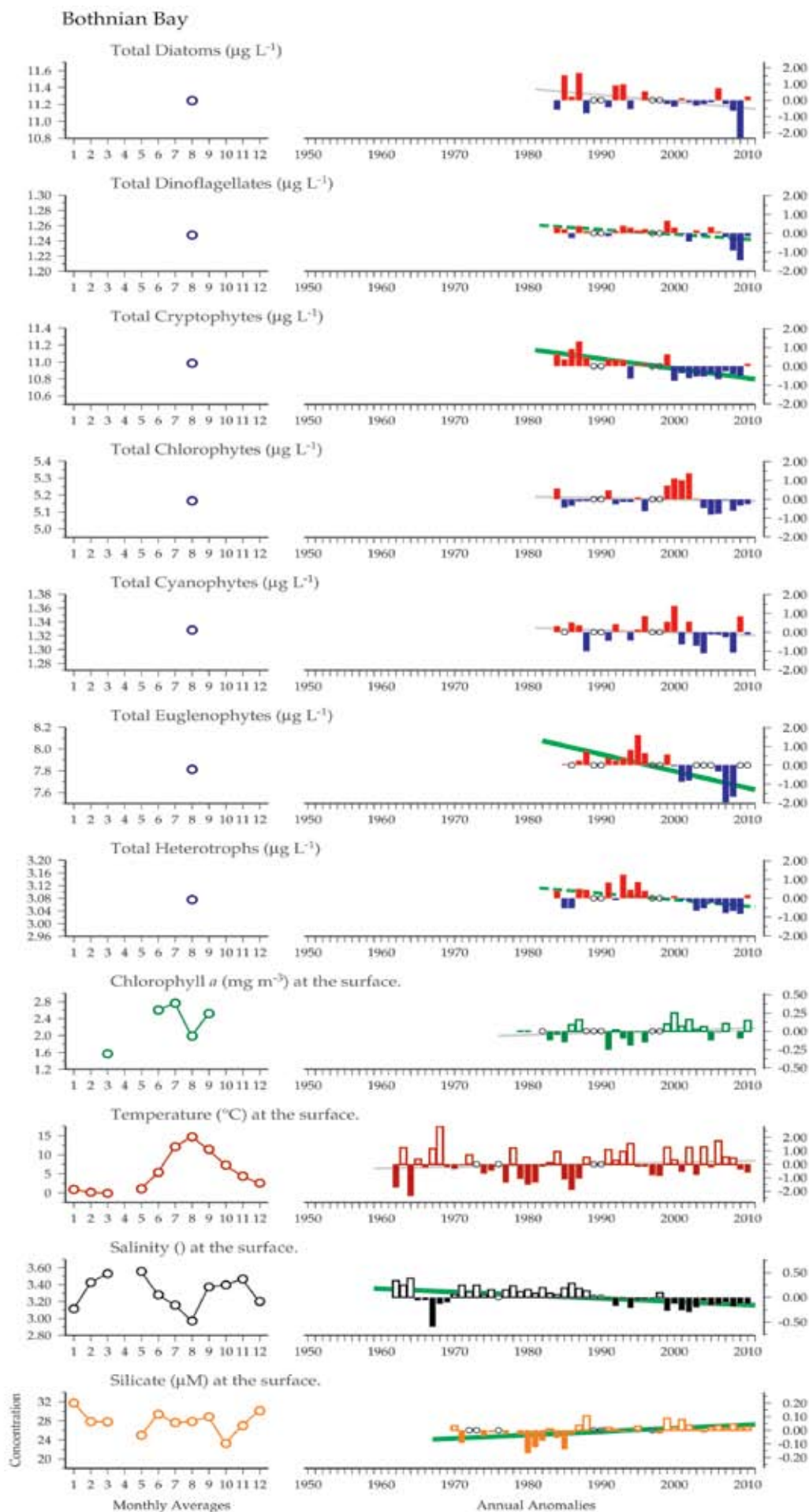
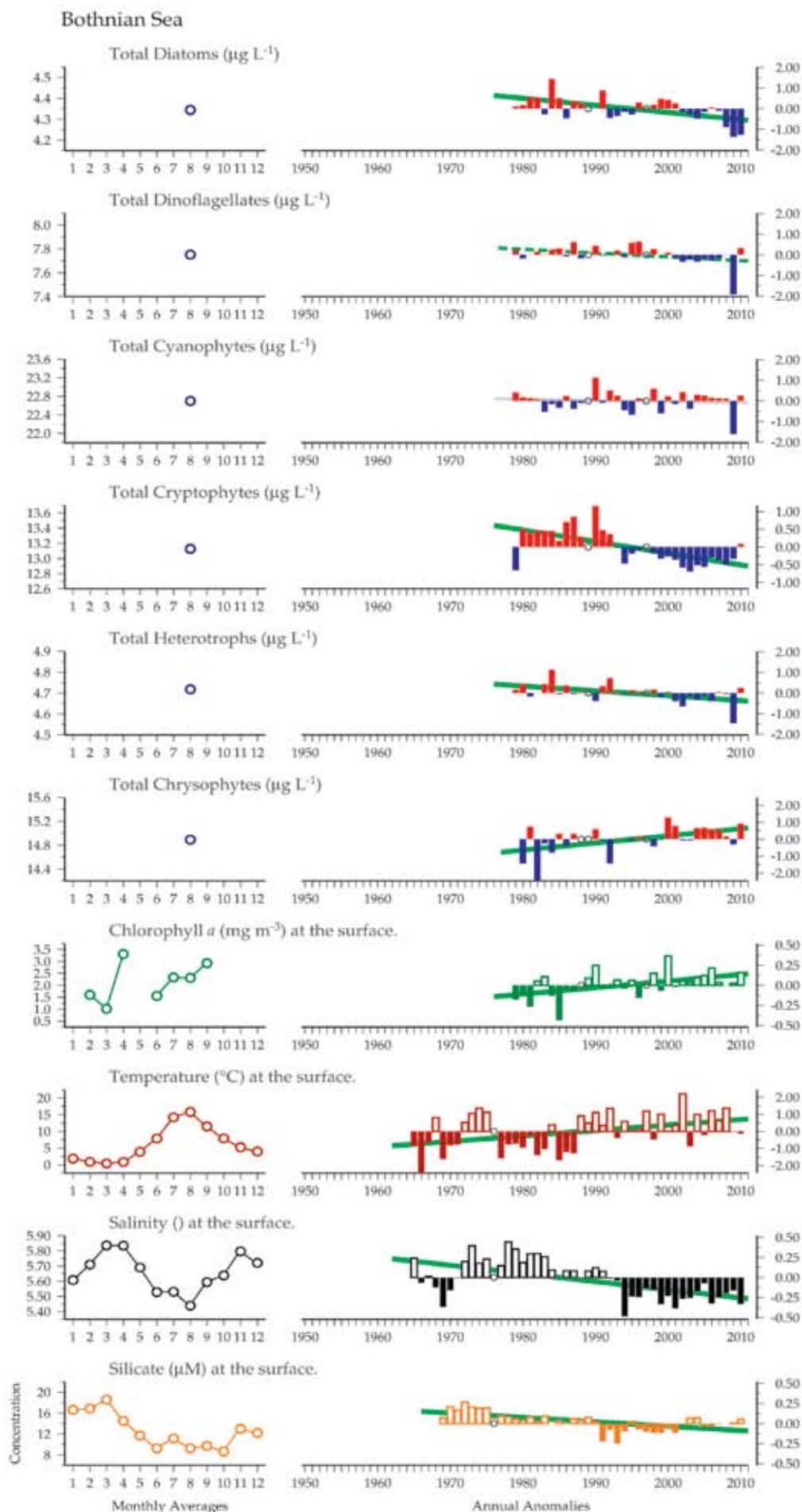


Figure 5.1.2
Multiple-variable comparison plot (see Section 2.2.2) showing the seasonal and interannual properties of select cosampled variables at the Bothnian Bay plankton monitoring site. Additional variables from this site are available online at <http://wgpmc.net/time-series>.

Figure 5.1.3
Multiple-variable comparison plot (see Section 2.2.2) showing the seasonal and interannual properties of select cosampled variables at the Bothnian Sea plankton monitoring site. Additional variables from this site are available online at <http://wgpme.net/time-series>.



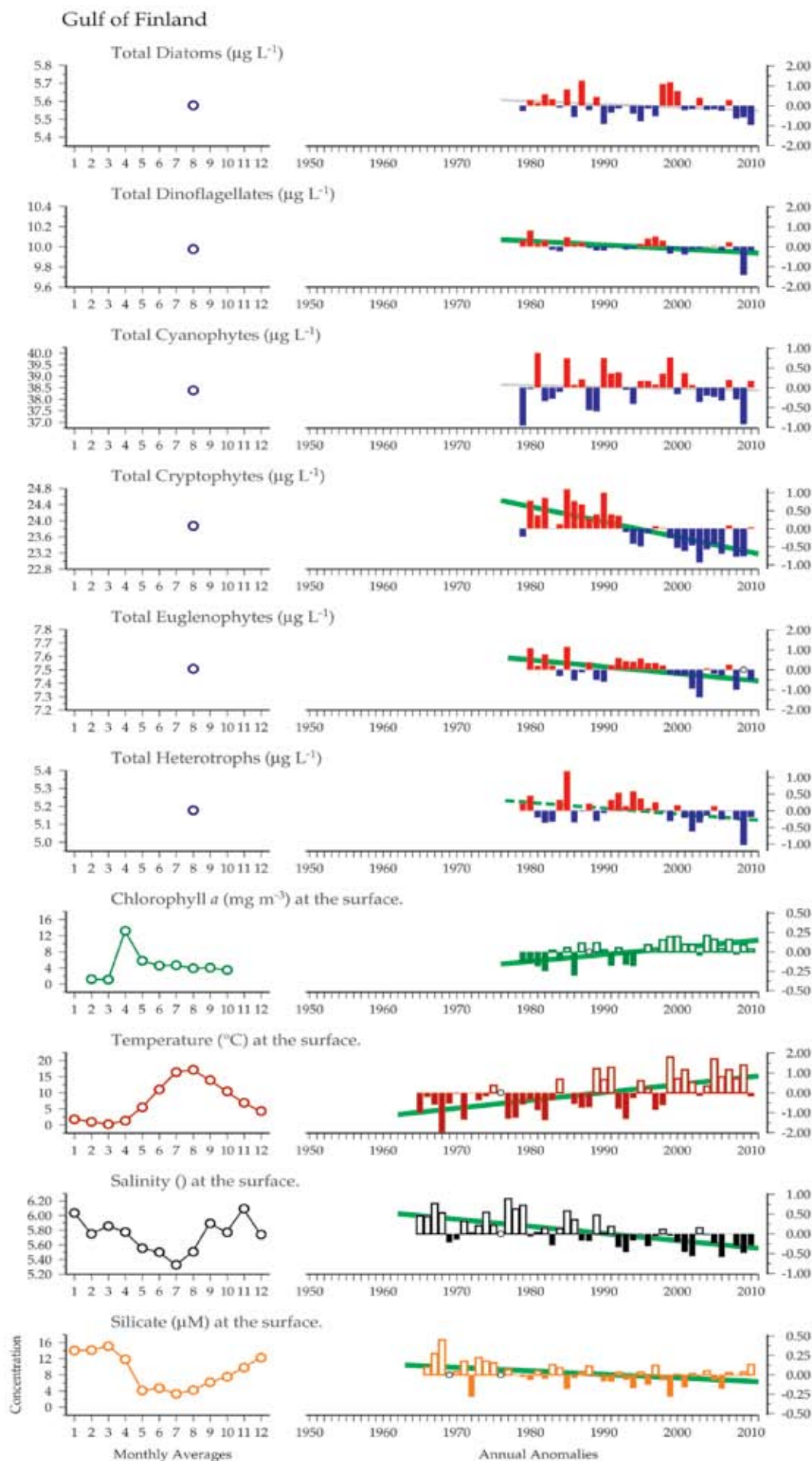


Figure 5.1.4
Multiple-variable comparison plot (see Section 2.2.2) showing the seasonal and interannual properties of select cosampled variables at the Gulf of Finland plankton monitoring site. Additional variables from this site are available online at <http://wgpmc.net/time-series>.

5.1.4 Northern Baltic Proper (Sites 18–21)

Surface salinity in the northern Baltic Proper ranges from 6.6 to 7.6. Bottom depths in the Baltic Proper can exceed 400 m. The open-sea sampling stations in the northern Baltic Proper are LL17 (Site 18, 59°02'N 21°08'E), LL23 (Site 19, 58°35'N 18°14'E), BY15 (Site 20, 57°19'N 20°03'E), and BY38 (Site 21, 57°07'N 17°40'E).

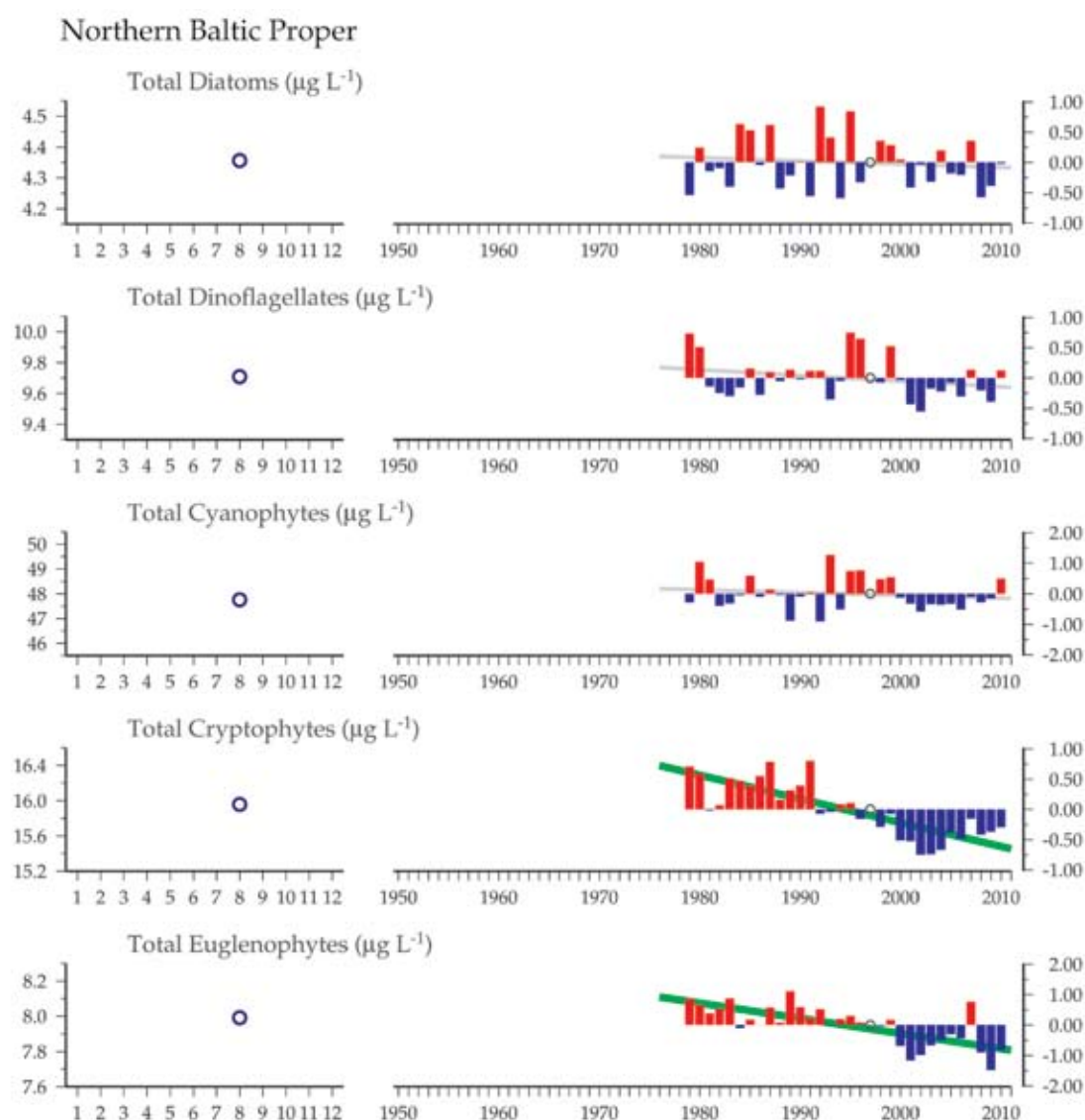
Seasonal and interannual trends (Figure 5.1.5)

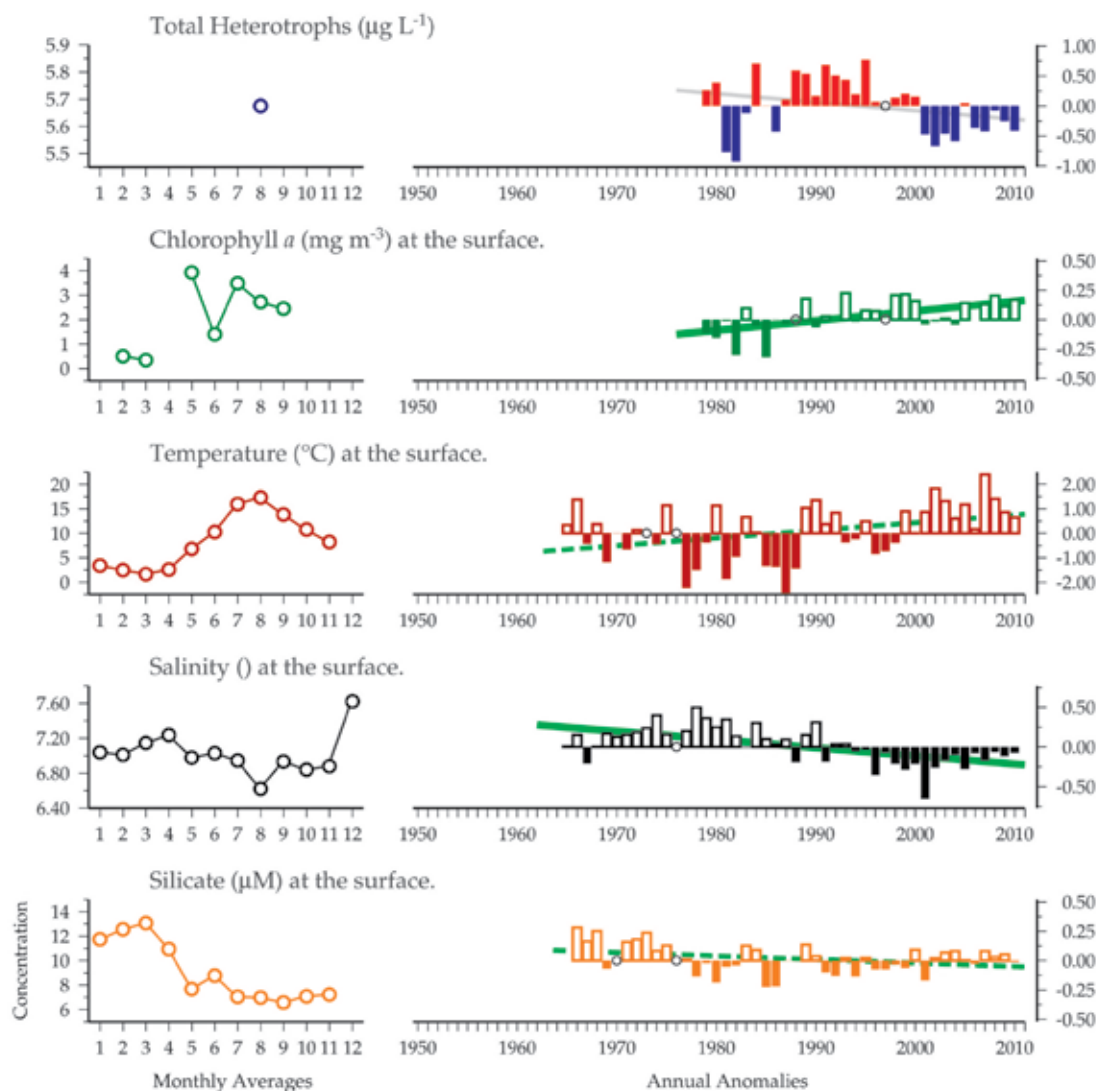
Dinoflagellates *Scrippsiella* sp., *Biecheleria baltica*, and *Gymnodinium corollarium* are dominant spring-bloom species in the northern Baltic Proper, and cyanobacteria blooms are typical in late summer (Wasmund *et al.*, 2011).

Since the start of the monitoring programme in 1979, temperature and chlorophyll *a* have increased, whereas silicate and salinity have decreased. Cryptophytes and euglenophytes have also decreased significantly.

Figure 5.1.5 (continued on facing page)

Multiple-variable comparison plot (see Section 2.2.2) showing the seasonal and interannual properties of select cosampled variables at the northern Baltic Proper plankton monitoring site. Additional variables from this site are available online at <http://wgpme.net/time-series>.





5.1.5 Overall northern Baltic trends

Since the start of the monitoring programme in 1979, chlorophyll *a* has increased in all northern subareas. Although chlorophyll *a* has increased, the biomass of major phytoplankton groups has generally decreased based on the results of microscopic phytoplankton counts. The chlorophyll *a* increase could be the result of, for example, an increase in picoplankton, which is not included in the phytoplankton results because its analysis would require special samples that need to be counted with an epifluorescence microscope. Also, for some reason, chlorophyll *a* production may have been more efficient than in earlier years. Diatoms have decreased, especially in the Bothnian Bay and the Bothnian Sea, and dinoflagellates have also decreased significantly in all subareas except

the northern Baltic Proper. In this long-term data from August, the diatoms:diatoms+dinoflagellates ratio did not show any trend (figure not shown), although Klais *et al.* (2011) have demonstrated that in the spring bloom, the share of dinoflagellates has generally increased in the Baltic Sea owing to the increase in dinoflagellate biomass and decrease in diatom biomass.

Cryptophytes, euglenophytes, and heterotrophic flagellates have decreased in all subareas. Chrysophytes have increased in the Bothnian Sea, and the endosymbiotic ciliate *Mesodinium rubrum* has increased in the Bothnian Sea (figure not shown, but available online). There is a possibility that *M. rubrum* has not been counted consistently from all earlier samples, which may affect the results.

5.2 Gdańsk Basin (Site 22)

Anetta Ameryk, Sławomira Gromisz, Janina Kownacka, Marianna Pastuszek, and Mariusz Zalewski

Figure 5.2.1

Location of the Gdańsk Basin plankton monitoring area (Site 22), plotted on a map of average chlorophyll concentration, and its corresponding environmental summary plot (see Section 2.2.1).



The National Marine Fisheries Research Institute (NMFRI) has a long-term database which covers a number of parameters measured in the southern Baltic Proper. NMFRI has been monitoring chlorophyll *a* concentrations since 1977, phytoplankton species since 1987, and additional microbial plankton since 1995. The database has, however, some gaps, especially in phytoplankton and bacterial parameters. Cruises were made 6–10 times a year in the 1980s in all seasons, and only two times a year, in spring and summer, over the last ten years. The data were collected at numerous sampling stations in the Gdańsk Basin, and the whole study area was placed into one box (longitude 017°54' 019°36'; latitude 55°36' to the coastline). The Gdańsk Basin includes waters sheltered by the Hel Peninsula (Gulf of Gdańsk) and the open waters. This region is relatively deep (60–80 m) and it is influenced by the Vistula River (the second largest river in the Baltic catchment).

Samples were collected with 2–5 l Nansen or Niskin bottles at five fixed depths from 0 to 10 m. Over the first 15 years of the studies, measurements of chlorophyll *a* concentrations were carried out with spectrophotometers, whereas in the years that followed, two parallel techniques were used: spectrophotometric and fluorometric. The phytoplankton samples were preserved with Lugol's solution (Edler, 1979) and then analysed using an inverted microscope (Utermöhl, 1958). Autotrophic dinoflagellates were distinguished from the heterotrophic ones using chlorophyll autofluorescence excited with blue light. Thecate dinoflagellates were determined after staining

with fluorochrome Calcofluor White MR2, which is a specific stain for cellulose in the thecal plates. Phytoplankton taxa were identified to species or general groups. Both abundance and average bacteria cell volume were determined by direct counting and by measuring the length and width of bacteria (dyed with acridine orange) under epifluorescence microscopes.

Seasonal and interannual trends (Figure 5.2.2)

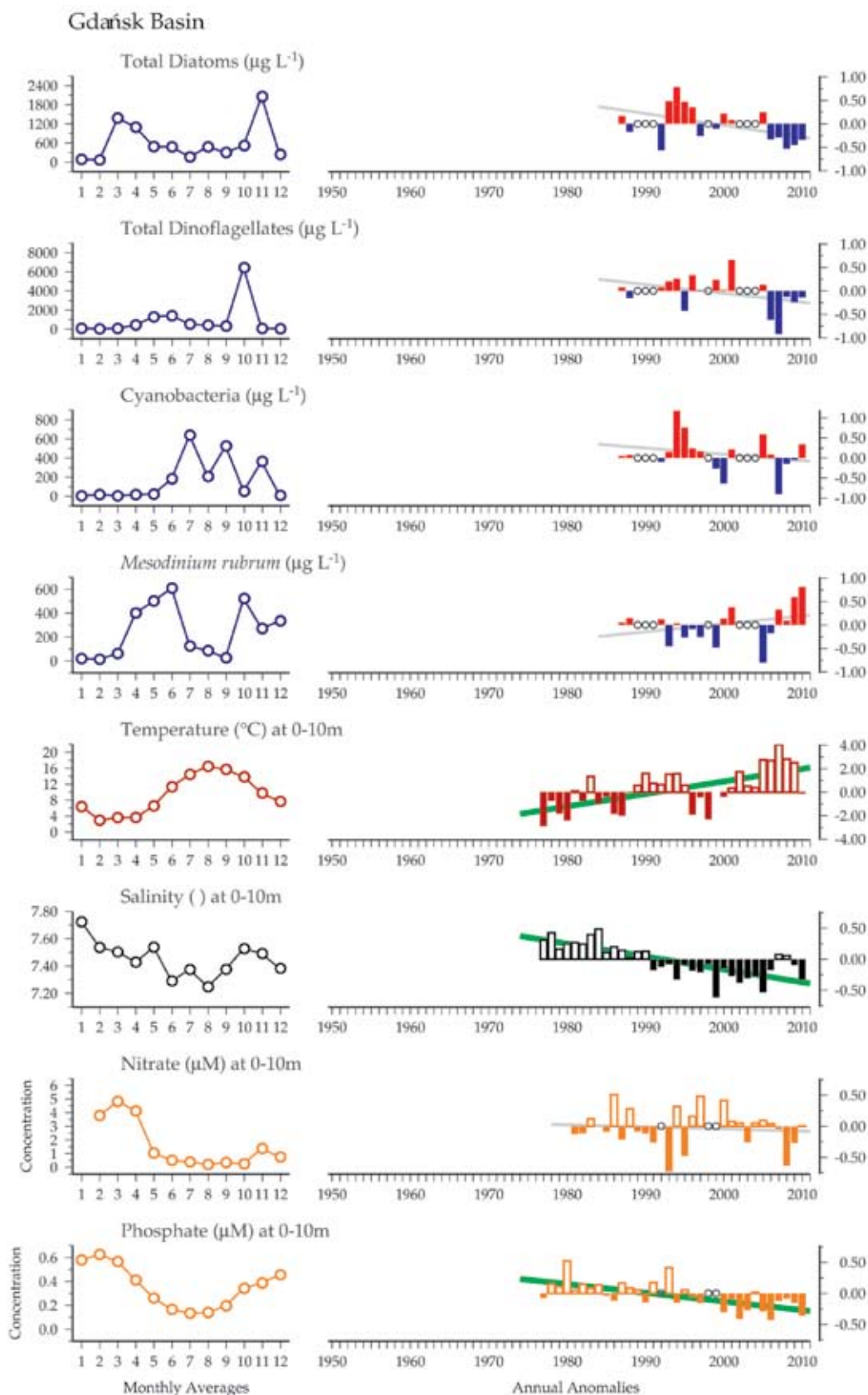
In the Gdańsk Basin, the spring bloom of small, rapidly growing diatoms is followed by the post-bloom peak of dinoflagellates. Cyanobacteria and nanoflagellates (not shown) bloom later, as they prefer conditions of thermal stratification in summer. A second peak of large diatoms is observed in autumn, usually accompanied by the photosynthetic ciliate *Mesodinium rubrum*, whereas winter is characterized by the phytoplankton minimum (Niemi, 1975; Smetacek *et al.*, 1984; Bralewska, 1992; Gromisz and Witek, 2001; Feistel *et al.*, 2008).

Nitrogen-fixing cyanobacteria dominate the phytoplankton communities in summer, when the N:P ratio is very low and water stratification is well established. Observations show a shift in time of appearance of cyanobacterial blooms. Over the years, the blooms shifted from July–August to June–July. Summer is also the time of highest microbial activity, which depends on phosphorus concentrations (Ameryk *et al.*, 2005).

Since the beginning of hydrographic sampling, temperature has increased significantly, whereas surface salinity and phosphate have decreased. Diatoms, dinoflagellates, and cyanobacteria show

slight, but non-significant, decreases. This may be the result of the biological variables' shorter year coverage compared with the hydrographic data.

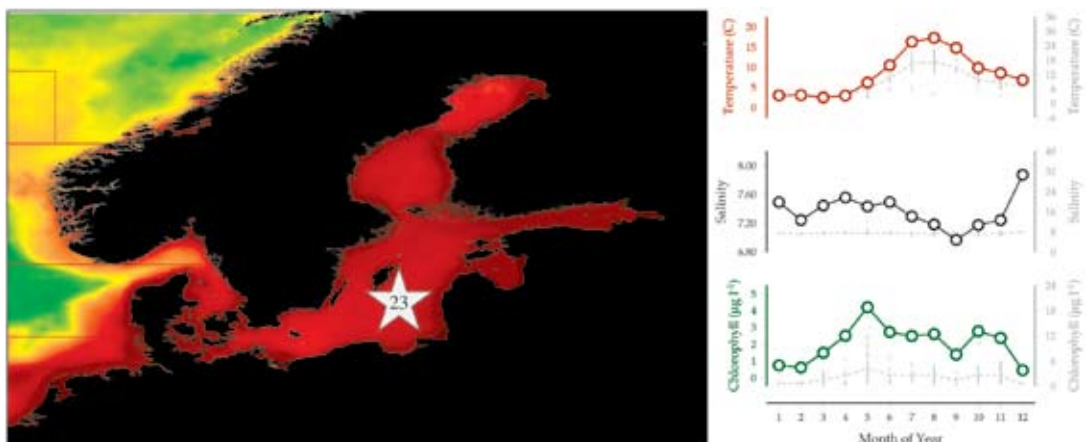
Figure 5.2.2
Multiple-variable comparison plot (see Section 2.2.2) showing the seasonal and interannual properties of select cosampled variables at the Gdańsk Basin plankton monitoring site. Additional variables from this site are available online at <http://vgpme.net/time-series>.



5.3 Eastern Gotland Basin (Site 23)

Norbert Wasmund and Günther Nausch

Figure 5.3.1
Location of the Eastern Gotland Basin plankton monitoring area (Site 23), plotted on a map of average chlorophyll concentration, and its corresponding environmental summary plot (see Section 2.2.1).



The Eastern Gotland Basin is part of the Baltic Proper, with a maximum depth of 249 m. In the frame of the international monitoring programme of the Helsinki Commission (HELCOM), two representative stations were sampled and combined for this report: BMP J1 at the Gotland Deep (57°18.3'N 20°4.6'E) and BMP K1 of the southern part of the Gotland Basin (55°33'N 18°24'E). Only integrated surface samples of the upper 10 m are considered. Sampling and processing of the samples and the data was carried out according to the compulsory manual (HELCOM, 2010).

This analysis is based on data collected in the frame of the monitoring programme of the Helsinki Commission (HELCOM) and contributed by the riparian countries of the Baltic Sea. The data are available from the ICES databank. Some data were personally supplied by Susanna Hajdu and Svante Nyberg (Stockholm University, Sweden), Sławomira Gromisz and Janina Kownacka (NMFRI Gdynia, Poland), as well as by Irina Olenina (Centre of Marine Research Klaipeda, Lithuania).

Seasonal and interannual trends (Figure 5.3.2)

The annual development of the phytoplankton is characterized by three blooms of different intensity, from which the summer bloom demonstrates a surprisingly high biomass, whereas the spring (May) and autumn blooms are mainly reflected in the chlorophyll data. The spring bloom is dominated by

dinoflagellates in recent times, but it is accompanied by *Mesodinium rubrum*, which may appear very early. Blooms of nitrogen-fixing cyanobacteria are typical in summer. The autumn bloom is dominated by diatoms, mainly *Coscinodiscus granii* (Wasmund and Siegel, 2008).

Since the start of the monitoring programme in 1979, the biomass in most phytoplankton groups is increasing. The major group, the dinoflagellates, forms blooms in spring, primarily in May, with the intensity of these spring blooms increasing mainly from 1986 to 1987. The long-term increase from 1979 to 2010 does not contradict the finding of a long-term decrease in dinoflagellate spring biomass in this area by Klais *et al.* (2011), because they considered only the period 1995–2004.

Another important group, the diatoms, contributed less to the spring bloom and mainly to the early stages of the bloom. Diatoms exhibited a strongly decreasing trend, especially in May, with the steepest decrease from 1988 to 1989, mainly owing to the decrease in *Achnanthes taeniata* (Wasmund *et al.*, 2011). The diatoms:diatoms+dinoflagellates ratio during the spring bloom period exhibited a significant decrease. Klais *et al.* (2011) demonstrated that dinoflagellates dominate in the open waters, but diatoms in the coastal waters of the Eastern Gotland basin during spring. The main appearance of diatoms was in August. The occurrence of diatoms is not highly correlated to other phytoplankton groups or abiotic parameters in this region.

The autotrophic ciliate *Mesodinium rubrum* has established itself as the third important group. It is strongly increasing in all seasons, but this may be partly an artefact because some contributors may have started counting that ciliate only in the 1990s.

Changes in the smaller groups are statistically more significant, but the ecological importance of these groups is rather low owing to their small biomass. Prasinophytes and prymnesiophytes are increasing in almost all seasons. Especially the prymnesiophyte *Chrysochromulina polylepis* increased suddenly since the end of 2007 (Hajdu *et al.*, 2008). Cryptophytes increased if July and October were considered. Chrysophytes (including Dictyochophyceae) shifted from negative to positive anomaly in the mid-1990s. Cyanobacteria have been increasing since the start of monitoring in 1979. Additional

analysis at the monthly level shows that the bulk of this increase occurs over the period March–June, a period of lower cyanobacteria biomass. During the July–August period of peak biomass, this trend disappears.

In contrast to the other areas of the Baltic Proper, the increasing tendency of temperature was not significant. The decrease in the components of dissolved inorganic nitrogen ($\text{NO}_3 + \text{NO}_2 + \text{NH}_4$) was only slightly significant. This is an important trend, as nitrogen is considered to be the limiting nutrient in the Baltic Proper. Chrysophytes, cryptophytes, and prasinophytes are strongly correlated with the DIN trend ($p < 0.01$). As the chlorophyll *a* concentrations are increasing, they show a slightly negative correlation with the DIN concentrations ($p < 0.05$).

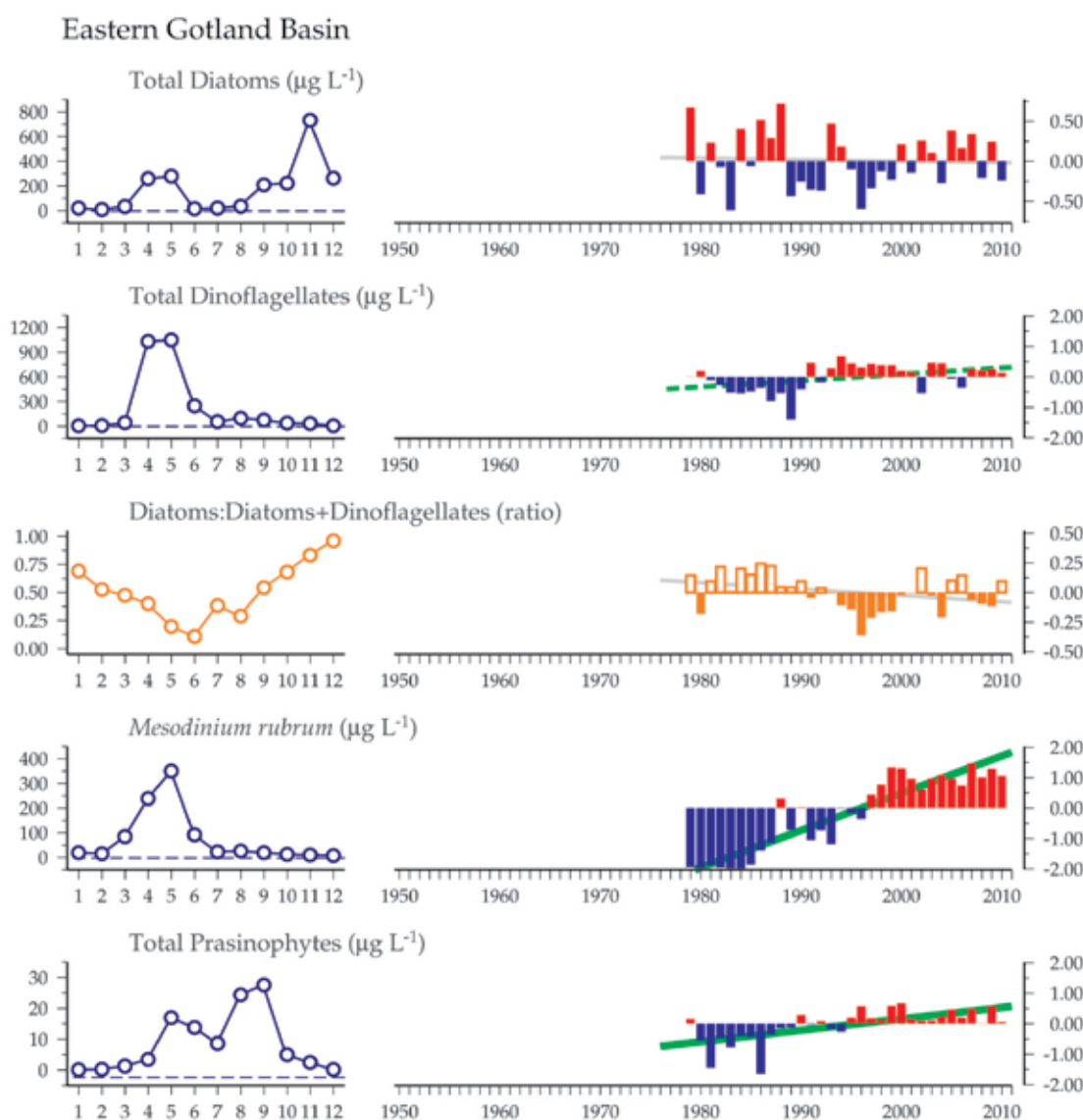
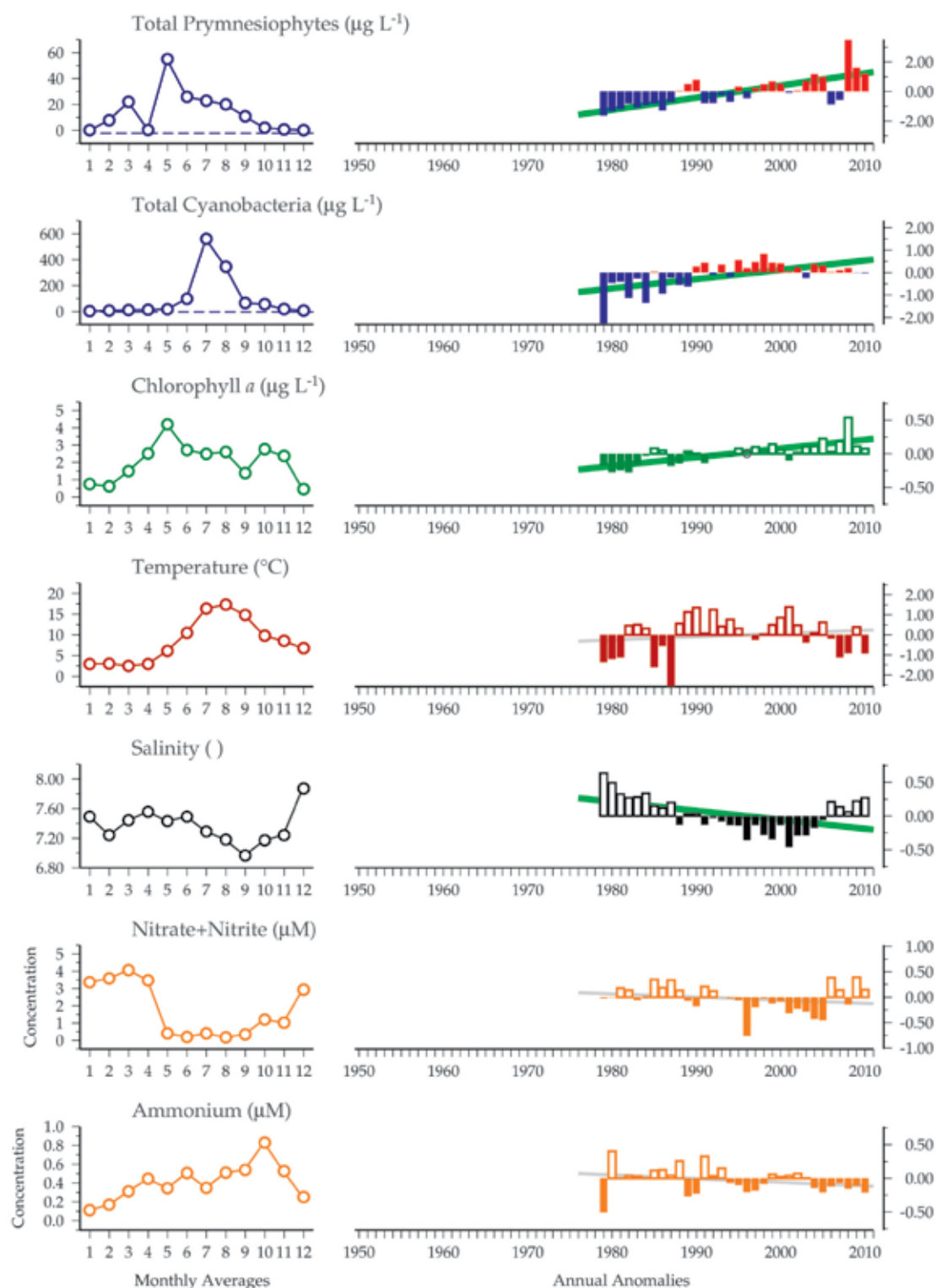


Figure 5.3.2 (continued overleaf)
Multiple-variable comparison plot (see Section 2.2.2) showing the seasonal and interannual properties of select cosampled variables at the Eastern Gotland Basin plankton monitoring site. Additional variables from this site are available online at <http://wgpmc.net/time-series>.

Figure 5.3.2 (continued from previous page)



5.4 Bornholm Sea (Site 24)

Norbert Wasmund and Günther Nausch

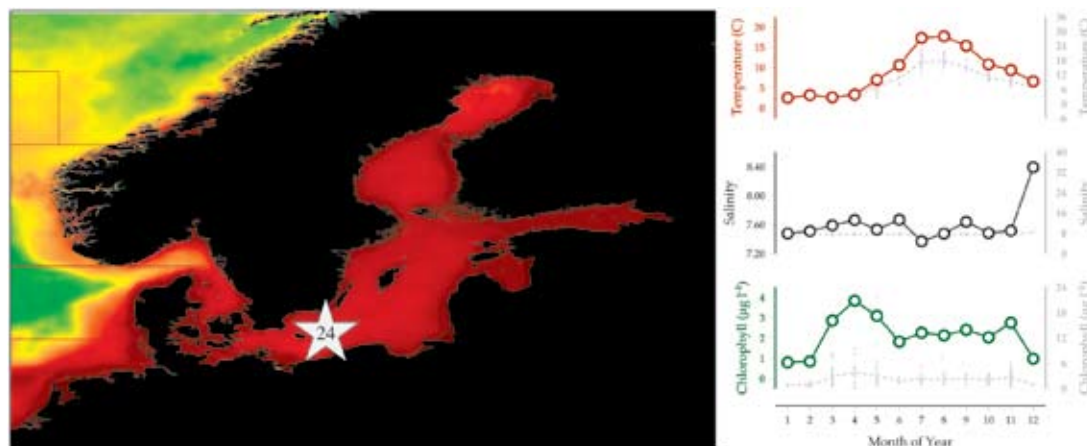


Figure 5.4.1

Location of the Bornholm Sea plankton monitoring area (Site 24), plotted on a map of average chlorophyll concentration, and its corresponding environmental summary plot (see Section 2.2.1).

The Bornholm Sea is part of the southern Baltic Proper, with a maximum depth of 92 m. In the frame of the international monitoring programme of the Helsinki Commission (HELCOM), the central station BMP K2 of the open sea was sampled: 55°15'N 15°59'E. Only integrated surface samples of the upper 10 m are considered. Sampling and processing of the samples and the data was carried out according to the compulsory manual (HELCOM, 2010).

This analysis is based on data collected in the frame of the monitoring programme of the Helsinki Commission (HELCOM) and contributed by the riparian countries of the Baltic Sea. The data are available from the ICES databank. Some data were personally supplied by Susanna Hajdu and Svante Nyberg (Stockholm University, Sweden), Sławomira Gromisz and Janina Kownacka (NMFRI Gdynia, Poland), as well as by Henrik Jespersen (Bornholms Regionskommune, Denmark) and Bente Brix Madsen (Orbicon, Denmark).

Seasonal and interannual trends (Figure 5.4.2)

The annual development of the phytoplankton is characterized by three blooms of different intensity, from which the summer bloom demonstrates a surprisingly high biomass whereas the spring and autumn blooms are mainly reflected in the chlorophyll data. In the spring bloom, a succession from diatoms to dinoflagellates occurs, but it is accompanied by *Mesodinium rubrum*, which

may appear very early. Blooms of nitrogen-fixing cyanobacteria are typical in summer. The autumn bloom is dominated by diatoms (Wasmund and Siegel, 2008).

Since the start of the monitoring programme in 1979, the biomass in most phytoplankton groups is increasing. Dinoflagellates frequently form blooms in spring, and the intensity of their spring blooms has been increasing, mainly from 1990 to 1991. Another major group, the diatoms, forms spring, summer, and autumn blooms. Diatoms dominate the spring bloom in this area (Klais *et al.*, 2011). A slight, but non-significant, increasing trend is found in the diatoms. The annual-only analysis of this report does not show the decreasing trend in spring blooms, based on silicate consumption, noted in Wasmund *et al.* (1998). Obviously, some diatom blooms of the 1980s were not properly recorded owing to undersampling; therefore, the decreasing trend could not be proven on the basis of biomass data (Wasmund *et al.*, 2011). Despite the lack of a trend in diatom biomass, the diatoms:diatoms+dinoflagellates ratio during the spring bloom period demonstrated a slightly significant decrease.

The autotrophic ciliate *Mesodinium rubrum* has established itself as the third important group. It is strongly increasing in all seasons, especially from 1993 to 1994. Its short-term shift may be an artefact, because some contributors may have counted that ciliate to the phytoplankton only after 1993.

Changes in the smaller groups are statistically more significant, but the ecological importance of these groups is rather low owing to their small biomass. Prasinophytes and prymnesiophytes are increasing in almost all seasons. Especially the prymnesiophyte *Chrysochromulina polylepis* increased suddenly since the end of 2007 (Hajdu *et al.*, 2008). Cryptophytes increased if May and July were considered, and euglenophytes in the months March and November. Chrysophytes (including Dictyochophyceae) shifted from negative to positive anomaly from 1998 to 1999.

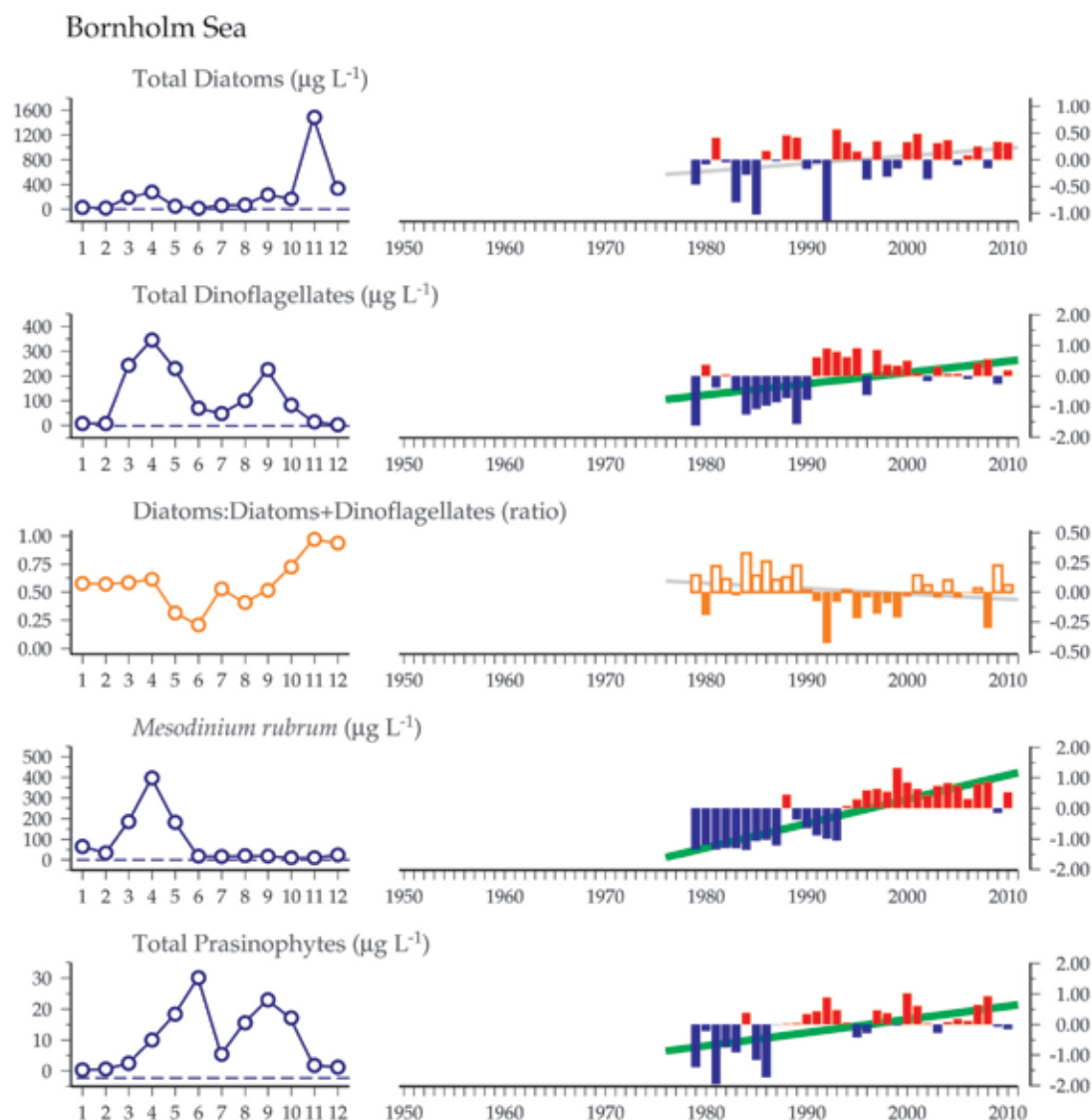
Cyanobacteria, which form blooms in July and August, decrease if only August is considered. The slight increase in April and May is less relevant as the biomass level is low in spring. Also, the chlorophytes

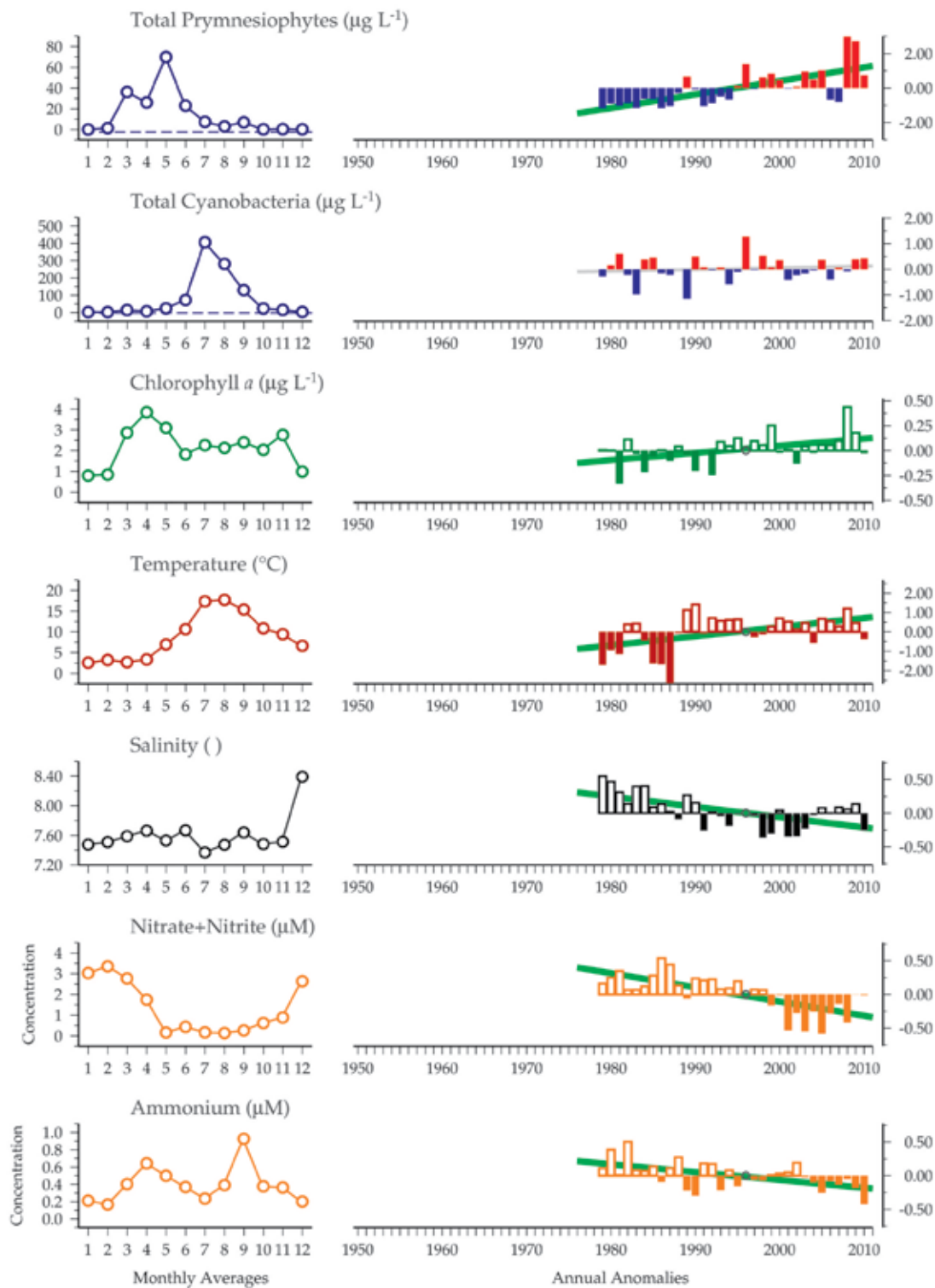
decrease in July, August, and September, but this group is unimportant in the brackish water.

The general increase in phytoplankton biomass may be related to increasing temperature. The component concentrations of dissolved inorganic nitrogen (where $DIN = NO_2 + NO_3 + NH_4$) are decreasing in the data collected since 1979. Nitrogen is considered to be the limiting nutrient in the Baltic Proper, but its trend does not agree with that of the phytoplankton biomass. Only the decrease in chlorophytes is related to the DIN trend. Euglenophytes, dinoflagellates, and *Mesodinium rubrum* are negatively correlated to salinity. The increase in phytoplankton biomass was verified by an increase in chlorophyll *a* concentrations (Wasmund and Siegel, 2008).

Figure 5.4.2 (continued on facing page)

Multiple-variable comparison plot (see Section 2.2.2) showing the seasonal and interannual properties of select cosampled variables at the Bornholm Sea plankton monitoring site. Additional variables from this site are available online at <http://wgpme.net/time-series>.



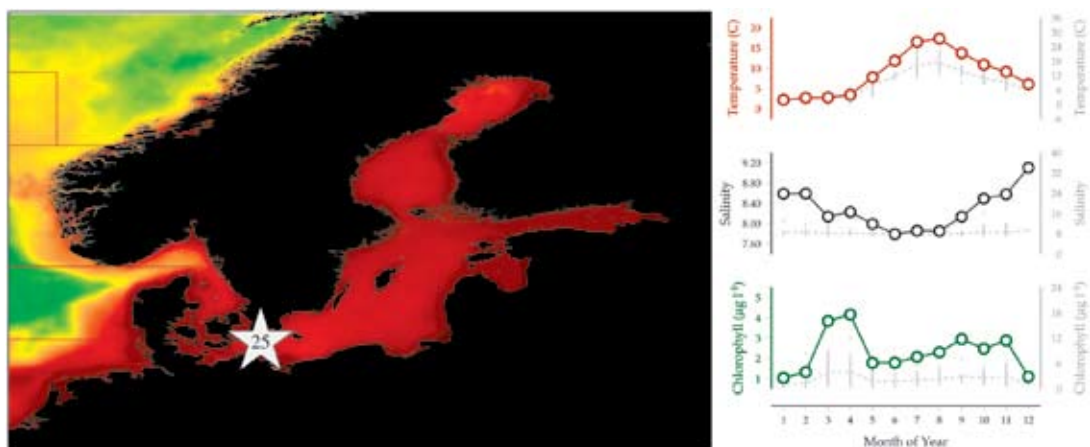


5.5 Arkona Sea (Site 25)

Norbert Wasmund and Günther Nausch

Figure 5.5.1

Location of the Arkona Sea plankton monitoring area (Site 25), plotted on a map of average chlorophyll concentration, and its corresponding environmental summary plot (see Section 2.2.1).



The Arkona Sea is part of the southern Baltic Proper, with a maximum depth of 47 m. In the frame of the international monitoring programme of the Helsinki Commission (HELCOM), four stations of the open sea were sampled: BMP K4, BMP K5, BMP K7, and BMP K8. The data from these stations are pooled to a representative dataset of this sea area. Only integrated surface samples of the upper 10 m are considered. Sampling and processing of the samples and the data were carried out according to the compulsory manual (HELCOM, 2010).

This analysis is based on data collected in the frame of the monitoring programme of the Helsinki Commission (HELCOM) and contributed by the riparian countries of the Baltic Sea. The data are available from the ICES databank. Some data were personally supplied by Susanna Hajdu and Svante Nyberg (Stockholm University, Sweden), as well as by Henrik Jespersen (Bornholms Regionskommune, Denmark) and Bente Brix Madsen (Orbicon, Denmark).

Seasonal and interannual trends (Figure 5.5.2)

The annual development of the phytoplankton is characterized by three blooms of different intensity. In the spring bloom, a succession from diatoms to dinoflagellates and/or *Mesodinium rubrum* occurs. In summer, large-celled diatoms may dominate the diverse community, whereas cyanobacteria blooms are only sparsely developed. The autumn bloom is dominated by diatoms (Wasmund and Siegel, 2008).

Since the start of the monitoring programme in 1979, the biomass in many phytoplankton groups is increasing. The important group of dinoflagellates may contribute to the spring blooms. It increased slightly if March and April are considered, but this increase was absent in the annual-level results of this study. Another important group, the diatoms, showed a spring bloom in March–April, but again had no general long-term trend at the annual level. The diatoms:diatoms+dinoflagellates ratio during the spring bloom is decreasing, but not as sudden as in the Bornholm Basin and the Eastern Gotland Basin. The autotrophic ciliate, *Mesodinium rubrum*, has established itself as the third most important group. It is strongly increasing in all seasons, especially from 1993 to 1994. This short-term shift may be an artefact because some contributors may have counted that ciliate to the phytoplankton only after the early 1990s. Independently of this problem, *Mesodinium rubrum* has also increased in datasets that included that species from the beginning of the observation.

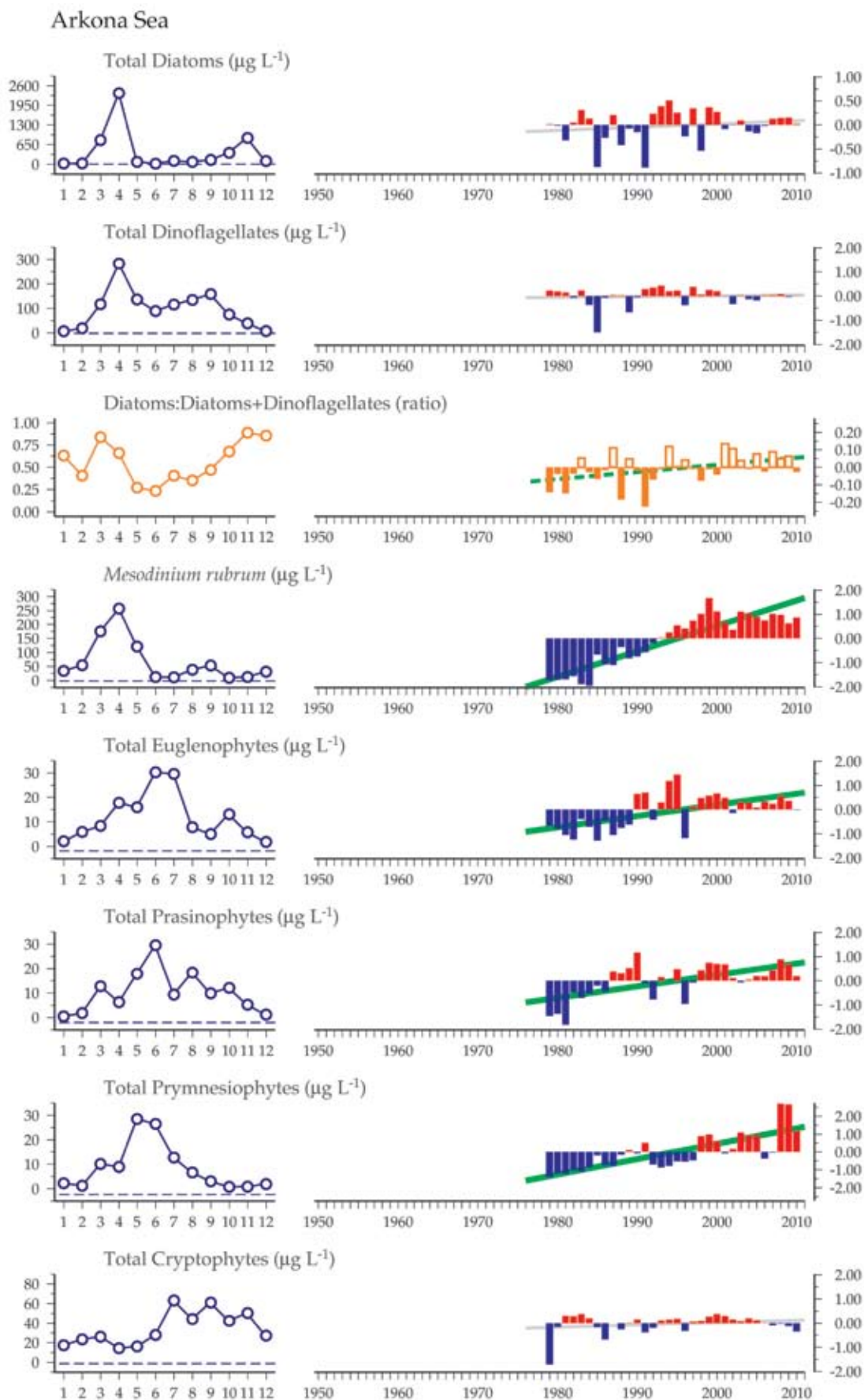
Changes in the smaller groups are statistically more significant, but the ecological importance of these groups is rather low owing to their small biomass. Euglenophytes, prasinophytes, and prymnesiophytes are increasing in all seasons, especially the prymnesiophyte, *Chrysochromulina polylepis*, which increased suddenly since the end of 2007 (Hajdu *et al.*, 2008). Cryptophytes exhibited a long-term increase in April and May mainly after 1991, but this may be caused only by a better identification after phytoplankton courses by the HELCOM Phytoplankton Expert Group (PEG). Chrysophytes (including Dictyochophyceae) shifted from negative to positive anomaly from 1998 to 1999 in all seasons.

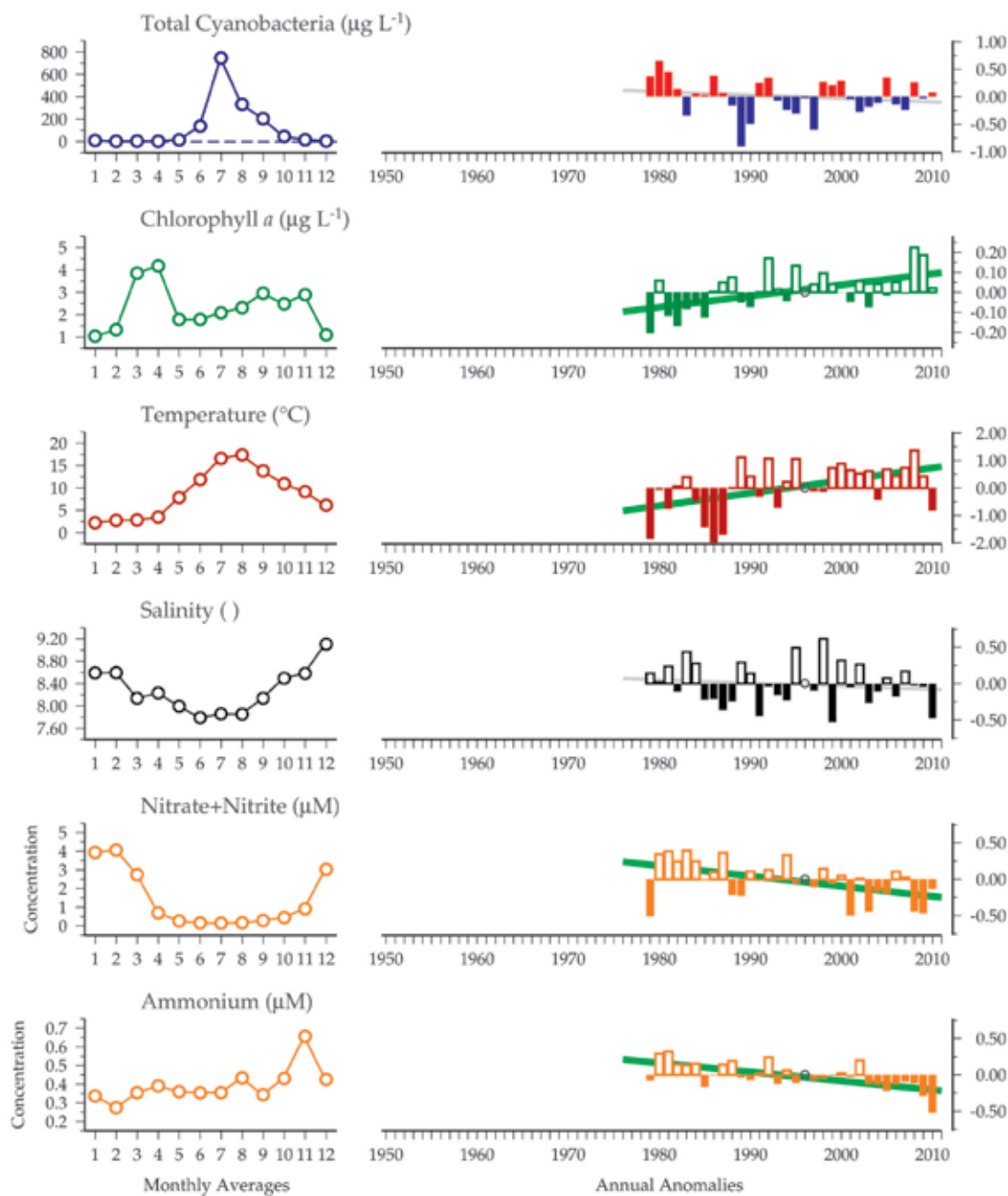
The only major group that is strongly decreasing is the cyanobacteria. In July and August, when they may form blooms in the Arkona Sea, they showed mostly positive anomalies until 1987, and negative anomalies since the year 2000. On the other hand, cyanobacteria biomass increased strongly in March, April, and May. This increase is less relevant because the biomass level in spring is low compared with summer. This tendency was already found and thoroughly discussed by Wasmund *et al.* (2011).

The general increase in phytoplankton biomass may be related to increasing water temperatures. The concentrations of dissolved inorganic nitrogen (represented as $\text{NO}_2 + \text{NO}_3 + \text{NH}_4$) are decreasing in the long-term dataserie. Nitrogen is considered to be the limiting nutrient in the Baltic Proper, but its trend does not agree with that of the phytoplankton biomass. The increase in phytoplankton biomass was verified by an increase in chlorophyll *a* concentrations (Wasmund and Siegel, 2008).

Figure 5.5.2 (continued on facing page)

Multiple-variable comparison plot (see Section 2.2.2) showing the seasonal and interannual properties of select cosampled variables at the Arkona Sea plankton monitoring site. Additional variables from this site are available online at <http://wgpmc.net/time-series>.

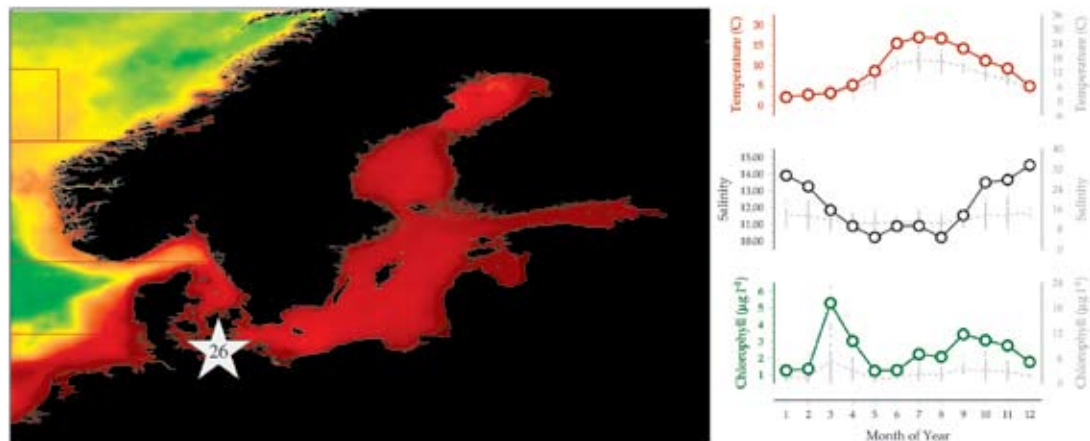




5.6 Mecklenburg Bight (Site 26)

Norbert Wasmund and Günther Nausch

Figure 5.6.1
Location of the Mecklenburg Bight plankton monitoring area (Site 26), plotted on a map of average chlorophyll concentration, and its corresponding environmental summary plot (see Section 2.2.1).



The Mecklenburg Bight is part of the Belt Sea within the western Baltic Sea. Its maximum depth is 27 m. The area is influenced by periodical inflow of marine water or outflow of Baltic brackish water and, therefore, is highly variable. In the frame of the international monitoring programme of the Helsinki Commission (HELCOM), three stations were sampled: BMP M1 (54°28'N 12°13'E), BMP M2 (54°18.9'N 11°33'E), and O22 (54°6.6'N 11°10.5'E). The data of these stations are pooled to a representative dataset of this sea area. Only integrated surface samples of the upper 10 m are considered. Sampling and processing of the samples and the data was carried out according to the compulsory manual (HELCOM, 2010).

This analysis is based on data collected in the frame of the monitoring programme of the Helsinki Commission (HELCOM) and contributed by the riparian countries of the Baltic Sea. The data are available from the ICES databank.

Seasonal and interannual trends (Figure 5.6.2)

The annual development of the phytoplankton is characterized by three blooms of different intensity, from which the summer bloom demonstrates a surprisingly high biomass, whereas the spring and autumn blooms are mainly reflected in the chlorophyll data. The spring bloom is, in most years, dominated by diatoms, but in some years also by Dictyochophyceae, which are included in the chrysophytes in this study. Dinoflagellates and *Mesodinium rubrum*, which contribute significantly to the spring bloom in the Baltic Proper, are of minor importance in the Mecklenburg Bight in spring. Also, cyanobacteria biomass does not normally grow up to bloom concentrations. However, the diatoms can reach a second peak in summer. The autumn bloom is dominated by dinoflagellates and/or diatoms (Wasmund and Siegel, 2008).

Since the start of the monitoring programme in 1979, the biomass of phytoplankton groups is decreasing in spring but increasing in summer in this area, as demonstrated by Wasmund *et al.* (2011). The important group of dinoflagellates is increasing, mainly in March. On the other hand, diatom spring biomass is decreasing. As a result, the diatoms:diatoms+dinoflagellates ratio during the spring bloom period is decreasing. The Dictyochophyceae (i.e. chrysophytes) become more important in spring. The autotrophic ciliate *Mesodinium rubrum* increased in the Baltic Proper, but probably the result of a changed counting strategy (cf. chapter on the Arkona Sea). The cyanobacteria biomass is increasing. Monthly

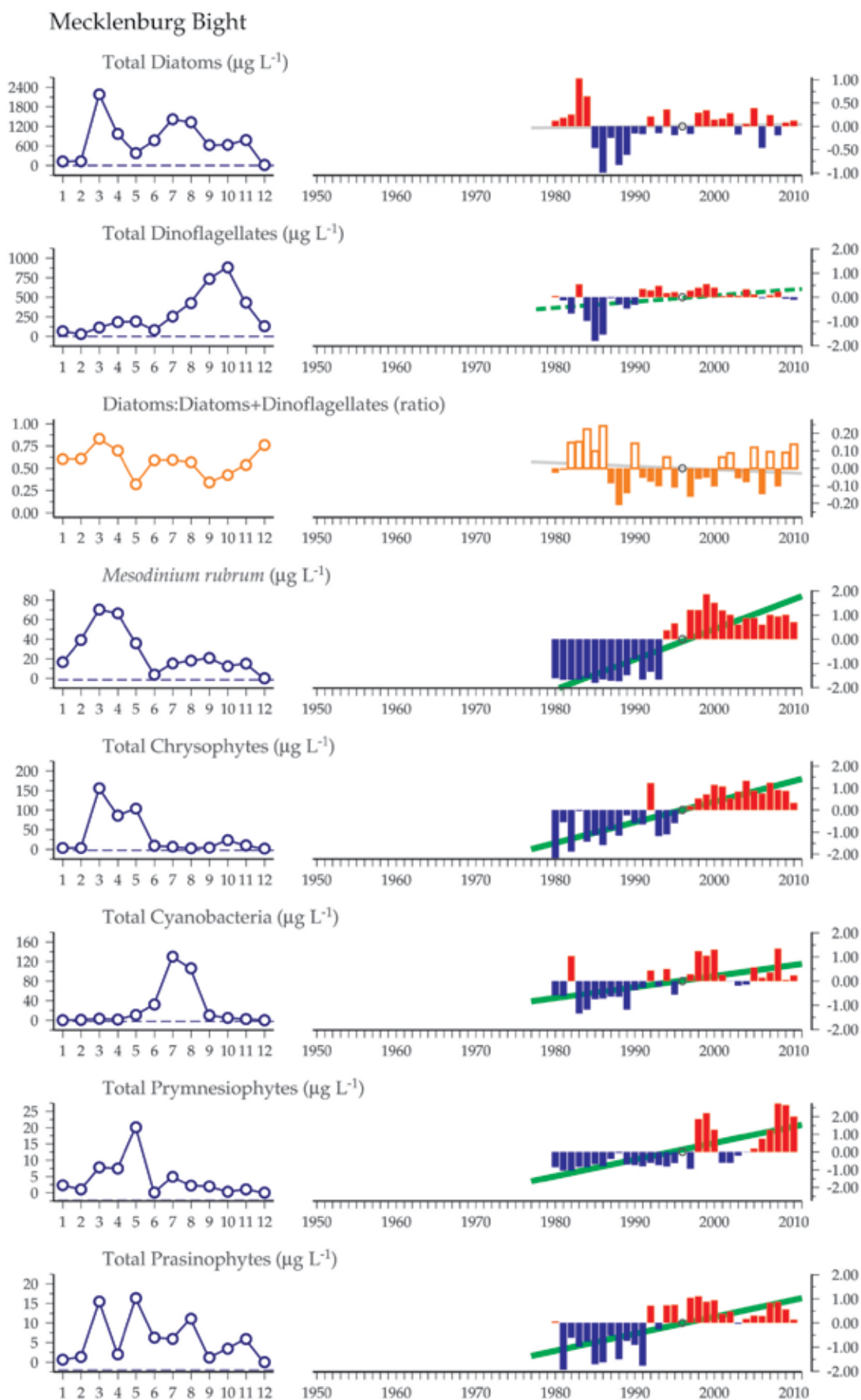
analysis finds no trend in summer, and the increase is evident only in the months of April and September, when their biomass is generally low, and an increase can be detected.

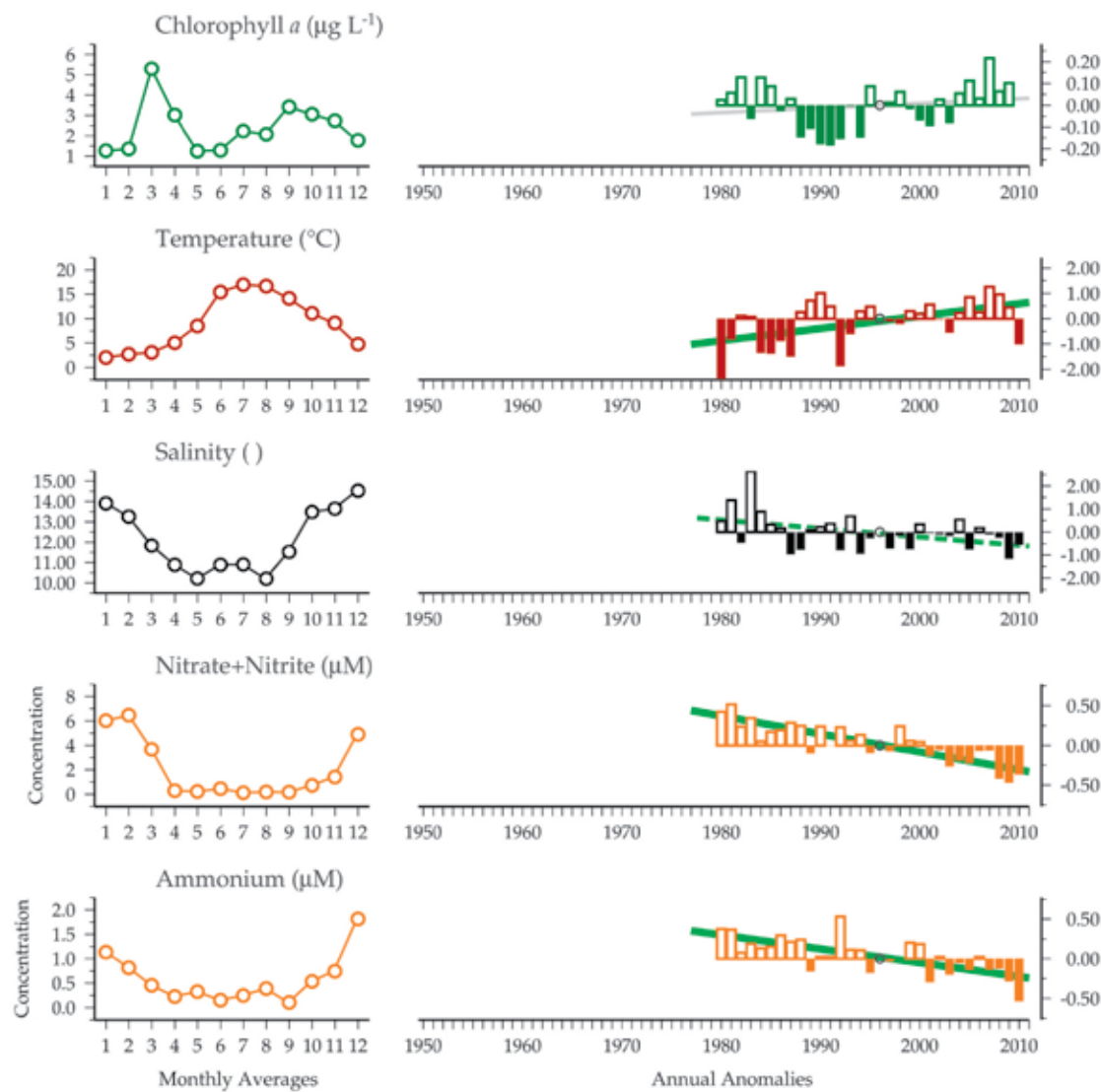
Changes in the smaller groups are statistically more significant, but the ecological importance of these groups is rather low owing to their small biomass. The prymnesiophytes and prasinophytes increased in all seasons, with the prymnesiophytes increasing especially since the end of 2007 (Hajdu *et al.*, 2008).

A general increase in temperature was also detected in the Mecklenburg Bight. The concentrations of the main components of dissolved inorganic nitrogen (i.e. $\text{DIN} = \text{NO}_2 + \text{NO}_3 + \text{NH}_4$) were decreasing in the long-term dataserie. Nitrogen is considered to be the limiting nutrient in the Baltic Proper, but its trend does not agree with that of the phytoplankton biomass. Chrysophytes, prymnesiophytes, prasinophytes, and *Mesodinium rubrum* are negatively correlated to this DIN trend. The chlorophyll *a* concentration is not correlated to any other parameter and demonstrates no general trend. Only seasonal-level trends (January–March) reveal a significantly decreasing trend in the chlorophyll *a* concentrations.

Figure 5.6.2 (continued on facing page)

Multiple-variable comparison plot (see Section 2.2.2) showing the seasonal and interannual properties of select cosampled variables at the Mecklenburg Bight plankton monitoring site. Additional variables from this site are available online at <http://wgpmc.net/time-series>.



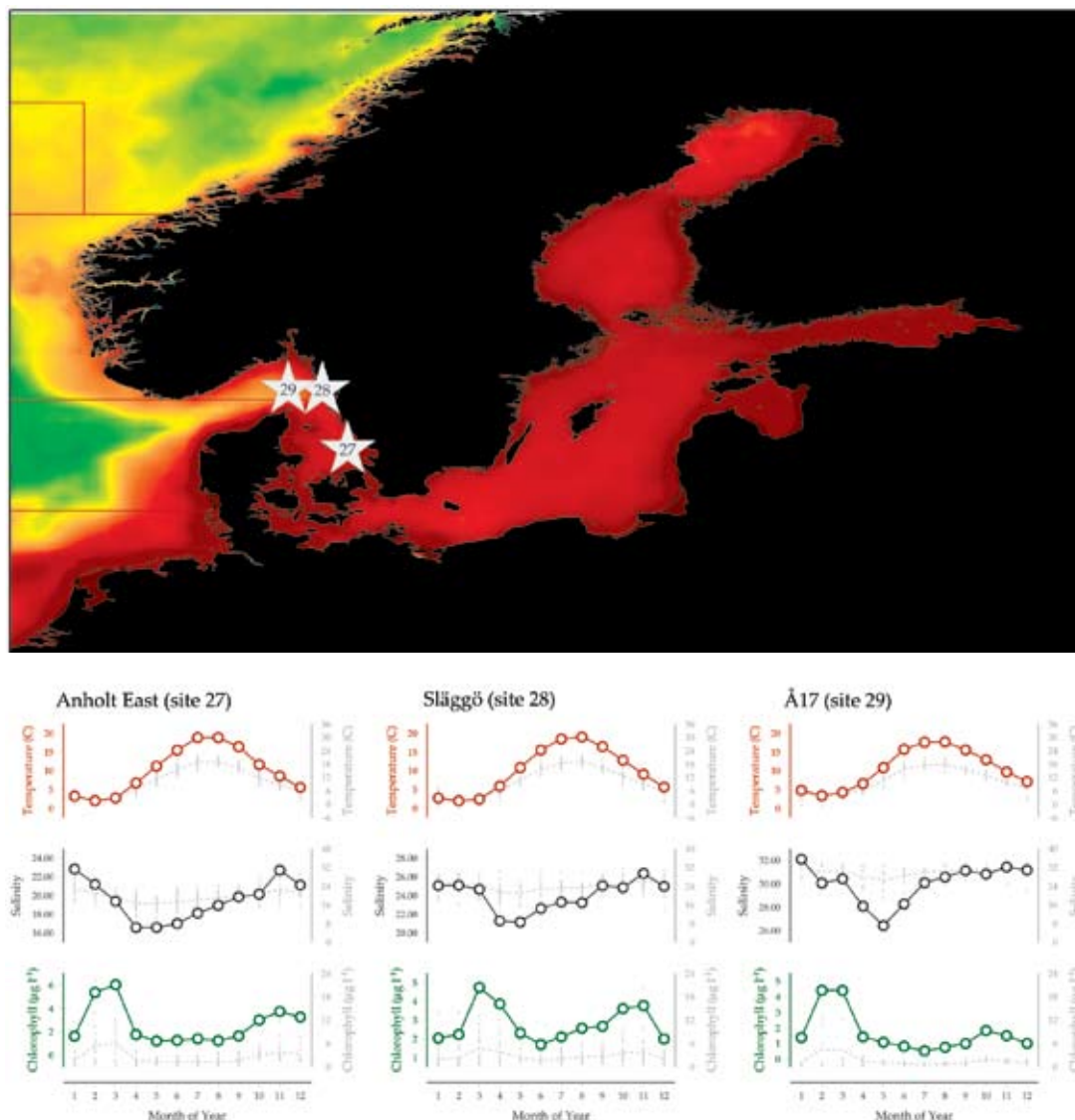


5.7 Kattegat and Skagerrak Monitoring (Sites 27–29)

Marie Johansen

Figure 5.7.1

Locations of the Kattegat and Skagerrak plankton monitoring areas (Sites 27–29), plotted on a map of average chlorophyll concentration, and their corresponding environmental summary plots (see Section 2.2.1).



The Kattegat is the transition area between the Baltic and North seas. It is included as part of the Baltic Sea in the HELCOM Convention area, but also as part of the North Sea in the OSPAR Convention. The mean depth is only ca. 20 m, and half the area has a depth of < 25 m (Fonselius, 1995), although the maximum depth exceeds 90 m at the northern, Skagerrak boundary. Close to the Swedish coastline, it has a connection with Skagerrak deep water through a deeper channel with elongated basins that run in a mainly north–south direction. The Kattegat has a strong halocline, with an average salinity of around 23 in the upper part (0–15 m) and ca. 32–33 in the deep water (below 60–80 m; Dyrssen, 1993). Surface water generally comes from the low saline Baltic Proper via the Danish

Straits, whereas the North Sea delivers more saline deeper waters from the north. The Baltic outflow from the Danish Straits coalesces in the eastern Kattegat to form the north-flowing Baltic Current. At the northern limit of the Kattegat, North Sea water from the Jutland Coastal Current splits, with some flowing as a bottom current into the Kattegat, whereas the remainder eventually combines with the Baltic Current, which is further augmented by significant freshwater outflows as it becomes the Norwegian Coastal Current in the Skagerrak. The Kattegat, thereby, forms a hydrographic transition zone between the Baltic Sea and the North Sea, with a substantially higher salinity range (and variability) than in nearby sea areas.

In the frame of the international monitoring programme of the Helsinki Commission (HELCOM), two stations are sampled by SMHI (Swedish Meteorological and Hydrological Institute) in the Kattegat; Anholt East (Site 27, 56°40'N 12°07'E) and N14 Falkenberg (56°56.40'N 12°12.7'E). Station N14 Falkenberg has only been sampled for a couple of years and is not included in the graphs. Two stations are sampled in the Skagerrak Släggö (Site 28, 58°15.5'N 11°26'E) and Å17 (Site 29, 58°16.5'N 10°30.8'E). Sampling and sample processing are conducted according to the HELCOM COMBINE manual for phytoplankton (HELCOM, 2010). All individuals were taxonomically identified to the lowest possible taxonomic level, but were presented as general taxonomic groups in the study. Data for 2002–2010 are presented, with a gap of no data in 2003.

Seasonal and interannual trends (Figures 5.7.2, 5.7.3, and 5.7.4)

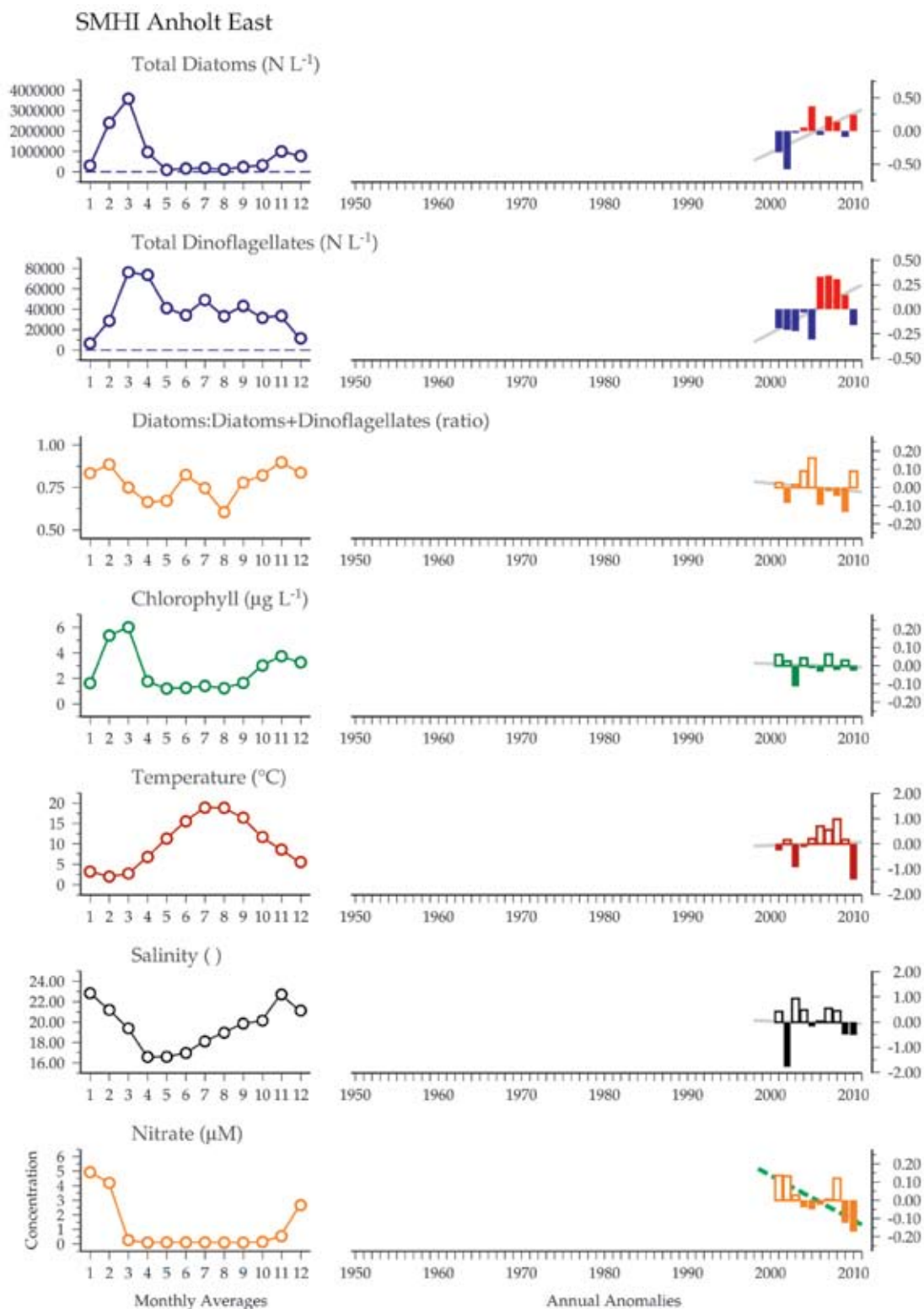
Although seasonal patterns and magnitudes of temperatures across the three sites were comparable, average salinities increased from 20 to 25 to 30 as the site location moved from east to west (approaching the North Sea). All three sites featured a 6–8 psu seasonal difference in salinity between the higher-salinity winter and lower-salinity summer periods. Chlorophyll concentrations exhibited a large March peak, followed by a significantly smaller October/

November peak. The spring phytoplankton population was numerically dominated by diatoms in all three sites. The seasonal abundance of dinoflagellates peaked during this spring period only at the Anholt East site, whereas this period was the seasonal lowest abundance for dinoflagellates at the other two sites. This relationship between diatoms and dinoflagellates was less clear in terms of the diatoms:diatoms+dinoflagellates ratio plots. In all three sites, the diatom maximum abundance and decrease corresponded to nitrogen availability, with dinoflagellates becoming more abundant during the low nitrogen periods.

Interannual trends within the three sites were not conclusive. This is likely the result of the combination of the relative shortness of sampling years in each site, combined with strong variability owing to the dynamic hydrographic conditions present within each of the sites.

Figure 5.7.2

Multiple-variable comparison plot (see Section 2.2.2) showing the seasonal and interannual properties of select cosampled variables at the Anholt East plankton monitoring site. Additional variables from this site are available online at <http://wgpme.net/time-series>.



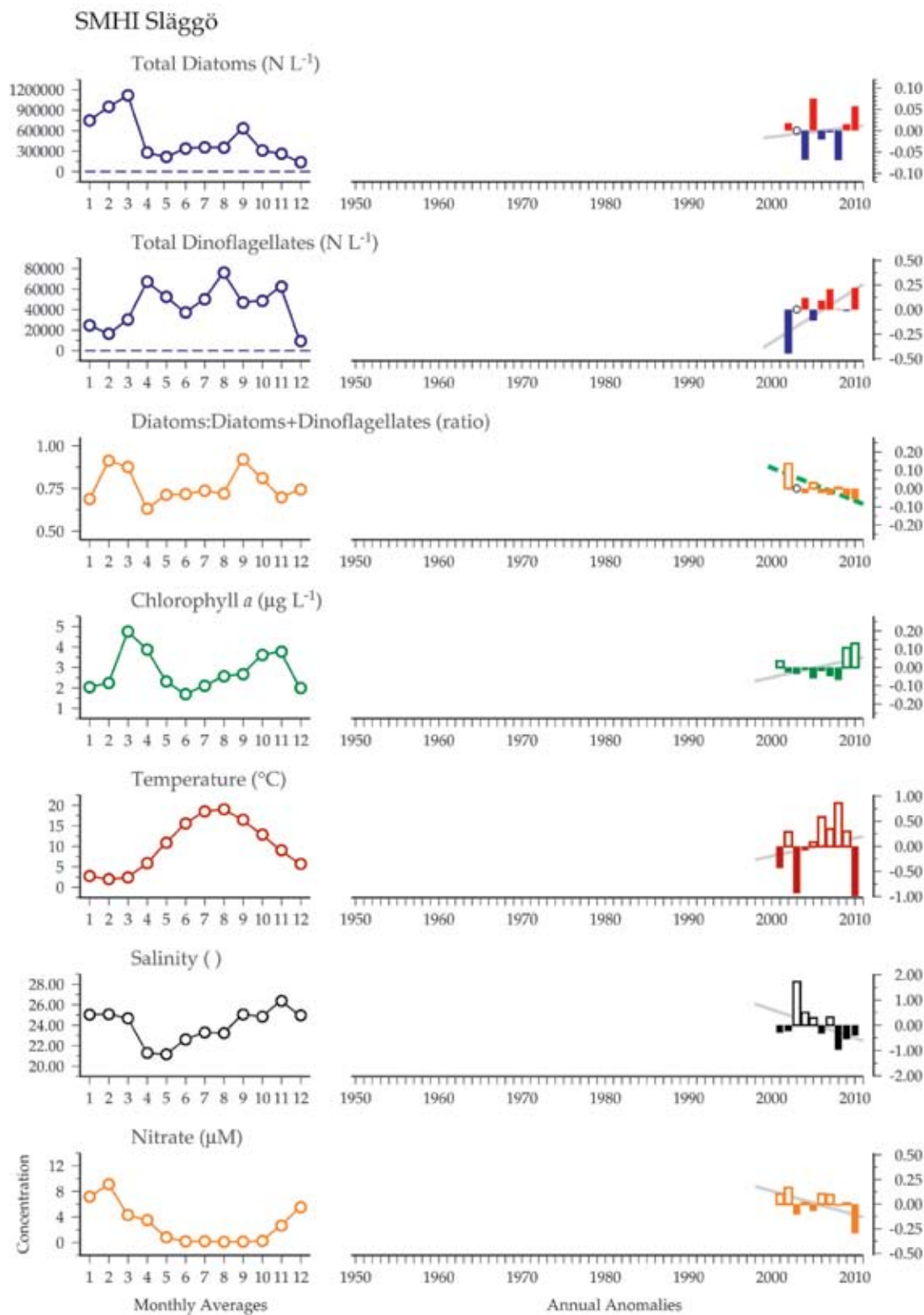
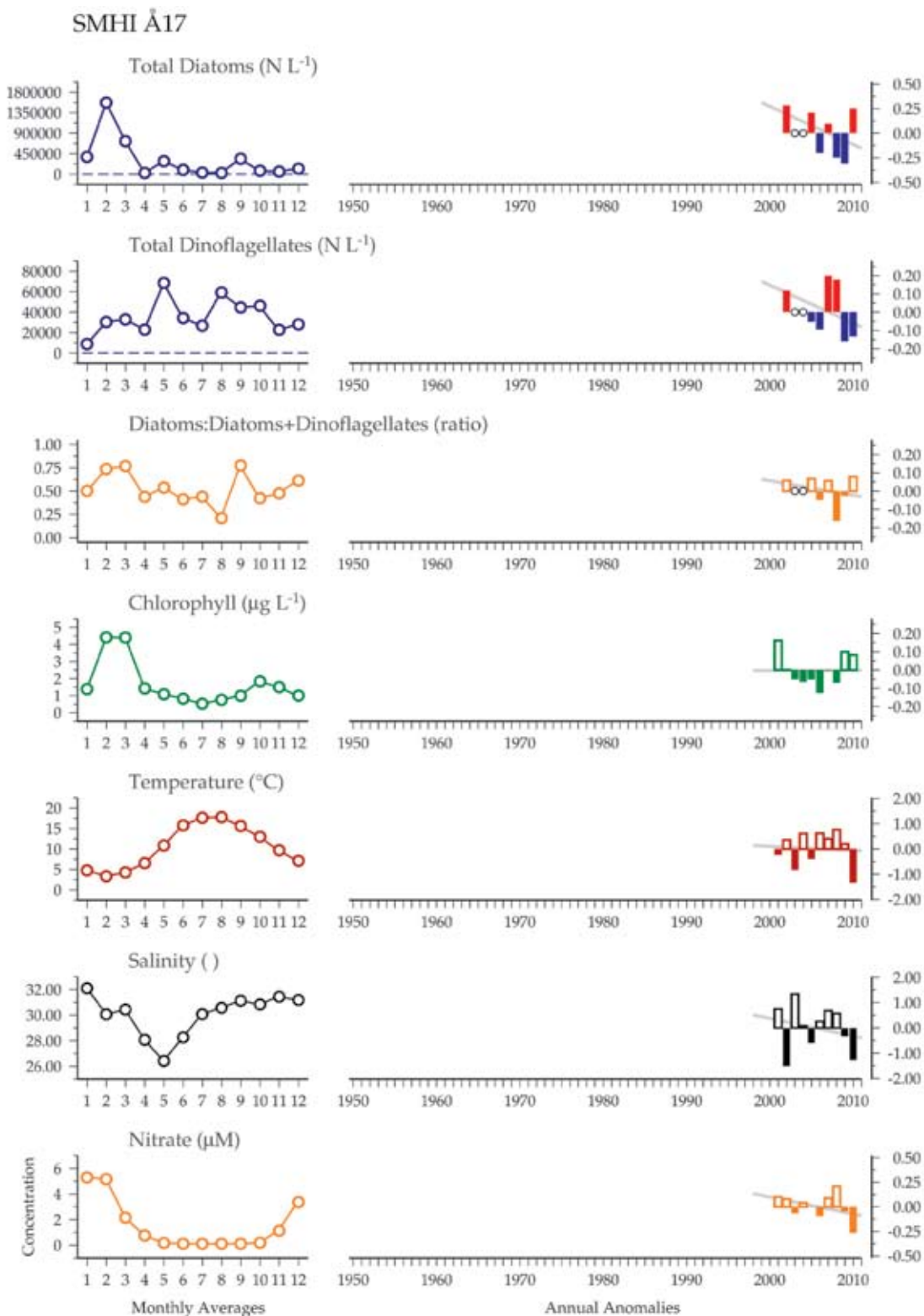


Figure 5.7.3
Multiple-variable comparison plot (see Section 2.2.2) showing the seasonal and interannual properties of select cosampled variables at the Släggö plankton monitoring site. Additional variables from this site are available online at <http://wgpme.net/time-series>.

Figure 5.7.4

Multiple-variable comparison plot (see Section 2.2.2) showing the seasonal and interannual properties of select cosampled variables at the Å17 plankton monitoring site. Additional variables from this site are available online at <http://wgpme.net/time-series>.





Deploying a Conductivity-Temperature-Depth instrument package in Bedford Basin, Canada. Photo: Fisheries and Oceans Canada.

6. PHYTOPLANKTON AND MICROBIAL PLANKTON OF THE NORTH SEA AND ENGLISH CHANNEL

Alexandra C. Kraberg, Claire Widdicombe, Karen Wiltshire, Eileen Bresnan, Dominique Soudant, Glen Tarran, and Tim Smyth

According to the classification of Longhurst (1998), the North Sea and English Channel belong to the Northeast Atlantic Shelf Province (NASP) extending from Cape Finisterre (Fisterra) in northwest Spain to the Skagerrak in Denmark and bordered in the north by the Faroe–Shetland Channel (Longhurst, 2007; McGinty *et al.*, 2011). This corresponds approximately to ICES Divisions IVa–c and VIIa–b. This region is characterized by seasonal patterns that are typical of temperate seas: well-mixed, nutrient-replete, and light-limited winter conditions; distinct blooms in spring; weak thermal stratification and nutrient depletion during summer; secondary blooms during late summer and/or autumn.

The hydrography of the North Sea and English Channel is complex and subject to considerable regional and interannual deviation through climatic and man-induced variability (Reid *et al.*, 2001). The North Sea receives tidally induced inputs of Atlantic water from the northwest, via the Faroe–Shetland Channel and, from the southwest, through the English Channel (Becker and Pauly, 1996; Callies *et al.*, 2011). The volume of water transported into the North Sea via either route also changes according to climatic conditions. Times of a high NAO index, for instance, are characterized by more southerly tracks of westerly winds, facilitating greater inflows of Atlantic water from the northwest. Water masses exit the North Sea along the Norwegian coast,

resulting in a anticlockwise current system that is driven by a combination of tidal and windstress forcing and considerable freshwater inputs from e.g. the Rhine and Elbe rivers (Simpson, 1994). The English Channel comprises continental shelf waters between the UK and French coasts, separated by a distinct frontal region (Groom *et al.*, 2008) that is directly influenced by Atlantic waters. The hydrography is generally seasonally stratified in the north and well-mixed, through strong tidal forcing, off the French coast, where freshwater inputs can also affect biogeochemical properties locally (e.g. the River Seine) (Goberville *et al.*, 2010). In addition to this complex hydrography, the North Sea and English Channel are also affected by a variety of anthropogenic pressures (Halpern *et al.*, 2008). They are, for instance, among the most heavily used shipping routes in the world, and coastal regions are of considerable importance for a range of ecosystem services, including recreation, tourism, and commercial fisheries. The North Sea is also exploited heavily for gas and oil, and increasingly its offshore areas are used for large-scale wind farms (Gee and Burkard, 2010). The impacts of these human activities on the North Sea's ecosystems are, as yet, largely unknown.

The complexity of the hydrography of the North Sea, with different physical drivers acting at a range of spatial and temporal scales coupled with

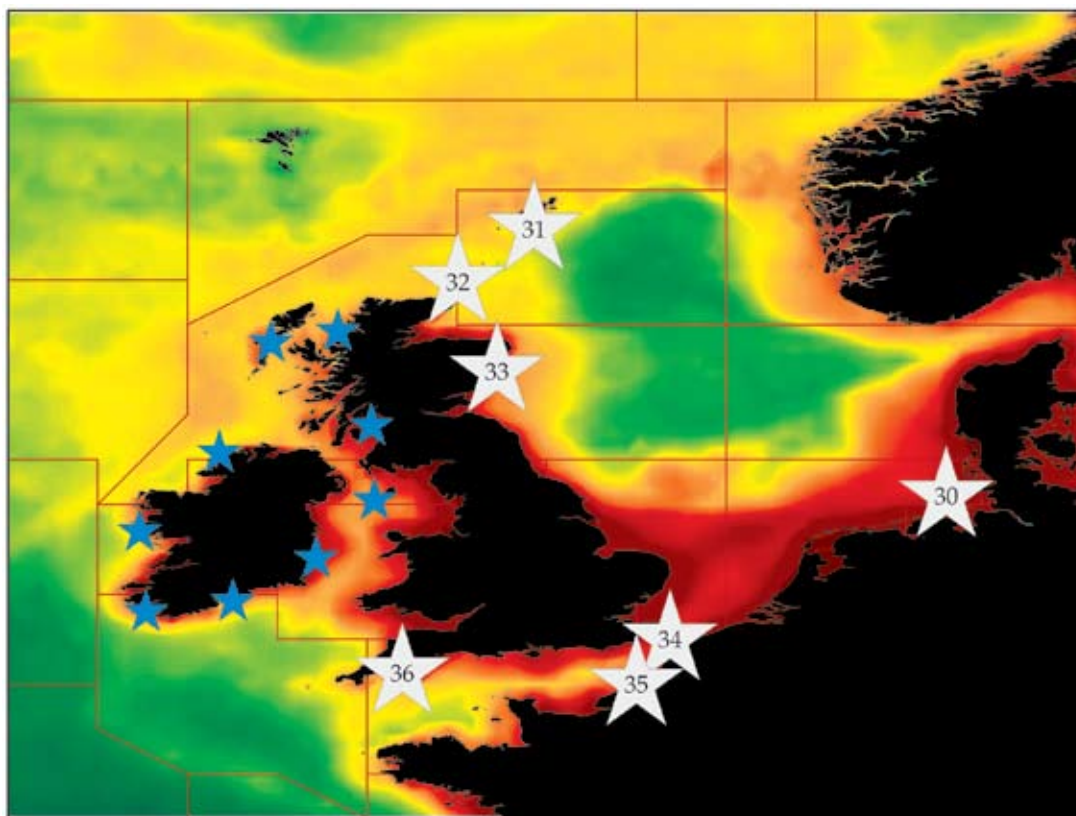


Figure 6.1
Locations of the North Sea and English Channel plankton monitoring areas (Sites 30–36) plotted on a map of average chlorophyll concentration. Blue stars indicate locations of sites described in the adjacent Northeast Atlantic Shelf region (see Section 7).

anthropogenic forcings, makes the detection and interpretation of biological trends in response to changing physico-chemical parameters difficult. Therefore, detailed time-series data are vital, and it is fortunate that a relatively large number of regular environmental and biological monitoring series exist, covering different regions of the North Sea and English Channel. Such data show that the phytoplankton (including heterotrophic protozoa or microzooplankton) and microbial communities in the North Sea and English Channel show distinct geographical (north-south; coastal-open water), seasonal, and interannual patterns in their abundance and biomass (Lefebvre *et al.*, 2011). Systematic assessments of the differences in phytoplankton community composition between the Channel regions are rare. Although the English Channel is seen as the northern geographical boundary for many warm-water species, it still has to be considered as a potential source of “new” species immigrating into the North Sea. This could happen by passive transport of either vegetative stages or cysts, which many diatoms or dinoflagellates produce as environmental conditions become unfavourable for vegetative growth. Accumulations of cysts on the seabed could then serve as seedbanks for future populations of a given species, for instance, if SSTs in the North Sea continue to rise (Nehring, 1995, 1998). Long-term studies also show that plankton are particularly sensitive to

climate change (Edwards and Richardson, 2004). For example, the rate of SST warming around the UK has increased by ca. 0.2–0.6°C per decade since the 1980s (MCCIP, 2008), and this rate has been fastest in the English Channel and southern North Sea (Wiltshire and Manly, 2004; Mackenzie and Schiedek, 2007; Hughes *et al.*, 2009, 2011; Smyth *et al.*, 2010). This warming coincides with an increase in dinoflagellates and diatoms in the northeastern and southeastern North Sea (Leterme *et al.*, 2005; Wiltshire *et al.*, 2008) and a decrease in diatoms in the English Channel (Widdicombe *et al.*, 2010).

Range extensions or contractions and changes in phenology of individual species or species groups have also been observed. Hays *et al.* (2005) described a range shift in the dinoflagellate genus *Ceratium*. For example, before 1970, *Ceratium trichoceros* was only found south of the UK, but it is now also found in the coastal waters of the west coast of Scotland and in the North Sea. Change in the timing of the annual spring bloom has also been reported. In some regions, the bloom appears to start earlier in response to increasing SSTs, although, if the warming also facilitates greater survival rates of zooplankton through winter, the opposite effect on bloom timing can be observed (relaxation of top-down control, see Wiltshire and Manly, 2004). Such changes can result in the complete reorganization of the ecosystem, for instance, as the result of the

decoupling between predator and prey phenology, known as match–mismatch phenomena (Edwards and Richardson, 2004). Such a regime shift occurred in the North Sea around 1988, evident as a stepwise alteration in all trophic levels, which coincided with the intrusion of warm-water plankton into the North Sea (Reid *et al.*, 2003; Schlüter *et al.*, 2008; Wiltshire *et al.*, 2008) and possibly in 1998 as well. This major regime shift was demonstrated to be strongly associated with warming sea temperatures and increased inflow of Atlantic water via the northern North Sea (Reid *et al.*, 2003).

The increases in sea surface temperatures, in particular, have also been linked to the appearance or greater prominence of species classed as invasive. The diatom *Coscinodiscus wailesii*, for instance, is thought to have originated in the Pacific. In the 1980s, it spread to the North Sea via the English Channel, where it was first observed in 1977 (as

C. nobilis) (Boalch and Harbour, 1977; Rincé and Paulmier, 1986). An exception, however, is the diatom *Mediopyxis helysia* (Kraberg *et al.*, 2011), which more commonly seems to be associated with negative salinity anomalies rather than temperature. The potential ecological role of such species is, as yet, unclear, but it has been hypothesized that, because many of them are large and, therefore, considered inedible for zooplankton, they also have considerable potential for modifying foodweb interactions.

Respective changes and trends in a considerable number of WGPME time-series will be described further in the individual site descriptions, which include the English Channel (Plymouth, Ifremer), German Bight (Helgoland Roads), and the northern North Sea (Stonehaven and northern Scottish Islands).

6.1 Helgoland Roads (Site 30)

Karen Wiltshire and Alexandra Kraberg

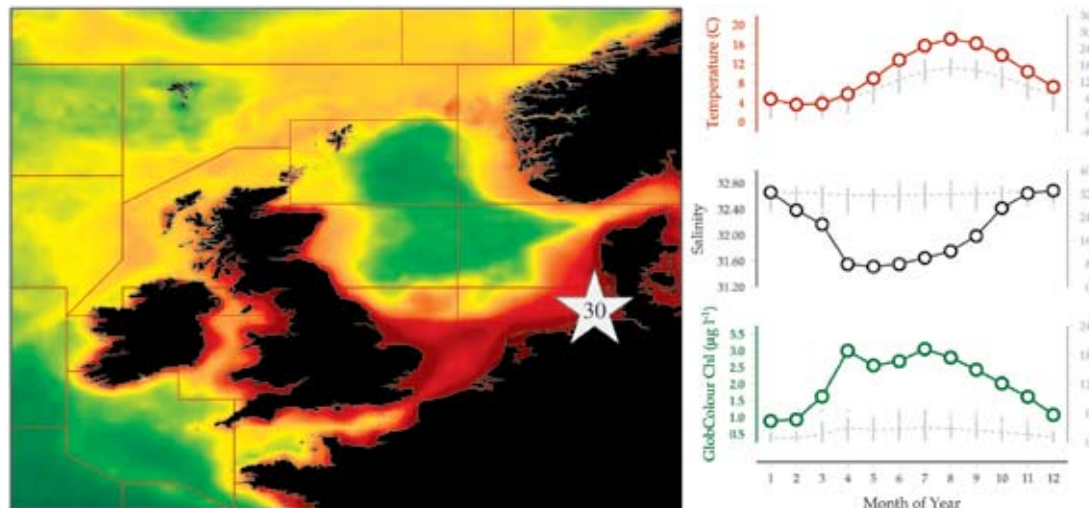


Figure 6.1.1
Location of the Helgoland Roads plankton monitoring area (Site 30), plotted on a map of average chlorophyll concentration, and its corresponding environmental summary plot (see Section 2.2.1).

The Helgoland Roads time-series, located at the island of Helgoland in the German Bight, approximately 60 km off the German mainland (54°11'N 7°54'E), is one of the richest temporal marine datasets available. The time-series was initiated in 1962 at the Helgoland Roads site, which is located between the main island of Helgoland and a small sandy outcrop, the so-called “dune”. The location near Helgoland is of particular interest because the site is essentially in a transitional zone between coastal and oceanic conditions, which is seen most clearly in the salinity patterns at Helgoland Roads. Initially, the sampling frequency was thrice weekly, but this was increased to daily in the early 1970s. Since then, the high sampling frequency has provided a unique opportunity to study long-term trends in abiotic and biotic parameters, but also ecological phenomena, such as seasonal interactions between different foodweb components, niche properties, and the dynamics and timing of the spring bloom (Mieruch *et al.*, 2010; Tian *et al.*, 2011).

The measured parameters comprise phytoplankton, temperature, salinity, and nutrient analyses. Inorganic nutrients are determined following the standard photometric method as described in Grasshoff (1976). Phytoplankton counts are carried out using the Utermöhl method. A sample of 25 ml is settled out, unless concentrations are so low as to jeopardize later statistical analyses. In these cases, 50 ml of settled sample are counted. The sampling procedure follows a strict protocol. The whole bottom

of the counting chamber is counted at an objective magnification of 5, 10, and 20 to count organisms of different size classes. For very abundant organisms, only tracks of a known area are counted. This indirect method is only used if the total number of cells of a given taxon amounts to at least 50 cells. Wherever possible, counts are made at the species level, but for problematic groups, a predefined set of size classes is used. The taxon list now contains over 300 entities. Both the phytoplankton and chemical dataseries are fully quality-controlled, based on original data sheets and metadata (Wiltshire and Dürselen, 2004; Raabe and Wiltshire, 2009). The phytoplankton time-series is augmented by the biological parameters zooplankton, rocky shore macroalgae, macro-zoobenthos, and bacteria, providing a unique opportunity to investigate long-term changes at an ecosystem scale.

Seasonal and interannual trends (Figure 6.1.2)

The multiple-comparison plot summarizes some of the general changes in abiotic and biotic conditions seen since 1962. The anomaly plots for temperature and salinity all show increases in these parameters over the last 50 years. Positive anomalies occurred particularly since the late 1980s, when a regime shift was also observed involving several foodweb components (Wiltshire *et al.*, 2008). The Helgoland temperature shifts are largely congruent with the Hadley SST dataset. Analyses by Wiltshire *et al.* (2010) have demonstrated the statistical

significance of these changes, with temperature since 1962 amounting to 1.7°C (Wiltshire *et al.*, 2010). In tandem with the increases in temperature and salinity, nutrient dynamics at Helgoland Roads have also changed considerably, with phosphate concentrations having declined significantly since 1962. Silicate, while exhibiting a more complex pattern of anomalies, has also demonstrated an overall increase. The simultaneous changes in parameters such as silicate, salinity, and Secchi depth (not shown) indicate a change towards more open-water, oceanic conditions.

Long-term trends are also seen in the biota, with diatoms in particular having exhibited an increase in abundance, with a concomitant increase in positive anomalies for total dinoflagellates (see also Wiltshire *et al.*, 2008). This was not a gradual change, but a rapid shift from negative to positive anomalies around 1998. The exact causes for this are still under investigation. Breaking this down to monthly trends, the swing seems to be largely

driven by shifts in autumn and winter. There was also a significant shift in seasonal densities of individual diatom species (*Guinardia delicatula*, *Paralia sulcata*) and in the numbers of large diatoms (e.g. *Cocinodiscus wailesii*), which are difficult for copepods to graze. The large diatom *Mediopyxis helysia* has recently been observed for the first time and now occurs almost throughout the year, with an intensive bloom in spring 2010 (Kraberg *et al.*, 2011). Generally speaking, the spring diatom bloom now appears to start later, if the preceding autumn was very warm (Wiltshire and Manly, 2004). Although not the focus of this report, it is worth noting that species introductions are also occurring in the zooplankton, with the ctenophore *Mnemiopsis leidyi* being the most obvious new species (Boersma *et al.*, 2007). The potential ecological consequences are currently being investigated.

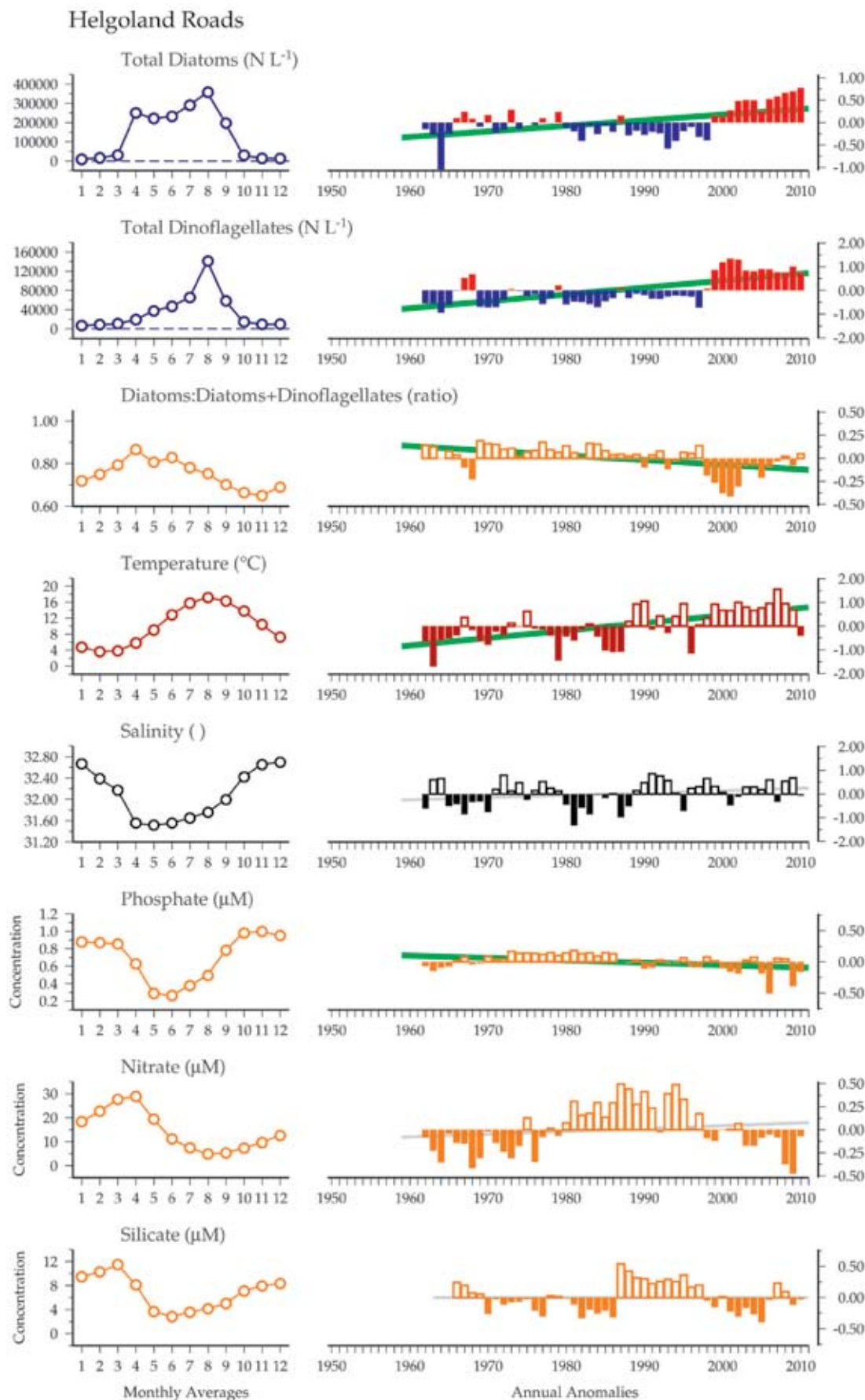
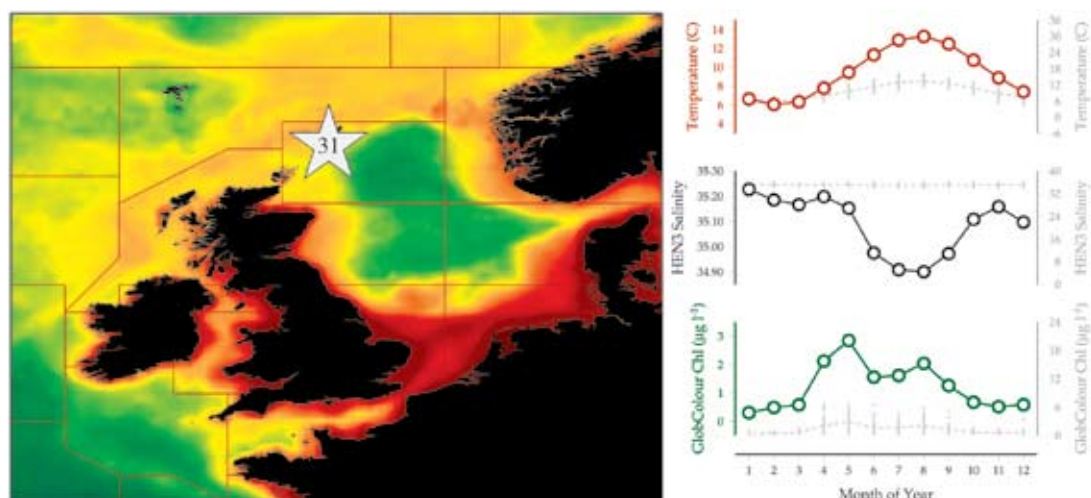


Figure 6.1.2
Multiple-variable comparison plot (see Section 2.2.2) showing the seasonal and interannual properties of select cosampled variables at the Helgoland Roads plankton monitoring site. Additional variables from this site are available online at <http://wgpmc.net/time-series>.

6.2 Scalloway, Shetland Isles (Site 31)

Eileen Bresnan

Figure 6.2.1
Location of the Scalloway, Shetland Isles plankton monitoring area (Site 31), plotted on a map of average chlorophyll concentration, and its corresponding environmental summary plot (see Section 2.2.1).



Marine Scotland Science (MSS) operates a Coastal Ecosystem Monitoring Programme at a number of sites around the Scottish coast. A variety of physical, chemical, and biological parameters are monitored in order to generate datasets that will allow variability and change in the marine ecosystem to be identified and investigated. Scalloway (60°08.06'N 1°16.95'W) in the Shetland Isles has been participating in this monitoring programme since 2002. Samples are collected by the North Atlantic Fisheries College (<http://www.nafc.ac.uk>), and their input to the success of this programme is gratefully acknowledged.

The Shetland Isles lie over 100 miles north of the UK mainland. Atlantic water from west of the UK enters the North Sea between the Orkney and Shetland Islands and also around northeast of Shetland through the Norwegian trench. Scalloway is located on the southwest coast of the Shetland mainland. The monitoring site is moderately exposed, and samples are collected from a pontoon close to the North Atlantic Fisheries College. The sampling site is less than 10 m deep. Temperature is measured using a minilogger, and surface-water samples are taken for salinity and chemical analysis. An integrated tube sampler is used to collect samples for phytoplankton community analysis. Phytoplankton samples are preserved in Lugol's iodine and analysed using the Utermöhl method (Utermöhl, 1958).

Seasonal and interannual trends (Figure 6.2.2)

Temperature demonstrates a distinct seasonality, with lowest temperatures in March and warmest in August. The lowest temperatures are observed during spring (ca. 6°C) and the warmest temperatures towards late summer. The temperature at this site rarely exceeds 14°C. A strong annual cycle can be seen in the phytoplankton community at this site. During winter, phytoplankton growth is reduced. Diatoms begin to increase in spring, whereas dinoflagellates become more abundant during summer. In contrast to other sites in the programme, the summer dinoflagellate *Ceratium* is rarely observed at this site. Instead, members of the dinoflagellate genera *Gonyaulax* and *Alexandrium* can become abundant. During some years, small thecate dinoflagellates such as *Heterocapsa* can form dense blooms during early summer.

Since 2006, diatom abundance has increased throughout summer. This community has been dominated by *Thalassiosira*, *Chaetoceros*, and *Pseudo-nitzschia*. Increased numbers of dinoflagellates during 2008 and 2009 were the result of the high abundance of thecate dinoflagellates such as *Gonyaulax*, *Heterocapsa*, and *Scrippsiella*. Blooms of *Karenia mikimotoi* have also been recorded in this area, and a bloom in 2003 resulted in significant mortalities of farmed fish. Further information and links to the data collected at this site can be found at the Marine Scotland website <http://www.scotland.gov.uk/Topics/marine/science/MSInteractive/Themes/Coastal>.

Scalloway - Shetland Isles

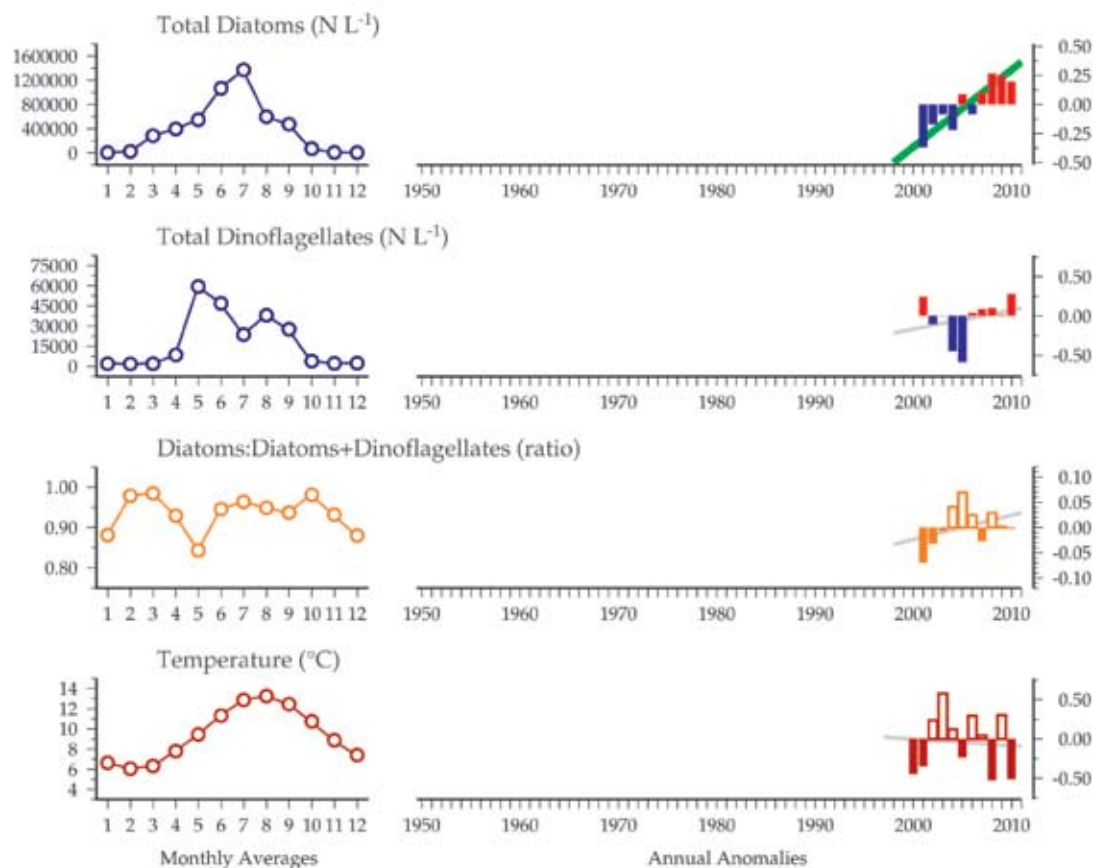


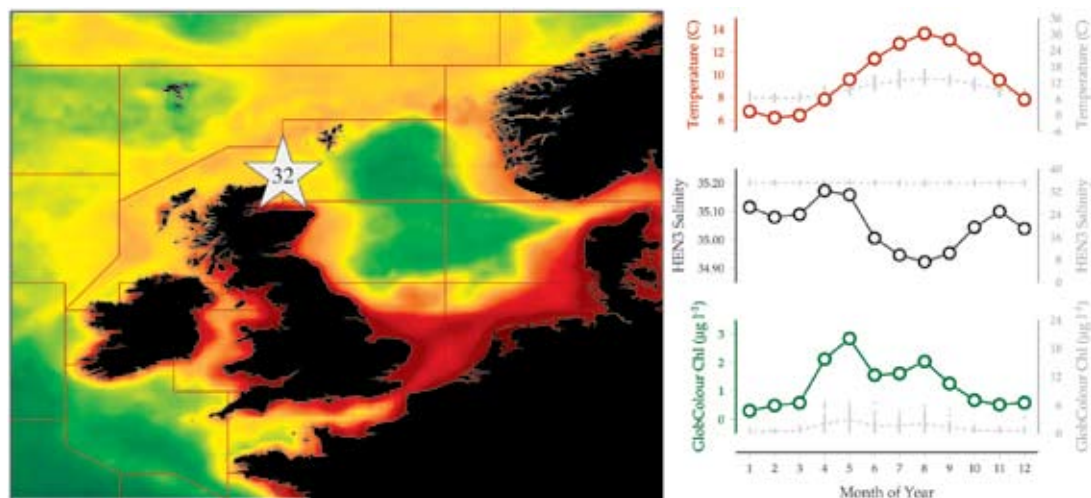
Figure 6.2.2
Multiple-variable comparison plot (see Section 2.2.2) showing the seasonal and interannual properties of select cosampled variables at the Scalloway, Shetland Isles plankton monitoring site. Additional variables from this site are available online at <http://wgpme.net/time-series>.

6.3 Scapa Bay, Orkney (Site 32)

Eileen Bresnan

Figure 6.3.1

Location of the Scapa Bay, Orkney plankton monitoring area (Site 32), plotted on a map of average chlorophyll concentration, and its corresponding environmental summary plot (see Section 2.2.1).



Scapa Bay in Orkney has been participating in the Marine Scotland Science Coastal Ecosystem Monitoring Programme since 2002. Samples are collected by Orkney Islands Council Marine Services and their input to the success of this programme is gratefully acknowledged.

The Orkney Isles are an archipelago of over 70 islands which lie just over 50 miles north of the Scottish mainland. They are separated from the mainland by the Pentland Firth, a tidally dynamic area where the waters of the Atlantic meet the waters of the North Sea.

The Scapa Bay monitoring site is located at Scapa Pier. Temperature is measured using a minilogger, and surface-water samples are taken for salinity and chemical analysis. A 10 m integrated tube sampler is used to collect samples for phytoplankton community analysis. Phytoplankton samples are preserved in Lugol's iodine and analysed using the Utermöhl method (Utermöhl, 1958).

Seasonal and interannual trends (Figure 6.3.2)

Temperature observes a strong seasonality at this site. The lowest temperatures are observed during spring (ca. 6°C) and the warmest temperatures towards late summer. The water temperature rarely exceeds 14°C at this site. Examination of the phytoplankton data reveals a similar pattern in the seasonality of the phytoplankton community as seen in other sites in the monitoring programme. During winter, phytoplankton growth is reduced. A spring

diatom bloom is succeeded by a summer community dominated by dinoflagellates. An autumn diatom bloom of larger diatoms such as *Rhizosolenia* and *Pseudo-nitzschia* spp. type cells is also observed. An increase in the abundance of the diatom *Skeletonema* has been observed since 2005. Since 2006, diatoms have become more abundant throughout summer, increasing the diatoms:diatoms+dinoflagellates ratio at this site. This summer diatom community consists of centric diatoms such as *Thalassiosira* and *Chaetoceros*.

A decrease in the abundance of the dinoflagellate *Ceratium* has been observed until 2009, and more recently, blooms of *Prorocentrum cf. minimum* have been observed during early summer. This site has also been subject to impacts from *Karenia mikimotoi* blooms, with mortalities of fish and lugworms recorded during 2001 and 2006. A *K. mikimotoi* bloom in 2003 resulted in significant mortalities of farmed fish in the area. Previous studies performed at this site have focused on the presence of harmful algal species and shellfish toxicity, as during the late 1990s, high concentrations of paralytic shellfish toxins were routinely recorded in shellfish tissue from Scapa Bay (Joyce, 2005; Bresnan *et al.*, 2005, 2009). Further information and links to the data collected at this site can be found at the Marine Scotland website <http://www.scotland.gov.uk/Topics/marine/science/MSInteractive/Themes/Coastal>.

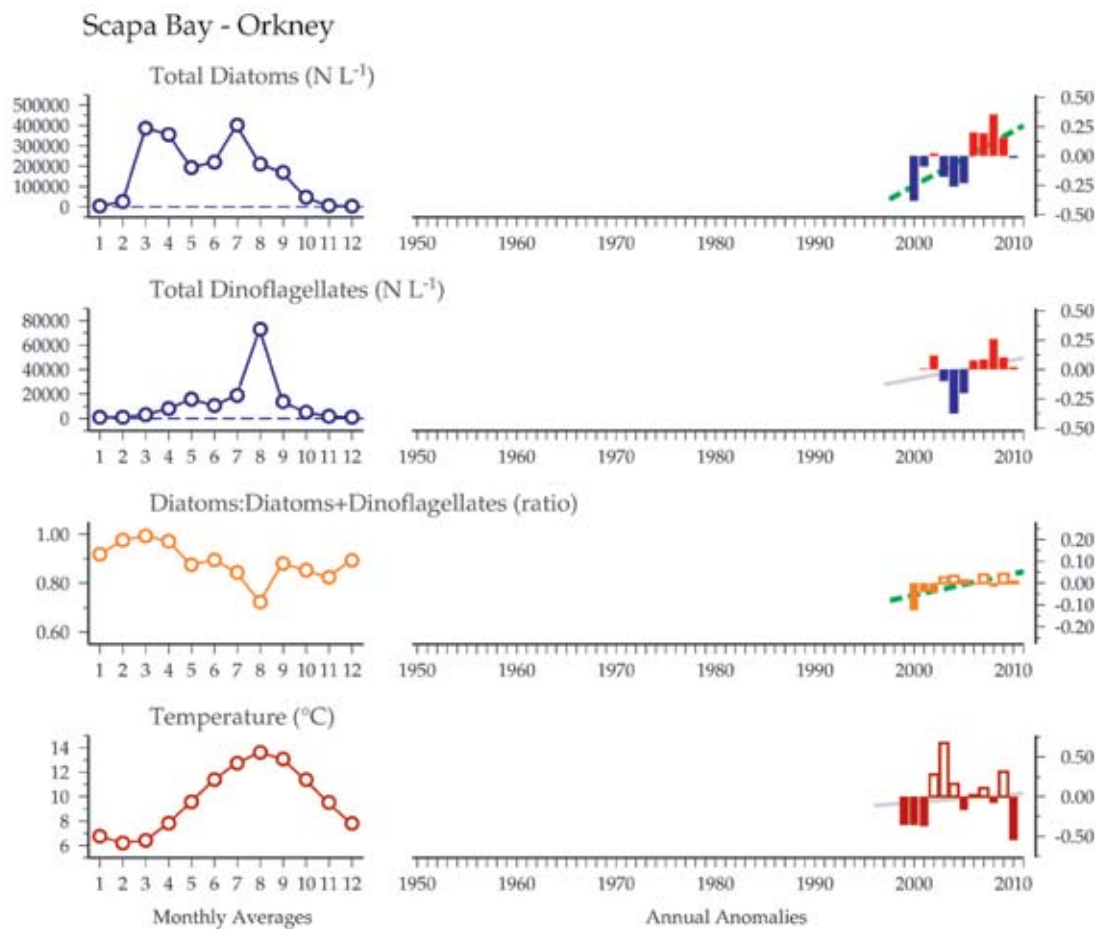


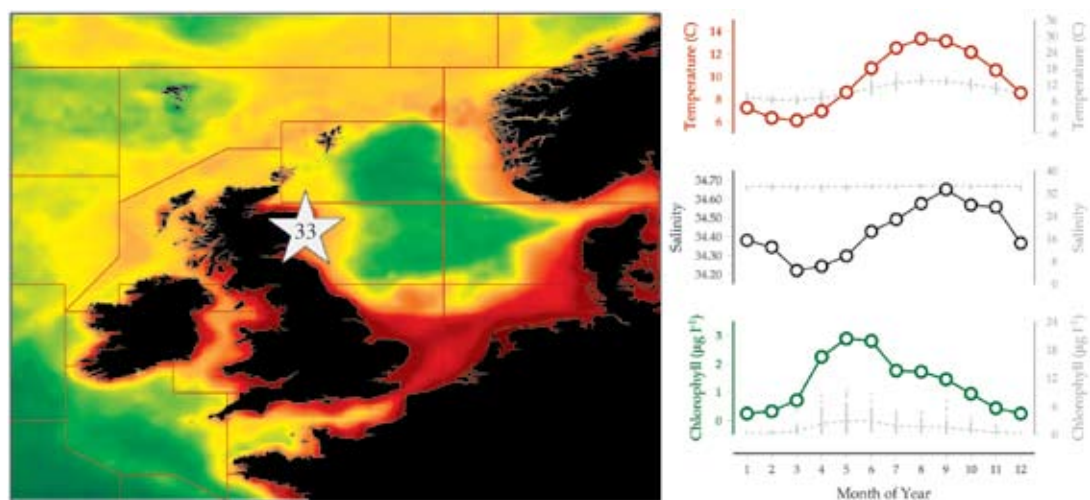
Figure 6.3.2
Multiple-variable comparison plot (see Section 2.2.2) showing the seasonal and interannual properties of select cosampled variables at the Scapa Bay, Orkney plankton monitoring site. Additional variables from this site are available online at <http://wgpme.net/time-series>.

6.4 Stonehaven (Site 33)

Eileen Bresnan

Figure 6.4.1

Location of the Stonehaven plankton monitoring area (Site 33), plotted on a map of average chlorophyll concentration, and its corresponding environmental summary plot (see Section 2.2.1).



The Stonehaven monitoring site (56°57.8'N 002°06.2'W) has been a part of the Coastal Ecosystem Monitoring Programme operated by Marine Scotland Science (MSS) since 1997. This site acts as a reference site to fulfill the requirements of the EU Water Framework Directive and test the development of tools to identify "Good Environmental Status" for the Marine Strategy Framework Directive.

The Stonehaven monitoring site is 50 m deep and is located 5 km offshore. Samples to measure temperature, salinity, and nutrients are collected using a reversing bottle and digital thermometer from surface (1 m) and bottom (45 m) depths. A 10 m integrated tube sampler is used to collect samples for chlorophyll and phytoplankton community analysis. Phytoplankton samples are preserved in Lugol's iodine and analysed using the Utermöhl method (Utermöhl, 1958). Zooplankton samples for community analysis are collected using a 200 µm mesh bongo net. Since 2009, weekly samples have also been taken for total alkalinity and dissolved inorganic carbon measurements. Scanning electron microscopy of selected samples to identify and enumerate the coccolithophores present is also being performed. Samples are collected weekly, weather permitting. Information about the zooplankton community at this site can be found in the ICES Zooplankton Status Report.

Seasonal and interannual trends (Figure 6.4.2)

The Stonehaven site is a dynamic site, with strong southerly flow. It is well mixed for most of the year. Temperature and salinity show a strong seasonality. The lowest temperatures are observed during spring (ca. 6°C) and the warmest towards late summer. The temperature at this site rarely exceeds 14°C. Salinity follows a similar pattern, with lowest salinity observed in spring and highest in late summer. Nutrients show a seasonal pattern typical to high latitudes, with the concentration of total nitrates, phosphate, and silicate increasing over winter, when phytoplankton growth is reduced, and decreasing during the phytoplankton growing period.

The phytoplankton community observes a strong seasonality at the Stonehaven monitoring site. During winter, phytoplankton growth is reduced. Diatom cells begin to increase in abundance from March, and during most years, there is a strong spring bloom dominated by diatom genera such as *Chaetoceros*, *Thalassiosira*, and *Skeletonema*. Dinoflagellates such as *Ceratium* become a more important part of the phytoplankton community during summer. In some years, but not all, an autumn diatom bloom of larger diatoms such as *Rhizosolenia* and *Pseudo-nitzschia* spp. type cells can be observed.

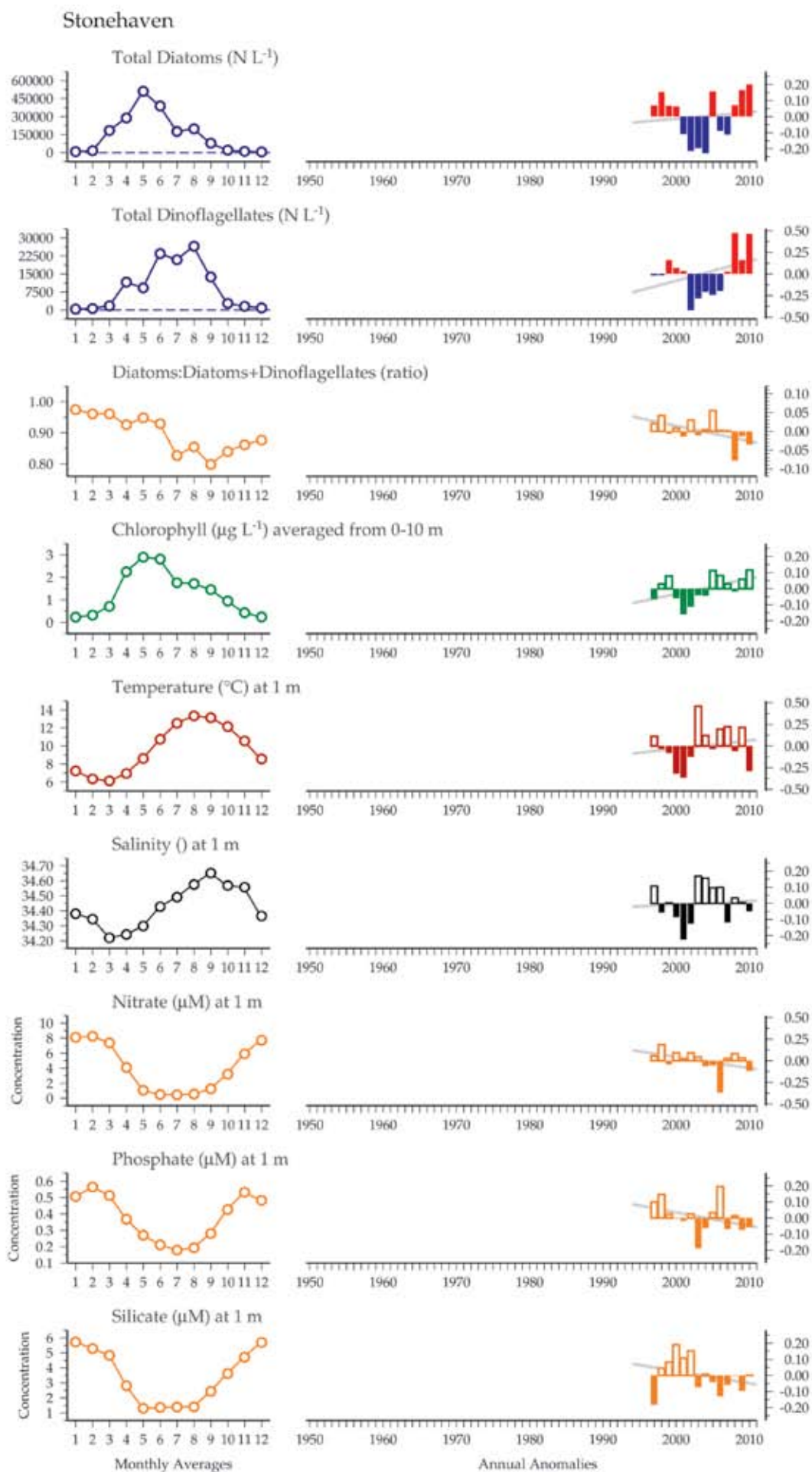
A number of changes have been observed in the phytoplankton community at this site since monitoring began. A period of reduced annual chlorophyll concentrations was observed from 2000 to 2004. This corresponds to a period when the intensity of the spring bloom was reduced. Chlorophyll concentrations increased again in 2005, with *Skeletonema* observed at high cell densities during the spring bloom. This increase in *Skeletonema* was also observed at the other monitoring sites in the programme.

Since 2000, a decrease has been observed in the large thecate dinoflagellates, such as *Ceratium*, that occur during summer, whereas dense blooms of small *Prorocentrum cf. minimum* cells have been observed in early summer. This change in *Ceratium* has also been observed at other sites in the programme and also in the Continuous Plankton Recorder data (Hinder *et al.*, 2012).

A preliminary description of the hydrography, chemistry, and phytoplankton community can be found in Bresnan *et al.* (2009). A description of a transect survey around this monitoring site can be found in McCollin *et al.* (2011). Further information and links to the data collected at this site can be found at the Marine Scotland website <http://www.scotland.gov.uk/Topics/marine/science/MSInteractive/Themes/Coastal>.

Figure 6.4.2

Multiple-variable comparison plot (see Section 2.2.2) showing the seasonal and interannual properties of select cosampled variables at the Stonehaven plankton monitoring site. Additional variables from this site are available online at <http://wgpme.net/time-series>.



6.5 English Channel REPHY sites (Sites 34–35)

Dominique Soudant (primary contact) and Alain Lefebvre

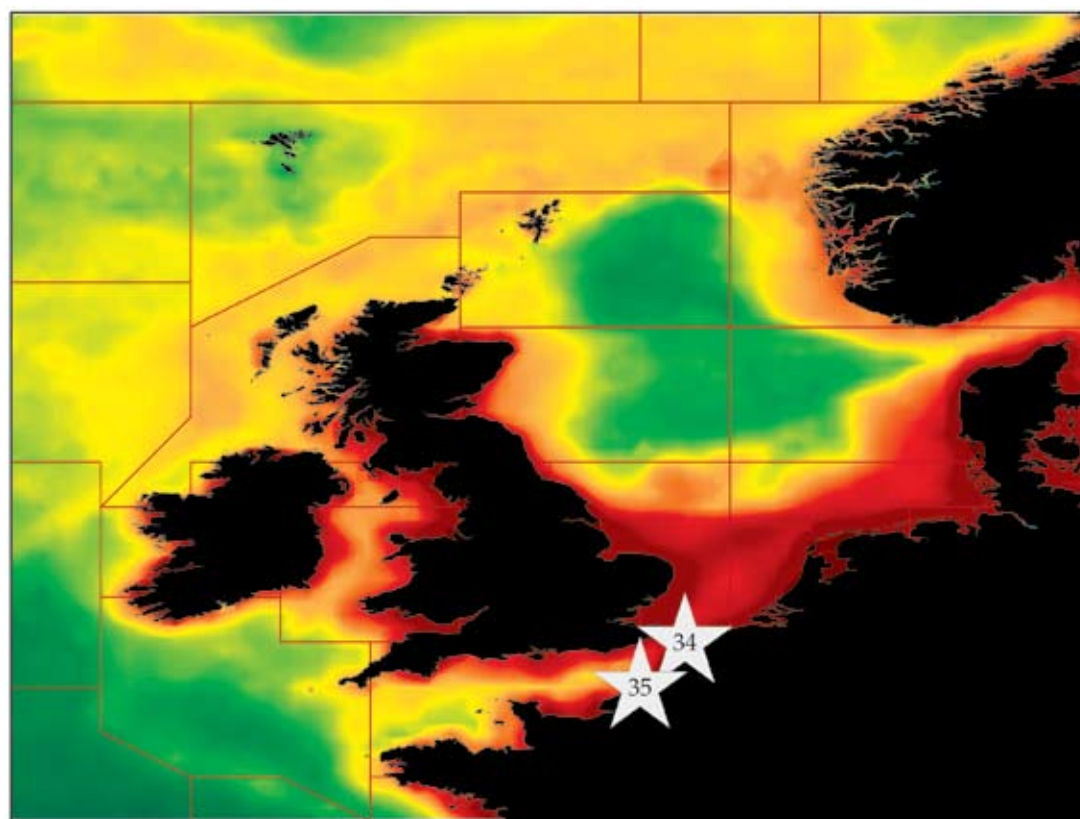
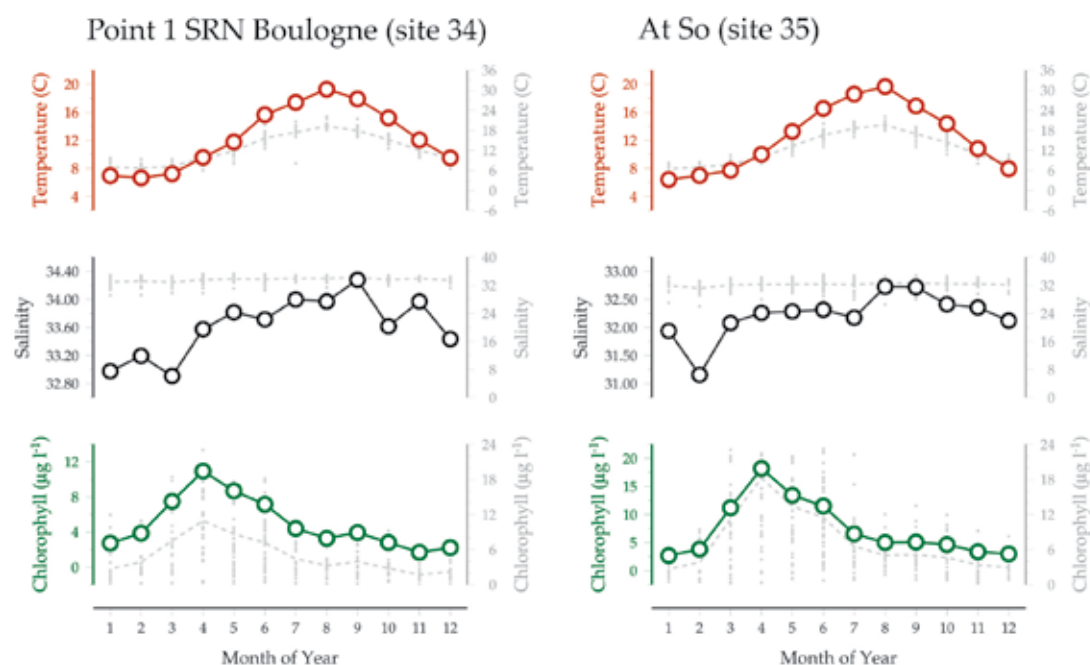


Figure 6.5.1

Locations of the REPHY English Channel plankton monitoring area (Sites 34–35), plotted on a map of average chlorophyll concentration, and their corresponding environmental summary plots (see Section 2.2.1).



The French Phytoplankton and Phycotoxin Monitoring Network (REPHY) was set up in 1984 with three objectives: to enhance knowledge of phytoplankton communities, to safeguard public

health, and to protect the marine environment (Belin, 1998). Phytoplankton along the French coast has been sampled up to twice a month since 1987 at 12 coastal laboratories. For that purpose, the French

coast is divided into a hierarchy of sites and subsites common to three regional networks: the English Channel, the Bay of Biscay, and the Mediterranean Sea.

Within the English Channel, the REPHY Point 1 SRN Boulogne and At So sites are both shallow and characterized by a macrotidal regime, especially the latter, which is also more sheltered. Sampling started in 1987 at At So and five years later at Point 1 SRN Boulogne. Ancillary measurements of temperature, salinity, chlorophyll *a* and phaeopigments, inorganic nutrients concentrations, and turbidity are also routinely measured (usually 15 samples per year). Oxygen was incorporated in 2007 at both sites.

Seasonal and interannual trends (Figures 6.5.2, 6.5.3)

Seasonal cycles of chlorophyll as a measure of total phytoplankton biomass are clearly unimodal at both sites, with maxima in April. Chlorophyll values are ca. 50% greater at At So, but peak values at both sites generally exceed 10 µg l⁻¹. Diatom seasonal cycles at both sites featured a summer high and a winter low. Maximum values at Point 1 SRN Boulogne are

usually observed in August after exhibiting relatively high values from March onwards, and then decline sharply until reaching minimum values in late autumn. In contrast, the seasonal maximum at At So was earlier in the year (June), with a smoother decline. The seasonal cycle of dinoflagellates at both sites was characterized by maxima in July–August and minima in December–February. A secondary peak in May was also observed at Point 1 SRN Boulogne. The diatoms:diatoms+dinoflagellates ratio covaries at both sites, with marked minima in August. Dominant taxa include *Chaetoceros socialis*, *Guinardia delicatula*, and various species of *Pseudo-nitzschia* among the diatoms and *Prorocentrum*, *Protoperidinium*, and *Gymnodinium* among dinoflagellates. *Phaeocystis globosa* is also abundant, especially during the first half of the year.

Increasing salinity has been observed for both time-series, along with significant chlorophyll increases. Total dinoflagellates abundance featured strong increases at both sites ($p < 0.01$), corresponding to strong decreases in the diatoms:diatoms+dinoflagellates ratio at both sites. Diatoms were increasing (non-significant) at the Point 1 SRN site, whereas no apparent trend was found in At So.

REPHY Point 1 SRN Boulogne

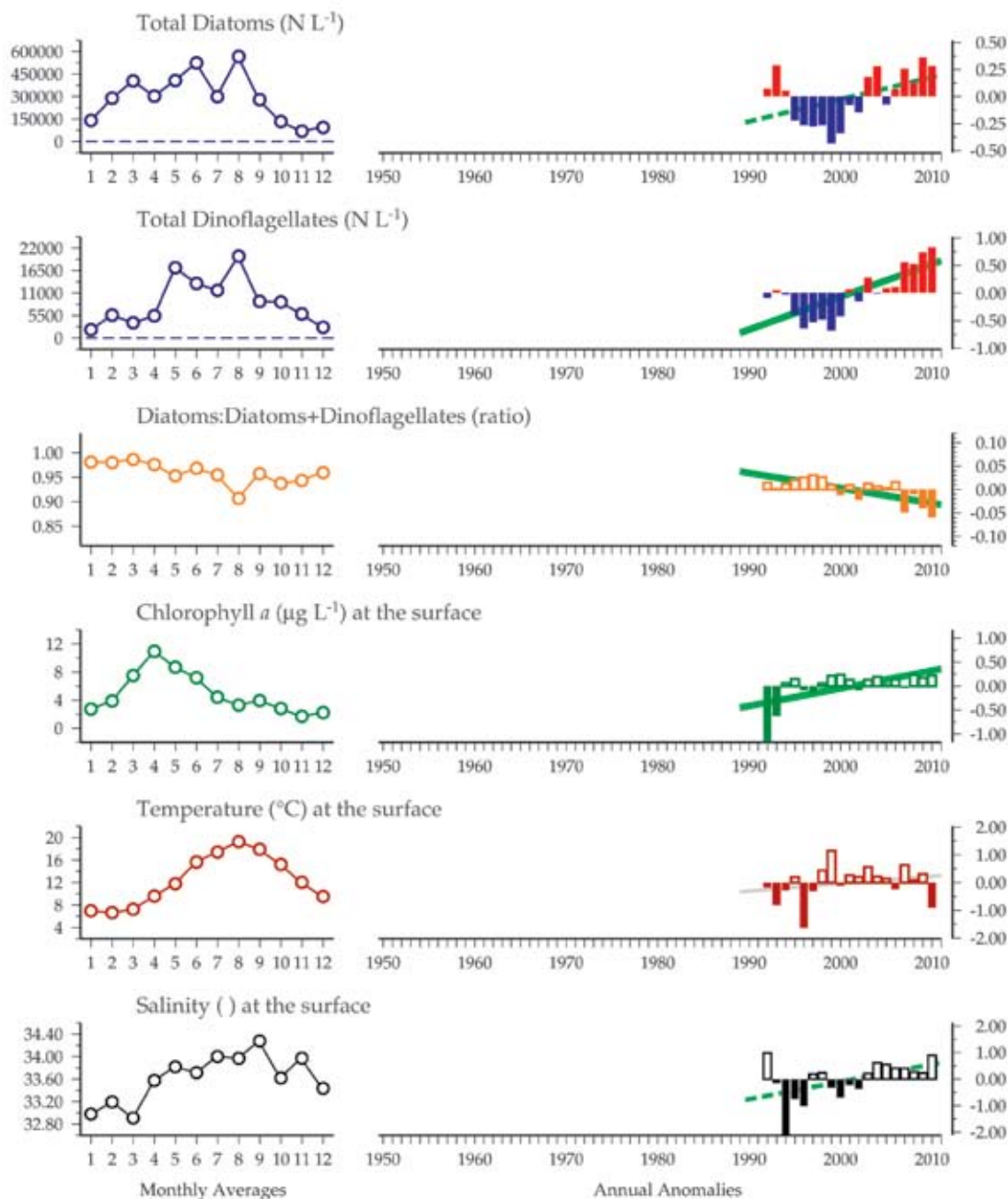
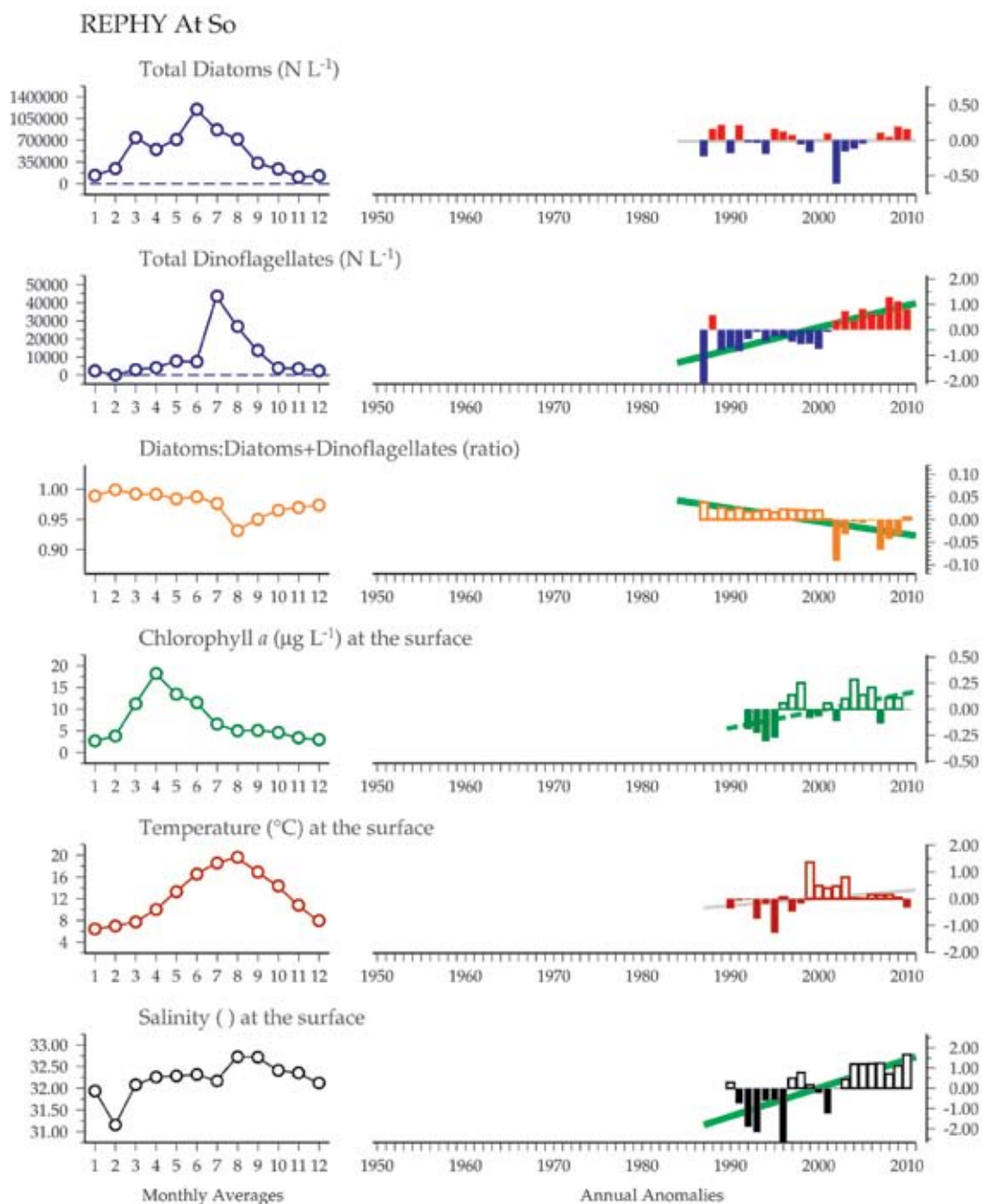


Figure 6.5.2
Multiple-variable comparison plot (see Section 2.2.2) showing the seasonal and interannual properties of select cosampled variables at the REPHY Point 1 SRN Boulogne plankton monitoring site. Additional variables from this site are available online at <http://vogpme.net/time-series>.

Figure 6.5.3

Multiple-variable comparison plot (see Section 2.2.2) showing the seasonal and interannual properties of select cosampled variables at the REPHY At So plankton monitoring site. Additional variables from this site are available online at <http://wgpme.net/time-series>.



6.6 Plymouth L4 (Site 36)

Claire Widdicombe, Glen Tarran, and Tim Smyth

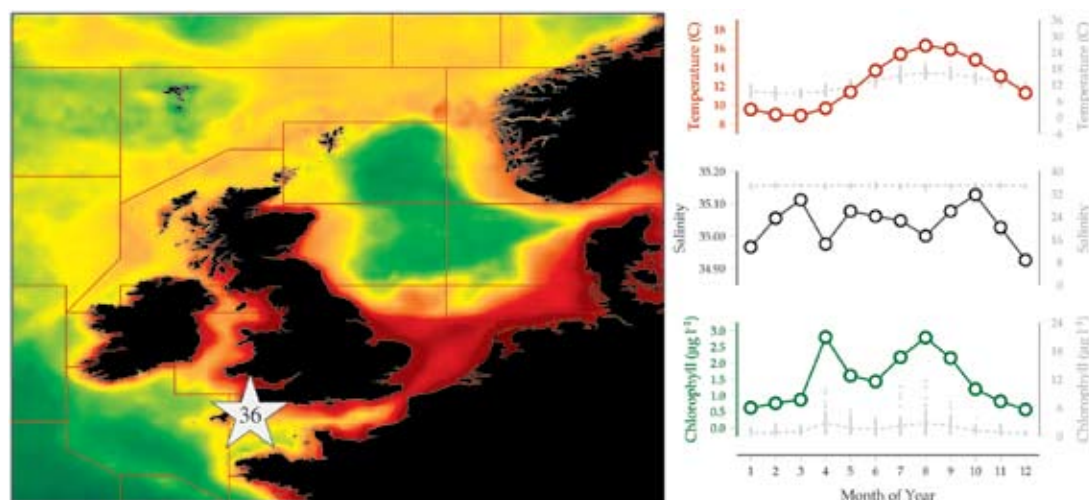


Figure 6.6.1
Location of the Plymouth L4 plankton monitoring area (Site 36), plotted on a map of average chlorophyll concentration, and its corresponding environmental summary plot (see Section 2.2.1).

The phytoplankton and microzooplankton time-series at Plymouth station L4 (Figure 6.6.1; 50°15'N 4°13'W) was established in 1992 to complement the ongoing zooplankton time-series (Harris, 2010), and continues to be sampled at weekly intervals (weather permitting). Station L4 is located in the western English Channel approximately 16 km southwest of Plymouth, where the water depth is ca. 50 m and conditions are typical of temperate coastal waters, with mixing during autumn and winter and weak stratification during spring and summer. Hydrodynamic variability, resulting from the interchange between wind-driven oceanic waters and rain-induced estuarine outflow, leads to a dynamic and variable plankton community.

Water samples for microscopy are collected using Niskin bottles from a depth of 10 m, and a 200 ml subsample is immediately preserved with acid Lugol's iodine solution for identifying and enumerating phyto- and microzooplankton species composition, and a second 200 ml subsample is preserved with buffered formaldehyde for the enumeration of coccolithophores (Widdicombe *et al.*, 2010). All analyses are conducted in the laboratory using light microscopy and the Utermöhl (1958) counting technique. Since April 2007, additional weekly samples are also collected from the surface, 10 m, 25 m, and 50 m for the live enumeration of small phytoplankton, bacteria, and heterotrophic flagellates by analytical flow cytometry. Sea surface temperature (SST) measurements have been made since 1988 using a mercury-in-glass thermometer submerged in an aluminium bucket containing

surface water. Triplicate surface chlorophyll *a* samples are collected and analysed using a Turner fluorometer after filtration and extraction in 90% acetone. Surface-water nutrient concentrations (nitrate, nitrite, phosphate, and silicate) are available as far back as 2000, and water-column profiles of temperature, salinity, and fluorescence have been recorded using a conductivity-temperature-depth (CTD) instrument since 2002. All data are generated at the Plymouth Marine Laboratory and are available for download or via the links to Pangea and BODC at the Western Channel Observatory website www.westernchannelobservatory.org.uk.

Seasonal and interannual trends (Figure 6.6.2)

The phytoplankton community at station L4 exhibits strong seasonal and interannual patterns in abundance and composition. Surface chlorophyll *a* concentrations show a distinct seasonal cycle, with lowest values recorded during autumn and winter, two distinct peaks during spring and late summer, and variable values in between. Phytoplankton, enumerated by microscopy, are also less abundant during autumn and winter, when the community composition is relatively stable. An abrupt change between March and early May heralds the onset of the spring bloom, when phytoplankton are more abundant and species composition is more variable. This continues throughout summer until autumn, when the phytoplankton community becomes relatively stable again. Phytoflagellates numerically dominate the phytoplankton (ca. 87%) and exhibit

similar seasonal patterns in total abundance. Diatoms, however, follow a pattern of low abundance during winter, show a small increase during spring, but peak in abundance during summer, and this can continue through autumn. The floristic composition of the diatoms is also highly variable both seasonally and interannually (Widdicombe *et al.*, 2010). Coccolithophores, dominated almost entirely by *Emiliania huxleyi*, regularly bloom in the western English Channel, typically during late summer, but occasionally blooms have been monitored at station L4 during late spring.

Dinoflagellate abundance is generally low during winter and spring months, but as sea surface temperatures warm during summer, dinoflagellates steadily increase in abundance, often culminating in intensive, but brief, blooms dominated by either *Karenia mikimotoi* or *Prorocentrum minimum*. Colourless dinoflagellates form a comparatively minor component and are, on average, sevenfold lower in abundance than the main group of dinoflagellates. However, they too are relatively rare during winter and most abundant between late spring and early autumn when phytoplankton prey are most numerous. Unsurprisingly, the ciliates also peak in abundance between spring and autumn, with a gradual transition to and from low levels in winter. Enumeration of the small phytoplankton and microbial fraction by flow cytometry since 2007 demonstrates a different seasonal pattern. Concentrations of *Synechococcus* cyanobacteria, as well as picoeukaryotes, are, on average, lower during spring and summer and highest during autumn. However, their abundance is highly variable, particularly during spring and summer. The patterns observed in the phytoplankton, microzooplankton, and microbial groups are reflected in the measured nutrient concentrations. Generally, nitrate and nitrite, phosphate, and silicate are highest during winter, but the onset of the spring bloom and weak stratification, coupled with continued phytoplankton growth throughout summer, rapidly depletes nutrient concentrations, and levels generally do not recover again until winter.

Analysis of the L4 time-series demonstrates a generally consistent year-on-year seasonal pattern in the different phytoplankton, microzooplankton, and microbial groups. However, interannual variability of the species composition and magnitude of their abundance is considerable, thus making it difficult to observe clear long-term changes in the different components. However, the data do suggest that diatoms, in general, are decreasing, whereas coccolithophores and dinoflagellates are increasing at certain times of the year. A series of negative anomalies since 2006 implies that diatoms are decreasing, particularly between January and June, which suggests that the magnitude of the spring diatom bloom is weakening. At the same time, coccolithophores are becoming more common, as demonstrated by positive anomalies for most years since 2003, particularly for the period between April and June. The observed warming magnitude of ca. 0.5°C in the western English Channel over the past 50 years or so (Smyth *et al.*, 2010) is likely to favour dinoflagellates (Widdicombe *et al.*, 2010). A change in the timing, magnitude, and floristic composition of phytoplankton communities may have an important impact upon zooplankton, meroplankton, and carbon export to the benthos, as well as the potential of harmful species to affect commercial fisheries and affect human health, and thus validates the importance of time-series studies such as at station L4.

Plymouth L4

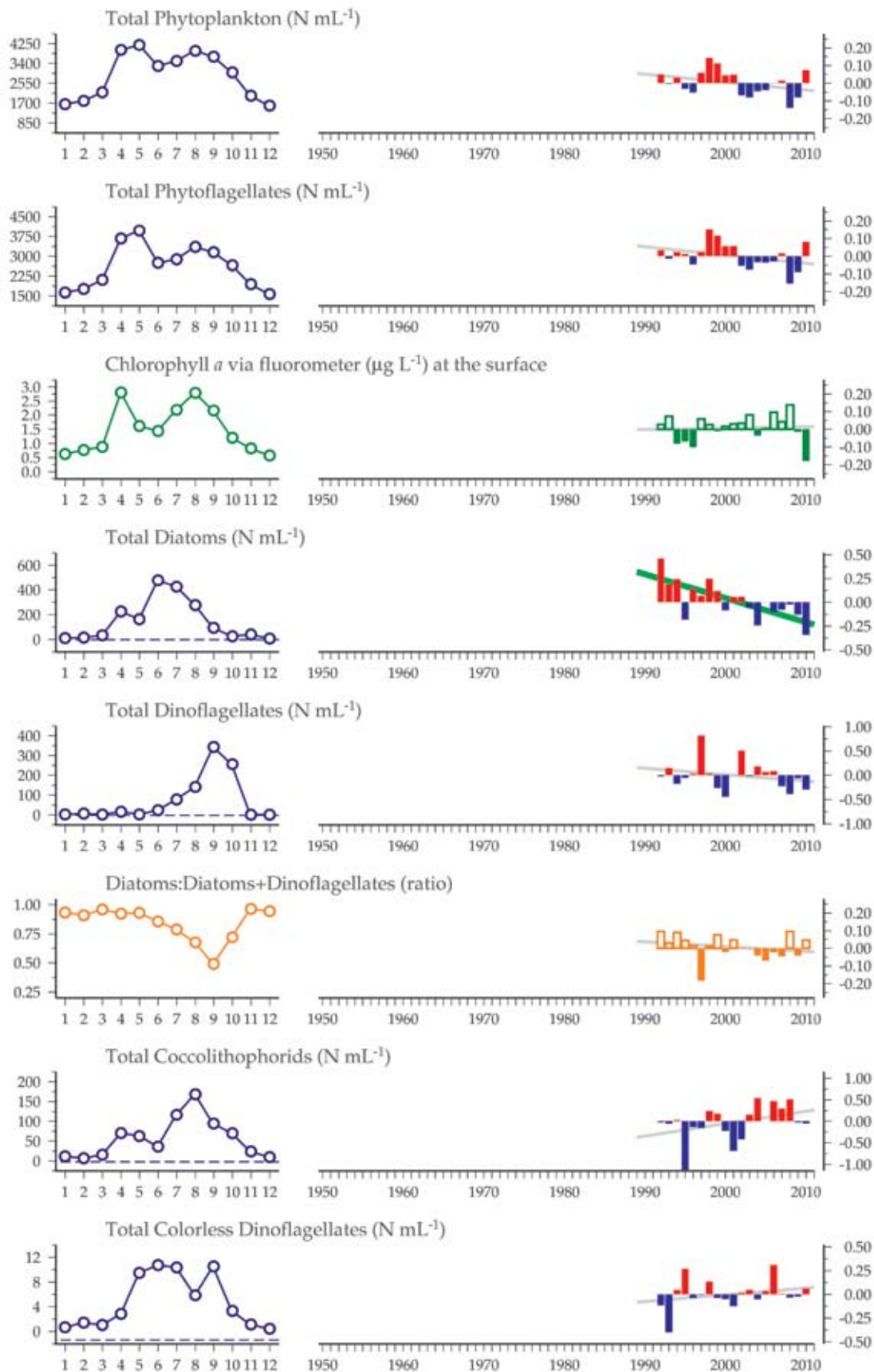
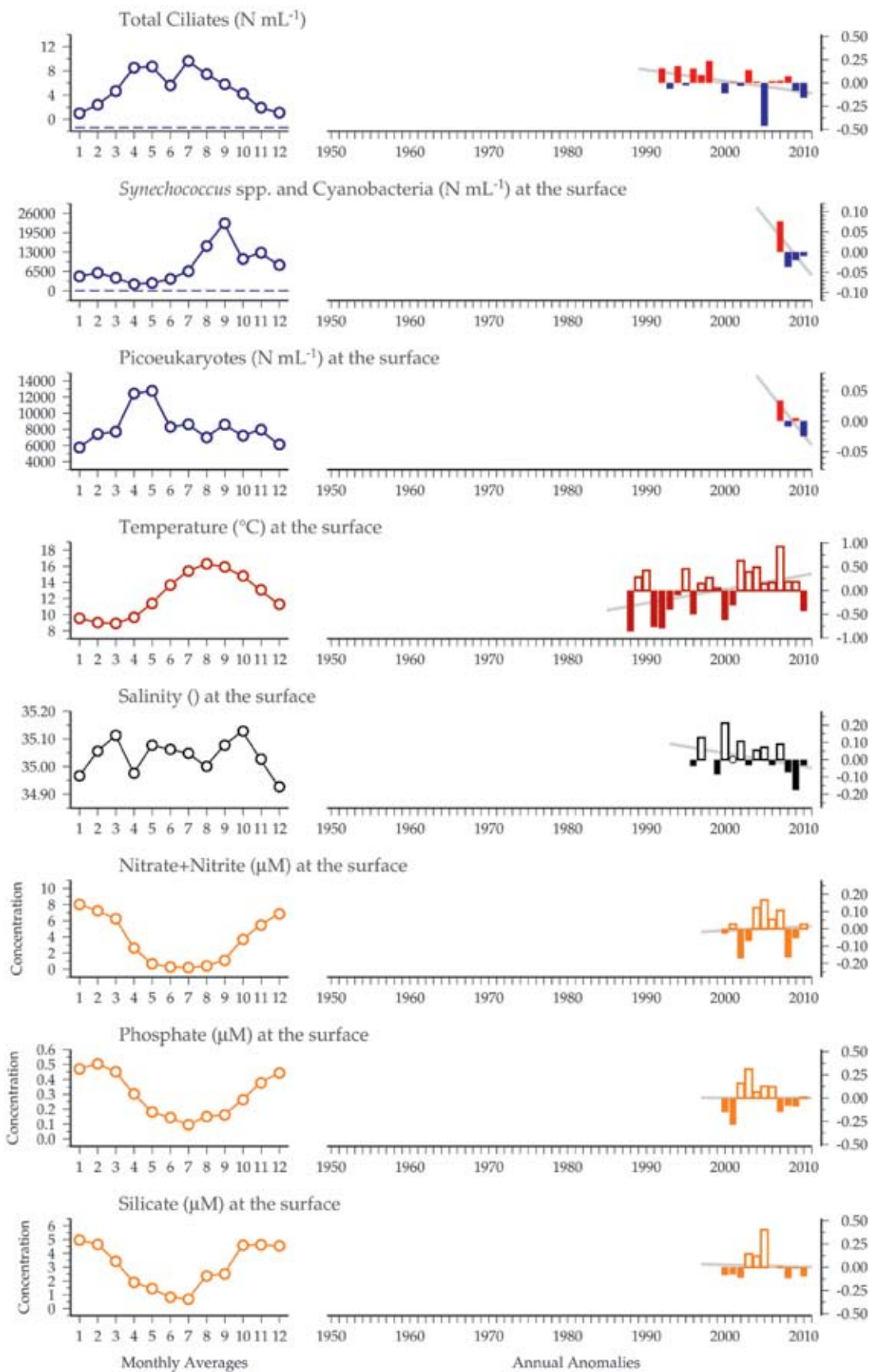


Figure 6.6.2 (continued overleaf)
Multiple-variable comparison plot (see Section 2.2.2) showing the seasonal and interannual properties of select cosampled variables at the Plymouth L4 plankton monitoring site. Additional variables from this site are available online at <http://hogpme.net/time-series>.

Figure 6.6.2 continued.





Preserved plankton samples being settled to concentrate cells for microscopic analysis.
Photo: Plymouth Marine Laboratory.

7. PHYTOPLANKTON AND MICROBIAL PLANKTON OF THE NORTHEAST ATLANTIC SHELF

Joe Silke, Kevin Kennington, Eileen Bresnan, and Caroline Cusack

The Northeast Atlantic Shelf region includes the sites from all coastal waters of Ireland, the Irish Sea, and western Scottish and Norwegian Sea waters. The region was defined by WGPME to include locations on the northern margin of Europe that were outside the North Sea/English Channel influence. The character of sites in the region are shallow, coastal-water sites ranging from sheltered bays on the south coast of Ireland and fjordic sea lochs of Scotland to fully exposed locations on the west coasts of Ireland and Scotland. Bathymetry of the region ranges from shallow embayments to regions of shallow, exposed continental-shelf waters. The topography of the shelf drops rapidly to 80–100 m within 20 km of the coast, where it extends to the shelf edge as a relatively flat plateau.

Waters are generally fully saline, with all of the bay sites fully open to oceanic waters. Although the sites would all be considered marine, local impact on salinity from regional river-basin discharge may be observed during seasonal run-off. In terms of anthropogenic inputs, the sites ranged from isolated areas, with little adjacent habitation, to sites close to densely populated areas, moderately industrial zones, and, in some cases, land intensively used for agriculture.

Water currents in the region are dominated by a north-flowing coastal current which flows during summer in a continuous pathway from the northern Cornish coast along the west of Ireland to Malin Head and onwards to The Minch, with average residual velocities $>7.5 \text{ cm s}^{-1}$ (Fernand *et al.*, 2006). This pathway is potentially a rapid transport mechanism for contaminants and exotic species of plankton. The region is also exposed to Atlantic weather systems, with average wind speeds in January of 12 m s^{-1} . Even during the calmest month of June, the average is 7 m s^{-1} . Consequently, wind plays a significant role in determining the residual circulation of the region. There is evidence that circulation around the southwestern tip of Ireland exists. It has also been demonstrated that this “gateway” may be closed by prevailing southwesterly winds leading to a gyre in the northwestern Celtic Sea. When easterly winds are established, this gateway opens and Celtic Sea water flows around into the mouths of the bays of southwest Ireland. It has been demonstrated that this may determine the advection and dispersion of nutrients and phytoplankton, and is likely to play a significant role in determining the timing and location of harmful algal events in the region (Raine *et al.*, 1993). Water circulation in the Irish Sea is modulated by the presence of fronts and gyres in the central west Irish Sea.

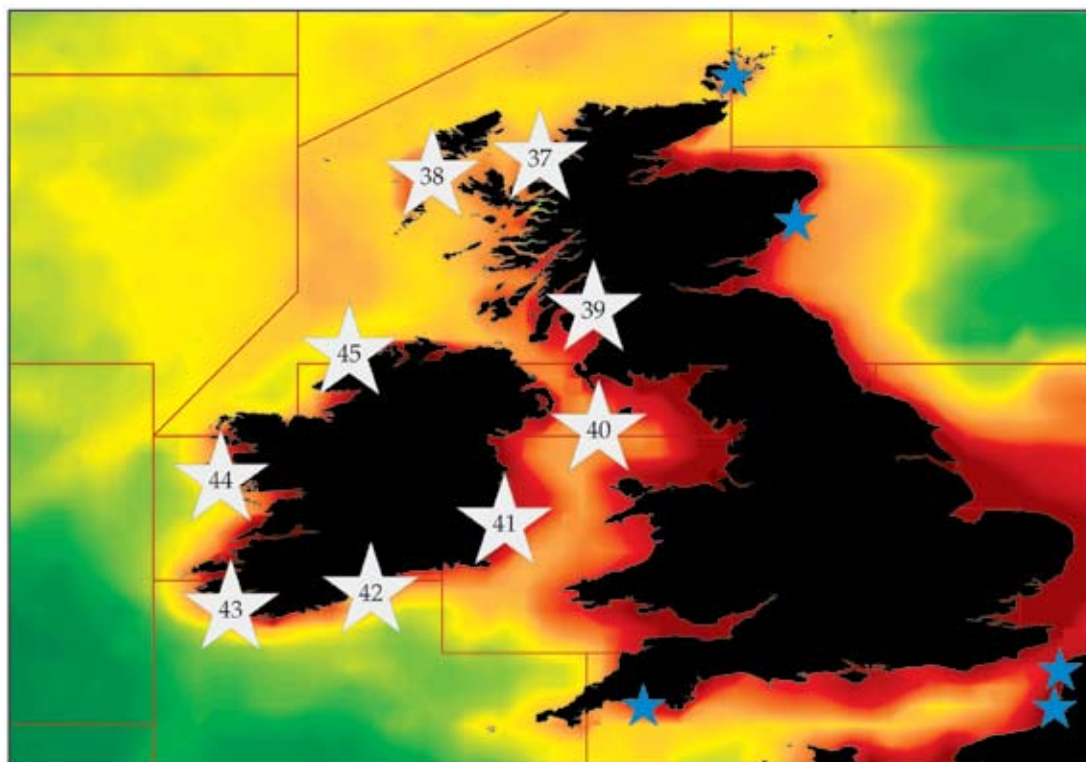


Figure 7.1
Locations of the Northeast Atlantic Shelf plankton monitoring areas (Sites 37–45) plotted on a map of average chlorophyll concentration. Blue stars indicate locations of sites located in the adjacent North Sea and English Channel region (see Section 6).

Time-series of phytoplankton data from the Atlantic Shelf exhibit a typical seasonal pattern of temperate waters, with considerable geographical and temporal variation. The well-mixed winter conditions lead to a region-wide strong spring bloom observed at all sites. The ensuing decrease in nutrient levels lead to a variable summer period characterized by stratified conditions in coastal areas and periodic blooms of mixed or occasionally monospecific diatom and dinoflagellate composition. The growth period tails off in autumn, when a secondary bloom may occur in response to increased mixing and breakdown of the summer thermocline. The seasonal cycle returns to a quiescent winter phase, with generally mixed conditions, light limitation, and increased nutrients return.

Seasonal stabilization and destabilization of the water column in this region accounts for most of the natural variation in both phytoplankton species composition and biomass. Much of the remaining natural variability can be explained by the interaction of phytoplankton with a number of oceanographic features and processes, such as the presence of tidal and thermohaline fronts, wind, topographically associated coastal upwelling, advection landward of offshore water masses, and the flow of coastal and oceanic currents. In estuarine waters, the scenario is somewhat reversed, and although seasonality is important in broad terms, the structure of

phytoplankton populations is determined more by local factors operating over much smaller time-scales in the order of days and weeks.

Scottish sites

The northern sites of this region were selected from Scottish coastal waters and were monitoring sites maintained by Marine Scotland Science as part of their Coastal Ecosystem Monitoring Programme. The most northerly, Loch Ewe, is a sea loch on the northwest coast of Scotland. Monitoring has been performed at this site since 2002. Loch Ewe is a fjordic sealoch that opens to the north and has a strong tidal circulation. Situated on the island of North Uist on the Western Isles, Loch Maddy has also been included in the programme since 2003. It is a unique site with a diverse saline lagoon system opening into the sea loch, which contains a mix of rocky reefs and soft sediment habitats. It has been designated a marine special area of conservation. Farther south, within the Firth of Clyde, is Millport on the island of Cumbrae. The Clyde is a wide fjord containing a deep basin separated from a north channel by a sill. A front exists above the sill throughout the year, separating the tidally mixed water in the north channel from the more stratified Firth. Phytoplankton monitoring has been performed at this site since 2005.

Irish Sea

Two sites were included in the Irish Sea proper, which were located at the Isle of Man and one of the Irish coastal regions along the east coast.

The Isle of Man Cypris Station was established in the 1950s, approximately 5 km west of Port Erin in water of 37 m depth. Initially, measurements of salinity, temperature, and soluble reactive phosphorus were recorded (1954). Over the years, other variables were also added, including silicate (1958), total oxidized nitrogen (1960), chlorophyll (1966), and phytoplankton (1995).

This programme continues today and provides one of the longest nutrient chemistry time-series in existence. Data collected from this site have been published in several peer-reviewed publications. Mean annual sea surface temperature at the site has risen by approximately 0.7°C over the duration of the time-series (1904–2012). These temperature increases follow the broad-scale northern hemisphere atmospheric temperature shifts. Eight of the ten warmest ranked years for local SST have occurred in the last 10 years. There is a positive correlation between the Port Erin breakwater salinity measurements and the North Atlantic Oscillation (NAO) index, reflecting the tendency for warmer European winters during NAO positive years.

Nutrient salt concentrations are at a maximum during winter. There is considerable interannual variation in the timing of the winter nutrient maxima, which, at the Cypris Station, occurs

between January and March. In spring, with increasing insolation and phytoplankton growth, stocks of nutrient salts are rapidly depleted, reaching a minimum around late spring. Levels remain low until late summer and early autumn, when organic-decay cycles regenerate nutrient salts to the water column. Winter inorganic nutrient data represent the basal or resting state when biological processes have come to a halt and the regeneration of nutrients is complete (Gowen *et al.*, 2002).

Irish coastal sites

The remaining sites are located in coastal areas around Ireland. These five sites are the combination of a national monitoring programme in place since 1990 for the monitoring of harmful algal blooms. The five sites are made up of five coastal stretches (east, south, southwest, west, and northwest), and the individual sample sites where full phytoplankton counts were made within each of these regions were quality checked and combined to represent each of these regions. The east stretch represents sites on the Irish Sea side of Ireland consisting of two sheltered shallow coastal bays. The southern sites are more exposed, with openings to the Celtic Sea. Sites in the southwest were made up of locations in the long inlets in this area. These sites were also in locations important to the aquaculture industry, particularly mussel farming. Farther up along the west coast were locations of both shellfish farming and salmon farms, which have a particular interest in the phytoplankton monitoring programme and provide useful access to samples.

7.1 Loch Ewe (Site 37)

Eileen Bresnan

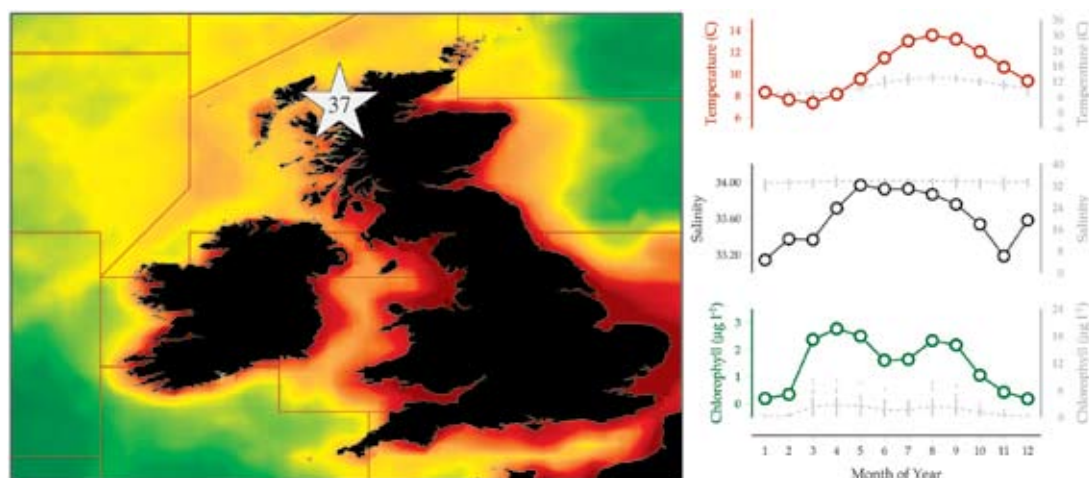


Figure 7.1.1

Location of the Loch Ewe plankton monitoring area (Site 37), plotted on a map of average chlorophyll concentration, and its corresponding environmental summary plot (see Section 2.2.1).

Loch Ewe (Site 37, 57°50.14'N 5°36.61'W), a sea loch on the west coast of Scotland, has been part of the Marine Scotland Science Coastal Ecosystem Monitoring Programme since 2002. This site acts as a reference site to fulfill the requirements of EU Water Framework Directive and to test the development of tools to identify "Good Environmental Status" for the Marine Strategy Framework Directive. Samples have been collected by Isle of Ewe Shellfish and their input to the success of the programme is gratefully acknowledged.

The Loch Ewe monitoring site is 40 m deep and located at the northerly face of the sea loch. Samples are collected weekly. Samples to measure temperature, salinity, and nutrients are collected using a reversing bottle and digital thermometer from surface (1 m) and bottom (35 m) depths. A 10m integrated tube sampler is used to collect samples for chlorophyll and phytoplankton community analysis. Phytoplankton samples are preserved in Lugol's iodine and analysed using the Utermöhl method (Utermöhl, 1958).

Seasonal and interannual trends (Figure 7.1.2)

Water movement in this loch is strongly influenced by wind and tide. The loch faces north and has variable exchange with the North Minch, which is influenced by influxes of Atlantic water. Temperature and salinity show a strong seasonality. The lowest temperatures are observed during spring (ca. 7°C) and the warmest towards late summer. The temperature at this site rarely exceeds 14°C. The

temperature at this and other west coast sites can be up to 1–2°C warmer during spring than the sites at the east coast, Orkney, and Shetland. Salinity follows a similar pattern, with lowest salinity observed in spring and highest in late summer.

Nutrients show a seasonal pattern typical to high latitudes, with concentration of total nitrates, phosphate, and silicate accumulating over winter, when phytoplankton abundance is reduced and concentrations decrease during the phytoplankton growing period.

The phytoplankton community observes a similar seasonal pattern to other sites in Scotland, with a strong spring bloom dominated by diatoms. The spring bloom occurs earlier on the west coast (February/March) than on the east (March/April), likely the result of the warmer water temperature. Dinoflagellates become an important component of the phytoplankton community during summer. The autumn diatom bloom is more intensive than on the east coast and is dominated by larger diatoms, such as the *Rhizosolenia* and *Pseudo-nitzschia* spp. type species.

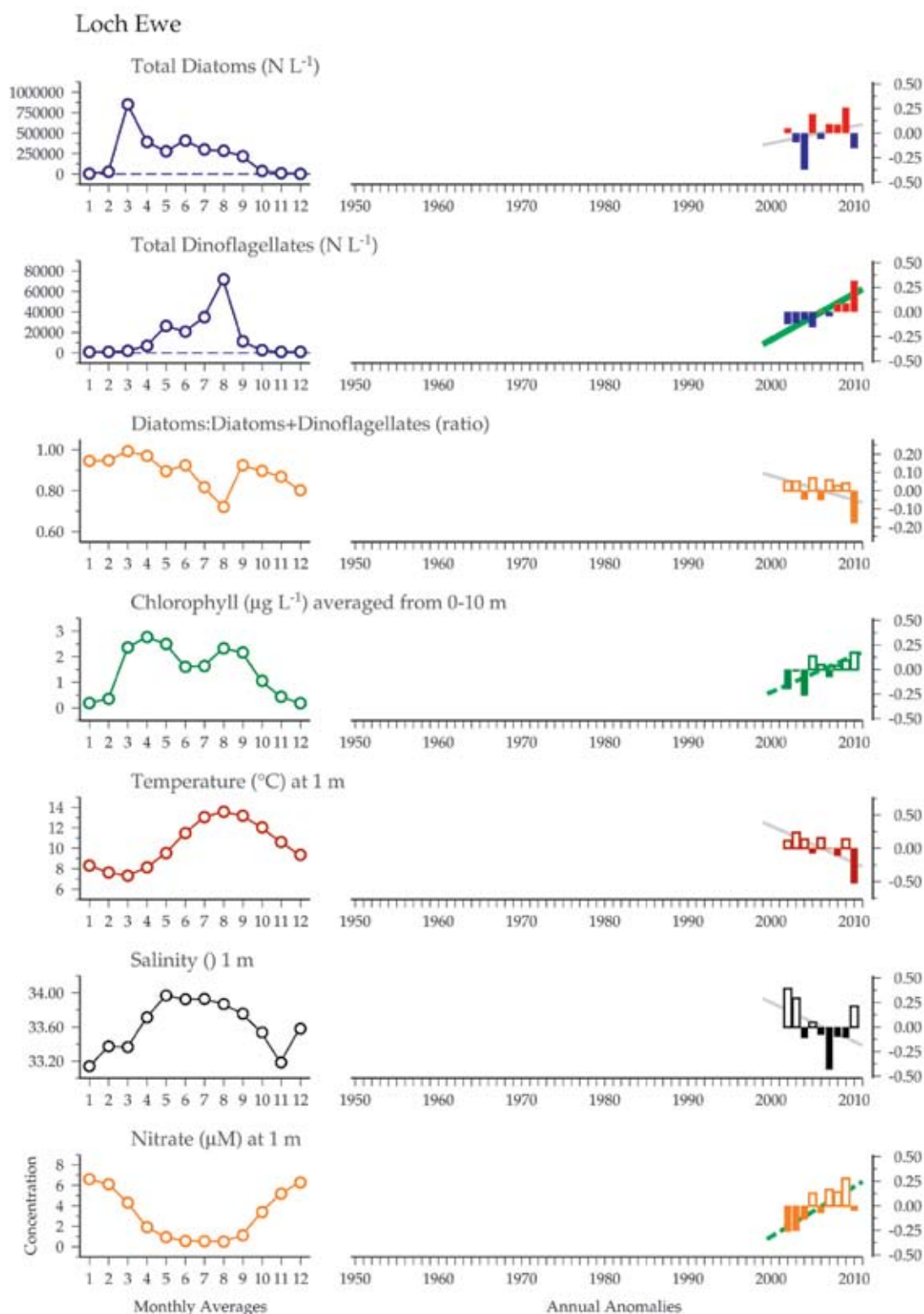
Annual average plots show an increase in dinoflagellates over the last five years. Increased numbers of athecate dinoflagellates have been observed during summer. The pattern of diatom abundance during the spring bloom is similar to that on the east coast, with an increase in abundance of *Skeletonema* observed since 2005 at this site. Chlorophyll data demonstrate an increase, primarily occurring during winter over the last

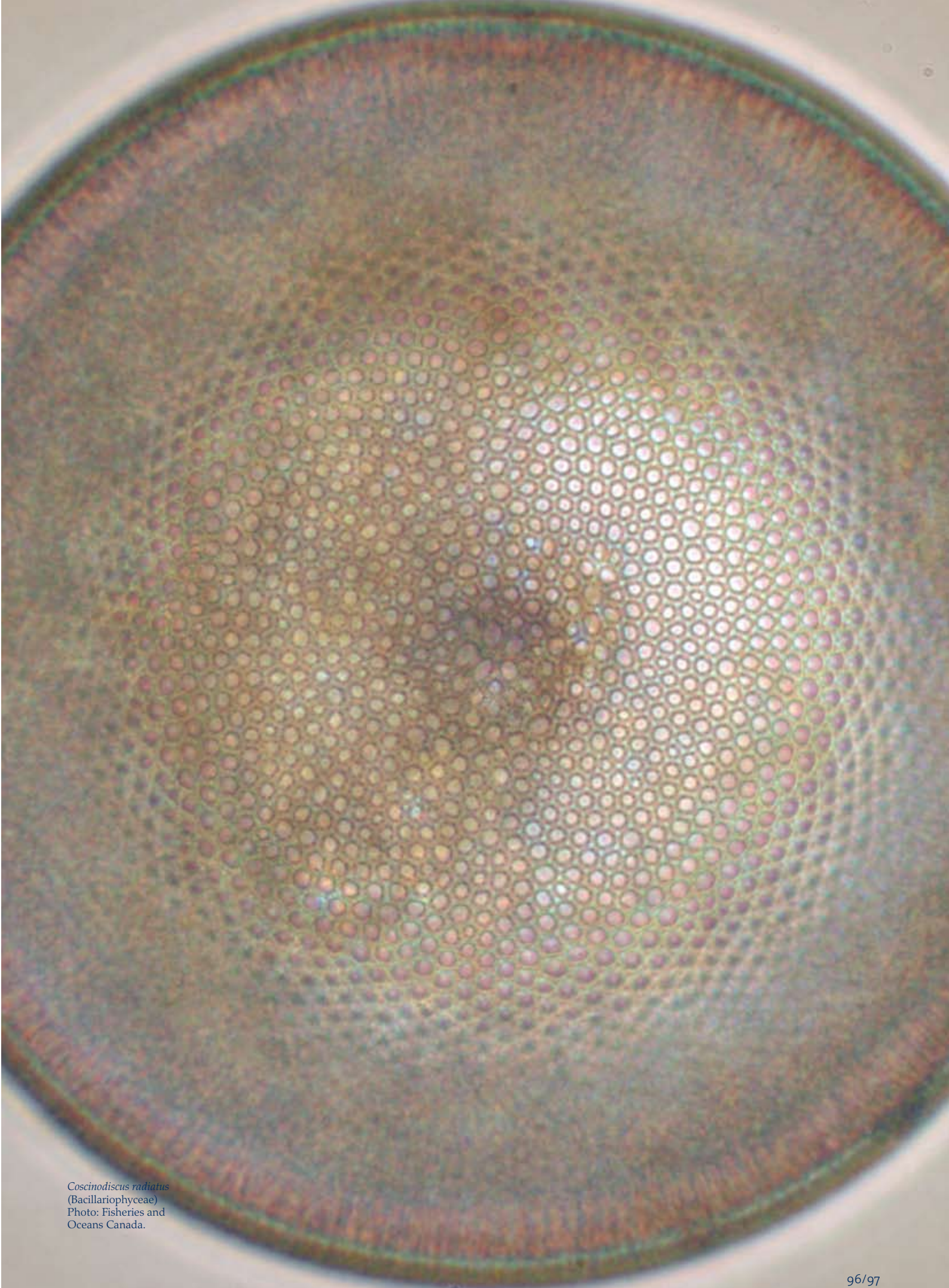
three years. Similar to other sites, a decrease in the abundance of *Ceratium* has been observed over the last decade. This site also experienced a devastating *Karenia mikimotoi* bloom in late summer 2006 (Davidson *et al.*, 2009), with significant mortalities of benthic fauna recorded.

This site was the focus of an intensive study of the presence of shellfish toxin-producing species and algal toxins (Bresnan *et al.*, 2005). Further information and links to the data collected at this site can be found at the Marine Scotland website <http://www.scotland.gov.uk/Topics/marine/science/MSInteractive/Themes/Coastal>.

Figure 7.1.2

Multiple-variable comparison plot (see Section 2.2.2) showing the seasonal and interannual properties of select cosampled variables at the Loch Ewe plankton monitoring site. Additional variables from this site are available online at <http://wgpmc.net/time-series>.





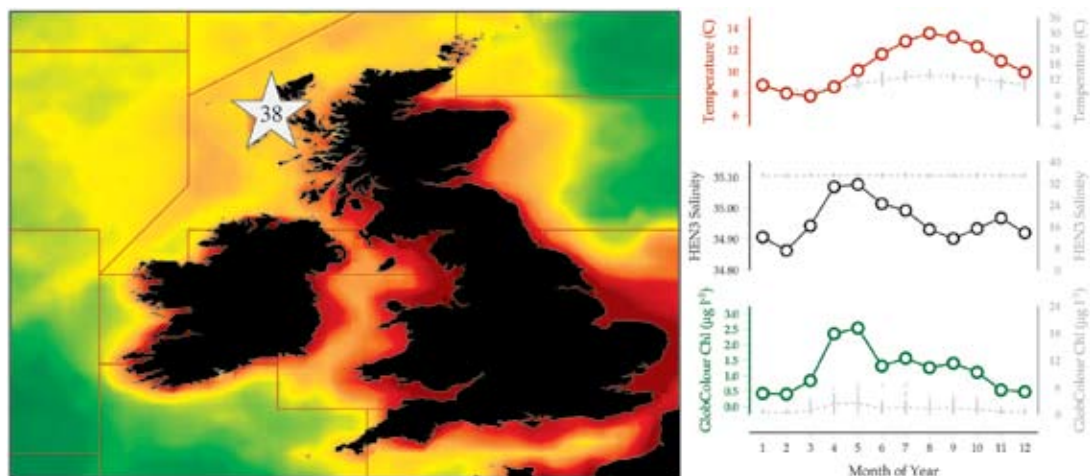
Coscinodiscus radiatus
(Bacillariophyceae)
Photo: Fisheries and
Oceans Canada.

7.2 Loch Maddy (Site 38)

Eileen Bresnan

Figure 7.2.1

Location of the Loch Maddy plankton monitoring area (Site 38), plotted on a map of average chlorophyll concentration, and its corresponding environmental summary plot (see Section 2.2.1).



Loch Maddy (Site 38, 57°36.09'N 7°08.48'W) is located on the Island of North Uist, part of the Western Isles. It is a unique site with a diverse saline lagoon system opening into the sea loch, which contains a mix of rocky reefs and soft sediment habitats. This system supports a rich diversity of marine life and, as a result, has been designated a marine special area of conservation (SAC). Loch Maddy has been participating in the Marine Scotland Science Coastal Ecosystem Monitoring Programme since 2003. Samples have been collected by Comann na Mara and Loch Duart Salmon and their input to the success of this programme is gratefully acknowledged.

Temperature is measured using a minilogger, and surface water samples are taken for salinity and chemical analysis. An integrated tube sampler is used to collect samples for phytoplankton community analysis. Phytoplankton samples are preserved in Lugol's iodine and analysed using the Utermöhl method (Utermöhl, 1958).

Seasonal and interannual trends (Figure 7.2.2)

Temperature demonstrates a distinct seasonality, with lowest temperatures in March and warmest in August. The lowest temperatures are observed during spring (ca. 7°C) and the warmest towards late summer. The temperature at this site rarely exceeds 14°C. In common with the other sites from Scotland, this site demonstrates a similar pattern in the seasonality of the phytoplankton community, with a spring bloom of diatoms dominated by *Skeletonema* and *Chaetoceros*. Dinoflagellates become more abundant in summer, and blooms of the dinoflagellate *Prorocentrum balticum/minimum* have been observed during early summer. High abundance of *Karenia mikimotoi* was observed at this site during 2006. In contrast to other sites along the west coast, diatom blooms can occur during summer, and the autumn diatom bloom is not as pronounced. Owing to the relative shortness of the sampling programme, long-term trends in hydrography or biology are not conclusive at this point.

Further information and links to the data collected at this site can be found at the Marine Scotland website <http://www.scotland.gov.uk/Topics/marine/science/MSInteractive/Themes/Coastal>.

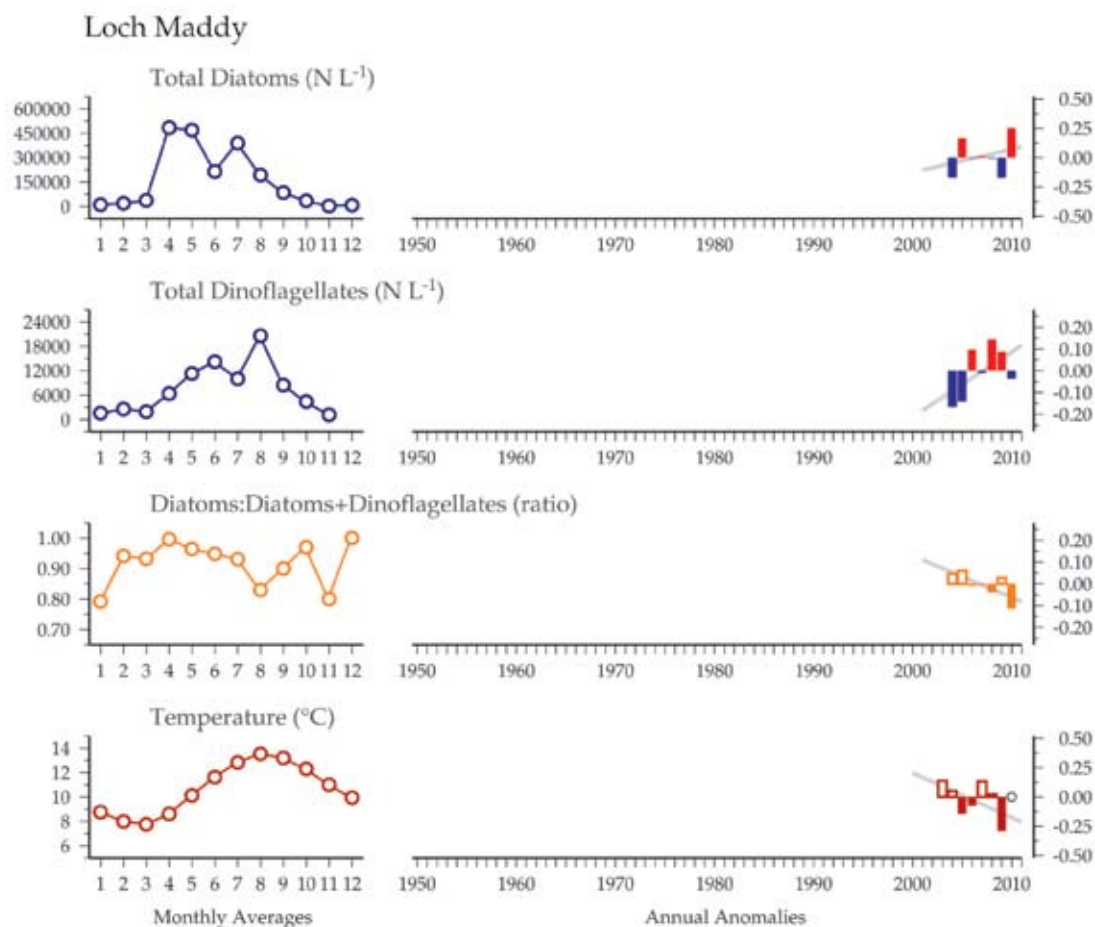


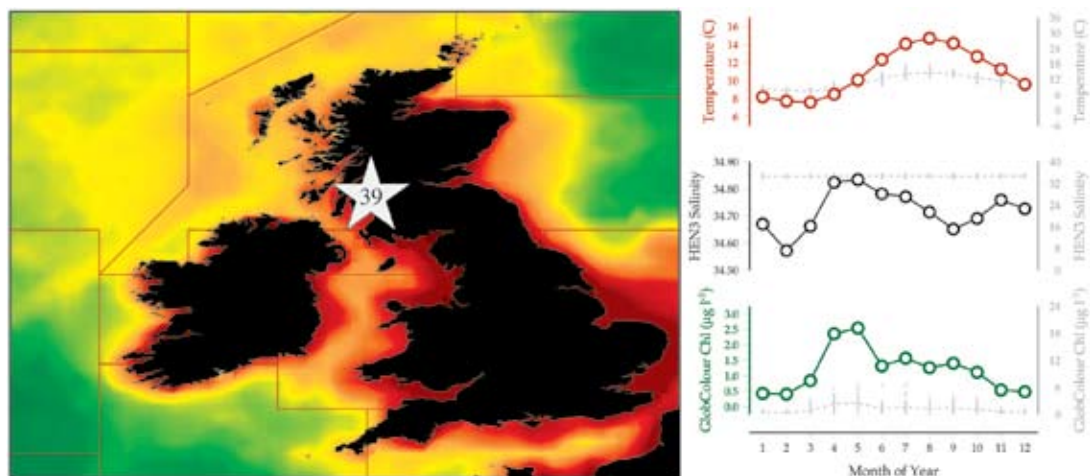
Figure 7.2.2
Multiple-variable comparison plot (see Section 2.2.2) showing the seasonal and interannual properties of select cosampled variables at the Loch Maddy plankton monitoring site. Additional variables from this site are available online at <http://wgpme.net/time-series>.

7.3 Millport (Site 39)

Eileen Bresnan

Figure 7.3.1

Location of the Millport plankton monitoring area (Site 39), plotted on a map of average chlorophyll concentration, and its corresponding environmental summary plot (see Section 2.2.1).



Millport (Site 39, 55°44.97'N 4°54.33'W) has been participating in the Marine Scotland Science Coastal Ecosystem monitoring programme since 2005. Samples are collected by the University Marine Biological Station Millport (<http://www.gla.ac.uk/centres/marinstation/index.php>) and their input to the success of this programme is gratefully acknowledged.

Temperature is measured using a minilogger at Keppel Pier. An integrated tube sampler is used to collect samples for phytoplankton community analysis at Fairlie Channel. The sampling site is approximately 35 m deep. Phytoplankton samples are preserved in Lugol's iodine and analysed using the Utermöhl method (Utermöhl, 1958).

Seasonal and interannual trends (Figure 7.3.2)

Temperature demonstrates a distinct seasonality, with lowest temperatures in March and warmest in August. The phytoplankton time-series at this site is relatively short. A strong phytoplankton spring bloom, dominated by *Skeletonema*, can be observed at this site. Dinoflagellates become more abundant during summer, and large thecate dinoflagellates, such as *Dinophysis* and *Ceratium*, are observed at higher cell densities at this site than at other sites in the programme. Blooms of *Karenia mikimotoi* can be observed during some years. An increase in diatom cell densities during autumn is not observed at this site.

Further information as well as data collected at this site can be found at the Marine Scotland website <http://www.scotland.gov.uk/Topics/marine/science/MSInteractive/Themes/Coastal>.

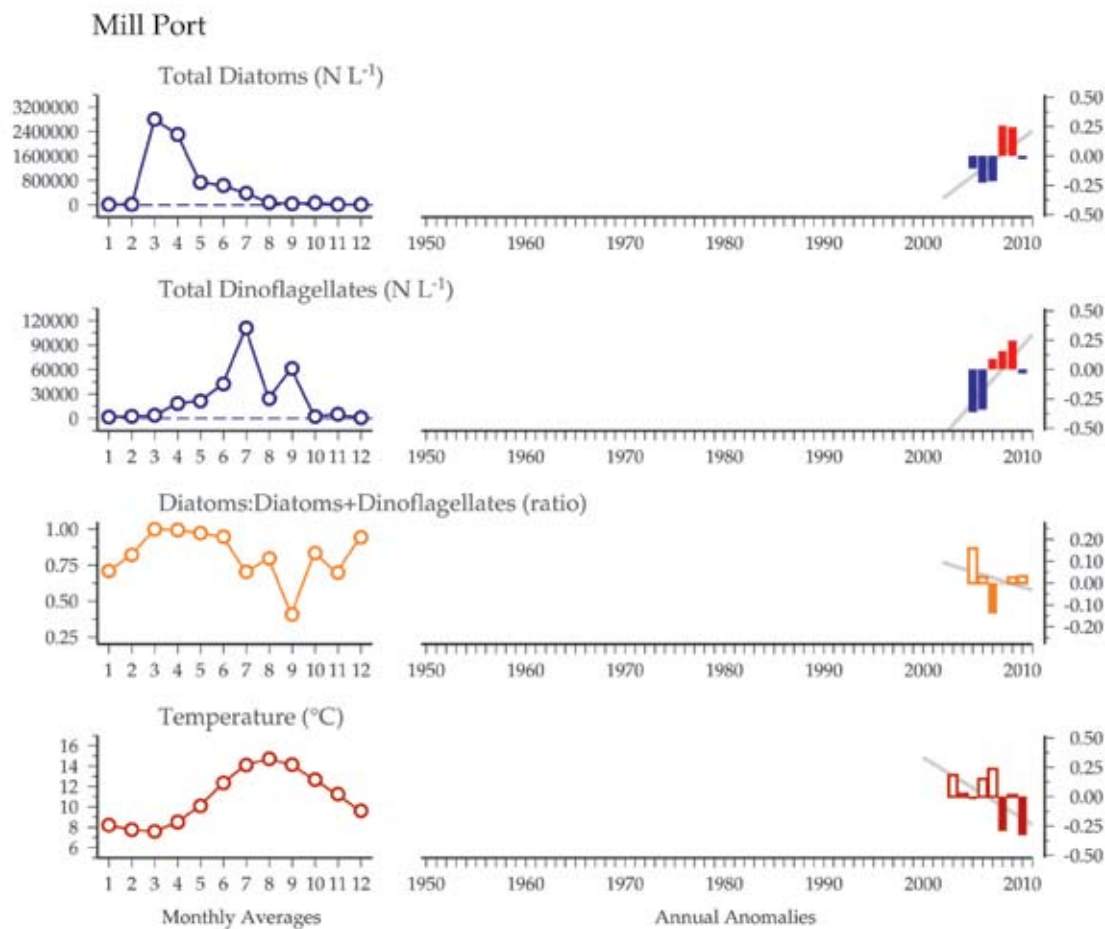


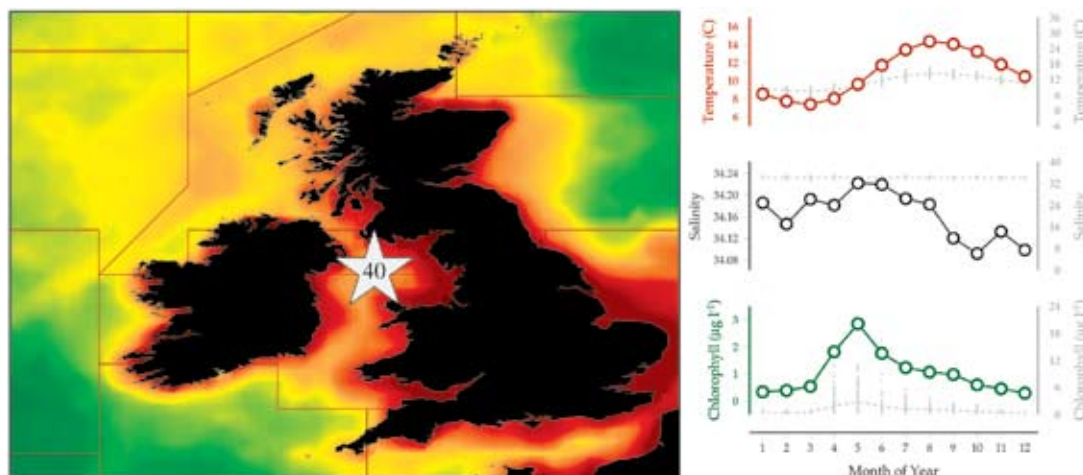
Figure 7.3.2
Multiple-variable comparison plot (see Section 2.2.2) showing the seasonal and interannual properties of select cosampled variables at the Millport plankton monitoring site. Additional variables from this site are available online at <http://wgpme.net/time-series>.

7.4 Cypris Station, Isle of Man (Site 40)

Kevin Kennington

Figure 7.4.1

Location of the Cypris Station, Isle of Man plankton monitoring area (Site 40), plotted on a map of average chlorophyll concentration, and its corresponding environmental summary plot (see Section 2.2.1).



The dataset comprises measurements of temperature, salinity, nutrients, chlorophyll, oxygen, and phytoplankton from two locations near Port Erin (Isle of Man, Irish Sea). Sea surface temperature measurements began to be recorded from the breakwater in Port Erin in 1904. Between 1904 and 2006, SST was recorded twice daily; salinity was also measured at this location between 1965 and 2006. Recordings continue at this location via a digital temperature logger attached to the lifeboat slip in Port Erin Bay. A second station, the so-called "Cypris" station located approximately 5 km due west of Port Erin Bay, was adopted as an offshore monitoring station in 1954. The Cypris data have been collected at frequencies ranging from weekly to monthly, depending on season, boat availability, and weather, and comprise measurements of temperature at 0, 5, 10, 20, and 37 m since 1954; salinity, dissolved oxygen, and phosphate at 0 and 37 m since 1954; silicate at 0 and 37 m since 1958; nitrate and nitrite at 0 and 37 m since 1960; chlorophyll *a* at 0 m since 1966; ammonia at 0 and 37 m since 1992; total dissolved nitrogen at 0 and 37 m from 1996 to 2005; and total dissolved phosphorus at 0 and 37 m from 1996 to June 2002.

At the Cypris station, water samples were collected with either a Nansen–Pettersen or an NIO bottle from 1954 to 2005. Phytoplankton counts have been undertaken on surface samples since 1996. The Nansen–Pettersen bottle was used in conjunction with an insulated thermometer, whereas the NIO bottle was used in conjunction with a mercury reversing thermometer. From 2006

onwards, an RTM 4002 X digital, deep-sea reversing thermometer has been used with an NIO bottle. Salinity was determined by titration against silver nitrate until 1965, thereafter using inductively coupled salinometers (Plessey 6230N until June 1998; Guildline Portasal from July 1998). Nutrients are estimated colorimetrically, and dissolved oxygen is determined by the Winkler technique. Until 2006, chlorophyll *a* was estimated using the trichromatic methods recommended by the SCOR–UNESCO Working Group 17 (SCOR, 1964). Since that year, the spectroscopic methods of Aminot and Rey (2002) have been used. Dissolved nitrogen and phosphorus were measured using the persulphate digestion method adapted from Valderama (1981). The Cypris station data are frequently split into the Cypris I (D. John Slinn) dataset comprising data from 1954 to 1992 and the Cypris II dataset from 1992 to the present.

Data from the Port Erin and Cypris stations are sometimes known collectively as the "Port Erin Bay dataset". Data from Port Erin Bay form part of the Isle of Man GAL Coastal Monitoring Sites network. The data were collected by the Port Erin Marine Laboratory (part of the University of Liverpool) until its closure in 2006. Sampling has since been taken over by the Isle of Man Government Laboratory (Department of Environment, Food and Agriculture). Data collected from Port Erin have been published in several peer-reviewed publications (see reference list).

Seasonal and interannual trends (Figure 7.4.2)

Mean annual sea surface temperature at the site has risen by approximately 0.7°C over the duration of the time-series (1904–2012). These temperature increases follow the broad-scale northern hemisphere atmospheric temperature shifts. Eight of the ten warmest ranked years for local SST have occurred in the last 10 years. There is a positive correlation between the Port Erin breakwater salinity measurements and the North Atlantic Oscillation index (NAO), reflecting the tendency towards warmer European winters during NAO positive years.

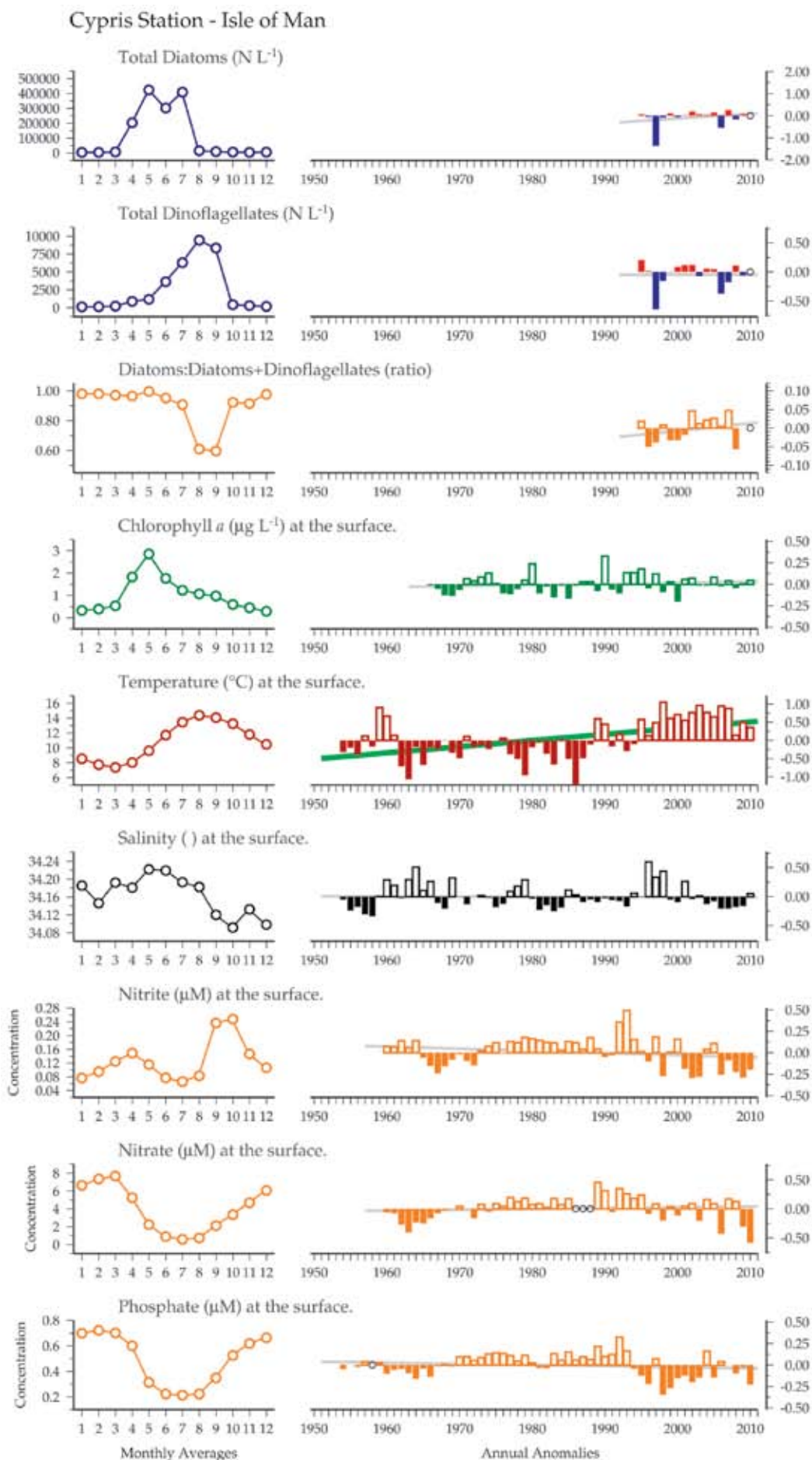
No significant long-term trends in salinity have yet been established. Differentials of annual means with reference to the 1966–2010 grand mean have demonstrated a noteworthy period of low salinity around the early 1980s and a period of higher salinity around the late 1990s. Salinity measurements have been below the grand mean since 2002. There is a negative correlation between the winter NAO and Port Erin winter salinity. In NAO negative years, local salinity tends to be less affected by freshwater inputs, reflecting lower precipitation in these years.

Nutrient concentrations are at a maximum during winter. There is considerable interannual variation in the timing of the winter nutrient maxima, which, at the Cypris station, occurs between January and March. In spring, with increasing insolation and phytoplankton growth, stocks of nutrient salts are rapidly depleted, reaching a minimum around late spring. Levels remain low until late summer and early autumn, when organic-decay cycles regenerate nutrient salts to the water column. Winter inorganic nutrient data represent the basal or resting state when biological processes have come to a halt and the regeneration of nutrients is complete.

Phytoplankton analysis at the Cypris station began in 1996 as part of the Isle of Man toxic algae monitoring programme. No significant long-term trends in phytoplankton abundance have been found, which may be the result of the relatively short time-span of the dataset. The results show that phytoplankton at this site are typical of northern temperate coastal waters. The spring bloom is generally dominated by diatoms, with peak abundance found during April/May. Microflagellated algae can also contribute significantly to the spring bloom and can have peak abundance between April and September. Dinoflagellates have a peak in abundance during summer (July/August), whereas microzooplankton (not shown) are most abundant between May and September.

Figure 7.4.2

Multiple-variable comparison plot (see Section 2.2.2) showing the seasonal and interannual properties of select cosampled variables at the Cypris Station, Isle of Man plankton monitoring site. Additional variables from this site are available online at <http://wgpmc.net/time-series>.



7.5 Irish National Phytoplankton Monitoring (Sites 41–45)

Joe Silke and Caroline Cusack

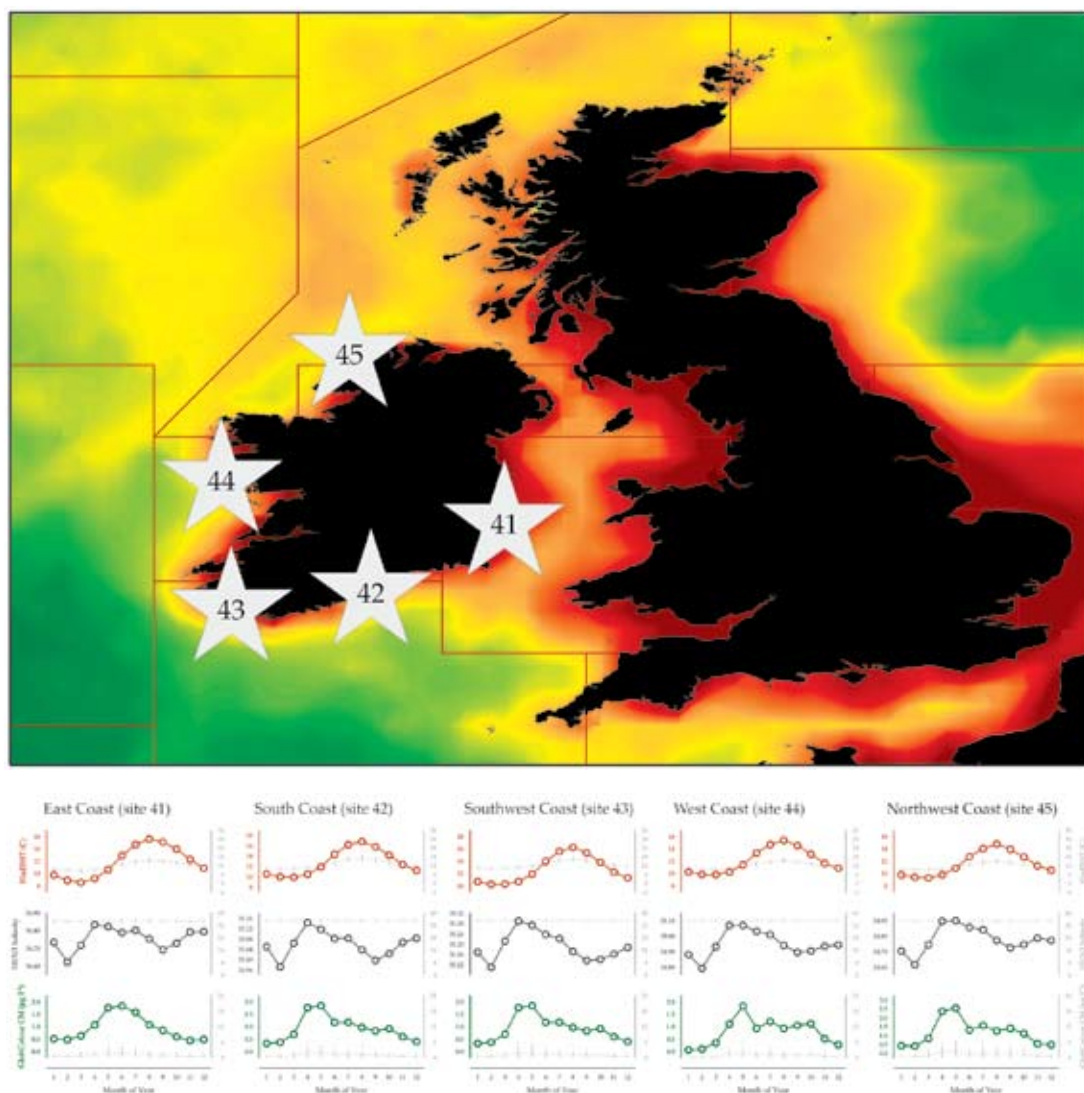


Figure 7.5.1
Locations of Ireland's national phytoplankton monitoring areas (Sites 41–45) area and their corresponding environmental summary plots (see Section 2.2.1).

The Marine Institute in Ireland carries out a national phytoplankton monitoring programme which extends back to the late 1980s. This includes a harmful algal blooms (HABs) monitoring service that warns producers and consumers of concentrations of toxic plankton in Irish coastal waters that could contaminate shellfish or cause fish deaths.

Cusack *et al.* (2001, 2002) summarized the objectives of the monitoring programme. This programme is primarily located along the Atlantic seaboard and Celtic Sea. Scientists working on this monitoring programme have developed an understanding of phytoplankton populations and dynamics around the Irish coastline, especially in relation to those that cause shellfish toxicity. Particular emphasis is put on the detection and enumeration of harmful species;

however, the importance of phytoplankton as an indicator of water quality is also studied and is a key component of the European Water Framework.

Since 1990, data have been captured in a systematic manner and logged into an electronic database. Many of the sites were only analysed for toxic and harmful species, because this was the main purpose of the monitoring programme. In addition, however, there were a selected number of sites around the country analysed for total phytoplankton. Over the years, these sentinel sites changed periodically for a number of reasons, mainly the unavailability of persons to take regular samples. Therefore, in order to construct time-series for this report, it was decided to construct regional groups of all of the sentinel sites in the complete database, based on

a principal component analysis of the dataset. This resulted in five groups of sentinel sites, which are presented in these maps and graphs as regional locations (Figure 7.5.2). Based on the data extracted and amalgamated from these regions, it is deemed to be a good representation of the phytoplankton flora for these regions. The number of sites used to construct each region varies from region to region, and also within each region over time as sites came and went.

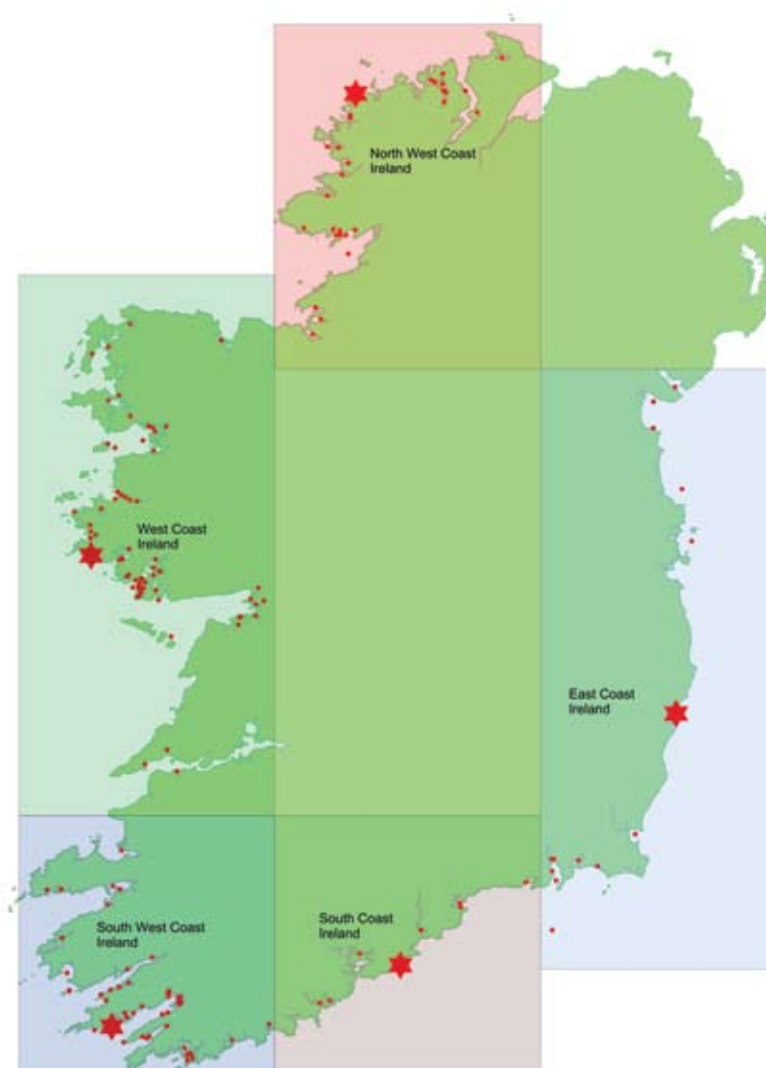
Sites were sampled by a variety of methods, either surface samples, discrete Ruttner sampling bottles, or tube samplers. They were preserved on site with neutral Lugol's iodine, and returned to the laboratory where 25 ml samples were settled for 24 h in Utermöhl chambers before analysis on an inverted microscope. Species were identified and enumerated and cell counts were expressed in cells l^{-1} .

Average sea surface temperatures for western and southern waters of Ireland range from 8 to 10°C in winter to 14–17°C in summer (Lee and Ramster,

1981; Elliott, 1991), and temperatures tend to be several degrees higher compared with the eastern waters. This difference is the result of the entry of warm Atlantic water onto the western Irish Shelf. In winter, Irish coastal and shelf waters are vertically well mixed, with little difference in the surface-to-bottom distribution of temperature within the water column. As the water column stratifies in summer, a surface-to-bottom temperature difference of up to 6°C is typical of waters along the Atlantic Shelf and Celtic Sea (Cooper, 1967; Raine and McMahon, 1998). Along the coast, turbulent tidal currents are sufficient to prevent establishment of stratification, and the water remains mixed throughout the year. The boundary between mixed and stratified waters in summer is marked by tidal fronts that influence the composition and density of phytoplankton community in these areas.

Further information on the sampling programme and results of individual locations can be accessed at the Marine Institute's HABs website <http://www.marine.ie/habs>.

Figure 7.5.2
Combined regions of Irish phytoplankton monitored sites, showing the location of individual sites combined into each region represented in this report.



Seasonal and interannual trends along the east coast (Site 41, Figure 7.5.3)

Seasonal diatom abundances peaked in June, with a second but smaller peak in September. The seasonal abundance of dinoflagellates also peaked in September. The diatoms:diatoms+dinoflagellates ratio is lowest during the warm-water summer period, but the phytoplankton remain dominated by diatoms, such as *Leptocylindrus danicus*, *Chaetoceros* spp., and *Rhizosolenia styliformis*. Total diatom abundance has been decreasing since 1992, possibly correlated with increasing water temperatures over the same period. Long-term trends in the dinoflagellates were inconclusive, following a large peak in the early 1990s.

There is very little shellfish aquaculture along the east coast, apart from the fjord-like inlet of Carlingford Lough, and some mussel fishing in the Wexford and Waterford areas of the southeast coastline. Because of this, there has been limited sampling activity in the region by the Marine Institute for phytoplankton.

There have been some historical studies carried out in the region, notably a study by Gowen *et al.* (2000), where the temporal distribution of phytoplankton and chlorophyll data were described from coastal waters adjacent to the mouth of the Boyne estuary between March and October 1997. During the spring bloom, peak chlorophyll levels up to 11.4 mg l^{-1} were reported during late April–early May. The dominant species at this time was the diatom *Guinardia delicatula*, which represented more than 90% of total phytoplankton abundance (excluding microflagellates). It was also reported that blooms of *Phaeocystis* spp. and other microflagellates occurred before the spring peak in diatoms.

The presence of *Phaeocystis* was also observed occasionally in the Marine Institute time-series with very high counts of up to $48 \times 10^6 \text{ cells l}^{-1}$ observed in spring and early summer months. Other high counts including *Chaetoceros* spp. (up to $6.2 \times 10^6 \text{ cells l}^{-1}$), *Leptocylindrus danicus* (up to $4.2 \times 10^6 \text{ cells l}^{-1}$), *Asterionellopsis glacialis* (up to $2.4 \times 10^6 \text{ cells l}^{-1}$), and *Prorocentrum balticum/minimum* (up to $2.2 \times 10^6 \text{ cells l}^{-1}$) were observed during summer.

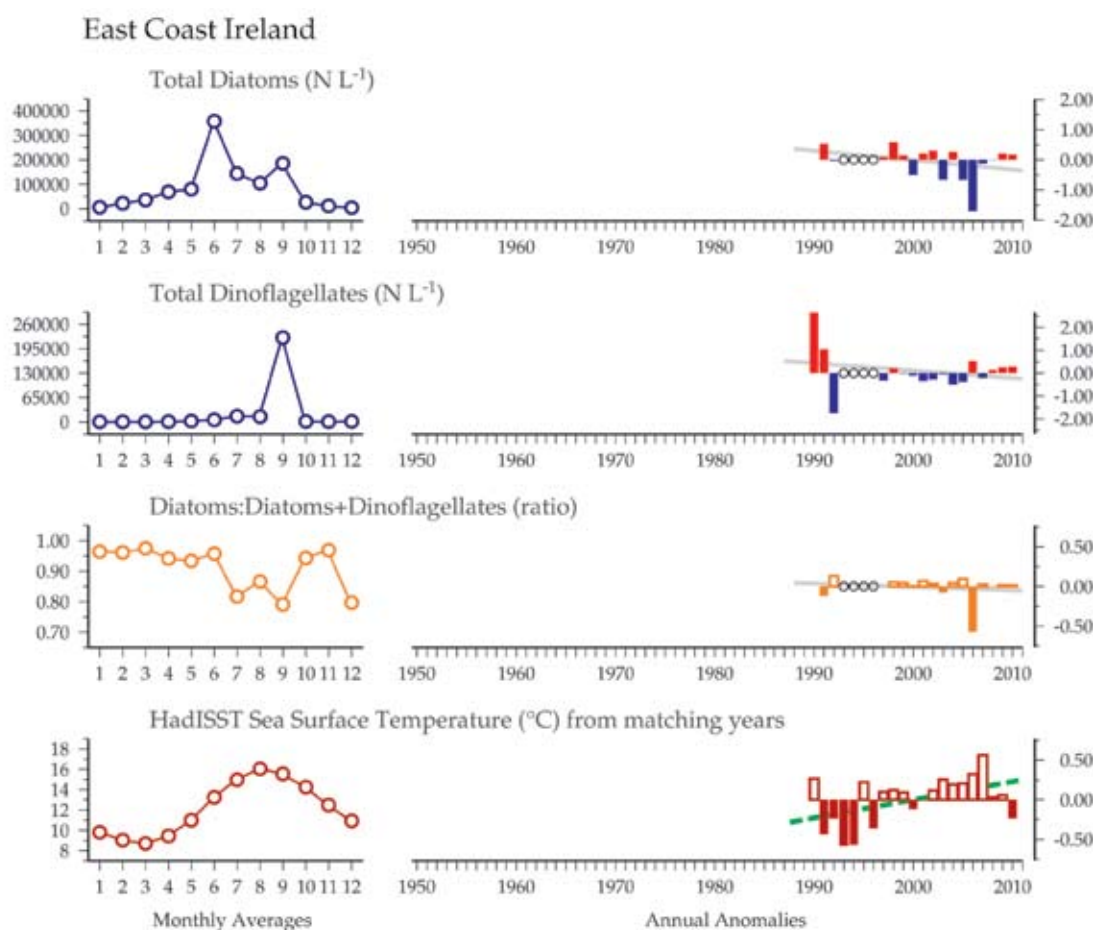


Figure 7.5.3
Multiple-variable comparison plot (see Section 2.2.2) showing the seasonal and interannual properties of select cosampled variables at the east coast of Ireland plankton monitoring site. Additional variables from this site are available online at <http://wgpmc.net/time-series>.

Seasonal and interannual trends along the south coast (Site 42, Figure 7.5.4)

Seasonal diatom abundance peaked in July/August, with a smaller peak in March/April. The seasonal abundance of dinoflagellates peaked in October. The diatoms:diatoms+dinoflagellates ratio is lowest in June, and has been increasing since 1990. Total diatoms have also been increasing since 1990. Dinoflagellate abundance was variable over this time span, with no clear trend.

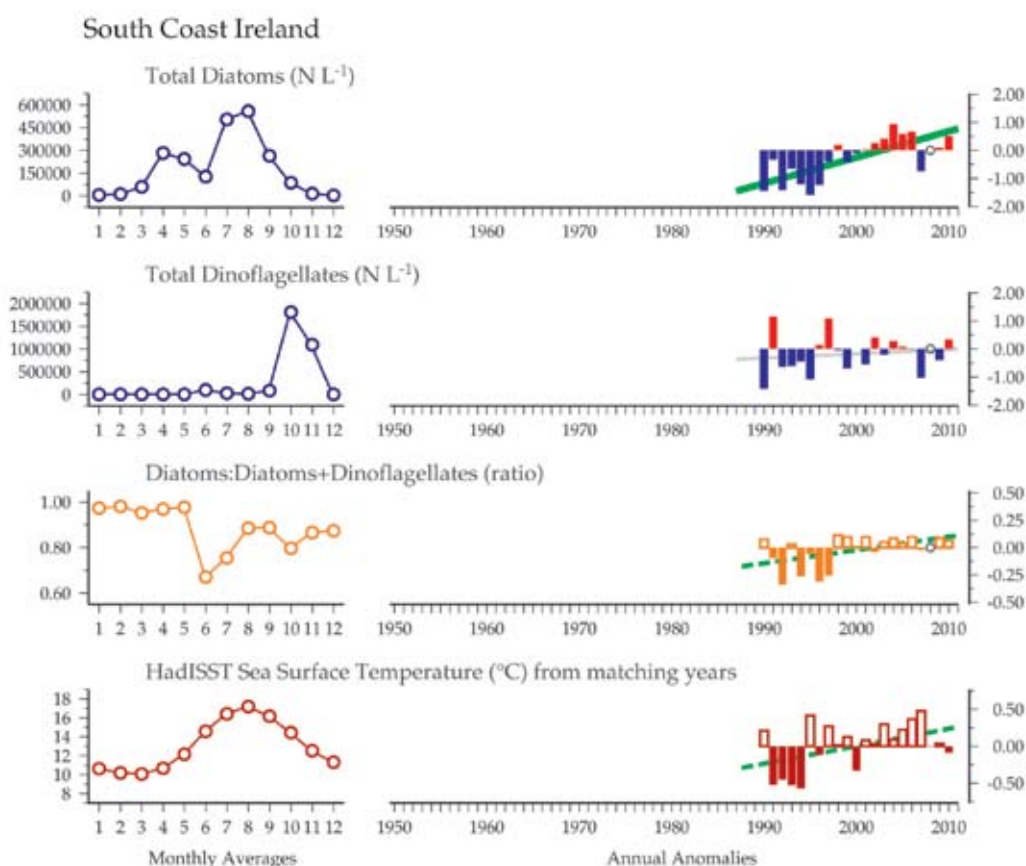
Historical information regarding phytoplankton is sparse for this region apart from some studies on *Alexandrium* spp. in Cork Harbour and descriptions of phytoplankton communities in the Celtic Sea. Pingree *et al.* (1976) and Fasham *et al.* (1983) observed that the spring bloom and the seasonal cycle of phytoplankton production in the Celtic Sea are related to the stratification of the water column. Spring blooms develop in April south of Ireland in an area of weak tidal streaming, with increases in phytoplankton biomass tracking the spatial development of stratification. The Celtic Sea Front forms a boundary between mixed and stratified waters of the southern Irish Sea, and there have been some observations of exceptional blooms of *Karenia mikimotoi* during summer on the stratified side of this front (Holligan *et al.*, 1980). This may be a source for blooms that extend around the west coast using the transport mechanism of the Irish Coastal Current to move the bloom around the coast in a

clockwise direction, where it establishes blooms as observed in years such as 2005 (Silke *et al.*, 2005). Other large numbers of important dinoflagellates, particularly *Dinophysis acuminata* (up to 125 cells ml⁻¹ in July 1992) and *K. mikimotoi* (up to 4300 cells ml⁻¹ in August 1994 and 1995), appear to be associated with a region of slack residual flow located off the southern Irish coast. The presence of blooms of toxic species establishing in this area is important for the downstream aquaculture bays to the southwest (Raine and McMahon, 1998).

The north channel of Cork Harbour is also an area of particular note in this region because of the presence of a population of *Alexandrium tamarense* and *A. minutum*. It has been the presence of *A. minutum* (counts of up to 845 000 cells l⁻¹) in this area that has resulted in the only detection of PSP toxins in shellfish in Ireland that exceeded the EU threshold and required closure of the shellfishery (Marine Institute, unpublished data; Touzet *et al.*, 2007).

Notable blooms detected from samples analysed for the national phytoplankton monitoring programme in this region include *Heterocapsa triquetra* (36×10^6 cells l⁻¹), *Prorocentrum balticum/minimum* (20×10^6 cells l⁻¹), *Phaeocystis pouchetii* (16×10^6 cells l⁻¹), *Bacteriastrum* (7.5×10^6 cells l⁻¹), undetermined coccolithophorids (4×10^6 cells l⁻¹), *Leptocylindrus danicus* (3.3×10^6 cells l⁻¹), and *Asterionellopsis glacialis* (3×10^6 cells l⁻¹).

Figure 7.5.4
Multiple-variable comparison plot (see Section 2.2.2) showing the seasonal and interannual properties of select cosampled variables at the south coast of Ireland plankton monitoring site. Additional variables from this site are available online at <http://wgpme.net/time-series>.



Seasonal and interannual trends along the southwest coast (Site 43, Figure 7.5.5)

Seasonal diatom abundance peaked in May and July, whereas dinoflagellates peaked in September. The diatoms:diatoms+dinoflagellates ratio is lowest in August, and has been increasing since 1990. Total diatoms have also been increasing since 1990, whereas dinoflagellate abundance has been variable over this time-span, with no clear trend.

This area is dominated by a series of embayments (similar to the Gallician rías of northwest Spain) along the coast, which are glacial-flooded river valleys, orientated in a northwest–southwest direction. These sheltered bays have become the location for a successful shellfish aquaculture industry, predominated by the culture of blue mussels (*Mytilus edulis*). Rope culture in these bays accounts for 80% of the national production. The hydrography of the areas is characterized by coastal upwelling, which is highly variable in both its periodicity and magnitude. During periods when there is stable water structure in this area, the microalgal flora is typical of the greater Atlantic Shelf area. The other key feature of this area was described by Raine and McMahon (1998), who noted that the composition of phytoplankton in samples collected from shelf waters off the southwest coast between 1992 and 1995 changed markedly in relation to the position of the Irish Shelf Front. It has been demonstrated that the sudden appearance of blooms such as *Karenia mikimotoi* resulted from advection of offshore populations into the southwest bays. The transport mechanism of these blooms was not known until the presence of the seasonal jet-like Irish Coastal Current was established (Fernand *et al.*, 2006). The strength of this clockwise flow around the southwest tip of Ireland is modulated by the presence of the Shelf Front, which is close to the shore in the presence of dominant southwesterly winds. When these winds relax, the front is weakened and the Irish Coastal Current can establish, bringing populations of dinoflagellates from the Celtic Sea to the mouth of the southwest bays, where they can be advected inshore by wind-induced residual flow in a two-layered stratified system (Edwards *et al.*, 1996).

Historically, there have been several studies of the plankton in this region, owing to the aquaculture presence and importance to the regional economy. A study by Raine *et al.* (1990) presents results of investigations into the distribution of phytoplankton for coastal waters off the southwest coast of Ireland during summers of 1985–1987. In general, diatom populations were associated with the cooler regions,

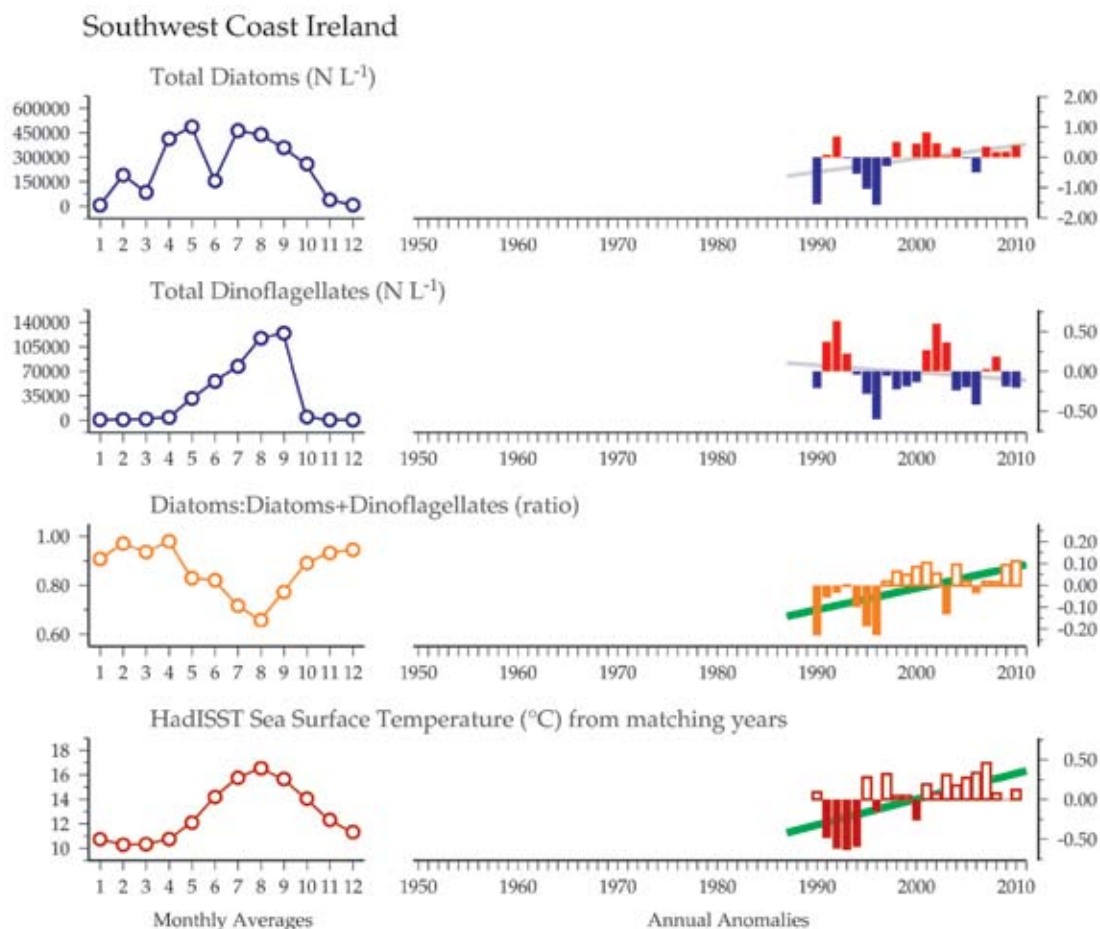
whereas dinoflagellates tended to predominate in stratified water. In 1985 and 1987, during upwelling events, diatoms dominated the flora in the vicinity of the Fastnet Rock and west of Bantry Bay, particularly species such as *Chaetoceros* spp., *Leptocylindrus danicus*, *Guinardia delicatula*, and *Thalassiosira* spp. In 1987, *Rhizosolenia alata* was the dominant diatom species. Farther offshore, where the water column was more stratified than in the previous two years, dinoflagellates increased in numbers, but *Proboscia alata* was still numerically dominant.

The National Monitoring Programme has identified some very dense blooms of diatoms and dinoflagellates between 1990 and 2010. These have included *Rhizosolenia* spp. ($75 \text{ million cells l}^{-1}$) in July 1991, an unidentified *Microflagellate* sp. bloom ($53 \times 10^6 \text{ cells l}^{-1}$) in October 2007, and a bloom of *Skeletonema* spp. ($26 \times 10^6 \text{ cells l}^{-1}$) in May 1998. Other less numerically dense, but still significant, blooms included periodic blooms of *Phaeocystis* spp. (up to $17 \times 10^6 \text{ cells l}^{-1}$), *Leptocylindrus minimus* (up to $12 \times 10^6 \text{ cells l}^{-1}$), *Cylindrotheca closterium/Nitzschia longissima* (up to $10 \times 10^6 \text{ cells l}^{-1}$), *Skeletonema* spp. (up to $9 \times 10^6 \text{ cells l}^{-1}$), *Thalassionema nitzschioides* (up to $5.5 \times 10^6 \text{ cells l}^{-1}$), *Noctiluca scintillans* (up to $5.2 \times 10^6 \text{ cells l}^{-1}$), and *Thalassiosira* spp. (up to $4.8 \times 10^6 \text{ cells l}^{-1}$).

Blooms of *Dinophysis acuta* and *D. acuminata* were observed in the bays during most summers, but never in particularly dense blooms or dominating the phytoplankton community. They are of particular note, however, because they resulted in closures of shellfish farming most years, for periods of time ranging from weeks to several months. The transport mechanism of the Irish Coastal Current and its control by the Irish Shelf Front is believed to be important in the delivery of *Dinophysis* to these aquaculture bays (Raine *et al.*, 2010).

Figure 7.5.5

Multiple-variable comparison plot (see Section 2.2.2) showing the seasonal and interannual properties of select cosampled variables at the southwest coast of Ireland plankton monitoring site. Additional variables from this site are available online at <http://wgpmc.net/time-series>.



Seasonal and interannual trends along the west coast (Site 44, Figure 7.5.6)

Seasonal diatom abundance peaked in August, followed by a dinoflagellate peak in September. The diatoms:diatoms+dinoflagellates ratio is lowest in July. Diatoms, dinoflagellates, and their ratio have been increasing since 1990, but none of the trends were statistically significant.

The west-of-Ireland region covers the coastline from the mouth of the Shannon River north to the northern coastline of County Mayo. This area is made up of exposed coastline open to the Atlantic Shelf waters to the west, and several coastal embayments offering sheltered shallow waters, where both shellfish farming and finfish farming industries have successfully operated.

The spring phytoplankton of the area is typical of that investigated by O'Boyle (2002), who reported that the spring bloom in Galway Bay occurred in mid-April, when a maximum chlorophyll concentration of just over 11 mg l⁻¹ was recorded. The spring bloom was dominated by diatom species including *Thalassiosira* spp. and *Chaetoceros* spp., with maximum cell numbers of 167 and 39 cells ml⁻¹,

respectively. In May, this assemblage was replaced by other diatom species, such as *Dactylosolen fragilissima*, *Leptocylindrus danicus*, *Leptocylindrus minimus*, *Pseudo-nitzschia* spp., and *Ceratium pelagica*. Microflagellates were common throughout the study period, with cell numbers ranging from 2 to 27 × 10³ cells ml⁻¹.

Summer distribution of phytoplankton in Atlantic Shelf waters west of Ireland was reviewed by Raine *et al.* (1993), who concluded that the pattern of change in phytoplankton populations can be divided into two temporal phases separated by the full development of the thermocline, which can obtain a depth of 35–40 m by mid-July. In early summer, before the water column becomes fully stratified, intermittent vertical mixing promotes a series of diatom blooms that are usually dominated by *Chaetoceros* spp. and *Rhizosolenia setigera*, with dinoflagellate numbers remaining low, with the possible exception of *Scrippsiella*. Following stratification, these species are replaced by dinoflagellates including *Ceratium* spp., and also the diatoms *Proboscia alata* and *Leptocylindrus mediterraneus*.

A notable bloom in 2005 of *Karenia mikimotoi* extended along the west coast for most of the summer and resulted in severe benthic in-faunal and pelagic mortalities of macroinvertebrates and

fish (Silke *et al.*, 2005). A second bloom was detected in a later period of summer in the southwest, and was present the following year on both the east and west coasts of Scotland.

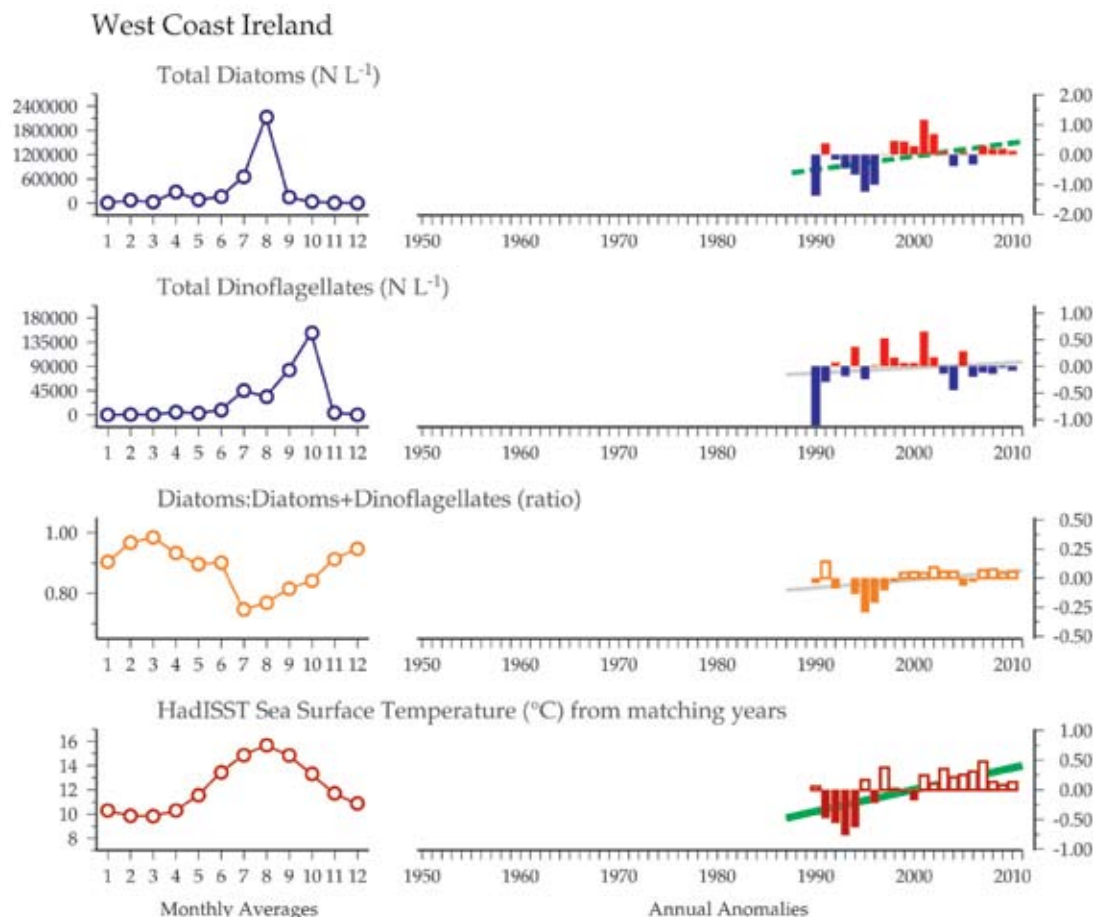


Figure 7.5.6
Multiple-variable comparison plot (see Section 2.2.2) showing the seasonal and interannual properties of select cosampled variables at the west coast of Ireland plankton monitoring site. Additional variables from this site are available online at <http://wvqpmc.net/time-series>

Seasonal and interannual trends along the northwest coast (Site 45, Figure 7.5.7)

Seasonal diatom abundance peaked in March and July, whereas dinoflagellates peaked in November. The diatoms:diatoms+dinoflagellates ratio is lowest in November/December. Diatoms have been increasing since 1990. Dinoflagellates also show a positive, but non-significant, trend. The diatoms:diatoms+dinoflagellates ratio was almost completely flat at this site.

This region represents sites from Sligo Bay up to the most northerly bay in Ireland: Trillick Bay. The rugged coastline of Counties Sligo and Donegal represents a diverse environment ranging from long shallow sandy bays of Sligo and sheltered coves along the north coast, to exposed bays and rocky shorelines in Donegal. These waters are all fully saline, with little significant freshwater input in the region.

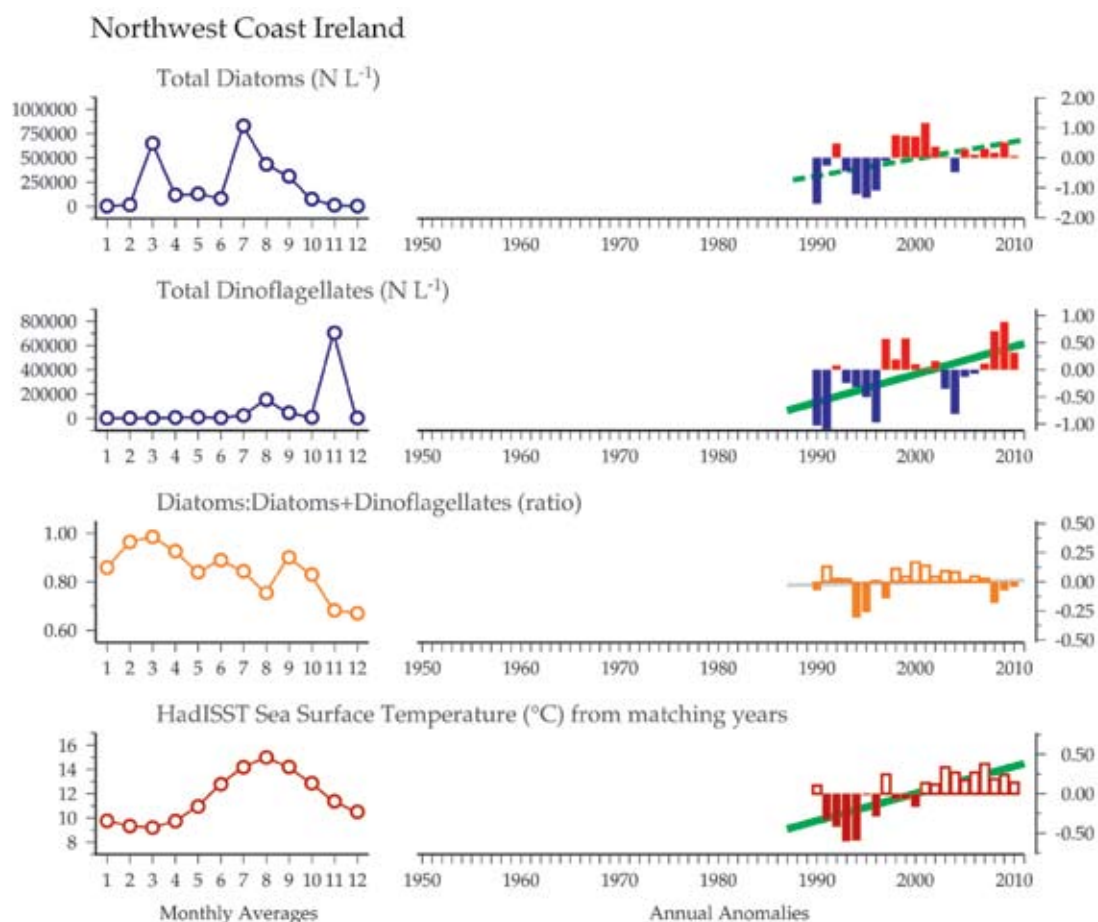
The distribution of phytoplankton in this area has been demonstrated to be related to the main oceanographic features of the region (O'Boyle and Raine, 2007). In that study, the authors presented the results of observations along the northwest coast in 1999. Inshore of the Irish Shelf Front, the phytoplankton species composition was dominated by diatoms, such as *Leptocylindrus danicus*, *Guinardia flaccida*, and *Pseudo-nitzschia* spp. The flora of the shelf region between the front and the outer shelf was characterized by the presence of *Halosphaera minor*, *Oscillatoria* sp., *Ptychodiscus noctiluca*, *Ceratium fusus*, and *Amphidoma caudata*. Farther offshore along the margins of the continental shelf, the floral assemblage was marked by the presence of *Gonyaulax polygramma*, *Ceratium furca*, *Oxytoxum scolopax*, *Podolampes palmipes*, *Prorocentrum compressum*, and *Prorocentrum dentatum*. The highest *Karenia mikimotoi* cell concentrations of up to 100 cells ml⁻¹ were found in proximity to bottom density fronts located inshore. Chlorophyll

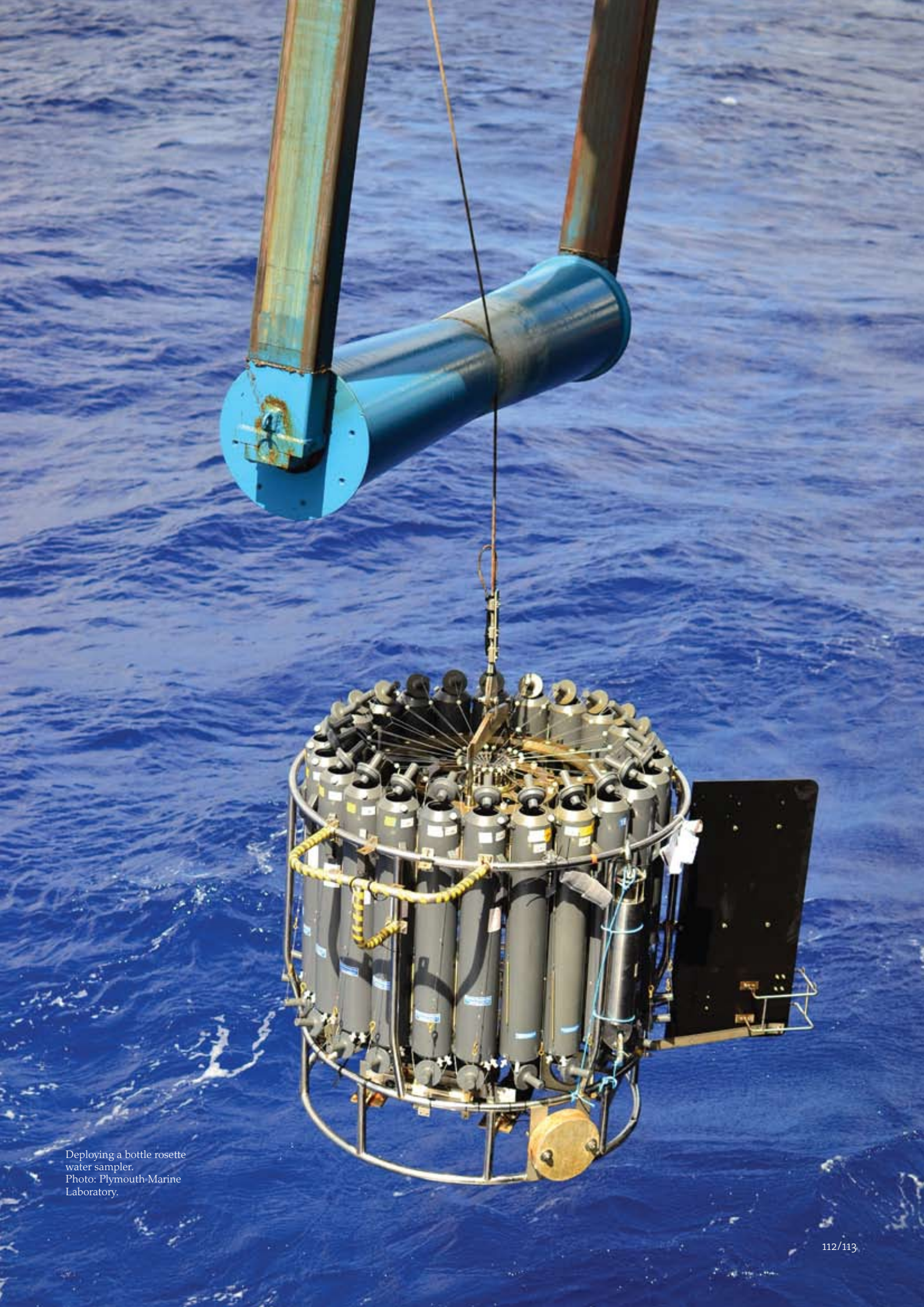
a concentrations (not shown) are generally low at 1.0 mg l^{-1} throughout the survey area, with the exception of some inshore coastal stations where values ranged from 1.8 to 3.4 mg l^{-1} , particularly in inlets along the west coast of Donegal.

The data extracted from the Marine Institute database demonstrates that coastal areas exhibit periodic blooms of both diatoms and dinoflagellates. The most frequent of these were *Asterionellopsis*

spp., with cell counts above $14 \times 10^6 \text{ cells l}^{-1}$. A significant dinoflagellate bloom of *Prorocentrum balticum* occurred off the north coast in 1997, with counts of up to $11 \times 10^6 \text{ cells l}^{-1}$ recorded. Other notable diatoms in this area include *Chaetoceros* spp. and *Skeletonema* spp., which have frequently bloomed with densities recorded up to $17 \times 10^6 \text{ cells l}^{-1}$. Dinoflagellate blooms are also recorded in this region, including blooms of *Heterocapsa triquetra*, *Gymnodinium* spp., and *Karenia mikimotoi*.

Figure 7.5.7
Multiple-variable comparison plot (see Section 2.2.2) showing the seasonal and interannual properties of select cosampled variables at the northwest coast of Ireland plankton monitoring site. Additional variables from this site are available online at <http://wgpmc.net/time-series>.





Deploying a bottle rosette water sampler.
Photo: Plymouth Marine Laboratory.

8. PHYTOPLANKTON AND MICROBIAL PLANKTON OF THE BAY OF BISCAY AND WESTERN IBERIAN SHELF

Xosé Anxelu G. Morán, Ana B. Barbosa, Marta Revilla, Antonio Bode, Emma Orive, and Dominique Soudant

This region of the Northeast Atlantic represents a gradient between two oceanographic regimes: (i) the subtropical waters of southern Portugal and southwestern Spain, and (ii) the temperate waters characterizing the northwestern and northern Iberian coasts (Cantabrian Sea) and the rest of the Bay of Biscay along the French coast. As a consequence, seasonal patterns in physico-chemical and biological variables typical of temperate pelagic ecosystems tend to be more conspicuous as we move northwards and into the Bay. Overall, a strong thermal stratification around summer is followed by vigorous winter mixing, frequently to the bottom of the continental shelf (Lavin *et al.*, 2006). Freshwater outflow from numerous rivers and coastal lagoons contributes to the existence of buoyant low-salinity plumes, particularly during late winter and spring, along the Bay of Biscay (Puillat *et al.*, 2004) and the western (western Iberian Plume) and southwestern Iberian coasts (Lafuente and Ruiz, 2007; Relvas *et al.*, 2007).

The western Iberian Peninsula and the southern Bay of Biscay continental shelves lie at the northernmost reaches of the northwest African upwelling system (Aristegui *et al.*, 2006). Upwelling and downwelling favourable periods, seemingly linked to the North Atlantic Oscillation (NAO) index, are variable in terms of duration, intensity, and phasing,

but generally occur during spring–summer and autumn–winter, respectively (Wooster *et al.*, 1976; Alvarez *et al.*, 2008). Upwelling-producing winds vary according to coastline orientation, ranging from northerly winds along the western Iberian coast, easterly winds in the southern Bay of Biscay, and westerly winds in southwestern Iberia. Along the Cantabrian Shelf, the intensity and frequency of upwelling events decrease eastward as temperature and stratification increase (Lavin *et al.*, 2006). The whole region is affected by a saline, warm-slope current flowing poleward during autumn and winter, the Portugal Coastal Counter Current (PCCC; Álvarez-Salgado *et al.*, 2003) also known as the Iberian Poleward Current (IPC). Similar to upwelling episodes, the influence of the IPC along the southern Bay of Biscay decreases eastwards (Pingree and Le Cann, 1990). Other important hydrographic features include: (i) the presence of slope-water anticyclonic eddies in offshore waters of the Bay of Biscay (Pingree and Le Cann, 1993), which affect planktonic assemblages (Fernández *et al.*, 2004); (ii) a persistent frontal structure between Eastern North Atlantic Central Water (ENACW) of subtropical and subpolar origin at the subsurface off Cape Fisterra (Aristegui *et al.*, 2006); and (iii) other mesoscale features such as upwelling filaments, fronts, and eddies off southwest Iberia (Lafuente and Ruiz, 2007; Relvas *et al.*, 2007). Overall, the



Figure 8.1
Locations of the Bay of Biscay and western Iberian Shelf plankton monitoring areas (Sites 46–54) plotted on a map of average chlorophyll concentration.

region comprises extreme variability with respect to coastal configuration, shelf width, coastal upwelling intensity, riverine outflow, mesoscale activity, and retentive vs. dispersive physical mechanisms (see Arístegui *et al.*, 2009).

Decadal trends in ocean–climatic observations within the area show a generalized sea surface warming, shallowing of the summer coastal thermocline depth, weakening of the upwelling intensity during most of the year along the western Iberian coast, and intensification in upwelling intensity during peak summer along the southwestern Iberian coast (Lemos and Sansó, 2006; Álvarez *et al.*, 2008; Relvas *et al.*, 2009; Pardo *et al.*, 2011; Santos *et al.*, 2011).

Time-series data on phytoplankton and microbes are available for nine sites distributed along the continental shelf of this region, with reasonably good coverage of the southern Bay of Biscay. Available sites include two confined coastal ecosystems at the land–ocean interface, the Nervión lower estuary and the Guadiana upper estuary. For these two sites, in addition to general oceanographic drivers described above, local conditions (e.g. rainfall and river-flow patterns) and anthropogenic pressures may cause departures from what is expected in coastal, temperate ecosystems (Cloern and Jassby, 2010).

Information available for all sites includes abiotic variables and phytoplankton, usually discriminated into functional groups (e.g. taxa or size classes), whereas data on heterotrophic bacterioplankton are limited to two sites.

Seasonal cycles of planktonic microbes globally reflect the stratification–destratification cycle, further enhanced by coastal upwelling events and riverine inputs. There is no common seasonal cycle of phytoplankton using surface chlorophyll concentration within the region. For instance, unimodal and bimodal annual cycles are found, likely related to site-specific differences in inorganic nutrient loading or light limitation. Sites less affected by coastal upwelling (e.g. Men er Roue, AZTI Station D2, and the lower Nervión estuary) show a classic bimodal cycle, with maxima around early spring and mid-autumn. When nutrients become limiting in the upper layers owing to strong summer thermal stratification, surface chlorophyll concentrations decrease in these locations to values $< 0.2 \mu\text{g l}^{-1}$. By contrast, if inorganic nutrients are available year-round, as usually found in most coastal areas and upper estuarine sites, or under frequent and strong upwelling episodes, phytoplankton tend to reach relatively high values (i.e. $> 1 \mu\text{g l}^{-1}$) also during summer, as found, for instance, off the city of A Coruña (Bode *et al.*, 2011b) and at Ouest Loscolo

and Le Cornard. Regardless of the seasonal pattern, chlorophyll peaks do not usually exceed $3 \mu\text{g l}^{-1}$ at any of the exposed coastal sites included here. The relative importance of the autumn bloom in bimodal annual patterns also varies, from similar or even greater in extent than the spring one to a clearly secondary position. Light limitation becomes important in the turbid Guadiana upper estuary during most of the year, in part explaining phytoplankton unimodal annual cycles.

Most of the sites lack significant interannual trends in phytoplankton biomass, although a significant increase was found in the upper layer (0–50 m) of the Basque coast (eastern Cantabrian Sea) for the 1986–2010 period. In the Guadiana upper estuary, a significant declining trend in phytoplankton abundance for the 1996–2010 period is apparently linked to the effects of increased river damming (Barbosa *et al.*, 2010). The overall lack of consistency in phytoplankton interannual trends across sites could be explained by the limited extension of available time-series (< 12 years at most sites) and/or site-specific differences at the level of long-term variability in environmental determinants, phytoplankton physiology, and mortality. Indeed, over the past two decades, primary production has increased significantly at A Coruña, but apparently decreased in the central Cantabrian Sea (Bode *et al.*, 2011b). Nitrate and phosphate concentrations, key phytoplankton resources, show a significant increasing trend only at the Gijón/Xixón site.

Contributions of larger (nano- and microplankton) phytoplankton groups also differ temporally and spatially. Diatoms tend to show variable annual patterns, ranging between bimodal cycles coincident with those of chlorophyll (e.g. Gijón/Xixón) to unimodal cycles with late spring–summer maxima (e.g. Nervión and Guadiana estuaries). As expected, generally single annual dinoflagellate maxima are usually detected 1–2 months after diatom blooms. Although most of the available time-series are too short to depict significant trends, increases in diatom abundance were significant at the Le Cornard and Ouest Loscolo sites on the French coast. Also significant or close to significant, but opposing, tendencies in diatom abundance over the last decade were detected in the Nervión and Guadiana estuaries, increasing and decreasing, respectively. In the latter site, the diatom decline was concomitant with significant reductions in other phytoplanktonic groups, an association also seen at several of the French coast sites (sharing

either increasing or decreasing trends), whereas the diatom increasing tendency was apparently contrary to that of dinoflagellates at Gijón/Xixón. Significant increases in dinoflagellate abundance are detected in the A Coruña and Le Cornard time-series.

Picoplankton in the area is strongly linked to oceanographic features such as the IPC or frontal areas (Calvo-Díaz *et al.*, 2004). Cyanobacteria as ecologically relevant members of this class show distinct seasonal cycles. Maximum abundance (up to 10^5 cells ml^{-1}) is usually found in summer. In the southern Bay of Biscay, highest annual abundance of *Synechococcus* during summer–autumn is accompanied by generally lesser abundance of *Prochlorococcus*, more abundant in open-ocean waters (Calvo-Díaz and Morán, 2006). One striking feature of the latter is its complete absence from the French continental shelf, whereas in the rest of the region, it is only detected for half of the year (roughly September–February). The construction of a river dam in the Guadiana estuary promoted a long-term decline in cyanobacterial abundance, probably owing to augmented summer river-flow and increased retention of water and cyanobacteria benthic life stages behind the dam (Barbosa *et al.*, 2010).

Heterotrophic bacterioplankton abundance ranges from 0.2 to 2×10^6 cells ml^{-1} in the two sites with available data. A Coruña and Gijón/Xixón show, however, clear differences in seasonal patterns, likely because of dissimilarities in phytoplankton annual cycles and trophic conditions. A sustained bacterial annual maximum around summer is found at the former site, whereas this period of the year coincides with minimum abundance at the latter (Morán *et al.*, 2011). Opposite tendencies in bacterial biomass for the period 2002–2010, increasing at Gijón/Xixón and decreasing at A Coruña are not significant, but suggest that climate-related changes in the region may be strongly dependent on local conditions.

8.1 Bay of Biscay REPHY sites (Sites 46-49)

Dominique Soudant (primary contact), Myriam Perrière Rumèbe, and Danièle Maurer

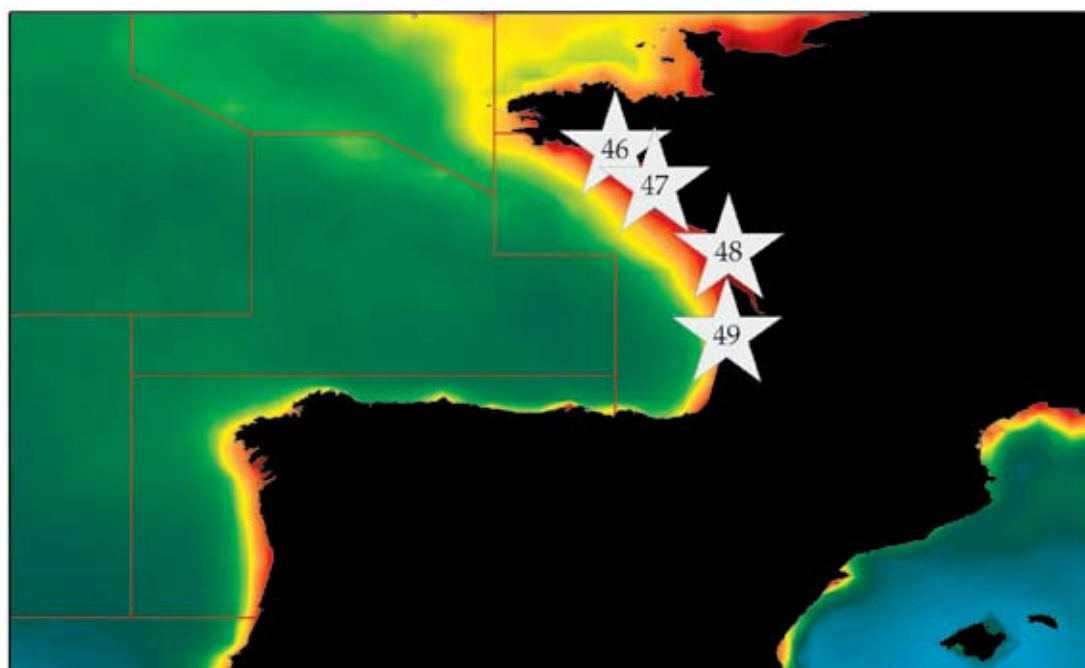
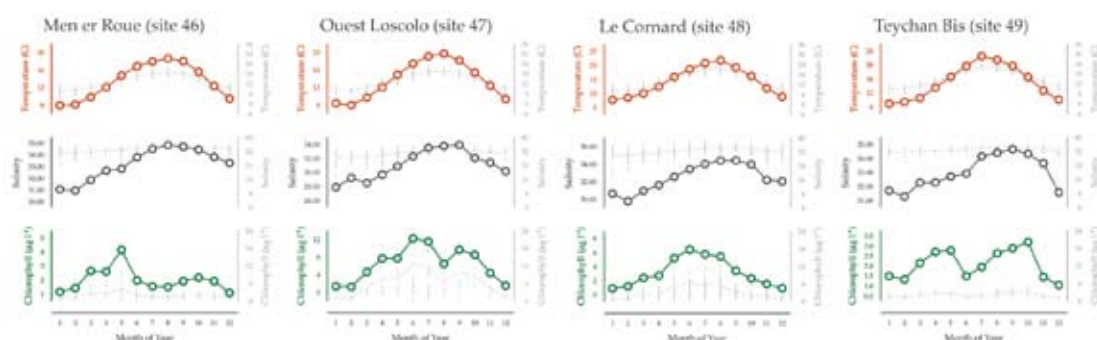


Figure 8.1.1

Locations of the REPHY Bay of Biscay plankton monitoring areas (Sites 46–49), plotted on a map of average chlorophyll concentration, and their corresponding environmental summary plots (see Section 2.2.1).



The French Phytoplankton and Phycotoxin Monitoring Network (REPHY) was set up in 1984 with three objectives: to enhance knowledge of phytoplankton communities, to safeguard public health, and to protect the marine environment (Belin, 1998). Phytoplankton along the French coast has been sampled up to twice a month since 1987 at twelve coastal laboratories. The French coast is divided into a hierarchy of sites and subsites common to three regional networks: the English Channel, the Bay of Biscay, and the Mediterranean Sea. Men er Roue, Ouest Loscolo, Le Cornard, and Teychan Bis are four REPHY sites in the Bay of Biscay. These sites are all shallow, meso- to macrotidal, with differing wave exposure from sheltered in Teychan Bis to moderately exposed at Ouest Loscolo and Le Cornard.

From 1987 onwards, the basic environmental variables salinity, temperature, and turbidity are measured together with phytoplankton composition and abundance. Variables such as inorganic nutrient concentrations chlorophyll *a*, pheopigments, and oxygen were included in the time-series of most of the sites later in different years.

Seasonal and interannual trends (Figure 8.1.2–8.1.5)

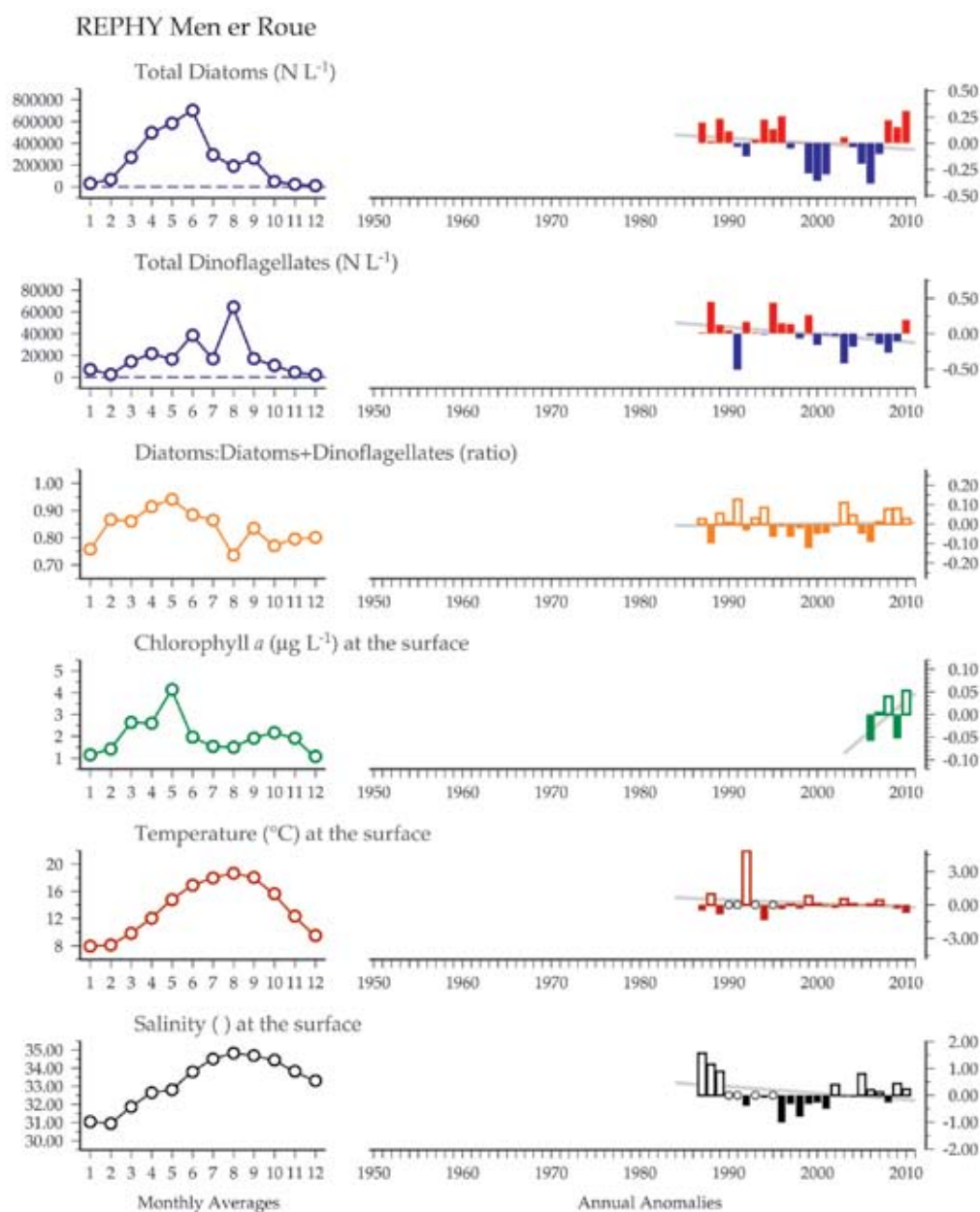
Seasonal cycles of chlorophyll as a measure of total phytoplankton biomass are bimodal at Men er Roue (Figure 8.1.2), Ouest Loscolo (Figure 8.1.3), and Teychan Bis (Figure 8.1.5), with maxima generally found in May/June and September/October, which, at the latter site, are even of greater magnitude than the spring peak, and unimodal

at Le Cornard (Figure 8.1.4), with an annual maximum in June. Although dinoflagellates at the sites usually exhibited unimodal cycles, peaking around August, the Teychan Bis site was bimodal, with a strong May peak followed by a weaker August increase. Diatoms at Men er Roue, Ouest Loscolo, and Le Cornard were bimodal, with peaks in May/June and September/October in accordance with chlorophyll cycles. Diatoms at Le Cornard were unimodal, with a strong peak in March and a slow, steady decrease onwards. Dominant diatom species common to all sites include *Skeletonema costatum* and *Leptocylindrus minimus*, with *L. danicus* important at Ouest Loscolo and Teychan Bis. *Asterionellopsis glacialis* may be frequent in blooms at Teychan Bis year-round. *Pseudo-nitzschia* sp. blooms appeared more frequently in the last two years. Dinoflagellates include several species

of *Prorocentrum* and *Protoperidinium*. *Lepidodinium chlorophorum* may form summer blooms locally.

Long-term trends for *in situ* temperature, salinity, and chlorophyll are not significant at any of the Bay of Biscay REPHY sites. However, some significant tendencies have been identified in the large phytoplankton groups. Total diatom abundance has increased significantly at the Ouest Loscolo ($p < 0.05$) and Le Cornard ($p < 0.01$) sites. Total dinoflagellate abundance has also increased at both sites, but only Le Cornard's trend was significant ($p < 0.05$). At the Men er Roue and Teychan Bis sites, diatoms and dinoflagellate totals were both decreasing (but without statistical significance). The diatoms:diatoms+dinoflagellates ratio was decreasing at the Teychan Bis site ($p < 0.05$) and at the Ouest Loscolo site (non-significant).

Figure 8.1.2
Multiple-variable comparison plot (see Section 2.2.2) showing the seasonal and interannual properties of select cosampled variables at the Men er Roue plankton monitoring site. Additional variables from this site are available online at <http://wgpmc.net/time-series>.



REPHY Ouest Loscolo

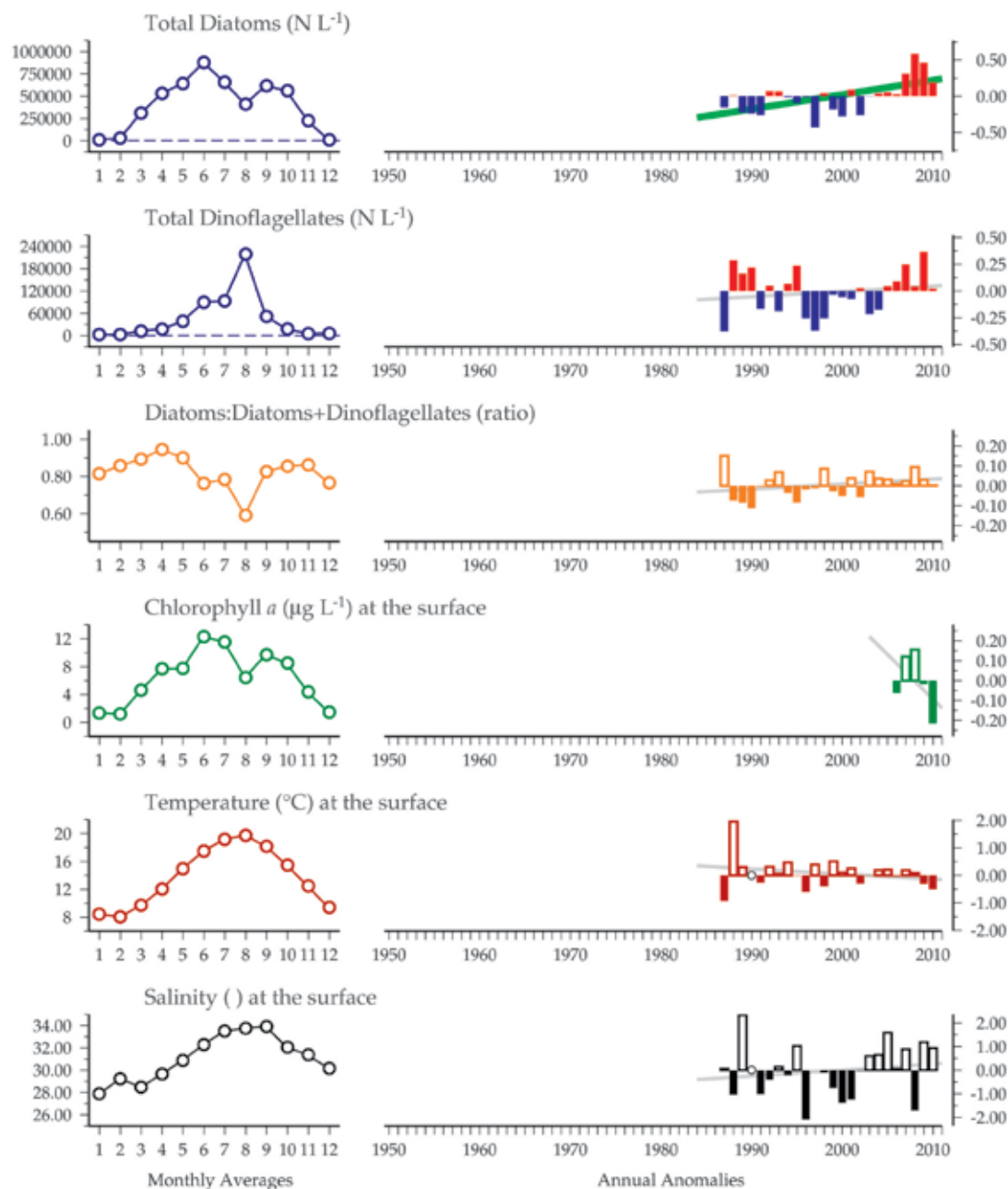
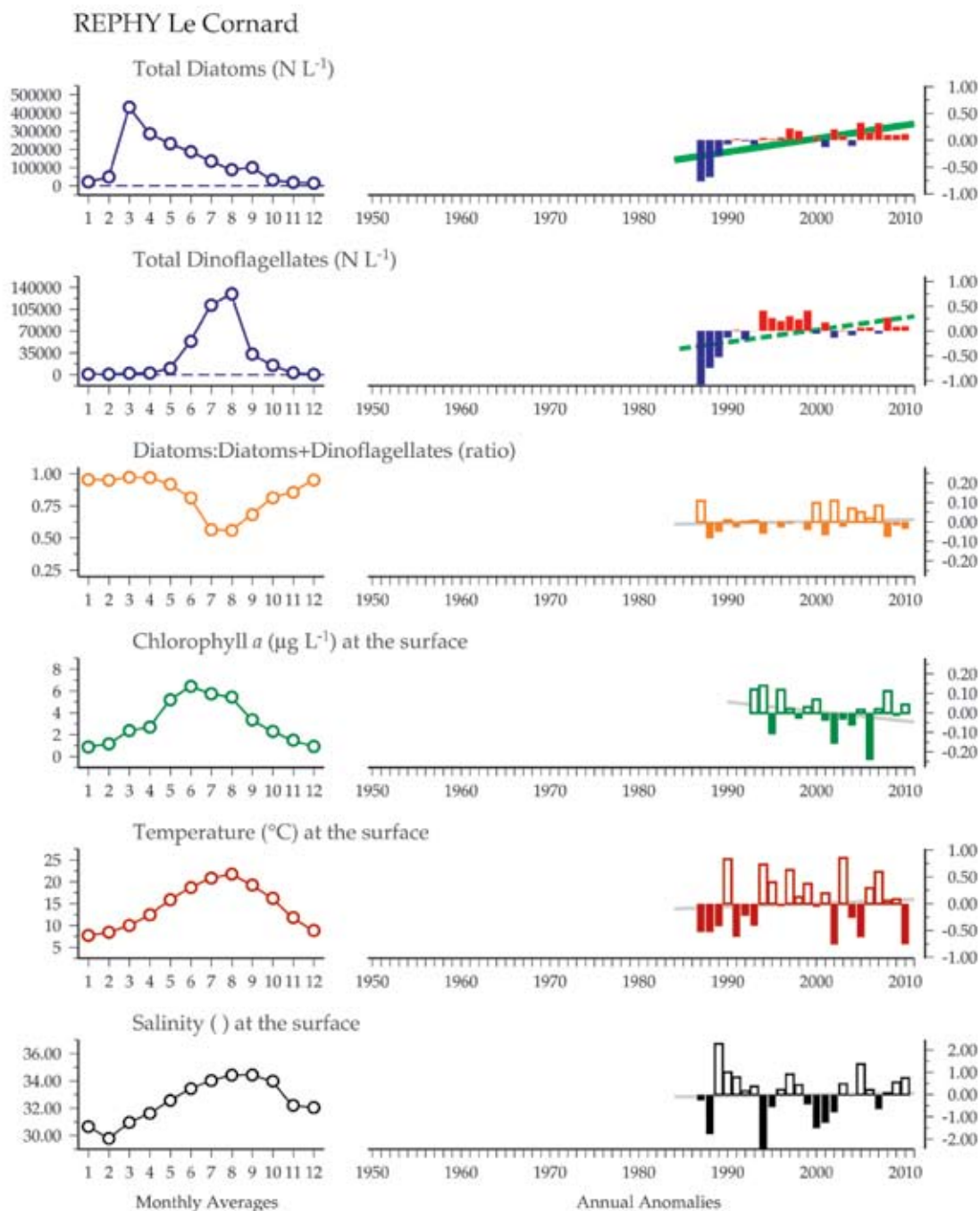


Figure 8.1.3
Multiple-variable comparison plot (see Section 2.2.2) showing the seasonal and interannual properties of select cosampled variables at the Ouest Loscolo plankton monitoring site. Additional variables from this site are available online at <http://wgpme.net/time-series>.

Figure 8.1.4
Multiple-variable comparison plot (see Section 2.2.2) showing the seasonal and interannual properties of select cosampled variables at the Le Cornard plankton monitoring site. Additional variables from this site are available online at <http://wgpme.net/time-series>.



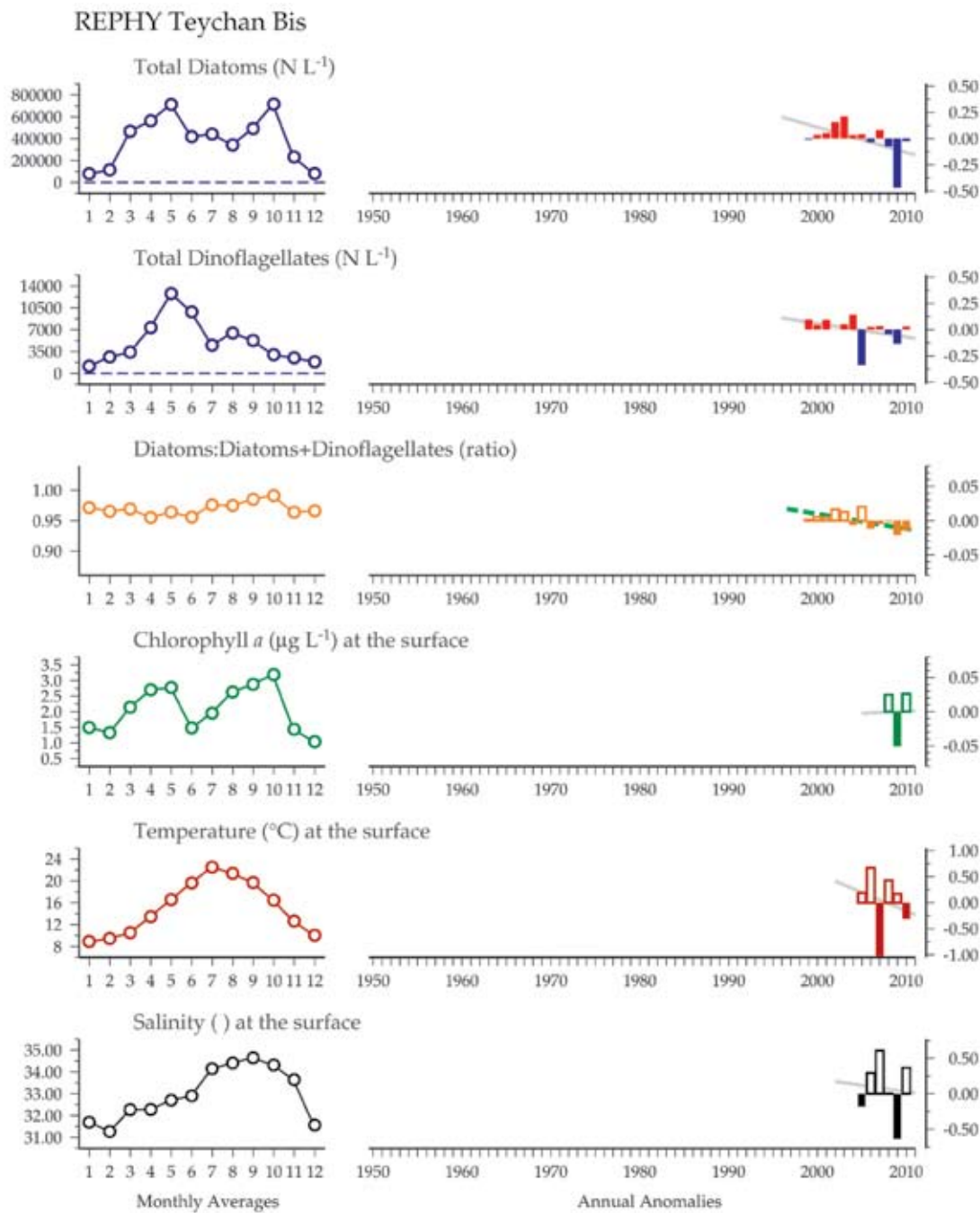
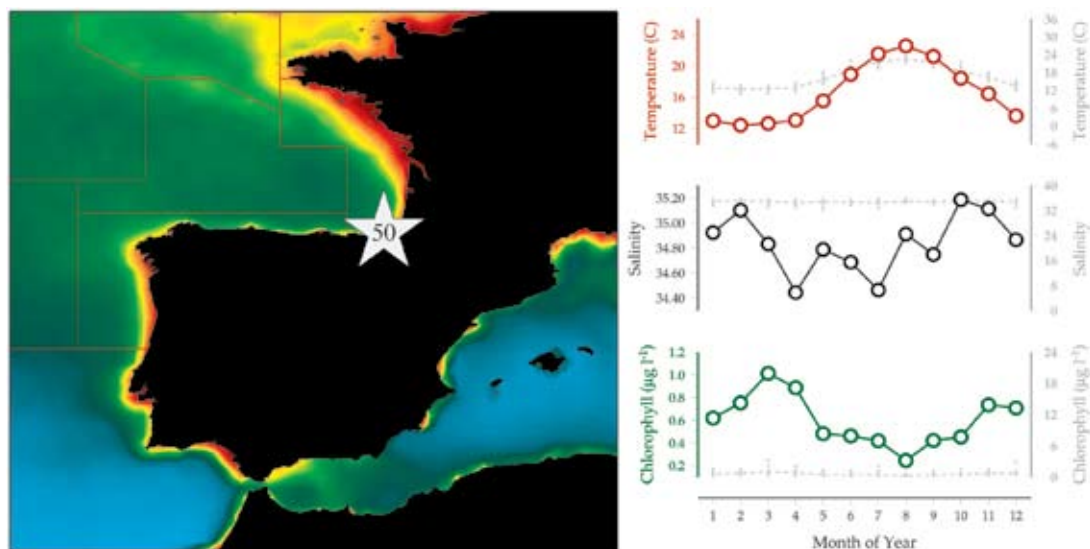


Figure 8.1.5
Multiple-variable comparison plot (see Section 2.2.2) showing the seasonal and interannual properties of select cosampled variables at the Teychan Bis plankton monitoring site. Additional variables from this site are available online at <http://wgpme.net/time-series>.

8.2 AZTI Station D2 (Site 50)

Marta Revilla, Ángel Borja, Almudena Fontán, and Victoriano Valencia

Figure 8.2.1
Location of the AZTI Station D2 plankton monitoring area (Site 50), plotted on a map of average chlorophyll concentration, and its corresponding environmental summary plot (see Section 2.2.1).



Along the Basque coast (southeastern Bay of Biscay), the longest series on phytoplankton biomass (chlorophyll *a* concentration) has been obtained at station D2 (Site 50, 43°27'N 01°55'W). This station is located 13.1 km offshore and at a water depth of 110 m. Data are collected since 1986 by AZTI-Tecnalia, within the project “Variaciones”, funded by the Department of Environment, Territorial Planning, Agriculture and Fisheries of the Basque Government. Surveyed months and total number of surveys per year are variable (3–12). On average, eight surveys per year are conducted. Details on sampling and analytical methods are available in Revilla *et al.* (2010). Generally, CTD continuous vertical profiles have been obtained. Here, long-term series on chlorophyll, salinity, and temperature are presented.

Additionally, phytoplankton abundance and composition, together with general environmental conditions (e.g. oxygen, nutrients, and optical properties) are shown from 2002 to 2010. This is part of the Littoral Water Quality Monitoring and Control Network of the Basque Country, conducted by AZTI-Tecnalia for the Basque Water Agency (URA). For this purpose, the station D2 is sampled every three months from February to November. Water samples for phytoplankton analyses (Utermöhl, 1958) are collected at the surface with a clean bucket and immediately fixed with glutaraldehyde. Field and laboratory methods are described in detail by Garmendia *et al.* (2011).

The offshore station D2 is considered to be unaffected by anthropogenic influence, owing to its distance from the main pollution sources on land. The main fertilization factor for the surface waters of this area is the continental run-off coming from the rivers around the southeastern Bay of Biscay (Valencia and Franco, 2004; Díaz *et al.*, 2007; Ferrer *et al.*, 2009). Surface salinity is 34.8 ± 0.67 (average \pm standard deviation) from 1986 to 2008 ($n = 174$), which indicates a low average freshwater content (2.3%).

Seasonal and interannual trends (Figure 8.2.2)

At station D2, sea surface temperature (SST) presents a distinct seasonal cycle, and chlorophyll in surface waters (0–1 m) is inversely correlated to SST. The cold season can be defined as November–April, with monthly averaged SST ranging from 12.5 to 16.5°C and surface chlorophyll ranging from 0.6 to 1.0 $\mu\text{g l}^{-1}$. The warm season can be defined as May–October (15.6–22.7°C, monthly averaged SST). During the warm months, the mean chlorophyll concentration is below 0.5 $\mu\text{g l}^{-1}$ in surface waters.

The surface waters at D2 station have warmed up over the past 20–30 years ($1.4 \pm 1.1 \times 10^{-2} \text{ }^{\circ}\text{C year}^{-1}$). The change could be faster for inshore waters, at around $2.4 \times 10^{-2} \text{ }^{\circ}\text{C year}^{-1}$ (González *et al.*, 2008; Revilla *et al.*, 2009). Warming patterns have also been described for other neighbouring areas (e.g. Goikoetxea *et al.*, 2009; Bode *et al.*, 2011b). In the

southern Bay of Biscay, Llope *et al.* (2007) linked the recent warming of the ocean surface with increasing stratification and weaker/shallower winter mixing, which could reduce nutrient inputs and cause stoichiometric changes. In this scenario, it has been hypothesized that primary production will be progressively lower and phytoplankton assemblages will change (Llope *et al.*, 2007).

At station D2, Revilla *et al.* (2010) found a slight decrease in the surface chlorophyll concentration between 1986 and 2008 ($-3.8 \pm 4.7 \times 10^{-3} \mu\text{g l}^{-1} \text{ year}^{-1}$). Further studies demonstrated that the photic-layer-averaged chlorophyll (0–50 m) had followed an opposite, increasing trend ($6.2 \pm 2.5 \times 10^{-3} \mu\text{g l}^{-1} \text{ year}^{-1}$). In addition, the location of the chlorophyll subsurface maximum could have moved progressively deeper in the water column, from 10 m at the beginning of the series to 30 m in the last decade. These trends could be related to climatic factors, such as the East Atlantic (EA) pattern (ICES, 2011).

The analysis of the annual anomalies at station D2 demonstrates a significant increase ($p < 0.05$) in the photic-layer-averaged chlorophyll over the 1986–2010 period. *In situ* surface temperatures taken immediately at the site had an increasing (but non-significant) trend, whereas HadISST date-matched data from the larger region did present a significant increasing trend ($p < 0.05$). These findings support previous results in the area that were obtained by other methods for trend analyses. Those were non-

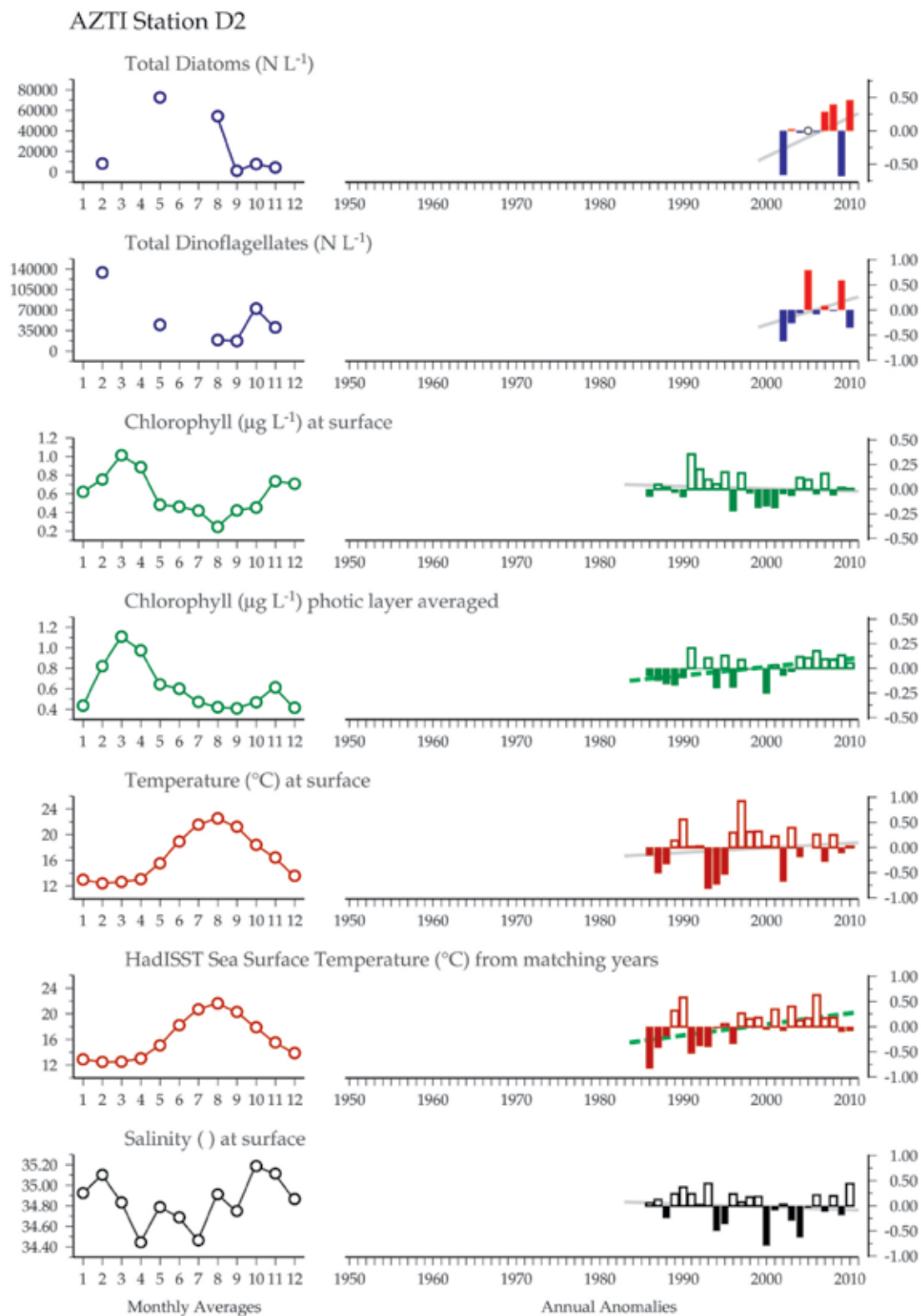
parametric methods based on seasonal variability removal and regression analysis, or KZA filter (Revilla *et al.*, 2010; ICES, 2011).

Decadal variations in climatic conditions have been described in this geographical area, with an increase in the positive phase of the EA occurring since 1997 (Borja *et al.*, 2008; Goikoetxea *et al.*, 2009). In the northern part of the Iberian Peninsula, the EA pattern is the most important variation pattern explaining temperature variability. In particular, in the southeastern Bay of Biscay, a positive EA involves warmer and drier winters, as well as stronger downwelling, caused by the southwesterly winds. At a larger scale, the positive phase of the EA is associated with above-average precipitation over northern Europe and Scandinavia, and with below-average precipitation across southern Europe (deCastro *et al.*, 2008).

At station D2, the oceano-meteorological variability coupled to the EA pattern could explain the decrease in phytoplankton biomass in surface waters and its increase in deeper waters in response to stronger downwelling and reduced cloudiness (ICES, 2011). Nevertheless, in other areas of the north Iberian Peninsula, the response of phytoplankton to climate variability could be different in relation to the relative influence of other hydrographic factors (e.g. upwelling activity and run-off) at the local scale (Bode *et al.*, 2011b).

Figure 8.2.2

Multiple-variable comparison plot (see Section 2.2.2) showing the seasonal and interannual properties of select cosampled variables at the AZTI Station D2 plankton monitoring site. Additional variables from this site are available online at <http://wgpme.net/time-series>.



8.3 Nervión River estuary (Site 51)

Emma Orive, Javier Franco, Aitor Laza-Martínez, Sergio Seoane, and Alejandro de la Sota

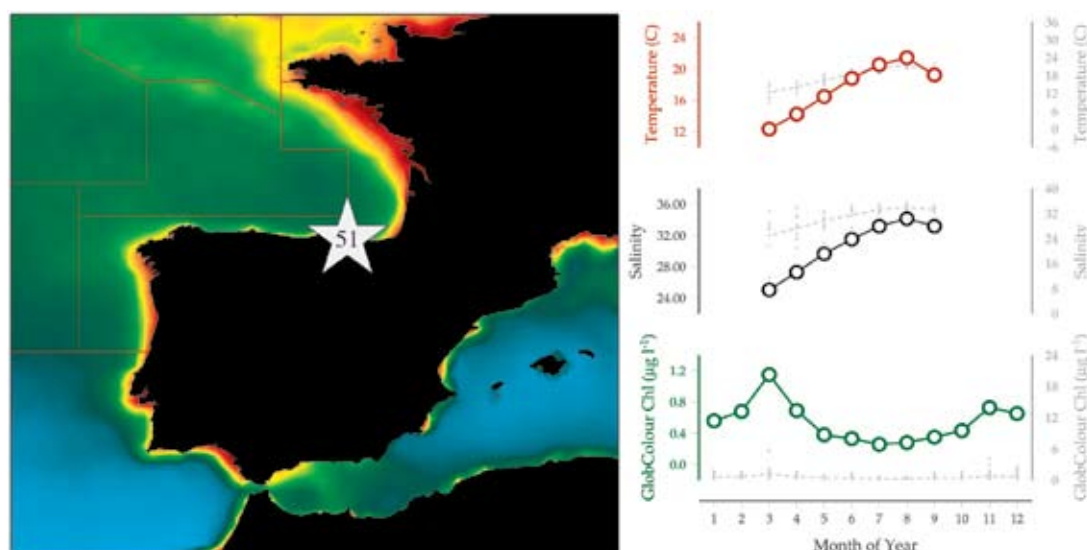


Figure 8.3.1
Location of the Nervión River Estuary plankton monitoring area (Site 51), plotted on a map of average chlorophyll concentration, and its corresponding environmental summary plot (see Section 2.2.1).

The Nervión River estuary (also named Nervión-Ibaizabal estuary) has been monitored for phytoplankton taxonomic composition and abundance since 2000. The Nervión catchment is densely populated, and this study forms part of a broader monitoring programme performed to follow the water quality evolution after the implementation of a sewerage scheme in the area (García-Barcina *et al.*, 2006). Phytoplankton samples are taken approximately monthly from March to September at eight stations (1–8, from the outer to the inner estuary) located along the longitudinal axis. Samples are analysed for cell identification and counted with the Utermöhl method; in addition, individuals from selected genera among those forming blooms or known to contain harmful species are isolated from live samples and grown in cultures for a more detailed morphological and genetic characterization. Stations 1 and 2 are located in the outer estuary (Abra of Bilbao), which, with a width of ca. 3 km and a maximum depth of ca. 30 m, contains most of the estuarine water. This estuarine area is dominated by marine water during most of the monitoring period and phytoplankton species are mainly of marine origin.

Seasonal and interannual trends (Figure 8.3.2)

The apparent increase in total diatoms and flagellates from 2000 to 2010 can be attributed to the improvement in water quality during this period, and is likewise evident in the

diatoms:diatoms+dinoflagellates ratio. Dinoflagellates are relatively scarce in the estuary, as determined by signature pigments from estuarine phytoplankton (Seoane *et al.*, 2005). Fucoxanthin is usually the dominant pigment in the total phytoplankton. Haptophytes are almost always present in the outer estuary (Seoane *et al.*, 2009), and blooms of *Apedinella spinifera* and *Heterosigma akashiwo* have been observed. Diatoms seem to constitute the bulk of chlorophyll *a* among fucoxanthin-containing microalgae. Alloxanthin is also relatively abundant, in agreement with the abundance of cryptophytes, which form frequent blooms both in the outer and inner estuary (Laza-Martínez, 2012). However, in the picoplankton, chlorophyll *b* is almost always the dominant pigment (Seoane *et al.*, 2006). FISH analysis (unpublished data) revealed the dominance of prasinophytes in this size fraction.

Cell density can be high in spring in the outer estuary because of the spring diatom bloom in adjacent coastal waters. During this period, which can be very short and start at different times each year, the outer estuary is dominated by large marine diatoms responsible for the annual maxima of chlorophyll *a*. However, the maximum abundance for most phytoplankton classes, in terms of cell numbers, is generally registered in summer. The size of the cells, generally larger in spring, can account for the absence of a clear relationship between chlorophyll *a* values and the number of cells. Summer maxima in cell numbers can be partially attributed to the

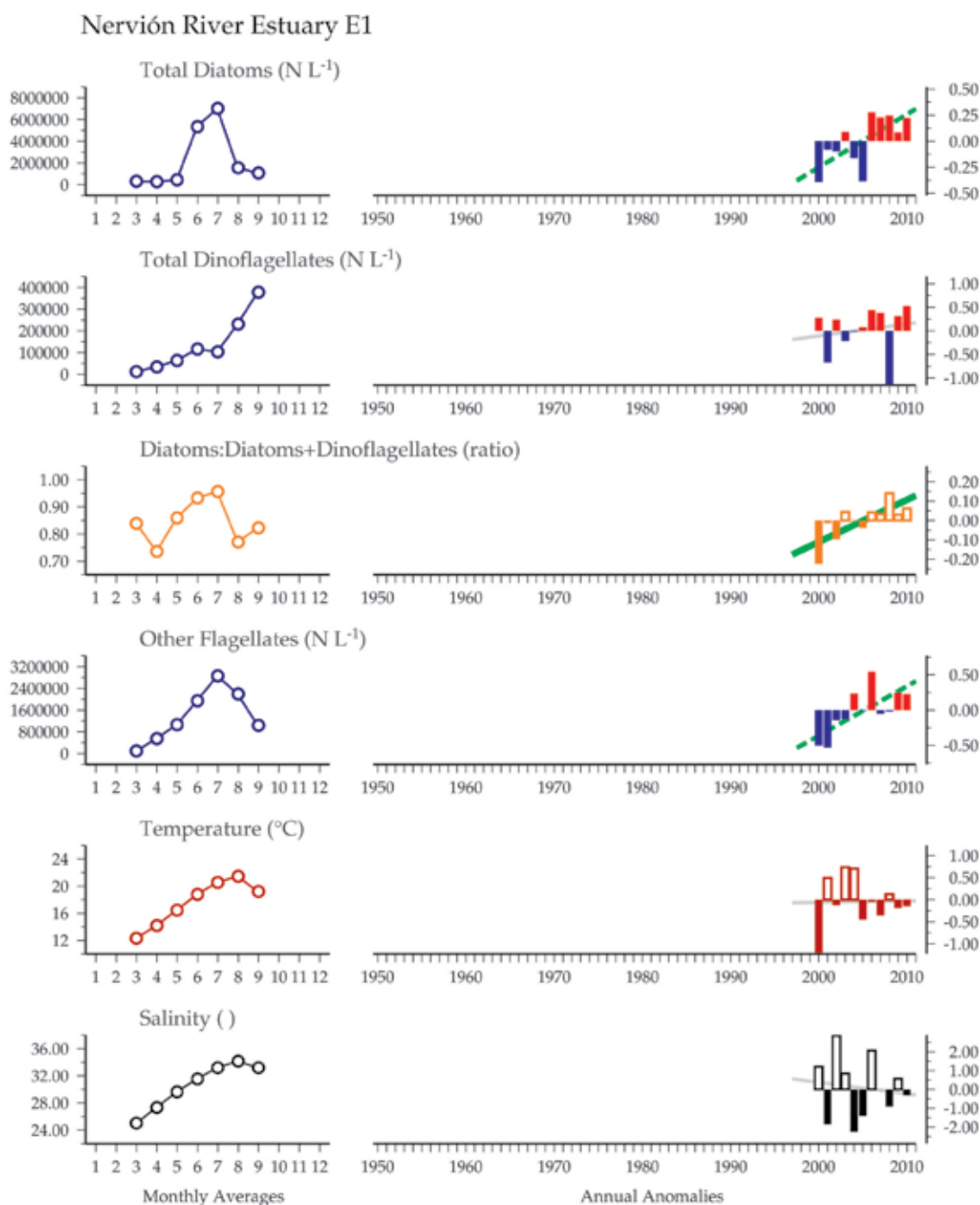
export to the outer estuary of eurihaline taxa that reach bloom proportions in the inner and middle estuary. In summer, these estuarine segments are a source of small centric diatoms and flagellated forms, belonging to Chlorophyta, Cryptophyta, and Haptophyta, to the outer estuary (Seoane *et al.*, 2006; Laza-Martinez *et al.*, 2007). In addition to these eurihaline species, the outer estuary contains marine forms which grow better in this area during summer than in the oligotrophic coastal waters (Orive, 1989; Orive *et al.*, 2010).

The shift between flagellates and diatoms in the outer estuary in summer is driven by river run-off after rainy periods and by stability of the water column. The raphidophycean *Heterosigma akashiwo*,

which is known to support high irradiance levels without experiencing photoinhibition (Martinez *et al.*, 2010), has been observed in bloom proportions in the outer estuary coinciding with very sunny days and elevated temperatures.

Lately, much attention is being paid to potentially toxic epiphytic dinoflagellates, which can appear in the water column as part of the phytoplankton. In addition to several species of the genera *Coolia* and *Prorocentrum*, toxic forms of the genus *Ostreopsis* have been found in the outer estuary and other localities of the southeastern Bay of Biscay that constitute the upper reported limit for the distribution of this pantropical genus in the Atlantic Ocean (Laza-Martinez *et al.*, 2011).

Figure 8.3.2
Multiple-variable comparison plot (see Section 2.2.2) showing the seasonal and interannual properties of select cosampled variables at the Nervión River estuary plankton monitoring site. Additional variables from this site are available online at <http://wgpmc.net/time-series>.



8.4 RADIALES Gijón/Xixón Station 2 (Site 52)

Xosé Anxelu G. Morán and Renate Scharek

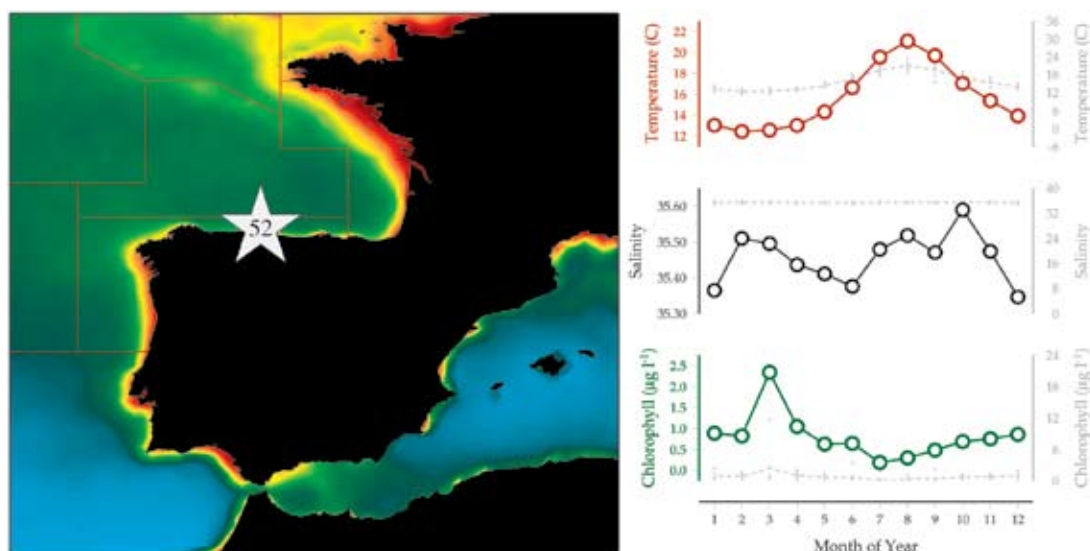


Figure 8.4.1

Location of the RADIALES Gijón/Xixón Station 2 plankton monitoring area (Site 52), plotted on a map of average chlorophyll concentration, and its corresponding environmental summary plot (see Section 2.2.1).

Sampling at the Gijón/Xixón transect started in March 2001, shortly after the opening of the Oceanographic Center of Gijón/Xixón, the latest laboratory of the Spanish Institute of Oceanography (IEO) to be built. Picoplankton began to be collected one year later. The Gijón/Xixón oceanographic time-series is part of the IEO programme RADIALES (<http://www.seriestemporales-ieo.com/>) and comprises three stations in the central Cantabrian Sea (southern Bay of Biscay) located over the ca. 37 km wide continental shelf off the city of Gijón/Xixón (Asturias, Spain). Only Station 2 data were used for this site summary.

Water samples are collected monthly on board RV “José de Rioja” from Niskin bottles in a rosette sampler attached to a CTD probe. The three stations are sampled for picoplankton at 10 m intervals from the surface down to 50 m, and additionally at 5 m at Station 1, at 75 and 100 m at Station 2, and at 75, 100, and 150 m at Station 3. Larger phytoplankton (nano- and microphytoplankton) is sampled at 0, 30, and 75 m at Station 2. Autotrophic and heterotrophic picoplanktonic groups are distinguished by flow cytometry analysis of 1% paraformaldehyde plus 0.5% glutaraldehyde preserved, ultrafrozen samples. Autotrophic picoplankton groups or picophytoplankton (*Synechococcus* and *Prochlorococcus* cyanobacteria and two groups of picoeukaryotes) are distinguished by red and orange fluorescence and size signals of thawed, unstained samples, whereas heterotrophic bacteria are first dyed with SYTO

13 fluorochrome. Nano- and microphytoplankton are fixed with acetic-acid Lugol’s solution (1% final concentration). Qualitative and quantitative analysis of nano- and microplankton is performed with an inverted microscope using the Utermöhl technique (Utermöhl, 1958). Cells are classified to species or genus level if possible or assigned to higher taxonomic levels divided into size classes.

The site displays the typical oceanographic conditions of a temperate shelf sea, with a well-mixed water column from November through April, broken occasionally by the presence of low-salinity water at surface layers and conspicuous stratification in late spring and summer, with a pycnocline usually developing at 10–20 m depth (Calvo-Díaz and Morán, 2006). Other hydrographic features include the presence of a saline and warm poleward slope current, especially during winter (Pingree and Le Cann, 1990; Álvarez-Salgado *et al.*, 2003) and short-lived, upwelling pulses more frequently found in late summer and early autumn (McClain *et al.*, 1986; Llope *et al.*, 2006). Warming trends have been described for the region for both surface (deCastro *et al.*, 2009) and deeper waters (González-Pola *et al.*, 2005), similar to those described for the whole North Atlantic basin (e.g. Johnson and Gruber, 2007).

Seasonal and interannual trends (Figure 8.4.2)

Total phytoplankton biomass (chlorophyll) demonstrates a unimodal distribution, with the annual maximum associated with the spring bloom in March and April, and minimum values usually recorded in July. As previously described (Calvo-Díaz and Morán, 2006), a marked seasonality in picophytoplankton becomes evident, with late summer–early autumn maxima in abundance ($>10^5$ cells mL^{-1}) and predominance of cyanobacteria ($>80\%$ of total abundance), and minima in early spring ($<10^4$ cells mL^{-1}), coincident with very small numbers of *Synechococcus*. One prominent feature is the absence of *Prochlorococcus* for roughly half of the year (March–July), probably due to a combination of low temperatures and high mortality rates in winter, with water-mass advection playing a role in its reappearance in late summer (Calvo-Díaz *et al.*, 2008). The abundance of this cyanobacteria appears related to water temperature, consistent with the predicted increase in picophytoplankton absolute and relative abundance in a warmer North Atlantic (Morán *et al.*, 2010).

Diatom spring blooms occur around April and, in some years, late summer–autumn diatom blooms are also found, which can be as pronounced as or even more pronounced (in terms of cell abundance) than the spring bloom. As expected for an open coastal area, big dinoflagellates ($>20\ \mu\text{m}$) do not form marked blooms. Small dinoflagellates ($<20\ \mu\text{m}$) formed a bloom in late autumn 2006, and

during the spring bloom in April 2007, increased to nearly half of the cell concentration of diatoms. Representative diatom species forming spring or autumn diatom blooms are *Chaetoceros* spp., *Hyalochaete* spp., *Pseudo-nitzschia* spp., *Rhizosolenia setigera*, *Rhizosolenia pungens*, and *Guinardia delicatula*.

Unlike most autotrophs, heterotrophic bacteria ($0.2\text{--}2.7 \times 10^6$ cells mL^{-1}) show a clearly bimodal distribution, with peaks in April and October and relative minima in February and July. Highly consistent changes in the relative distribution of the flow cytometric groups of cells with low and high nucleic acid content probably reflect distinct species succession (Morán *et al.*, 2011). Bacterial abundance off Gijón/Xixón has increased since the beginning of the time-series. Although this trend is not significant (grey line in Figure 8.4.2), an analysis decomposing the monthly time-series variance has demonstrated a significant increase in integrated bacterial biomass, with the 2009 annual mean value being 30% higher than that of 2002 (Morán *et al.*, 2011).

By 2012, we will have completed a decade of microbial records in this site. Although it will probably still be too short to draw concluding associations with the observed increases in oceanic temperature, our working hypothesis is that small plankton will become increasingly important in the near future.

Figure 8.4.2 (continued on facing page)

Multiple-variable comparison plot (see Section 2.2.2) showing the seasonal and interannual properties of select cosampled variables at the RADIALES Gijón/Xixón Station 2 plankton monitoring site. Additional variables from this site are available online at <http://wgpme.net/time-series>.

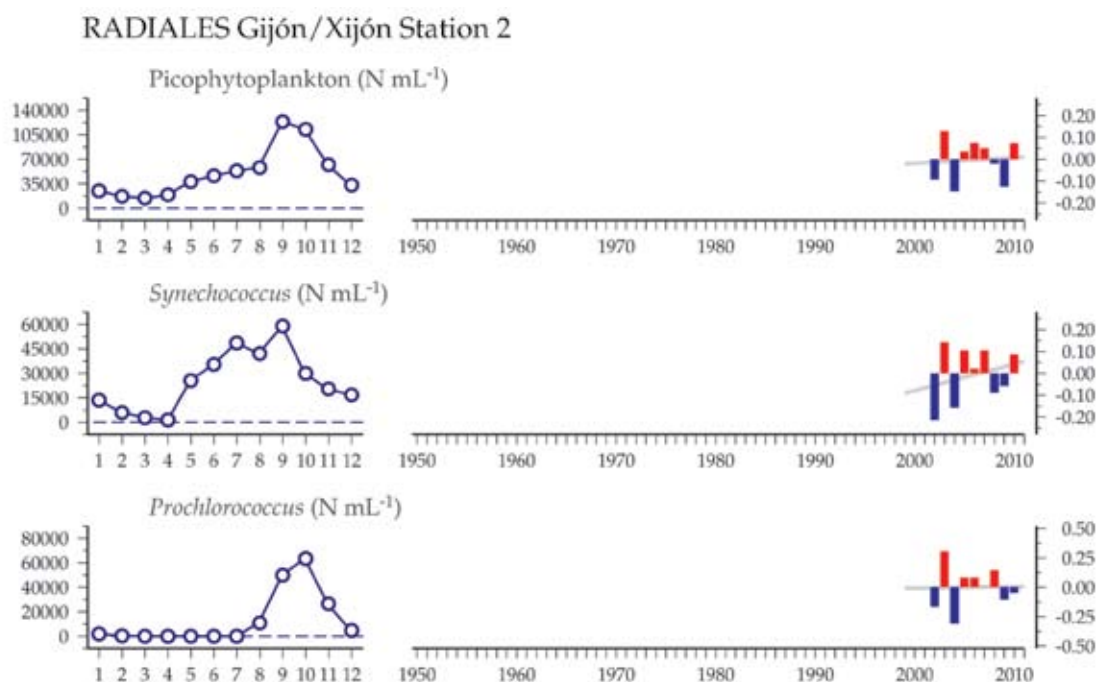
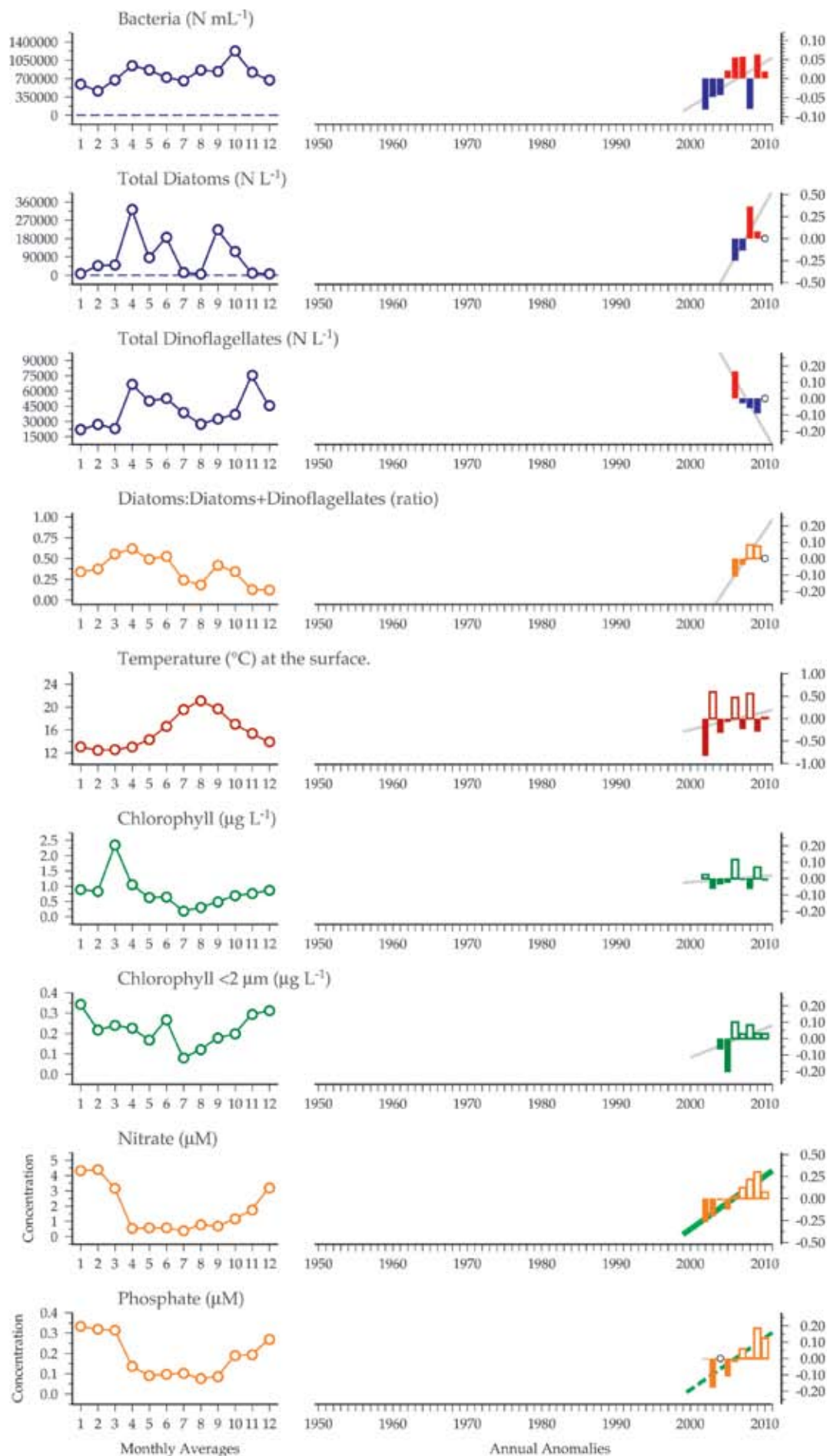


Figure 8.4.2 continued.

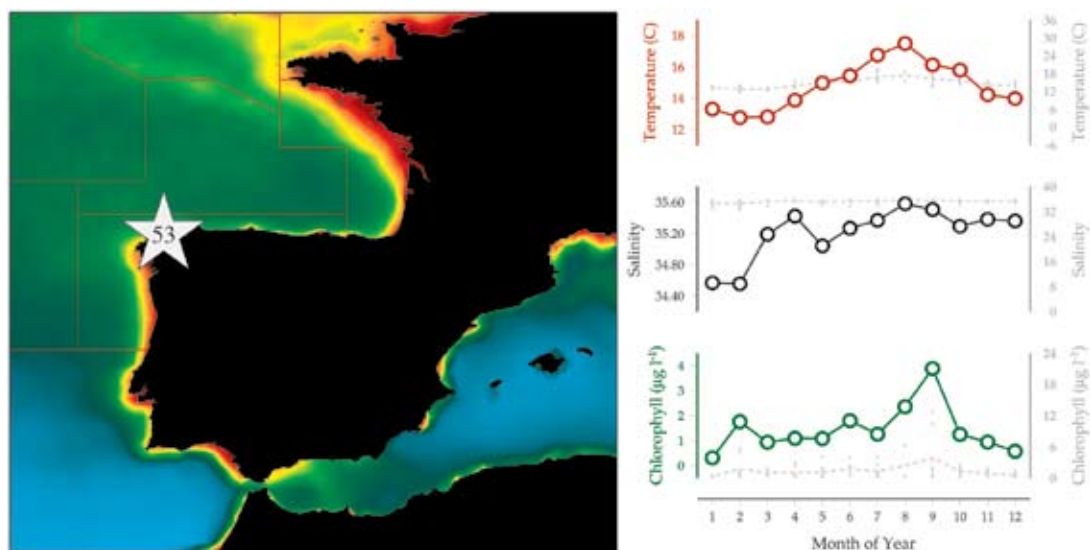


8.5 RADIALES A Coruña Station 2 (Site 53)

Antonio Bode, Manuel Varela, and Xosé Anxelu G. Morán

Figure 8.5.1

Location of the RADIALES A Coruña Station 2 plankton monitoring area (Site 53), plotted on a map of average chlorophyll concentration, and its corresponding environmental summary plot (see Section 2.2.1).



The A Coruña section is part of the time-series programme RADIALES (<http://www.seriestemporales-ieo.com>). Station 2 of the A Coruña section, which was used for this summary, is located off the northwestern Iberian coast at 43°25.3'N 8°26.2'W. Phytoplankton samples were collected at the depth equivalent to irradiance levels 100, 50, 25, 10, and 1% of surface photosynthetic active irradiance (PAR) using Niskin bottles. Sampling (starting in 1989) is made at monthly frequency. CTD casts were made simultaneously with sampling (Sea-Bird rosette from 2000 onwards) or just before bottle deployment (1989–1999) and temperature, salinity, *in situ* chlorophyll fluorescence, and PAR irradiance profiles were recorded. Aliquots of water for large phytoplankton samples were preserved in Lugol's iodine. Starting in 2004, picoplankton was sampled and analysed as described by Calvo-Díaz and Morán (2006). Additional water samples were collected for determination of chlorophyll (GF/F filters, acetonic extracts, fluorometry) and nutrients (nitrate, nitrite, ammonium, phosphate, and silicate by segmented flow analysis). Detailed description of sampling and analytical procedures can be found in Casas *et al.* (1997).

The phytoplankton cycle in this area demonstrates the general characteristics described for the temperate zone (Margalef, 1964; Varela *et al.*, 2001). There is an alternation between a mixing period in winter and a stratification period in summer, with blooms in the transition phases: mixing–stratification (spring blooms) and stratification–

mixing (autumn blooms). In this section, as in the whole coastal region off Galicia (northwestern Spain), this classical pattern of seasonal stratification of the water column in temperate regions is masked by upwelling events, especially during summer (e.g. Casas *et al.*, 1997). These upwelling events provide phytoplankton populations with favorable conditions for development well beyond the typical spring bloom of most seas in this latitude. As a consequence of these disturbances of the water column, phytoplankton abundance demonstrates a unimodal distribution, with annual maxima in summer and predominance of diatoms throughout the year. Only during stratification periods, coinciding with a decrease in upwelling intensity, is there a relative increase of dinoflagellates (Margalef *et al.*, 1955; Varela *et al.*, 1996; Casas *et al.*, 1997, 1999).

Seasonal and interannual trends (Figure 8.5.2)

Phytoplankton blooms can be observed from spring to autumn, including summer, when major phytoplankton abundance was also detected. Diatoms always dominate the microphytoplankton community. Several species of the genus *Chaetoceros*, especially *C. socialis* as well as *Leptocylindrus danicus*, *Pseudo-nitzschia pungens*, and *Skeletonema costatum*, are generally dominant during blooms in all seasons. During spring, *Cerataulina pelagica*, *Lauderia annulata*, *Detonula pumila*, and *Guinardia delicatula* are more typical, whereas in autumn,

outbursts of *Asterionellopsis glacialis*, *P. delicatissima*, and *Thalassiosira levanderi* were more representative of the diatom community. All of the above-mentioned species can be found in the summer upwelling blooms, although *L. danicus*, *S. costatum*, *P. pungens*, and *Nitzschia longissima* attained higher abundance in this season. During winter mixing, the phytoplankton community is characterized by species that are present throughout the year, but in very low densities, as well as resuspended diatoms from the sediment (Casas *et al.*, 1999). The diatom species composition is similar to those found in other Galician coastal areas (Bode *et al.*, 1996; Varela and Prego, 2003; Varela *et al.*, 2005, 2006; Prego *et al.*, 2007).

In contrast to studies conducted in neighboring temperate areas, dinoflagellates never dominated during summer stratification periods, probably because of the very frequent upwelling events, which caused destabilization of the water column. In these stratified periods, a relative increase in dinoflagellate populations was recorded. Small species (< 20 µm) of naked dinoflagellates are the most abundant, with average values around 60 cells ml⁻¹, followed by *Prorocentrum balticum*, *Katodinium glaucum*, and large (>20 µm) unidentified thecate species exhibiting concentrations lower than 7 cells ml⁻¹. In other periods, the composition is similar to total densities around 50 cells ml⁻¹ in autumn and upwelling periods, and ca. 30 in spring and winter. *Heterocapsa niei* is typical of winter mixing. *P. balticum* and *P. minimum* are frequently observed during spring and autumn blooms, whereas *Scrippsiella trochoidea* and *Ceratium lineatum* are more characteristic of summer upwelling. As in

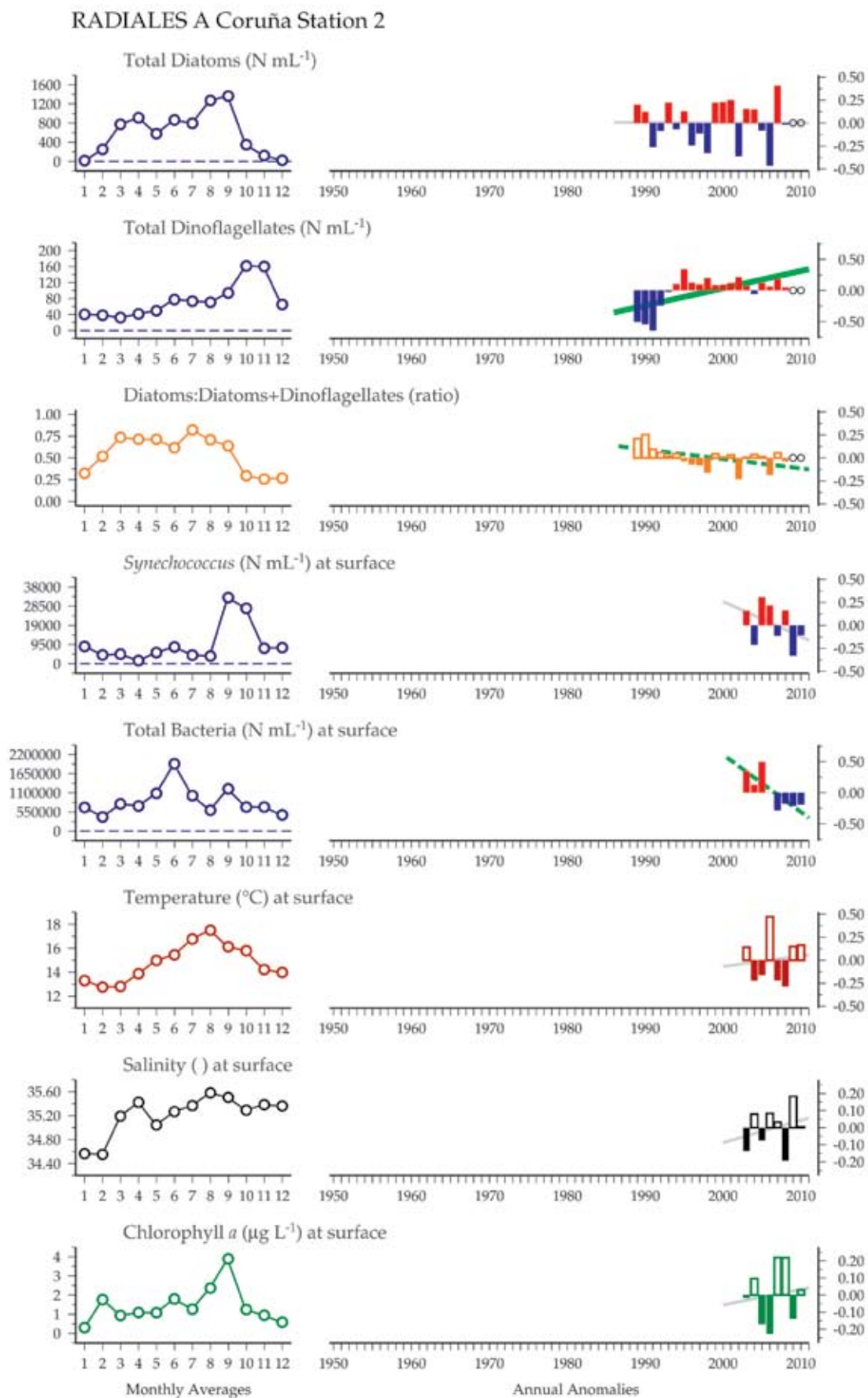
the case of diatoms, dinoflagellate species in the A Coruña transect are reported for other coastal areas of Galicia (Figueiras and Niell, 1987; Figueiras and Pazos, 1991; Bode and Varela, 1998; Varela *et al.*, 2005, 2008, 2010).

Picophytoplankton abundance at the surface, ranging over two orders of magnitude (10³–10⁵ cells ml⁻¹), tends to be higher during summer, in which cyanobacteria (mostly *Synechococcus*, with *Prochlorococcus* much less abundant and detected only from September through January) may contribute up to 80% of total cell counts. Similar to both large and small phytoplankton, surface heterotrophic bacteria (0.1–2.2 × 10⁶ cells ml⁻¹) show consistent unimodal distributions in A Coruña, with maxima found through spring and summer, and minima in February.

Recent studies of the historical data in the A Coruña section demonstrated a significant decrease in diatom abundance at interannual scales, along with an increase in dinoflagellates (albeit non-significant). These results are consistent with the decreasing upwelling intensity in the area (Bode *et al.*, 2011b; Varela *et al.*, 2012). The series revealed that there is no significant long-term trend in phytoplankton biomass, but primary production increased significantly, despite significant decadal changes in upwelling intensity (Bode *et al.*, 2011b). An increase in the use of remineralized nutrients from organic matter has been proposed to explain the increase in production (Pérez *et al.*, 2010). Additional annual observations are required for demonstrating the apparent trend of decreasing bacterial biomass at A Coruña Station 2.

Figure 8.5.2

Multiple-variable comparison plot (see Section 2.2.2) showing the seasonal and interannual properties of select cosampled variables at the RADIALES A Coruña station 2 plankton monitoring site. Additional variables from this site are available online at <http://wgpme.net/time-series>.



8.6 Guadiana estuary (Site 54)

Ana B. Barbosa, Rita B. Domingues, and Helena M. Galvão

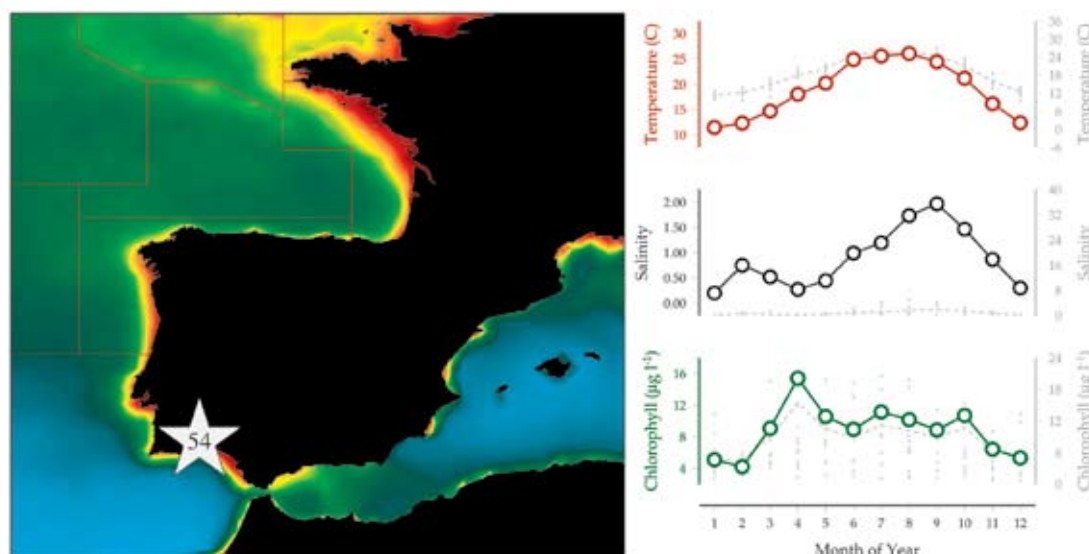


Figure 8.6.1

Location of the Guadiana estuary plankton monitoring area (Site 54), plotted on a map of average chlorophyll concentration, and its corresponding environmental summary plot (see Section 2.2.1).

The Guadiana estuary (GE) is located in southwestern Iberia and is a 22 km² mesotidal ecosystem (average depth: 6.5 m), ranging from partially stratified to well-mixed. GE is located in a Mediterranean climate area, classified as highly sensitive to climate change, and is currently considered one of the best preserved and most vulnerable estuaries of the Iberian Peninsula. The Guadiana River watershed is the fourth largest river basin in the Iberian Peninsula and demonstrates a torrential hydrographic regime, with concentrated rainy periods and a prolonged dry season, usually from May to September. Managing water availability under such demanding conditions led to the construction of hundreds of dams, almost 90 of which have a volume capacity over 1 hm³. Recent construction of the large Alqueva dam, built in the upper estuary in 1999 and completed in 2002, further increased freshwater flow regulation up to 81% (see Barbosa *et al.*, 2010, and references therein).

Phytoplankton monitoring in GE began in 1996 and was motivated by an anticipated increase in cyanobacterial blooms caused by the construction of the Alqueva dam. Physical-chemical variables (e.g. temperature, salinity, intensity of photosynthetic available radiation, light extinction coefficient, dissolved oxygen, concentration of dissolved inorganic macronutrients, particulate suspended matter) and phytoplankton abundance, composition, and biomass were routinely monitored at different stations in the upper, middle, and lower estuary in the framework of projects funded by the

Portuguese Foundation of Science and Technology (FCT) and the European Union. Abundance of heterotrophic bacterioplankton and phytoplankton and bacterial production were less frequently determined. Water quality and phytoplankton are also regularly monitored by the Portuguese Water Institute (INAG). Since 2008, water quality and hydrodynamics have been measured by an autonomous instrumented platform positioned at the estuary entrance (Garel *et al.*, 2009).

Data displayed in this site are average monthly values (1996–2010) collected at station “Alcouthim” (37°28'N 7°28'W; Datum WGS84) at subsurface levels (ca. 0.5 m). The station is located ca. 38 km from the Guadiana river mouth within the upper Guadiana estuarine region and has a mean depth of 9 m. Details on sampling and analytical methods are given in Barbosa *et al.* (2010). Samples were usually collected from the Alcouthim pier using a sampling bottle, and sampling frequency was usually monthly during autumn–winter and biweekly during the spring–summer productive period. Physical-chemical variables were analysed using standard methods. Chlorophyll *a* concentration, used as a proxy for phytoplankton biomass, was analysed using a spectrophotometric method, after GF/F sample filtration and acetone extraction. Abundance of picoplankton (< 2 µm) and nanophytoplankton (2–20 µm) was estimated using epifluorescence microscopy, after glutaraldehyde preservation and proflavin staining. Abundance of microphytoplankton (>20 µm) was analysed using

inverted microscopy, after Lugol preservation (see Barbosa *et al.*, 2010 for details).

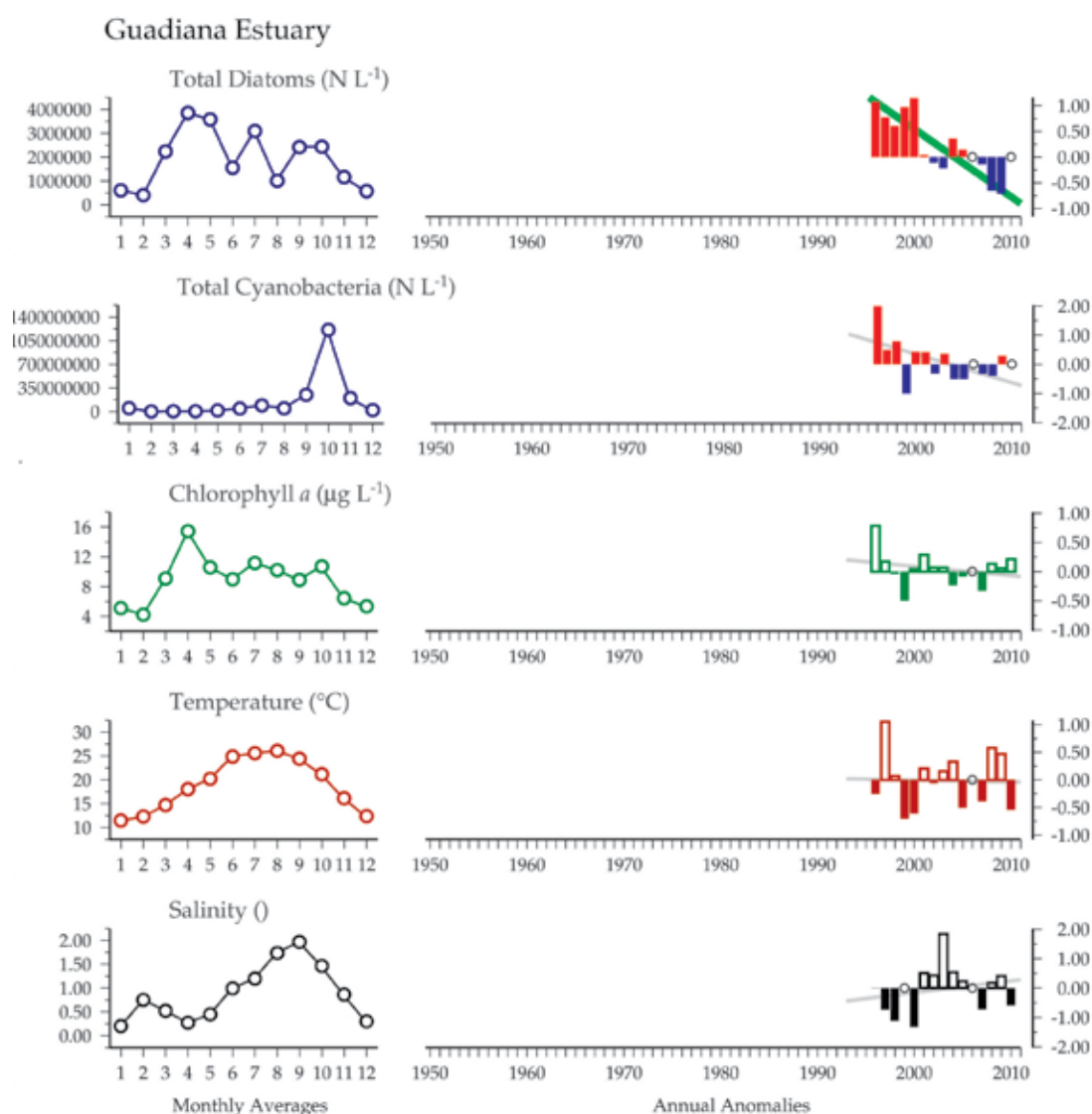
blooms, is driven by changes in nutrients, water temperature, and turbulence, clearly demonstrating the role of river flow and climate variability.

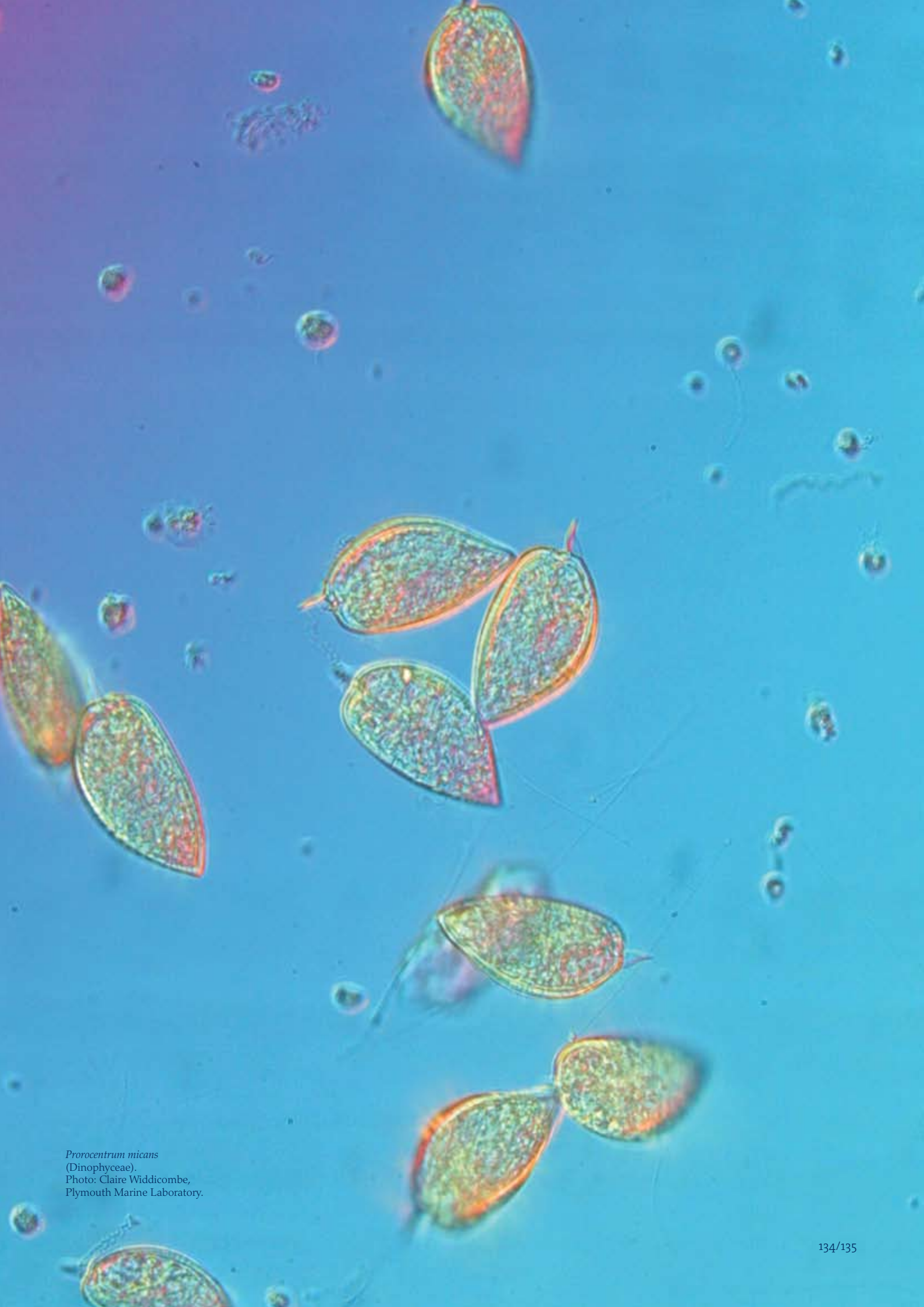
Seasonal and interannual trends (Figure 8.6.2)

Phytoplankton seasonal patterns, studied before, during, and after the construction of the Alqueva dam, revealed bimodal to unimodal annual cycles, with chlorophyll *a* maxima usually occurring between March and October. Seasonal patterns show an alternation between a persistent light limitation and episodic nutrient limitation (Rocha *et al.*, 2002; Domingues *et al.*, 2005, 2011a,b,c, 2012; Barbosa *et al.*, 2010). Phytoplankton succession, with spring diatom blooms and summer–early fall cyanobacterial

Diatom, green algae, cyanobacteria, and total phytoplankton abundance displayed significant interannual declining trends over the period 1996–2010. Light intensity in the mixed layer is a prevalent driver of phytoplankton interannual variability. Yet, increased water retention by the Alqueva dam led to interannual decreases not only in turbidity but also in nutrient inputs, promoting a shift from persistent light limitation towards a more nutrient-limited mode (see Barbosa *et al.*, 2010; Domingues *et al.*, 2012).

Figure 8.6.2
Multiple-variable comparison plot (see Section 2.2.2) showing the seasonal and interannual properties of select cosampled variables at the Guadiana estuary plankton monitoring site. Additional variables from this site are available online at <http://wgpme.net/time-series>.





Prorocentrum micans
(Dinophyceae).
Photo: Claire Widdicombe,
Plymouth Marine Laboratory.

9. PHYTOPLANKTON AND MICROBIAL PLANKTON OF THE MEDITERRANEAN SEA

Yves Collos, Josep M. Gasol, Mladen Šolíc, Dominique Soudant, and Adriana Zingone

Although located within a narrow latitudinal range (less than 3°), the seven western Mediterranean sites included in this report (from west to east: Blanes Bay, Thau, Lazaret, Diana, Naples, Kastela Bay, and Stončica) vary widely morphologically (from one offshore site to more or less open bays, gulfs, and lagoons) and in trophic status (from oligotrophic to eutrophic). Coverage in time ranges from 18 to 38 years for physical variables such as water temperature and salinity, and from 26 to 35 years for biological variables such as total diatoms and total dinoflagellates. Three sites (Blanes, Kastela, and Stončica) also report bacterial counts and production, but for more limited time-spans.

In situ water temperature increases significantly with time at Thau (1972 on), but not at the other four sites where data are available. *In situ* salinity increases significantly with time at three sites (Blanes, Lazaret, Diana), but not at the other sites where data were available. Concerning chemical variables such as nutrients, the only significant changes have been observed in Thau lagoon, with significant decreases in ammonium, nitrate, and phosphate, although a tendency towards oligotrophication is reported to occur at several sites (Blanes, Kastela).

As for biological variables, total diatoms increased at Lazaret (1987 on) and Naples (1984 on) and decreased in Thau lagoon (1975 on). Total dinoflagellates decreased at Diana (1987 on). Total flagellates (not dinoflagellates) increased at Naples (1984 on).

The picocyanobacteria *Synechococcus* are reported for two sites only, with a significant increase at Thau (1991 on) and no change in Blanes Bay (1997 on). Picoeukaryotes are also reported for these two sites only. Their cell densities are approximately an order of magnitude higher at Thau than in Blanes Bay. In addition, there is a striking contrast in the seasonal cycle, with minimum densities in August for Blanes and January for Thau, and maximum densities in February for Blanes and August for Thau, which probably indicates that we are pooling together as “picoeukaryotes” taxonomically different types of organisms.

Bacteria, either measured by DAPI or by flow cytometry, are seen to decrease in Blanes Bay, Kastela Bay, and Stončica. Bacterial heterotrophic production is also showing a tendency to decrease with time at these sites, which are the only ones for which a time-series exist. Heterotrophic nanoflagellates are decreasing at the two Croatian sites, with a similar tendency shown at the Catalan Blanes Bay site.



Figure 9.1
Locations of the Mediterranean Sea monitoring areas (Sites 55–61) plotted on a map of average chlorophyll concentration. The star for Site 61 is not visible as it is beneath the star for Site 60.

Previous attempts to synthesize phytoplankton trends in the Mediterranean indicate a decrease in phytoplankton biomass (chlorophyll *a*) over time-scales of two decades (CIESM, 2003, 2010) and an increase in cell numbers. This apparent contradiction is the result of a decrease in phytoplankton average cell size, a decrease determined using data primarily from coastal sites. The only offshore data used in the study indicated a general increase in phytoplankton biomass, mainly due to pico- and nanoplankton over a 9-year period (CIESM, 2010).

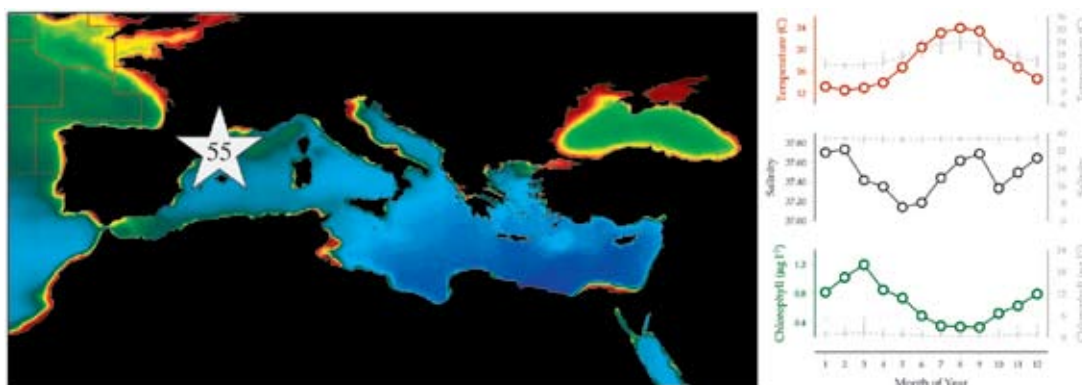
Data available in this report originate mostly from coastal sites, with influences from terrestrial environments that might induce site-specific variability. In addition, sites harbouring aquaculture (Leucate, Thau, Diana) represent high grazing environments where phytoplankton blooms may be “erased” by grazing pressure on time-scales of days/weeks and may mask relationships between phytoplankton standing stock and bottom-up processes. Still, large perturbations, such as the decrease in soluble reactive phosphorus in Thau lagoon, could be related to significant changes in phytoplankton community structure (emergence of picocyanobacteria and *Alexandrium catenella/tamarense*). Such dominance of coastal site features is likely to be the reason why no within-basin synchrony is apparent, in contrast to zooplankton studies based on more open-ocean time-series (Mackas *et al.*, 2012).

9.1 Blanes Bay (Site 55)

Josep M. Gasol, Ramon Massana, Rafel Simó, Celia Marrasé, Silvia G. Acinas, Carlos Pedrós-Alió, Carles Pelejero, M. Montserrat Sala, Eva Calvo, Dolors Vaqué, and Francesc Peters

Figure 9.1.1

Location of the Blanes Bay plankton monitoring area (Site 55), plotted on a map of average chlorophyll concentration, and its corresponding environmental summary plot (see Section 2.2.1).



Blanes Bay is an open, east-facing bay in the northwest Mediterranean Catalan coast ca. 70 km north of the city of Barcelona. It was selected as a monitoring site because it is a good example of an oligotrophic (relatively nutrient-poor) coastal ecosystem that is relatively unaffected by human influence. It is also one of the sites for which more information exists on the ecology of the Mediterranean planktonic environment, with papers on phytoplankton dating back to the 1940s (Margalef, 1945).

The site is placed at ca. 0.5 miles offshore over a water depth of 20 m. An oceanographic, fully operated buoy is placed nearby (http://atlantis.ceab.csic.es/~oceans/index_en.html), and the station is close to an automatic meteorological station and a directional wave buoy. The station is just placed at the limit between the rocky coast of the “Costa Brava” and the sandy coast southwards, with very limited riverine influence. The dominant southwestern water circulation that characterizes this location drives away the water from Tordera River, which outflows south of the site, a river system than only brings substantial amounts of water in winter (Guadayol *et al.*, 2009). The site is near a submarine canyon, which facilitates the arrival of offshore seawater to this coastal site.

The phytoplankton of Blanes Bay was studied intensively in the 1950s for its phytoplankton (Margalef, 1945, 1948, 1964), and again later, during the 1990s, with a focus on phytoplankton and biogeochemistry (Cebrián *et al.*, 1996; Agawin *et al.*, 1998; Duarte *et al.*, 1999, 2004; Lucea *et al.*, 2005; Olsen *et al.*, 2006). Since 1998, there has been a continuous effort and focus on microbial biodiversity and biogeochemical function (Schauer *et al.*, 2003; Massana *et al.*, 2004; Alonso-Sáez *et al.*, 2007; Unrein *et al.*, 2007). Owing to these scopes, it is now known as the “Blanes Bay Microbial Observatory”. DNA (and RNA) has been stored since 1998, and studies on archaeal, bacterial, and protist diversity are underway. Oceanographic data, nutrients, chlorophyll, bacterial and heterotrophic nanoflagellate abundance, picophytoplankton (by flow cytometry), and bacterial activity are some of the core variables monitored consistently over time. Variables for which a limited time-series exists include nano- and microphytoplankton species distribution, HPLC-determined pigments (Gutiérrez-Rodríguez *et al.*, 2011), primary production and respiration, organic sulphur (DMS, DMSP) concentrations and fluxes (Simó *et al.*, 2009), ectoenzymatic activities, CO₂ system parameters, particulate and dissolved organic nutrient concentrations, viral abundance, and impact on microbial foodwebs (Boras *et al.*, 2009). Other variables have been introduced at specific times over the last years, and a few synthesis papers have been published (e.g. Alonso-Sáez *et al.*, 2008; Simó *et al.*, 2009).

Seasonal and interannual trends (Figure 9.1.2)

As at most other coastal sites, this site experiences a strong seasonal forcing, with warm and not very productive (CHL ca. $0.2\text{--}0.3\text{ mg m}^{-3}$) summers and cold and richer winters (average CHL $>0.7\text{ mg m}^{-3}$). Though wind is much less forceful in summer, it does constrain water towards the coast, facilitating organic matter accumulation (Vila-Reixach *et al.*, 2012) simultaneously with nutrient deficiency and nutrient limitation (particularly P) of microbial growth (Pinhassi *et al.*, 2006).

Consequently, monthly average temperature correlates positively with Secchi disk depth, and negatively with chlorophyll *a* and with SiO_4 , PO_4 , NO_2 , and NO_3 concentrations. Summer demonstrates clearer waters, with low chlorophyll and low nutrients. Salinity does not exhibit a clear seasonal cycle, but tends to be lower in spring and autumn, which are the typical rainy seasons in such a Mediterranean-climate area. Bacterial production is higher in summer (positively correlated with temperature and Secchi depth and negatively correlated with chlorophyll *a* and with most nutrient concentrations). Heterotrophic bacterial abundance also tends to be higher in summer, but is very much buffered by predators and viruses (Unrein *et al.*, 2007; Boras *et al.*, 2009) and stays fairly stable. Heterotrophic nanoflagellates are more abundant in summer, whereas autotrophic nanoflagellates are more abundant in winter. The ratio between the two types exaggerates this difference.

The picophytoplankton has been well characterized with a dominance of picoeukaryotes in winter vs. *Synechococcus* in summer. *Prochlorococcus* appears only at the end of summer and throughout early winter, probably supplied with advected oceanic water. The main phytoplankton groups have been characterized by HPLC and consist of diatoms in spring, prasinophytes and cryptophytes in winter, *Synechococcus* and dinoflagellates in summer, and pelagophytes and *Prochlorococcus* in autumn, but with haptophytes appearing all year long (Gutiérrez-Rodríguez *et al.*, 2011).

Some of the techniques have changed from one of the three main periods to the others, which may influence interpretation of the data. This is in particular the case for salinity, which displays a long-term shift that might be associated with a change in the sensor used.

Temperature and Secchi depth show a slight non-significant positive trend with time. Chlorophyll *a* exhibits no clear trend, and all inorganic nutrients (exemplified in PO_4 and NH_4) show negative trends albeit non-significant, all indicating a very slow tendency towards oligotrophication (see also Sarmiento *et al.*, 2010), consistent with the implementation of wastewater treatment plants and P reduction policies over the last few decades.

The global temperature climatologies (HadISST) indicate a small temperature increase that agrees with the data measurements, and the ocean colour estimate of CHL (GlobColour Case-2) indicates a decrease that is barely observable. Winds are observed to increase over the sampled area according to the ICOADS, although with little changes during the period of observation.

Bacterial abundance is one of the variables that suffered from methodological inconsistencies. Measured by two sets of operators in two different periods by DAPI counts, it demonstrated dissimilar trends. The most consistent trend is that observed from 2002 to 2012 because it is observed in DAPI counts, but also in flow cytometry counts, including both fractions, the LNA and HNA bacteria. This trend goes towards bacteria being less abundant with time in this ecosystem.

Heterotrophic and phototrophic nanoflagellates show also the same declining trend. Bacterial production exhibits a similar trend.

Finally, the data show a somehow clear trend towards increased cyanobacteria and picoeukaryote concentrations and a decreased contribution of nanophytoplankton and cryptophytes, as determined by flow cytometry. *Synechococcus* enumerated by DAPI show the same trend.

All in all, this site shows a tendency towards oligotrophication, with decreased colour, chlorophyll, nutrients, increased transparency, decreased bacterial abundance and production, and increasing contribution of cyanobacteria and small eukaryotic algae to total chlorophyll. Most trends are consistent, although the still limited extension of the dataset precludes statistical confirmation of the observed tendencies.

Figure 9.1.2 (continued on facing page)

Multiple-variable comparison plot (see Section 2.2.2) showing the seasonal and interannual properties of select cosampled variables at the Blanes Bay plankton monitoring site. Additional variables from this site are available online at <http://wgpmc.net/time-series>.

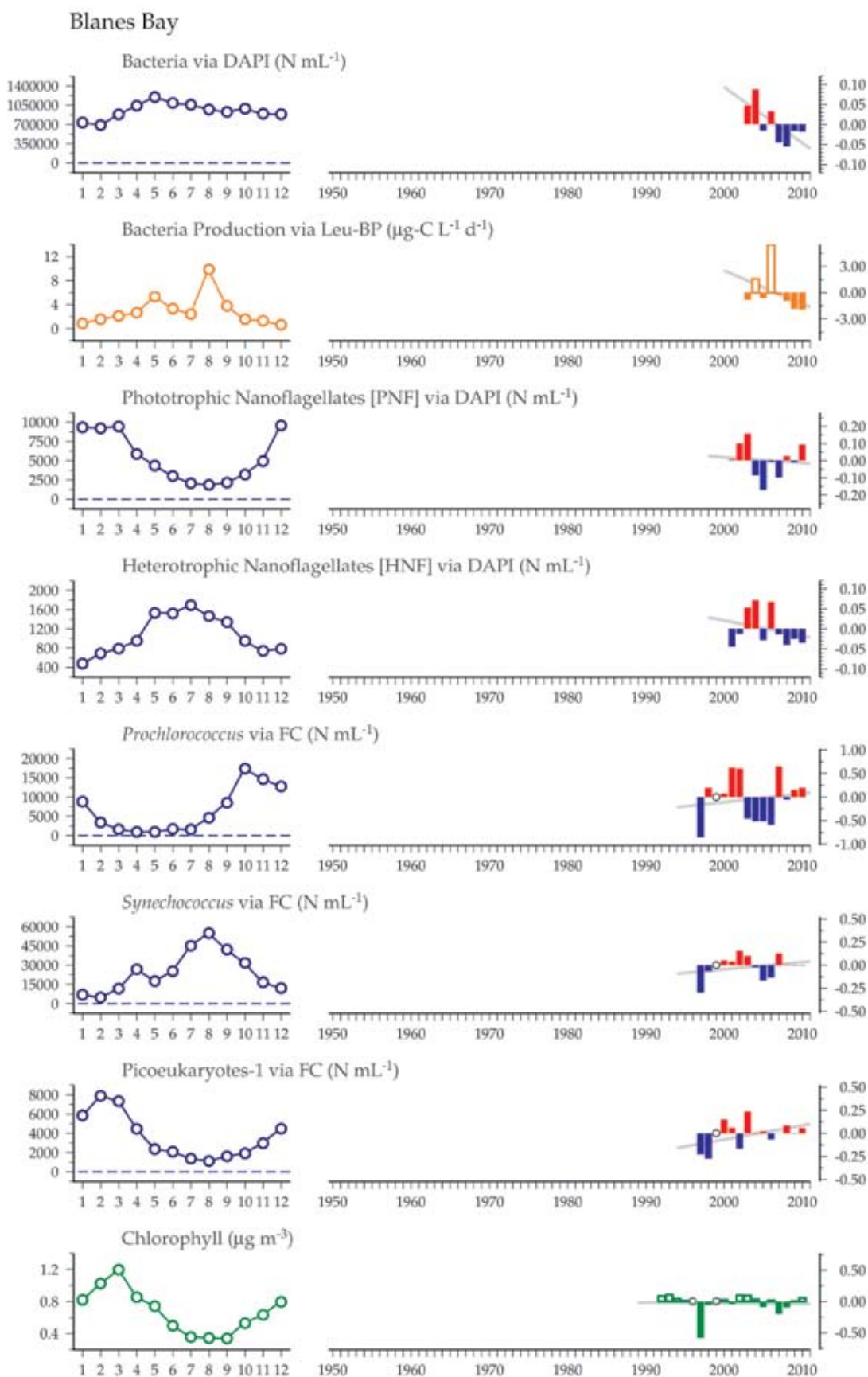
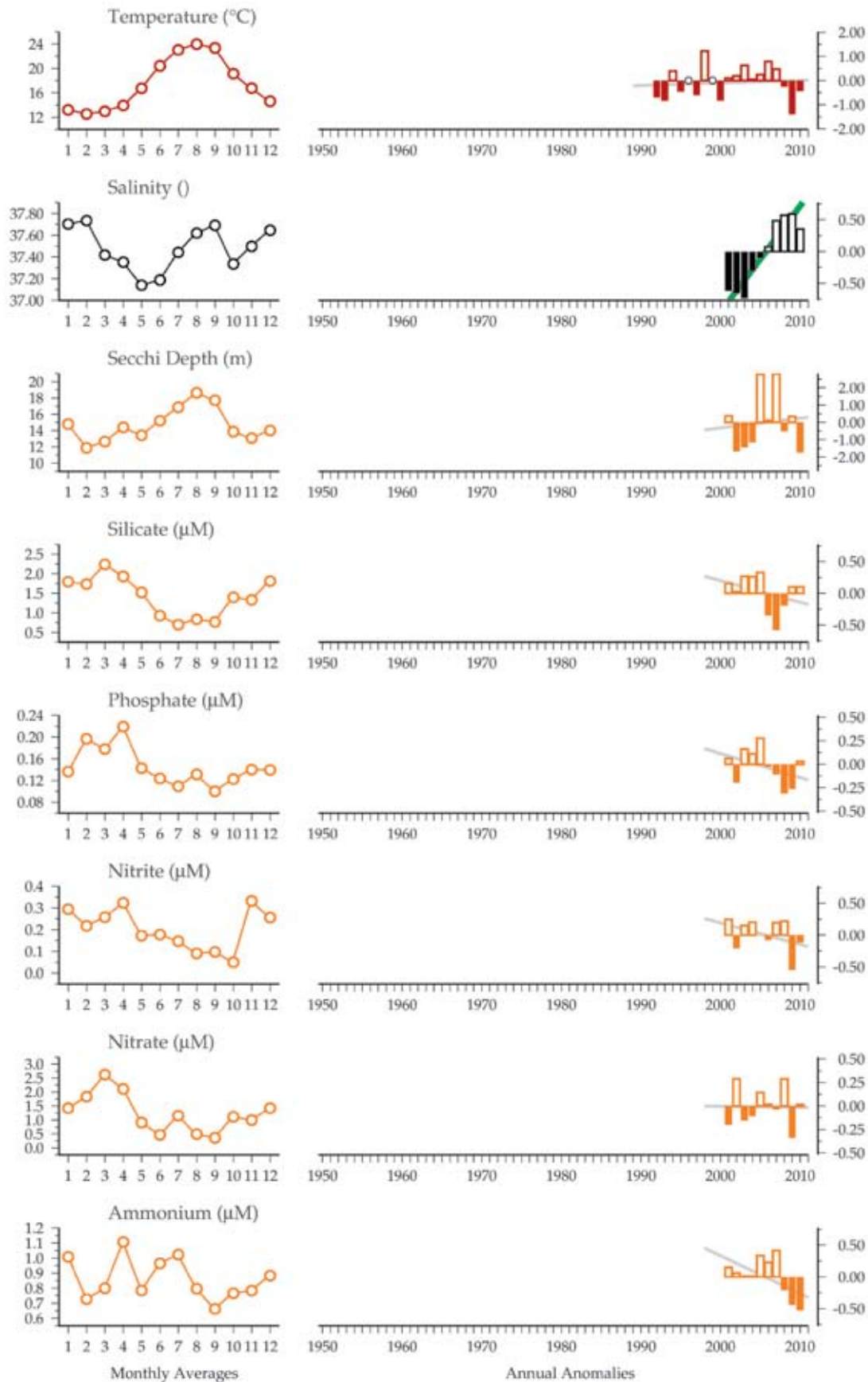


Figure 9.1.2 continued.

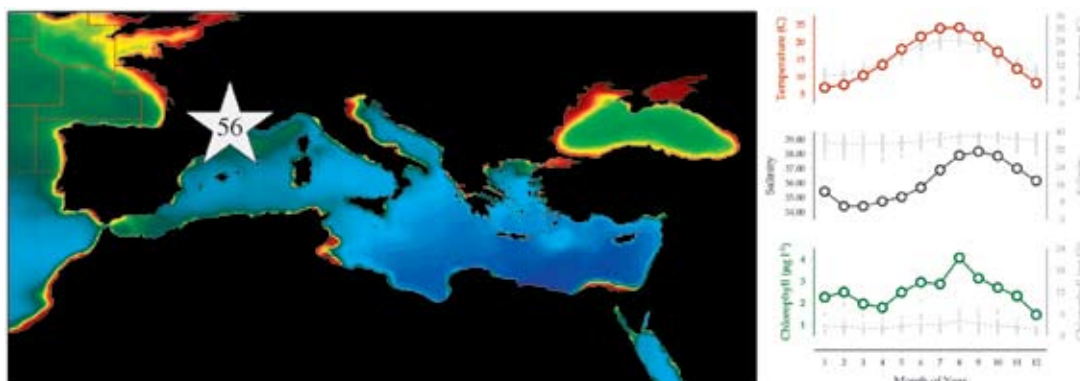


9.2 Thau Lagoon (Site 56)

Yves Collos, Béatrice Bec, and Eric Abadie

Figure 9.2.1

Location of the Thau Lagoon plankton monitoring area (Site 56), plotted on a map of average chlorophyll concentration, and its corresponding environmental summary plot (see Section 2.2.1).



Thau Lagoon is a shallow marine lagoon located on the French Mediterranean coast (43°24'N 3°36'E), with a mean depth of 4 m and a maximum depth of 8 m. The lagoon is connected to the sea by three narrow channels. Three oyster farming zones are located along the northwestern shore. The lagoon represents 10% of French oyster production and is the main oyster production centre in the Mediterranean, with an estimated standing stock of 20 000 t of oysters (*Crassostrea gigas*). Because of the weak tidal range (<1 m), the residence time of water masses (1–5 months) mainly depends on wind and barometric effects. However, it can be estimated that, in summer, the oyster standing stock can filter the whole lagoon in 24 h and thus change the biogeochemistry of the water masses (Souchu *et al.*, 2001).

Systematic observations of physical (temperature, salinity) and chemical (nutrient concentrations) properties have been made since 1972, and of biological (phytoplankton >5 µm) properties since 1987, with some monthly additional data for 1975–1976 from an unpublished doctoral thesis (Hénard, 1978). Picophytoplankton (picoeukaryotes and picocyanobacteria) has been counted by flow cytometry since 1991 (Vaquer *et al.*, 1996; Bec *et al.*, 2011). The lagoon harbours *Ostreococcus tauri*, the smallest eukaryote in the world (Courties *et al.*, 1994). Sampling frequency is twice a month, but can increase to once a week or more during periods favourable to harmful algae. Several stations are sampled, but data presented here belong to station B at the surface.

Well-identified phytoplankton species include *Cylindrotheca closterium*, *Dactyliosolen fragilissimus*, *Dinophysis acuminata*, *Dinophysis sacculus*, *Guinardia striata*, *Gyrodinium spirale*, *Heterocapsa triquetra*, *Leptocylindrus danicus*, *Leptocylindrus minimus*, *Nitzschia longissima*, *Peridinium quinquecorne*, *Protoperidinium bipes*, *Rhizosolenia pungen/setigera* complex, and *Thalassionema nitzschioides*. Other groups of diatoms not identified to the species level include *Chaetoceros* spp., *Pseudo-nitzschia* spp., *Rhizosolenia* spp., and *Skeletonema* spp.

Seasonal and interannual trends (Figure 9.2.2)

On a seasonal scale, diatoms generally show maxima in June and September, whereas dinoflagellates show maxima in March and November. The water temperature and chlorophyll *a* concentrations both show a maximum in August and a minimum in December.

Over the last 38 years, mean annual water temperature has increased by ca. 1.5°C, but this increase was not evenly distributed among seasons. On a seasonal basis, the highest rate of increase was in spring (+ 3.0°C), followed by summer (+2.0°C) and autumn (+1.7°C). In winter, no significant increase over the same period could be found.

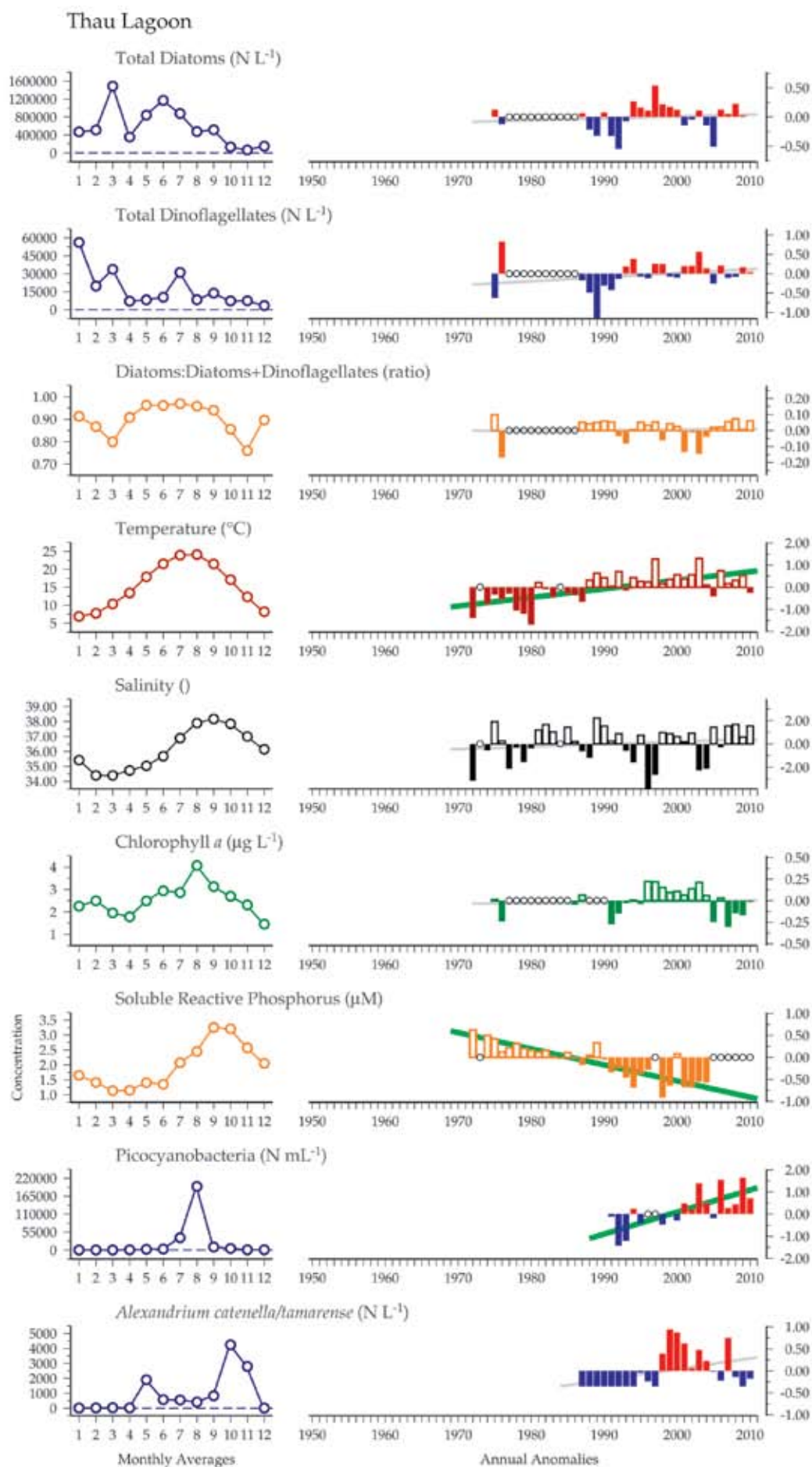
Concerning nutrients, a major perturbation has been a large decrease in soluble reactive phosphorus, with summer values decreased from 10 to 1 µM, whereas winter values decreased from 3 µM in 1972 to undetectable levels in 1995.

The recent (1995) and almost simultaneous appearance of both picocyanobacteria (mostly *Synechococcus*) and the toxic dinoflagellate *Alexandrium catenella*, following eight years of monitoring without reported presence in Thau, seems to be related to such reduced nutrient loading and the increase in water temperature (Collos *et al.*, 2009).

Long-term (1987–2010) trends for phytoplankton have seen a slight but non-significant increase in total diatoms, while significant increases have been found within individual species: *Dactyliosolen fragilissimus* ($p < 0.01$), *Guinardia striata* ($p < 0.01$), *Leptocylindrus danicus* ($p < 0.01$), and *Rhizosolenia pungens/setigera* complex ($p < 0.05$). Among the dinoflagellates, *Dinophysis acuminata* cell densities have increased ($p < 0.01$), and *Dinophysis sacculus* has decreased ($p < 0.05$) between 1987 and 2010. Other groups such as Euglenophytes have decreased ($p < 0.05$).

Figure 9.2.2

Multiple-variable comparison plot (see Section 2.2.2) showing the seasonal and interannual properties of select cosampled variables at the Thau Lagoon plankton monitoring site. Additional variables from this site are available online at <http://wgpmc.net/time-series>.



9.3 Mediterranean REPHY sites (Sites 57–58)

Dominique Soudant

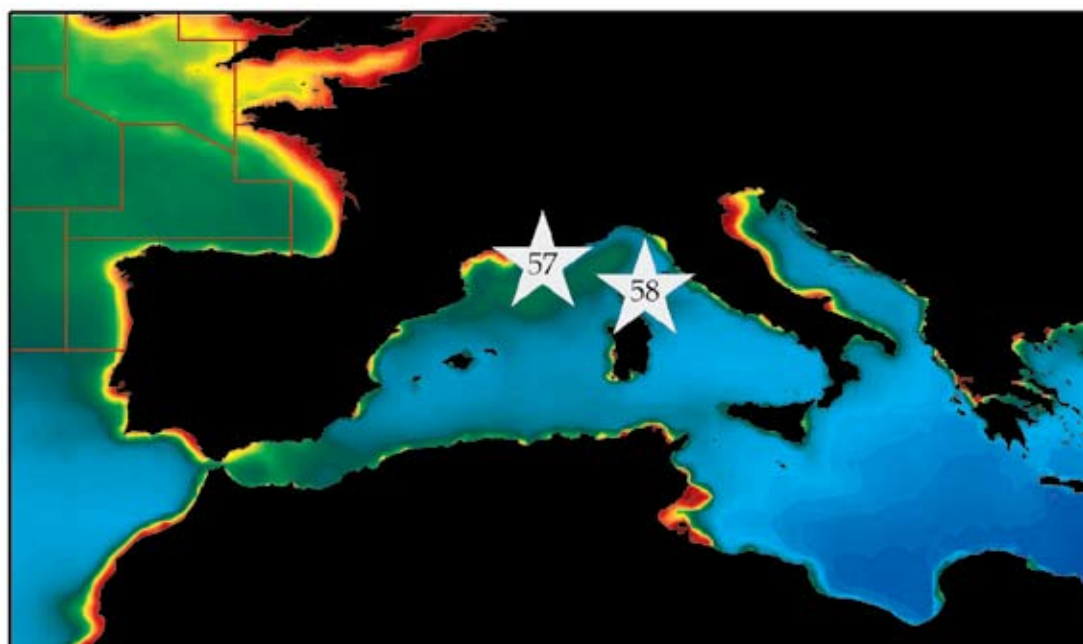
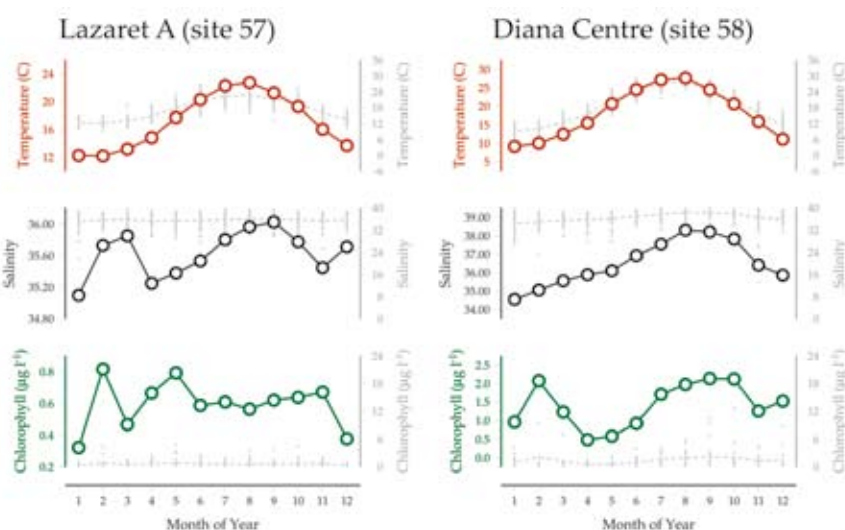


Figure 9.3.1

Locations of the REPHY Mediterranean Sea plankton monitoring areas (Sites 57–58), plotted on a map of average chlorophyll concentration, and their corresponding environmental summary plots (see Section 2.2.1).



The French Phytoplankton and Phycotoxin Monitoring Network (REPHY) was set up in 1984 with three objectives: to enhance knowledge of phytoplankton communities, to safeguard public health, and to protect the marine environment (Belin, 1998). Phytoplankton along the French coast has been sampled up to twice a month since 1987 at twelve coastal laboratories. For that purpose, the French coast is divided into a hierarchy of sites and subsites common to three regional networks: the English Channel, the Bay of Biscay, and the Mediterranean Sea. Lazaret A and Diana Centre (Figure 9.3.1) are two Mediterranean REPHY sites. Lazaret A is located in well-mixed waters, with a medium-depth, sandy bottom within Toulon Bay.

Diana Centre is located in shallow, less-mixed waters of a coastal lagoon in Corsica and features a muddy bottom.

As with the Bay of Biscay and English Channel REPHY sites, sampling started in 1987, with salinity, temperature, turbidity, and oxygen measured concomitantly from the beginning or one year thereafter. Chlorophyll *a* and pheopigments started at Diana Centre in 1988 and at Lazaret A in 1999. This latter site is sampled twice a month on average, whereas fewer samples (17 on average from 10 months) are taken annually at Diana Centre.

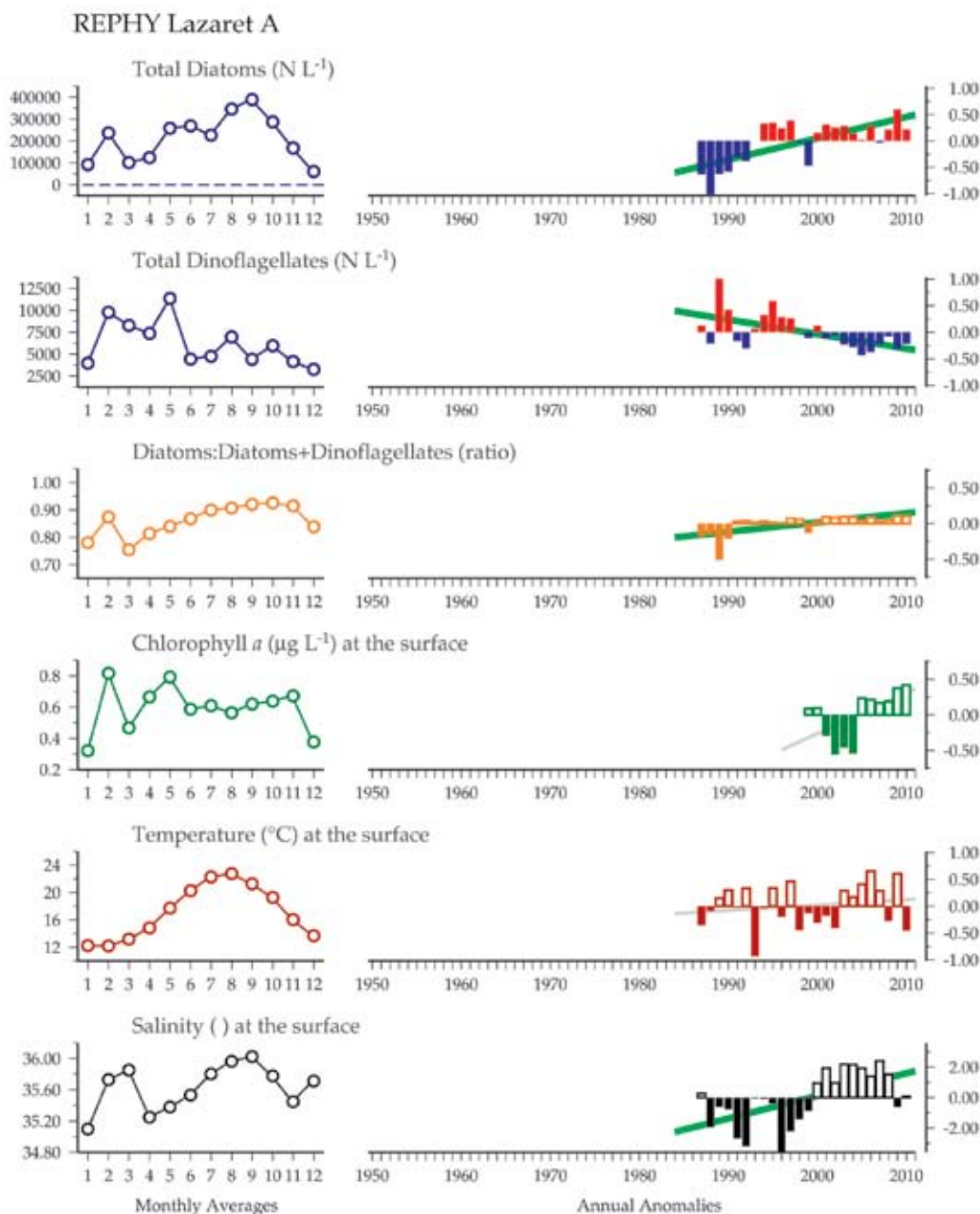
Seasonal and interannual trends (Figures 9.3.2–9.3.3)

Chlorophyll annual cycles show maximum values in late winter at both sites, but equally high values are also observed in late summer at Diana Centre. At this latter site, chlorophyll values are well above $1 \mu\text{g L}^{-1}$ for most of the year, whereas chlorophyll remains below this value through the year at Lazaret A. Diatom abundance tends to fluctuate year-round, exhibiting maxima in late summer (September) at both sites, with relatively high values also in February (Lazaret A) and December (Diana Centre). Dinoflagellates peaked early in the year (winter–spring) at Lazaret A, whereas those at Diana Centre peaked in October and December. Diatoms include *Chaetoceros* at both sites, with species such as *Skeletonema costatum* and

Pseudo-nitzschia more abundant at Lazaret A and *Asterionellopsis glacialis*, *Dactyliosolen fragilissimus*, and *Hemiaulus* sp. at Diana Centre. Common genera of dominant dinoflagellates are *Prorocentrum*, *Bysmatrum*, *Scrippsiella*, and *Ensiculifera*, although species may be different at both sites.

Salinity has been steadily increasing for more than two decades at both Mediterranean REPHY sites. A significant ($p < 0.05$) increase in total phytoplankton (as chlorophyll) is observed at Lazaret A, probably owing to a concomitant significant ($p < 0.01$) increase in diatom abundance, whereas a long-term decrease in dinoflagellate abundance was conspicuous ($p < 0.01$) at both sites. Consequently, a significant increase in the diatoms:diatoms+dinoflagellates ratio was observed at both sites, more marked at Lazaret A.

Figure 9.3.2
Multiple-variable comparison plot (see Section 2.2.2) showing the seasonal and interannual properties of select cosampled variables at the REPHY Lazaret A plankton monitoring site. Additional variables from this site are available online at <http://wgpmc.net/time-series>.



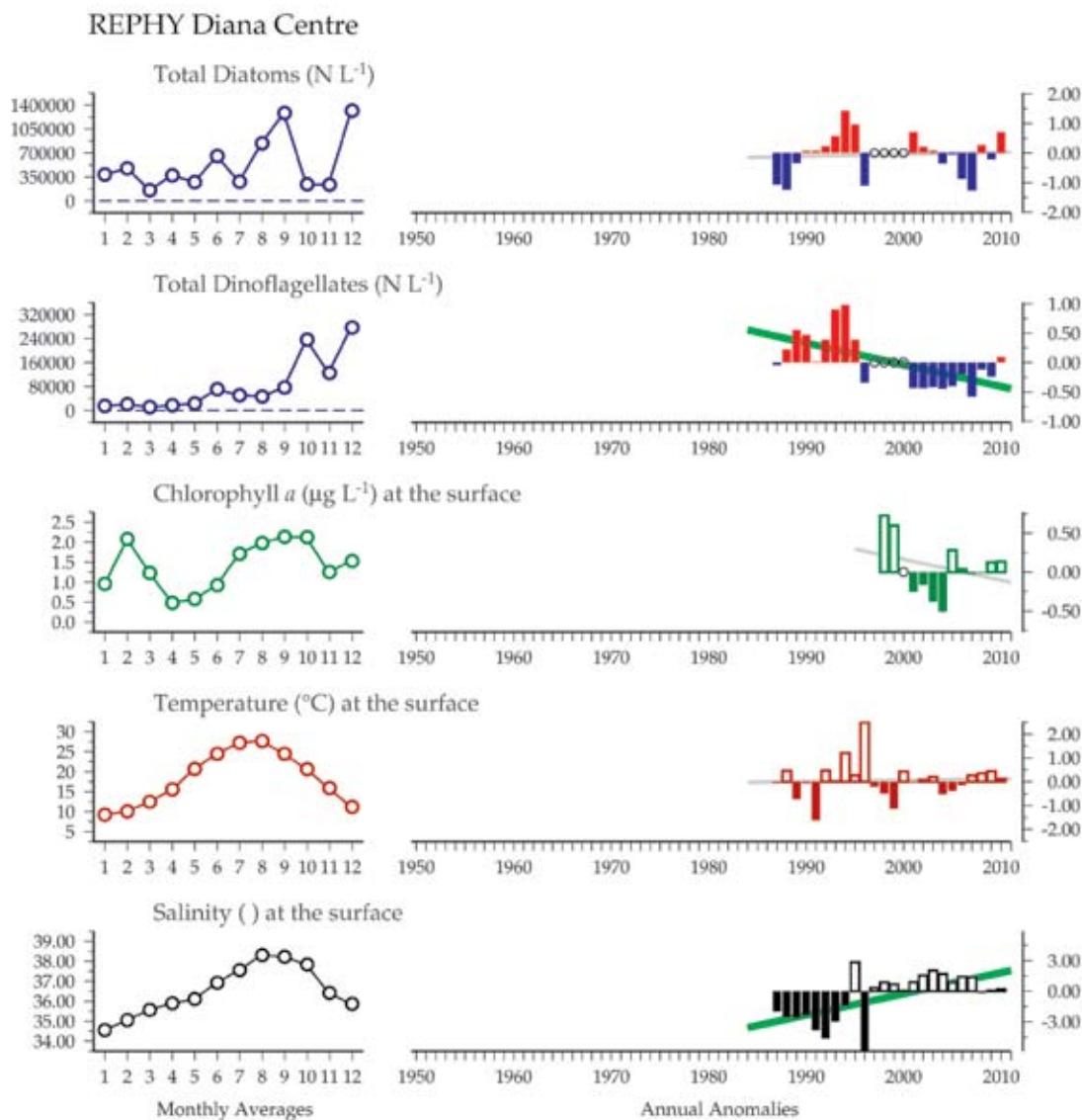


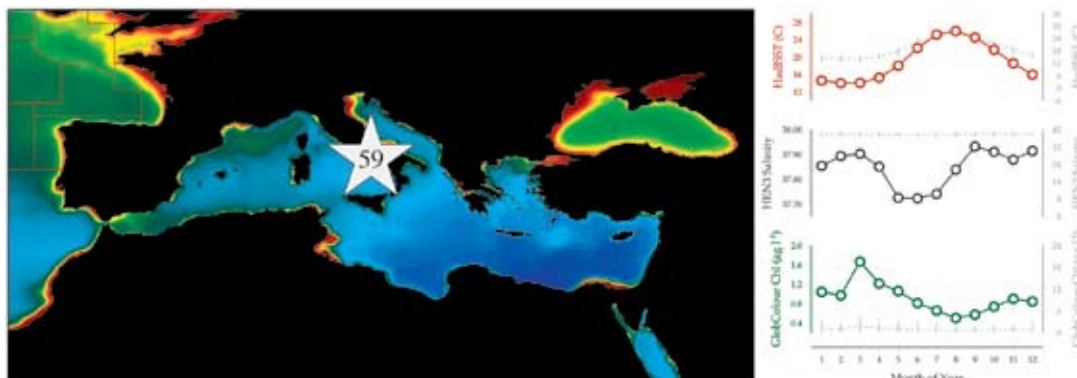
Figure 9.3.3
Multiple-variable comparison plot (see Section 2.2.2) showing the seasonal and interannual properties of select cosampled variables at the REPHY Diana Centre plankton monitoring site. Additional variables from this site are available online at <http://wgpme.net/time-series>.

9.4 Gulf of Naples LTER-MC (Site 59)

Adriana Zingone and Diana Sarno

Figure 9.4.1

Location of the Gulf of Naples LTER-MC plankton monitoring area (Site 59), plotted on a map of average chlorophyll concentration, and its corresponding environmental summary plot (see Section 2.2.1).



The first research on marine microalgae in the Gulf of Naples preceded the foundation of the Stazione Zoologica in 1876 (Costa, 1838). Since then, more than a century passed until the first ecological investigations were made on phyto- and zooplankton assemblages, dating back to the 1970s and, in a more continuous way, the 1980s. In 1984, a regular sampling project at a fixed station, MareChiara (MC), was started with the aim of understanding diversity, evolution, and functioning of plankton organisms, their dynamics in relation to environmental conditions, and their rôle in the biogeochemical cycles. In 2006, the MareChiara site joined the European (www.lter-europe.net) and international (www.ilternet.edu) networks of Long-Term Ecological Research as LTER-MC.

The sampling site is located ca. 3 km from the coastline near the 75 m isobath (40°48.5'N 14°15'E) and at the boundary between two subsystems, whose exchanges are very dynamic: the coastal eutrophic area, influenced by land run-off from a very densely populated region, and the offshore oligotrophic area, similar to the open Tyrrhenian waters. Sampling has been ongoing since January 1984, with a major interruption from January 1991 until February 1995. Sampling frequency was fortnightly until 1990, and weekly from 1995 to the present (Ribera d'Alcalà *et al.*, 2004).

The water column at the site is thoroughly mixed from December to March and stratified during the rest of the year. The annual cycle of surface temperature is characterized by lowest values in February–March (~14°C) and highest values in August (~26°C). Ranges for nutrient concentrations (annual average, 0–10 m) are 0.5–3 mM m⁻³ for TIN,

0.2–0.4 mM m⁻³ for PO₄, and 2–4 mM m⁻³ for SiO₄. Temperature, salinity, and chlorophyll demonstrate high interannual variability. Significant trends during 1984–2006 have been recorded in the increasing summer temperatures and in the decreasing annual chlorophyll *a* concentrations (Zingone *et al.*, 2010; Mazzocchi *et al.*, 2012).

Phytoplankton are numerically dominated by diatoms and small flagellates. In terms of biomass, diatoms are still predominant, but dinoflagellates are the second major group. Coccolithophores are the least represented group in terms of both abundance and biomass. Biomass may start increasing over the water column in February–early March, mainly owing to diatom peaks, but these winter blooms have decreased in frequency and abundance over the time-series, probably in relation to more unstable weather conditions in this season in recent years (Zingone *et al.*, 2010). Annual peak values for total biomass (both diatoms and dinoflagellates) are achieved in the upper layers in late spring (Ribera d'Alcalà *et al.*, 2004), whereas an increase over the whole water column is recorded in autumn (Zingone *et al.*, 1995).

Approximately 700 different phytoplankton species have been identified at Station LTER-MC, whereas abundance values exist for 344 taxa, including supraspecific and suprageneric groups. Of these, ca. 20 taxa constitute 90% of the total cell counts over the time-series. The most abundant diatoms are *Leptocylindrus danicus*, *Skeletonema pseudocostatum*, *Chaetoceros tenuissimus*, *C. socialis*, and several species belonging to the genera *Chaetoceros*, *Thalassiosira*, and *Pseudo-nitzschia*. Among the other groups, the most represented besides small

flagellates are *Emiliana huxleyi*, cryptophyceans, and naked, small ($< 15 \mu\text{m}$) dinoflagellates.

Seasonal and interannual trends (Figure 9.4.2)

A large number of species show regular timing in their occurrence over the years, despite marked interannual variations in environmental parameters and meteorological conditions (Zingone and Sarno, 2001; Zingone *et al.*, 2003; Ribera d'Alcalà *et al.*, 2004). Seasonal patterns investigated over shorter periods have also been found to be distinct for selected flagellates, i.e. the prasinophyte *Micromonas pusilla* (Zingone *et al.*, 1999), cryptomonads (Cerino and

Zingone, 2006), and for flagellate groups studied with molecular methods (McDonald *et al.*, 2007).

Over the time-series, an increase in total abundance has been accompanied by an increase of small species, which has resulted in a decrease in the average size of the phytoplankton assemblages (Ribera d'Alcalà *et al.*, 2004). Recent sampling and historical data were used to compare distribution of the dinoflagellate genus *Ceratium* in Ligurian and South Tyrrhenian waters, demonstrating that the Ligurian Sea populations are currently more similar to the South Tyrrhenian ones than before, probably related to increasing temperatures during recent decades (Tunin-Ley *et al.*, 2009).

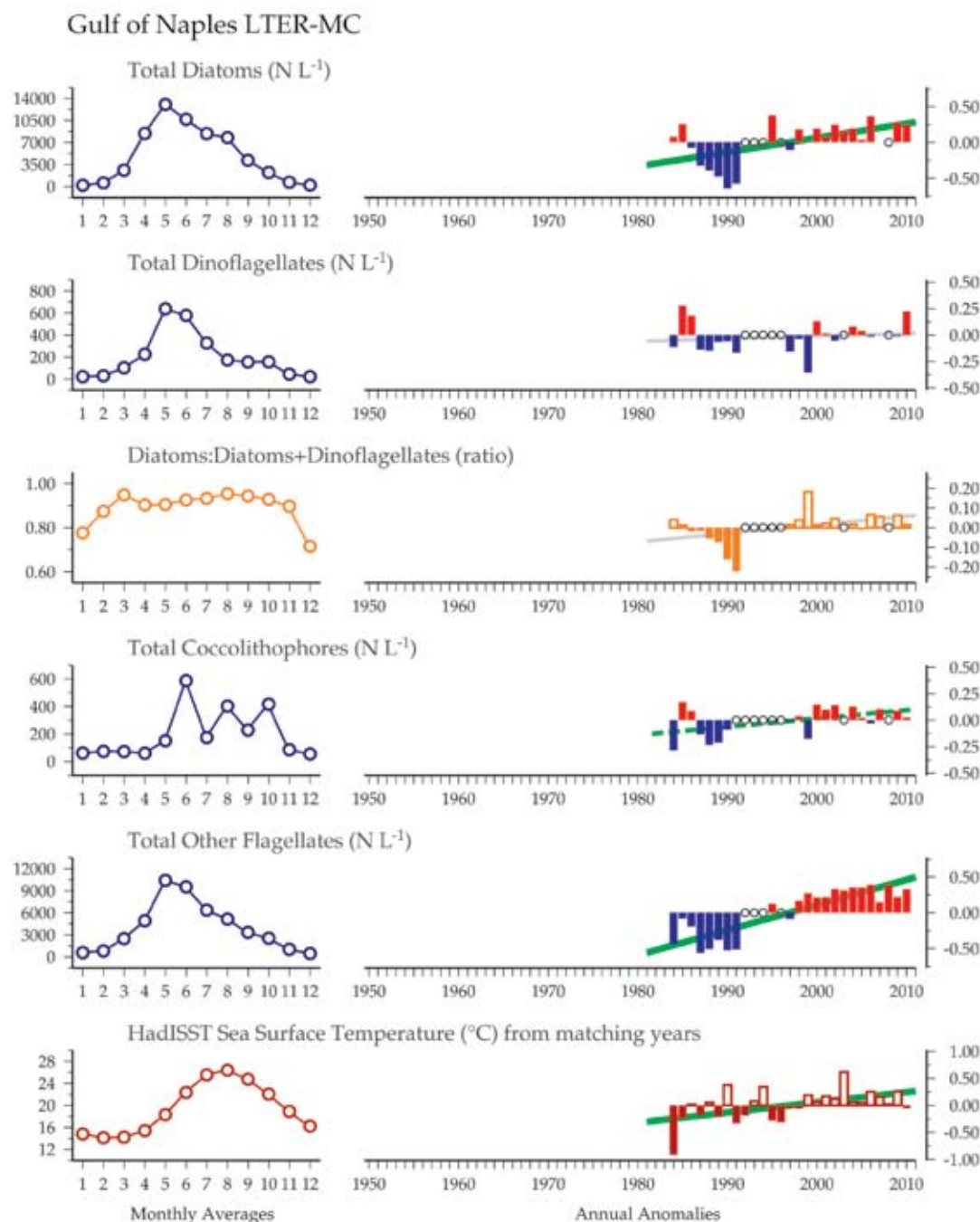


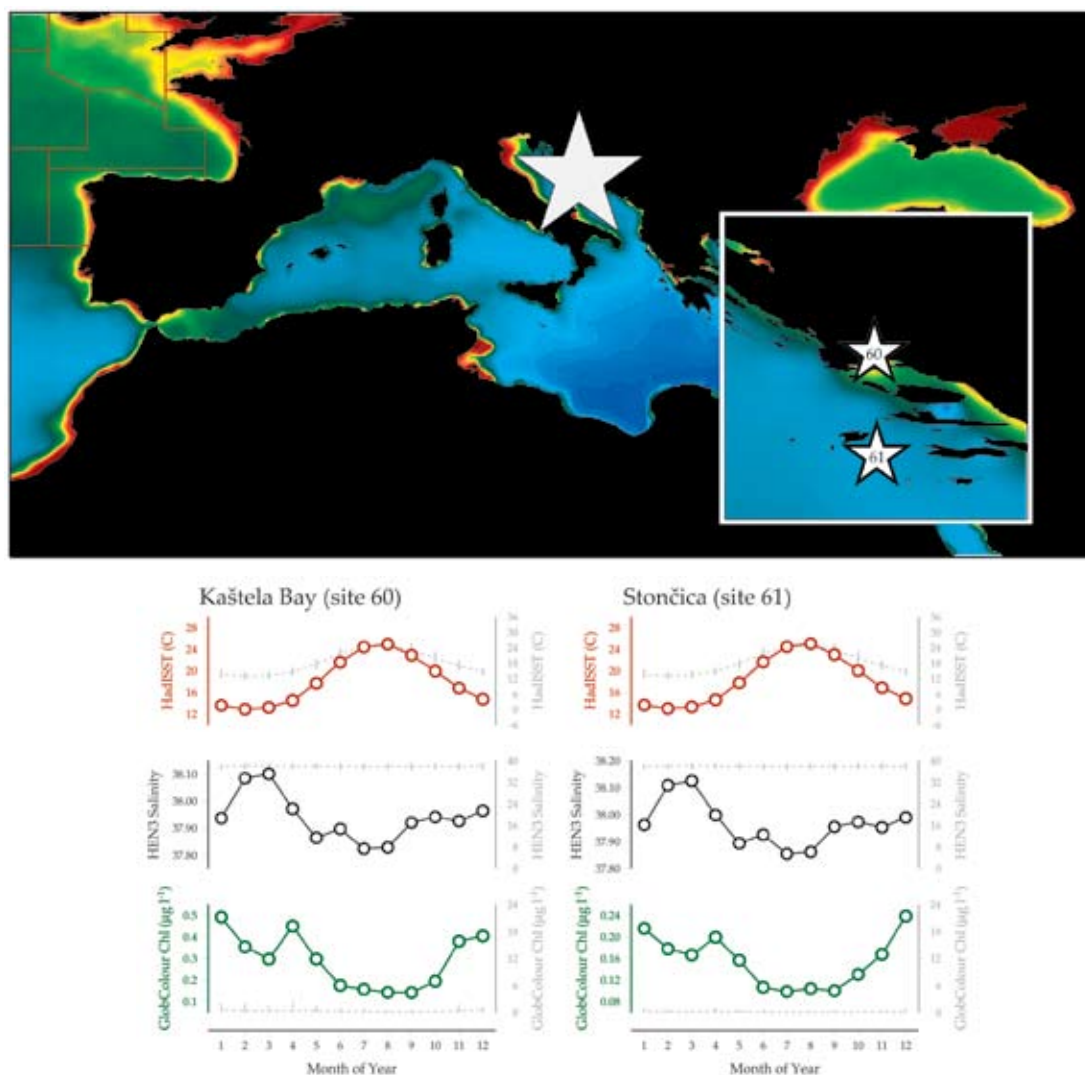
Figure 9.4.2
Multiple-variable comparison plot (see Section 2.2.2) showing the seasonal and interannual properties of select cosampled variables at the Gulf of Naples LTER-MC plankton monitoring site. Additional variables from this site are available online at <http://wgpmc.net/time-series>.

9.5 Kaštela Bay and Stončica (Sites 60–61)

Mladen Šolić, Nada Krstulović, Danijela Šantić, and Stefanija Šestanović

Figure 9.5.1

Locations of the Kaštela Bay and Stončica plankton monitoring areas (Sites 60–61), plotted on a map of average chlorophyll concentration, and their corresponding environmental summary plots (see Section 2.2.1).



Kaštela Bay has an average depth of 23 m and communicates with the adjacent channel through an inlet 1.8 km wide and 40 m deep. The River Jadro, which discharges into the eastern part of the bay, is the most important freshwater source, with an average annual inflow of $10 \text{ m}^3 \text{ s}^{-1}$. Wide oscillations in chemical and physical parameters in this area are the result of strong land influence. Water circulation in the bay is generated mostly by the local wind, which is related to the passage of mid-latitude cyclones over the area. The average water renewal time is approximately 1 month, whereas under strong wind conditions, it can be as short as 5 d. During the warm period of the year (July–September), windforcing is relatively weak and the freshwater inflow low, because the renewal time is rather long.

The Stončica site is located southeast of Cape Stončica on Vis Island ($43^{\circ}2'38''\text{N}$; $16^{\circ}17'7''\text{E}$) ca. 50 km offshore, and is 100 m deep. Located just out of the middle Adriatic island coastal waters and influenced by the largest east Adriatic river Neretva, this station feels these freshened waters in its surface layer, but also the open Adriatic circulation and water masses during dryer periods. In contrast, the deep layers are flooded by the open Adriatic water masses, mostly Levantine Intermediate Water (LIW) and North Adriatic Dense Water (NAdDW), which are characterized by smaller oscillations of chemical and physical parameters compared with the coastal area. Therefore, this station is quite suitable for detecting environmental changes in the open Adriatic Sea in relation to its circulation, water masses, and their long-term changes and anomalies.

Sampling was done on a monthly basis. Bacteria and heterotrophic nanoflagellates (HNF) were enumerated by epifluorescence microscopy ("Olympus" BX50 at a magnification of $\times 1000$), using the standard DAPI staining technique (Porter and Feig, 1980). Bacterial cell production was measured from DNA synthesis based on incorporation rates of ^3H -thymidine (Fuhrman and Azam, 1980).

Seasonal and interannual trends in Kaštela Bay (Figure 9.5.2)

Long-term bacterial and heterotrophic nanoplankton (HNAN) data from Kaštela Bay have been analysed in several papers (Šolić *et al.*, 1997, 1998, 2009, 2010). After increasing trends of all parameters during the 1980s (data not shown), decreasing trends (particularly in the coastal waters) were established owing to "de-eutrophication" or "oligotrophication". The switch from eutrophic to oligotrophic conditions was accompanied by quantitative (decrease in bacterial abundance,

bacterial production, and chlorophyll *a*, and an increase in HNF abundance and bacterial-specific growth rate), structural (phytoplankton species composition, phytoplankton size structure, seasonal cycles), and functional (trophic relationships, bottom-up vs. top-down control) changes within the microbial community.

Seasonal and interannual trends in Stončica (Figure 9.5.3)

Long-term bacterial and HNAN data from Stončica have been analysed in several papers (Šolić *et al.*, 1997, 2008, 2009). Since 1995, both have a slight (but non-statistically significant) decrease. Non-seasonal fluctuations during the last 15 years coincided with some specific meteorological and hydrographical conditions (strong influence of North Adriatic Dense Water in 1997, strong Levantine Intermediate Water ingression in 2004 or extremely warm winter, and the Po River run-off in 2000/2001).

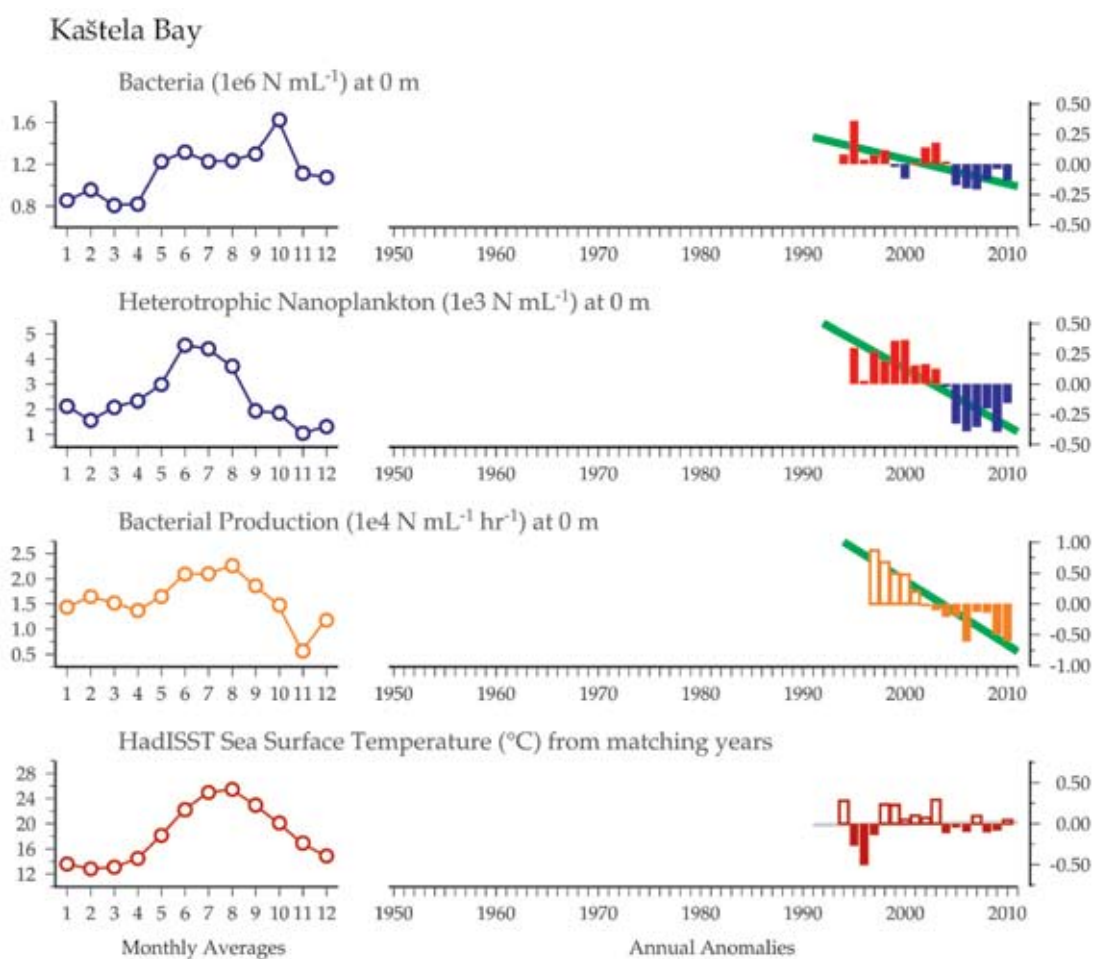
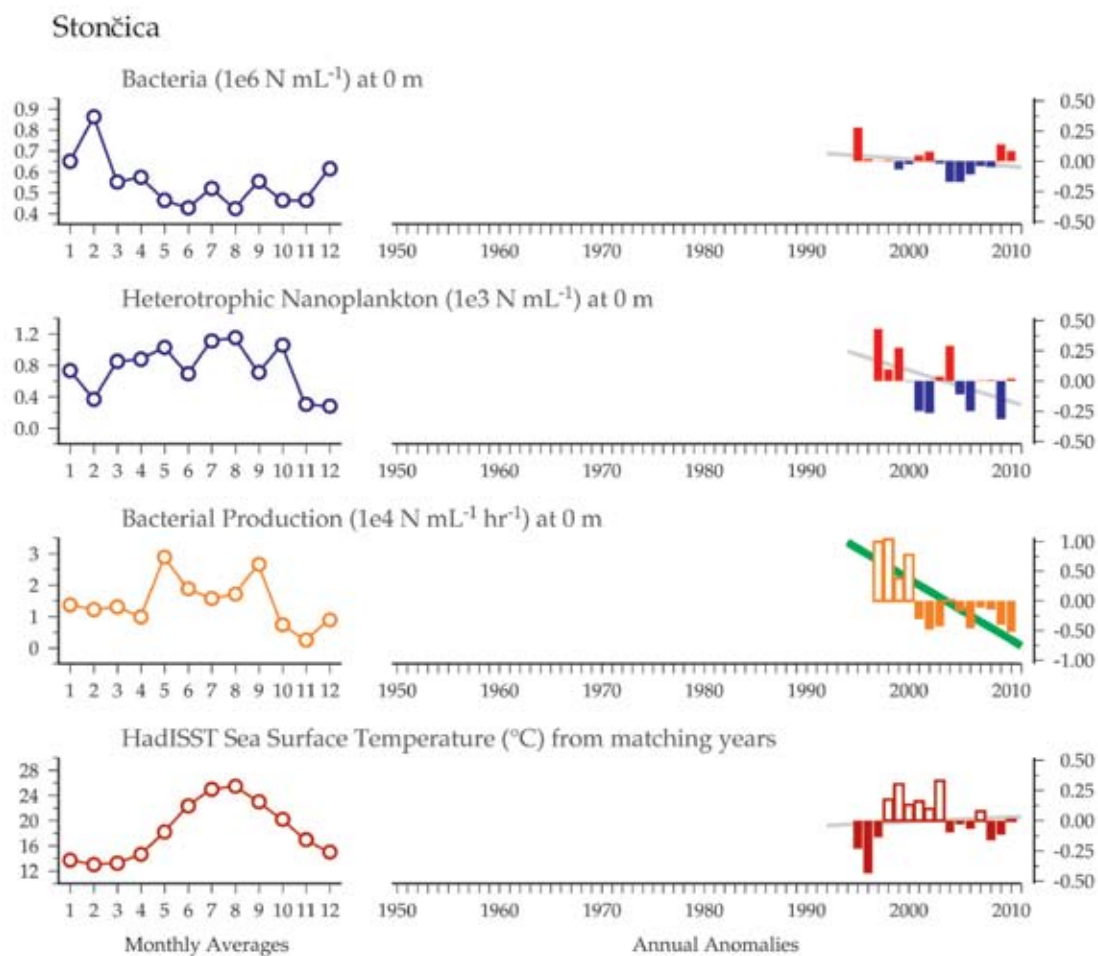


Figure 9.5.2
Multiple-variable comparison plot (see Section 2.2.2) showing the seasonal and interannual properties of select cosampled variables at the Kaštela Bay plankton monitoring site. Additional variables from this site are available online at <http://wgpmc.net/time-series>.

Figure 9.5.3

Multiple-variable comparison plot (see Section 2.2.2) showing the seasonal and interannual properties of select cosampled variables at the Stončica plankton monitoring site. Additional variables from this site are available online at <http://wgpme.net/time-series>.





Thalassiosira nordenskiöldii
(Bacillariophyceae).
Photo: Fisheries and
Oceans Canada.

10. PHYTOPLANKTON OF THE NORTH ATLANTIC BASIN

Martin Edwards and Rowena Stern

The Continuous Plankton Recorder (CPR) survey is a long-term, subsurface, marine plankton monitoring programme consisting of a network of CPR transects towed monthly across the major geographical regions of the North Atlantic. It has been operating in the North Sea since 1931 with some standard routes existing with virtually unbroken monthly coverage back to 1946. After each tow, the CPR samples are returned to the laboratory for routine analysis, including the estimation of phytoplankton biomass (Phytoplankton Colour Index, PCI) and the identification of up to 500 different phytoplankton and zooplankton taxa (Warner and Hays, 1994). Direct comparisons between the Phytoplankton Colour Index and other chlorophyll *a* estimates, including SeaWiFS satellite estimates, indicate strong positive correlations (Batten et al., 2003; Raitsos et al., 2005). The second step of the phytoplankton analysis involves counting phytoplankton cells under high magnification (x450) to identify and count taxa. Each CPR sample represents ~3 m³ of filtered seawater. Using this analysis method, 200 phytoplankton taxa have been routinely identified and counted by the CPR survey since 1958.

Because of the mesh size of CPR silks, many phytoplankton species are only semi-quantitatively sampled owing to the small size of the organisms. There is, thus, a bias towards recording larger armoured flagellates and chain-forming diatoms, and smaller-species abundance estimates from cell counts will probably be underestimated in relation to other water sampling methods. However, the proportion of the population that is retained by the CPR silk reflects the major changes in abundance, distribution, and specific composition (i.e. the percentage retention is roughly constant within each species even with very small-celled species; Edwards *et al.*, 2006). The CPR now has a water sampler housed on board certain units to provide additional data and sample the whole size-spectrum of plankton using molecular techniques from bacteria and viruses to flagellates and other taxa not normally identified using standard CPR analysis.

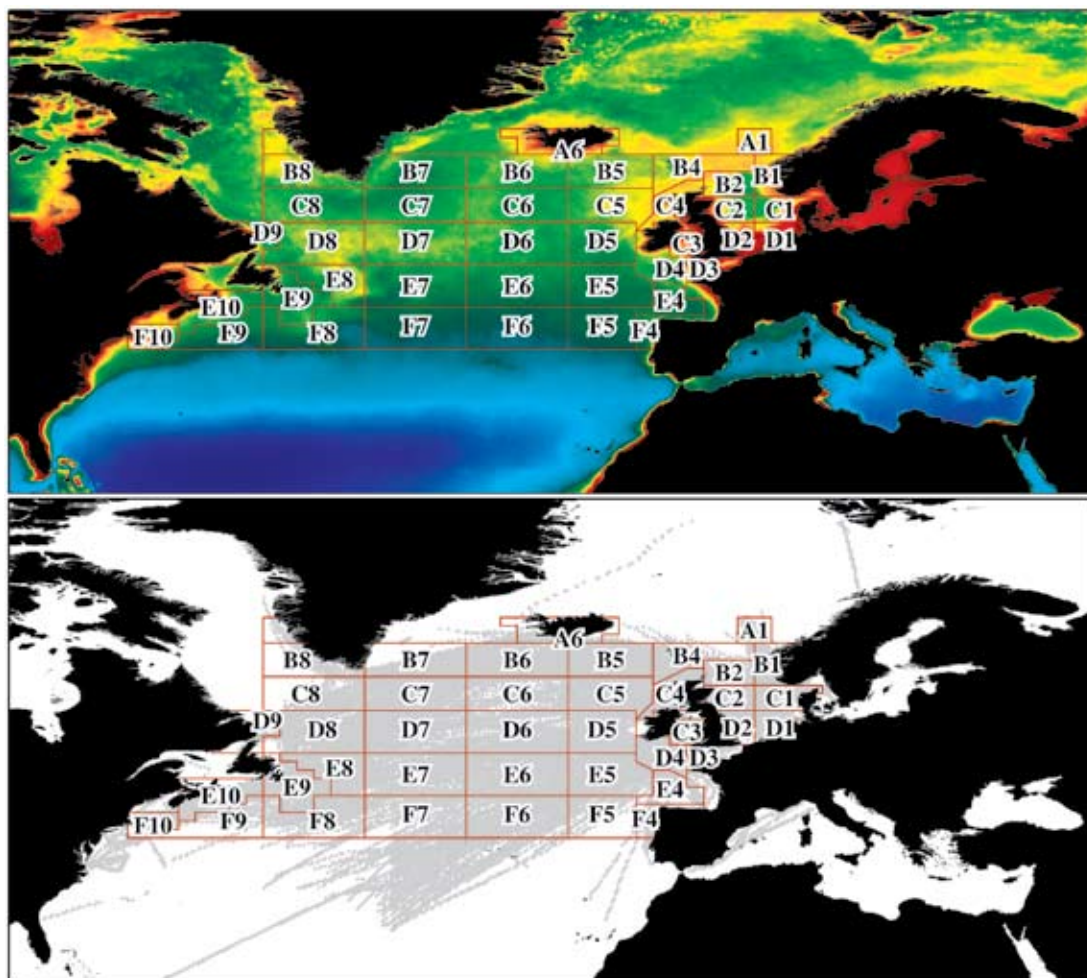


Figure 10.1
Locations of Continuous Plankton Recorder (CPR) standard areas (outlined in red). The top panel shows these areas on a map of average chlorophyll concentrations (see Section 2.3.2). The bottom panel shows the CPR transect and sampling coverage (grey dots) available within each of these areas.

For the purpose of the assessment in this report, the North Atlantic Basin has been geographically subdivided into different spatial regions (Figure 10.1). The 40 geographical regions shown in the figures are known as CPR standard areas and are referenced by their alphanumeric identifiers (e.g. “B2”, “D8”). Included in this assessment are some trends in the phytoplankton and microzooplankton, as well as trends in marine pathogens derived from molecular analysis of samples in the CPR sample archive.

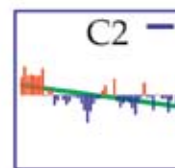
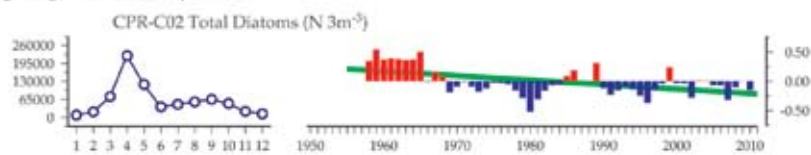
The CPR data from the standard areas were processed using standard report methods (see Section 2.1) as applied to the other plankton time-series presented in this report. For the purpose of viewing the long-term CPR trends in a spatial context, the standard report graphics (see Section 2.2) were truncated into the forms described in Figure 10.2 and used in the “Spatial Trends Plots” of this section (Figures 10.3–10.9).

Figure 10.2

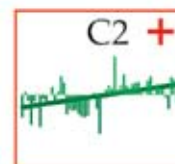
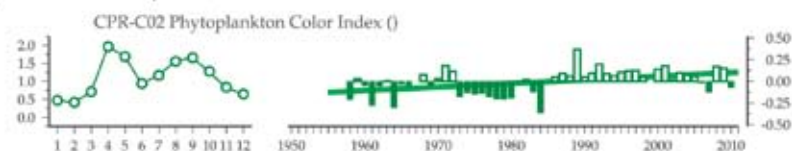
Examples of CPR standard area data shown in the standard report plot format (left column, see Section 2.2.2) and their corresponding truncated forms (right column) as presented in the "Spatial Trends Plots" shown later in this section.

The truncated form incorporates the standard annual anomaly trend representation (e.g. the green and grey slope lines) as described in Section 2.2. Positive significant trends ($p < 0.01$ or $p < 0.05$) are indicated with a red box outline, negative significant trends are indicated with blue box outline. Solid box outlines indicate $p < 0.01$, dashed boxed outlines indicate $p < 0.05$. Non-significant trends are outlined in grey. Trend directions ("+", "-") are also indicated in all cases.

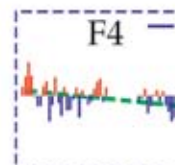
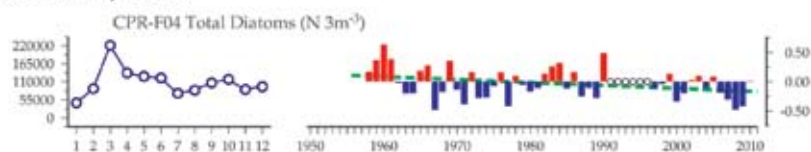
Strong Negative Trend ($p < 0.01$):



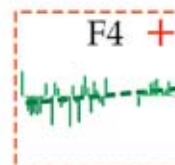
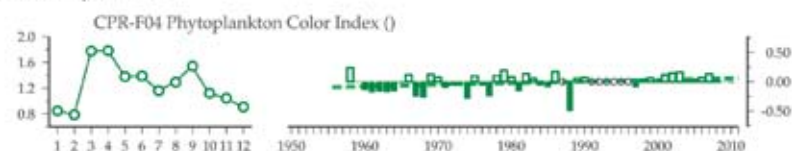
Strong Positive Trend ($p < 0.01$):



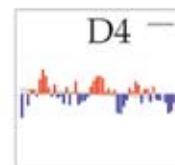
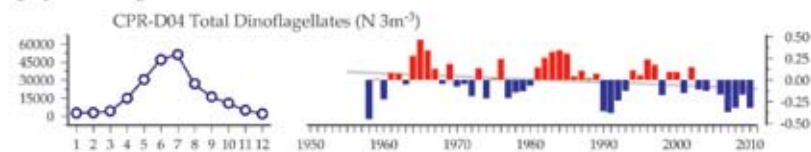
Negative Trend ($p < 0.05$):



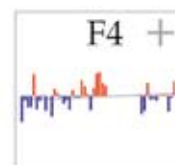
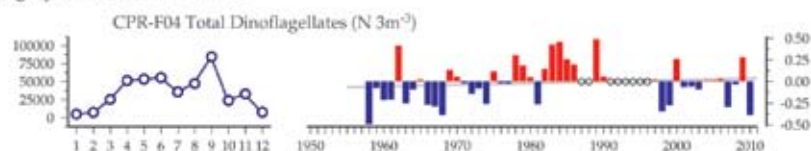
Positive Trend ($p < 0.05$):



Non-significant Negative Trend:



Non-significant Positive Trend:



10.1 Basin-scale trends in phytoplankton

To summarize the long-term trends in phytoplankton in the North Atlantic Basin, we used indices of phytoplankton that included the CPR Phytoplankton Colour Index and the sum of the abundance of all counted diatoms ("Total Diatoms") and all counted dinoflagellates ("Total Dinoflagellates"). Bulk indices like these are less sensitive to environmental change, and will quite often mask the subtleties that individual species will give you; however, it is thought that these bulk indices represent the general functional response of phytoplankton to the changing environment. In the North Atlantic, at the ocean basin-scale and over multidecadal periods, changes in phytoplankton species and communities have been associated with Northern Hemisphere Temperature (NHT) trends, the Atlantic Multidecadal Oscillation (AMO), the East Atlantic Pattern (EAP), and variations in the North Atlantic Oscillation (NAO) index. These have included changes in species distributions and abundance, the occurrence of subtropical species in temperate waters, changes in overall phytoplankton biomass and seasonal length, changes in the ecosystem functioning, and productivity of the North Atlantic (Edwards *et al.*, 2001, 2002; Reid and Edwards, 2001; Beaugrand *et al.*, 2002; Edwards and Richardson, 2004).

Contemporary observations using ten years of blended satellite and *in situ* chlorophyll records indicate that global ocean net primary production has declined over the last decade, particularly in the oligotrophic gyres of the world's oceans (Behrenfeld *et al.*, 2006). In contrast, trends based on 50 years of Phytoplankton Colour Index records (a proxy for chlorophyll) indicate there has been an steady increase in phytoplankton biomass for the whole temperate Northeast Atlantic (Richardson and Schoeman, 2004), which is visible in Figure 10.3. Both studies correlate these increases with sea surface temperatures (Figure 10.4). This increase in phytoplankton biomass is presumably the result of an initial increase in phytoplankton metabolic rates caused by these warmer temperatures in otherwise cooler-water regions. This positive response to warming is not unlimited, however, as nutrient limitations can take effect as warming of the surface layers increase water-column stability, enhancing stratification, and requiring more energy to mix deep, nutrient-rich waters into surface layers. Particularly warm winters will also limit the degree of deep convective mixing and thereby limit nutrient replenishment necessary for the following spring phytoplankton bloom. The amount of nutrients available in surface waters directly dictates

phytoplankton growth and is the key determinant of the plankton size, community, and foodweb structure.

Climate variability has a spatially heterogeneous impact on phytoplankton in the North Atlantic and not all regional areas are correlated to the same climatic index. For example, trends in the AMO are particularly prevalent in the oceanic regions and in the Subpolar Gyre of the North Atlantic, and the NAO has a higher impact in the southern North Sea where the atmosphere–ocean interface is most pronounced. This is also apparent with respect to the Northern Hemisphere Temperature, where the response is also spatially heterogeneous with areas of the Northeast Atlantic and shelf areas of the Northwest Atlantic warming faster than the North Atlantic average and some areas like the Subpolar Gyre actually cooling. Similarly, regime shifts or abrupt ecosystem shifts do not always occur in the same region or at the same time. The major regime shift that occurred in phytoplankton colour in the late 1980s was particularly prevalent in the North Sea and was not seen in oceanic regions of the North Atlantic. However, a similar regime shift occurred in the phytoplankton colour ten years later in the Icelandic Basin and in oceanic regions west of the British Isles. The different timing and differing regional responses to regime shifts have been associated with the movement of the 10°C thermal boundary as it moves north in the North Atlantic (Beaugrand *et al.*, 2008).

In examining the long-term trends in the three phytoplankton indices (PCI, Total Diatoms, and Total Dinoflagellates), the general pattern is an increase in PCI for most regions in the North Atlantic (Figure 10.3), with differing timings for the main stepwise increase being later in oceanic regions compared with the North Sea. Within the dinoflagellates (Figure 10.6), there has been a general increase in abundance in the Northwest Atlantic and a decline in the Northeast Atlantic over a multidecadal period. In particular, some regions of the North Sea have experienced a sharp decline over the last decade, mainly caused by the dramatically reduced abundance of the *Ceratium* genus in the North Sea. However, *Ceratium* abundance has recovered in the North Sea over the last two years. For the diatoms (Figure 10.5), there is not really a predominant trend for the North Atlantic Basin as a whole, but some regions show a strong cyclic behaviour over the multidecadal period. The time-signal resembles an oscillation of ca. 50–60 years and a minimum around 1980, reflecting changes in the AMO signal. In summary, although climate warming is a major driver for the overall biomass

of phytoplankton, diatoms are less influenced by temperature and show a strong correlation with the AMO signal and wind intensity in many regions. The increase in diatoms associated with the positive phase of the AMO and the decline in dinoflagellate abundance over the last ten years in the Northeast Atlantic can be reflected as an increase in the diatoms:diatoms+dinoflagellates ratio. Figure 10.7 shows a strong positive increase in this ratio in the North Sea, but a strong negative decrease in the Labrador Sea region.

Indirectly, the progressive freshening of the Labrador Sea region, attributed to climate warming and the increase in freshwater input to the ocean from melting ice, has resulted in the increasing abundance, blooms, and shifts in seasonal cycles of dinoflagellates because of the increased stability of the water column (Johns *et al.*, 2001). Similarly, increases in coccolithophore blooms in the Barents Sea and harmful algal blooms (HABs) in the North Sea are associated with negative salinity anomalies and warmer temperatures, leading to increased stratification (Edwards *et al.*, 2006; Smyth *et al.*, 2004). It seems likely that an important environmental impact caused by climate change is an increase in the presence of haline stratification in regions susceptible to freshwater inputs, resulting in an increase in bloom formation.

Globally, eutrophication is considered a major threat to the functioning of nearshore ecosystems, as it has been associated with the occurrence and perceived increase of HABs. HABs are, in most cases, a completely natural phenomenon and occur regularly throughout recorded history. Disentangling these natural bloom events, caused by natural hydroclimatic variability, from unnatural bloom events caused by global climate change or eutrophication, can be very difficult. For example, increasing temperature, nutrient input fluctuations in upwelling areas, eutrophication in coastal areas, and enhanced surface stratification all have species-specific responses. Prediction of the impact of global climate change is, therefore, fraught with numerous uncertainties. There is some evidence that biogeographical range extensions caused by regional climate change have increased the presence of certain HABs in some regions (Edwards *et al.*, 2006). Regional climate warming and hydrographic variability in the North Sea has also been associated with an increase in certain HABs in some areas of the North Sea, particularly along the Norwegian Coastal Current (Edwards *et al.*, 2006). The abundance of *Prorocentrum* spp. and *Noctiluca scintillans* abundance is strongly correlated with increasing SST, and the increase in

a number of diatom species in the North Sea over the last decade has been associated with increasing wind intensity (Hinder *et al.*, 2012), which has been increasing across the majority of the North Atlantic Basin (Figure 10.8). Phenological studies have also found strong correlations between the movement of dinoflagellates (up to 1 month earlier) in their seasonal cycle and regional climate warming (Edwards and Richardson, 2004). In summary, at the large ecoregional and provincial scale, trends in phytoplankton are associated with hydroclimatic variability. This is not to say, however, that eutrophication is not a problem; it may, in fact, be the primary driver in certain coastal regions and at the more localized scale.

10.2 Basin-scale trends in microzooplankton

Tintinnids are ciliates, often grouped under microzooplankton, and they are an important group of marine micrograzers of nanophytoplankton. Tintinnids help transport nutrients to higher trophic levels and remove 10–27% of phytoplankton from coastal waters (Verity, 1987). They show a pelagic distribution, highest between 20 and 30°N or S, and there is often a correlation in tintinnid abundance and chlorophyll *a* (Dolan *et al.*, 2006). The CPR tintinnid time-series (1993–2010) are significantly shorter than the other CPR variables (1958–2010), but some initial trends emerge (Figure 10.9). Tintinnids in the western North Atlantic, bordering Newfoundland and Labrador (standard area D8), are exhibiting an overall positive increase, whereas standard area boxes in the southern (C1, D2) and northern (B2) North Sea show an overall decline.

Total tintinnid measurements do not reflect individual genus or species patterns. Tintinnid species have specific abundance and seasonality (Urrutxurtu, 2004), which may be masked by assessing phenology at a higher taxon level (i.e. “totals”). Several genera of tintinnids, such as *Tintinnopsis*, were found to expand their winter seasonal presence into UK coastal waters (Hinder *et al.*, 2011). Surprisingly, the total tintinnid patterns in this study do not follow PCI trends or SST (which are universally increasing), but their phenology can potentially be related to dinoflagellate abundance, which may be a food source. As the CPR tintinnid time-series are relatively short, these trends may become more evident as monitoring continues.

10.3 Phytoplankton biodiversity and invasive species

At the ocean basin scale, biodiversity of phytoplankton is related to temperature, and an increase in warming over the last few decades has been followed by an increase in diversity, particularly for dinoflagellates (Beaugrand *et al.*, 2010). Phytoplankton as a whole show a relationship between temperature and diversity, which is linked to the phytoplankton community having a higher diversity, but an overall smaller size-fraction and a more complex foodweb structure (i.e. microbial-based vs. diatom-based production) in warmer, more stratified environments. Climate warming will, therefore, increase planktonic diversity throughout the cooler regions of the world's oceans as temperature isotherms shift poleward. Apart from thermal boundary limits moving progressively poleward and, in some cases, expanding, the rapid climate change observed in the Arctic may have even greater consequences for the establishment of invasive species and the biodiversity of the North Atlantic.

The thickness and areal coverage of summer ice in the Arctic have been melting at an increasingly rapid rate over the last two decades, reaching the lowest-ever recorded extent in September 2007. In spring, following the unusually large ice-free period in 1998, large numbers of a Pacific diatom *Neodenticula seminae* were found in samples taken by the CPR survey in the Labrador Sea in the North Atlantic. *N. seminae* is an abundant member of the phytoplankton in the subpolar North Pacific and has a well-defined palaeo history based on deep-sea cores. According to the palaeological evidence and modern surface sampling in the North Atlantic since 1948, this was the first record of this species in the North Atlantic for at least 800 000 years. The reappearance of *N. seminae* in the North Atlantic, and its subsequent spread southwards and eastwards to other areas in the North Atlantic, after such a long gap, could be an indicator of the scale and speed of changes that are taking place in the Arctic and North Atlantic oceans as a consequence of climate warming (Reid *et al.*, 2007). The diatom species itself could be the first evidence of a transarctic migration in modern times and be a harbinger of a potential inundation of new organisms into the North Atlantic. The consequences of such a change to the function, climatic feedbacks, and biodiversity of Arctic systems are, at present, unknown.

10.4 Trends in marine pathogens

As sea surface temperatures increase, predictions favour an increase in the number and range of pathogenic microorganisms. Such changes are difficult to determine over short periods, as one cannot separate short-term variations from long-term climate-change trends. In a unique long-term time-study, Vezzulli *et al.* (2011) investigated the spread of the pathogenic bacteria *Vibrio*, the causative agent of cholera, in the North Sea using 54 years of CPR-collected samples. Using DNA extract from CPR samples, the relative proportion of *Vibrio* bacteria in relation to total bacteria was calculated. This *Vibrio* Abundance Index (VAI) was found to have steadily increased over four decades, and the trend was correlated with SST and copepod abundance, but not PCI. *Vibrio* thrives best in water temperatures over 18°C (Vezzulli *et al.*, 2004). Within the southern Rhine region of the North Sea, an area which frequently has summer SST values over 18°C, the correlation between SST and VAI was significant. Within the northern Humber region, an area where SST never exceeds 18°C, there was no significant increase or clear trend. *Vibrio* attach to chitin surfaces, such as the shells of copepods and other chitinous zooplankton. The correlation with copepod abundance indicates this relationship is both a pathway for the pathogen and a potential monitoring proxy.

Phytoplankton Colour Index

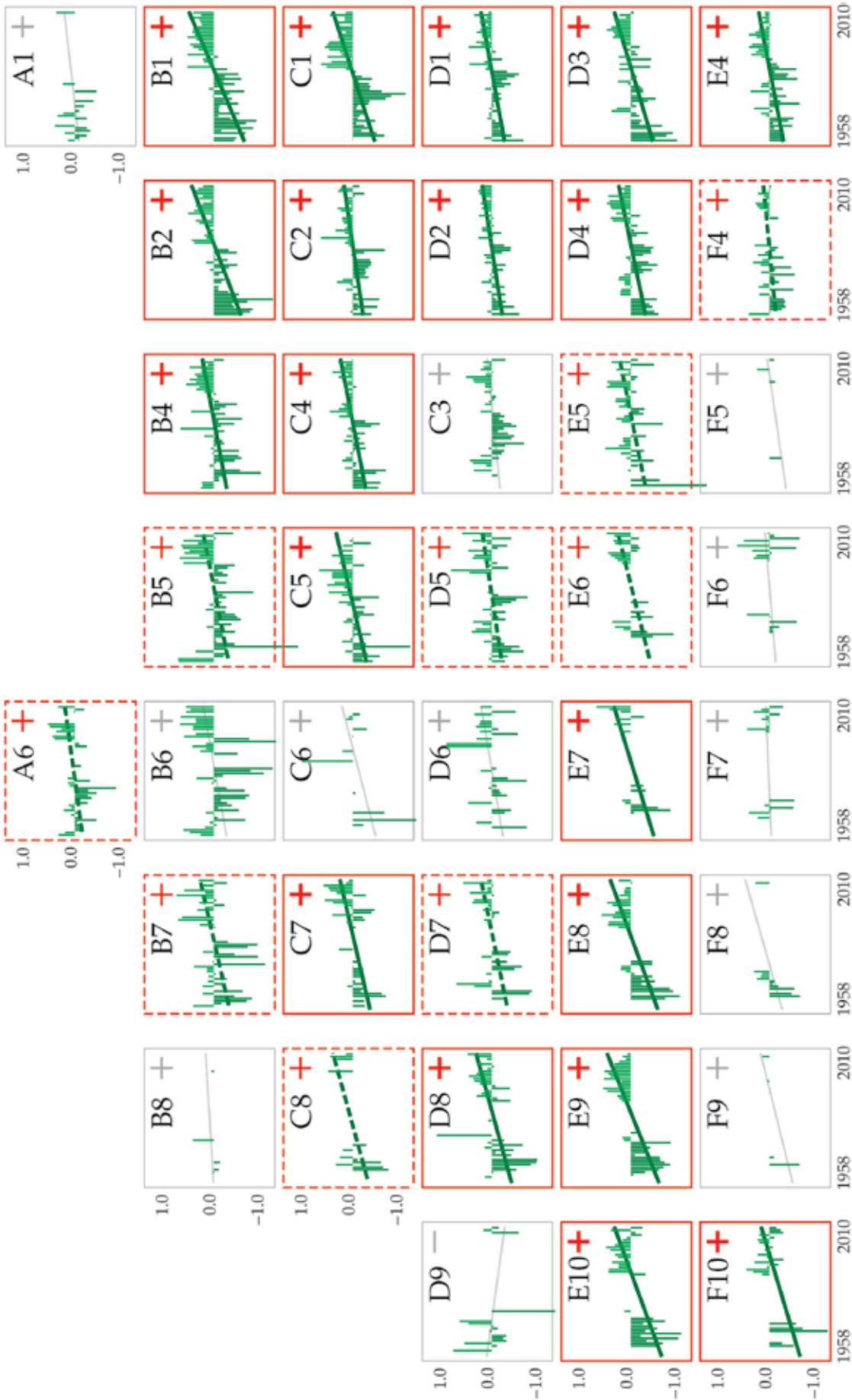


Figure 10.3
Spatio-temporal trends plot for
Phytoplankton Colour Index
time-series in the CPR standard
areas of the North Atlantic Basin
based on data for 1958–2010.

Sea Surface Temperature

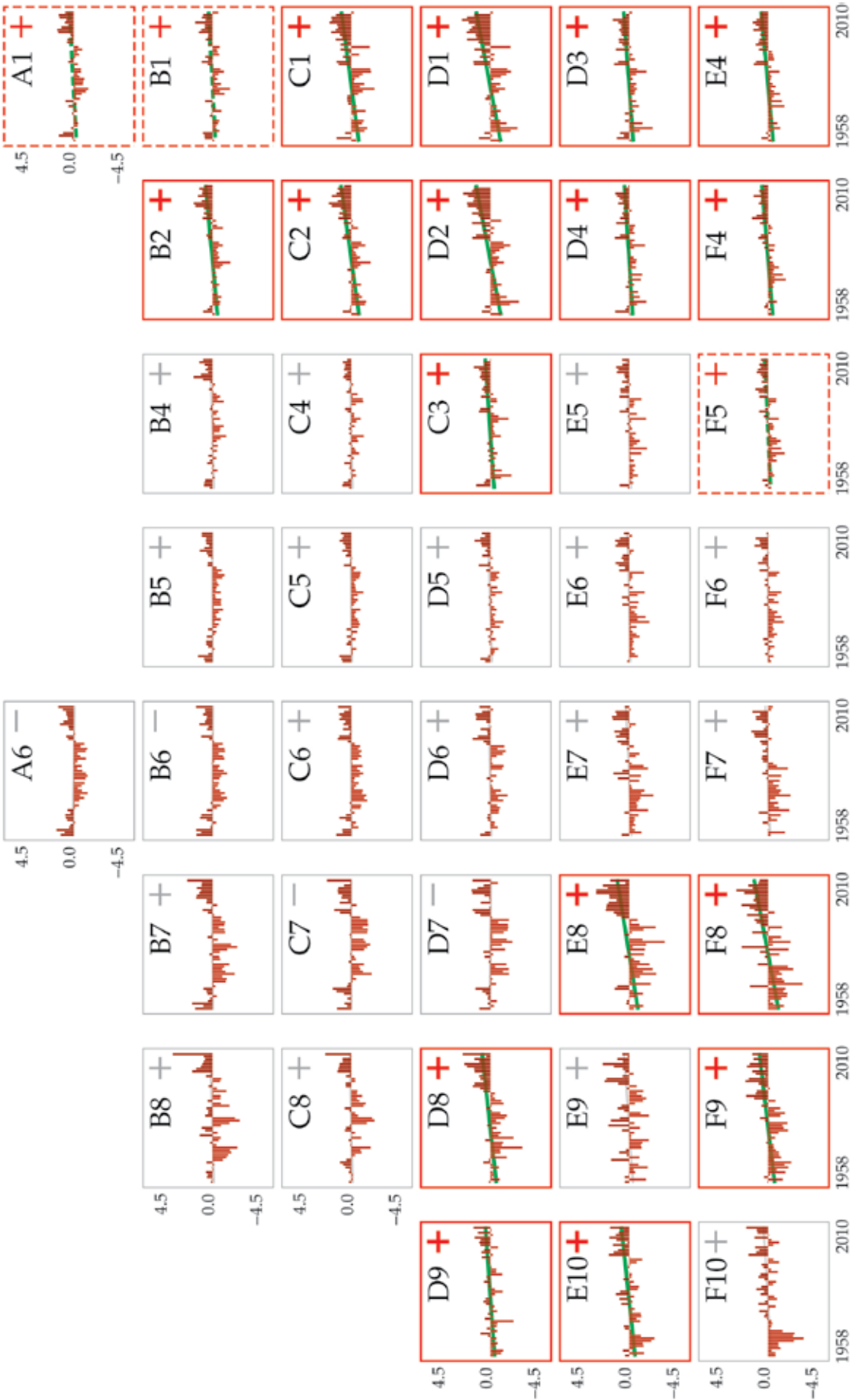


Figure 10.4
Spatio-temporal trends plot for
sea surface temperature time-
series in the CPR standard areas
of the North Atlantic Basin based
on data for 1958–2010.

Total Diatoms

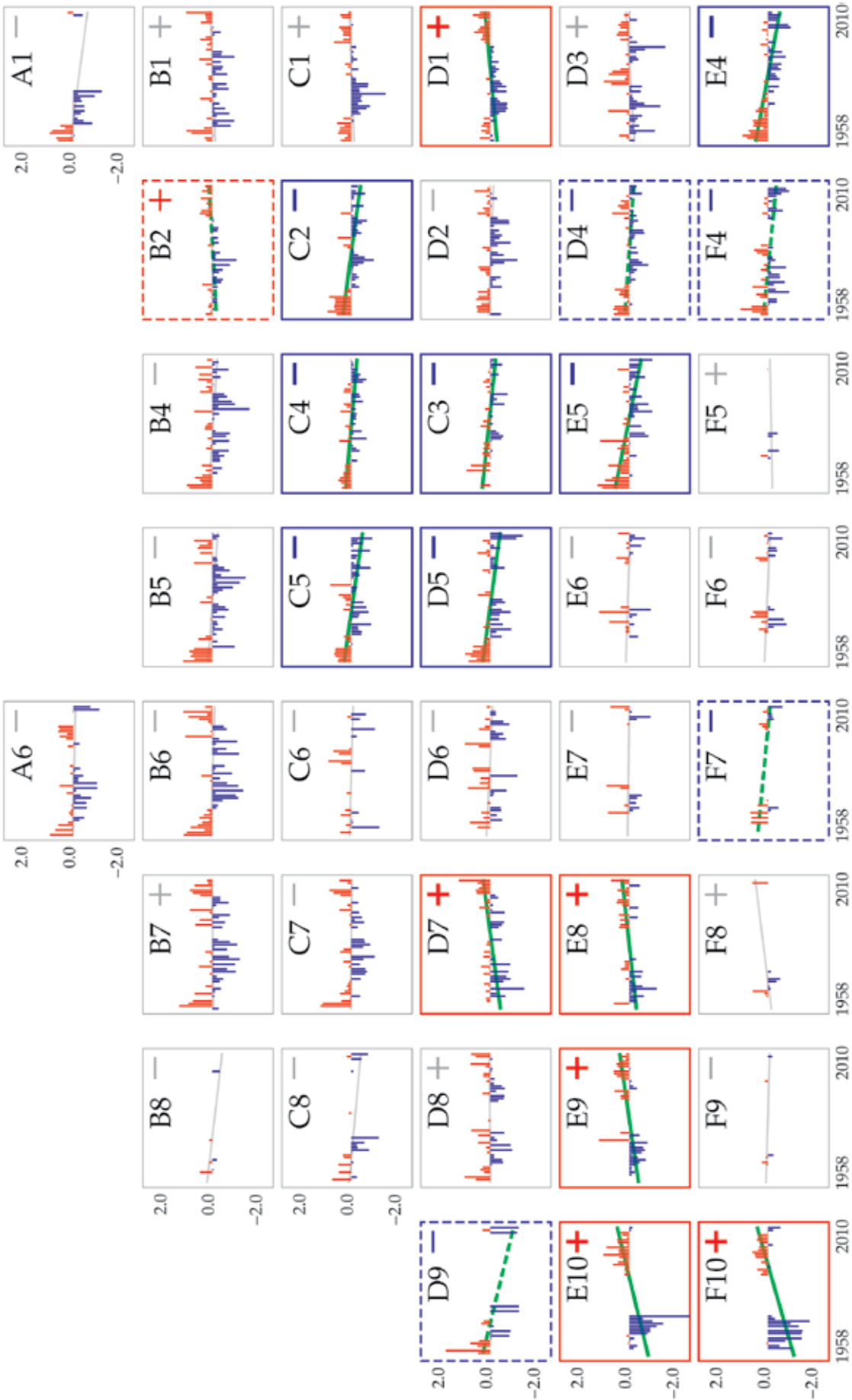


Figure 10.5
Spatio-temporal trends plot for
Total Diatoms time-series in the
CPR standard areas of the North
Atlantic Basin based on data for
1958–2010.

Total Dinoflagellates

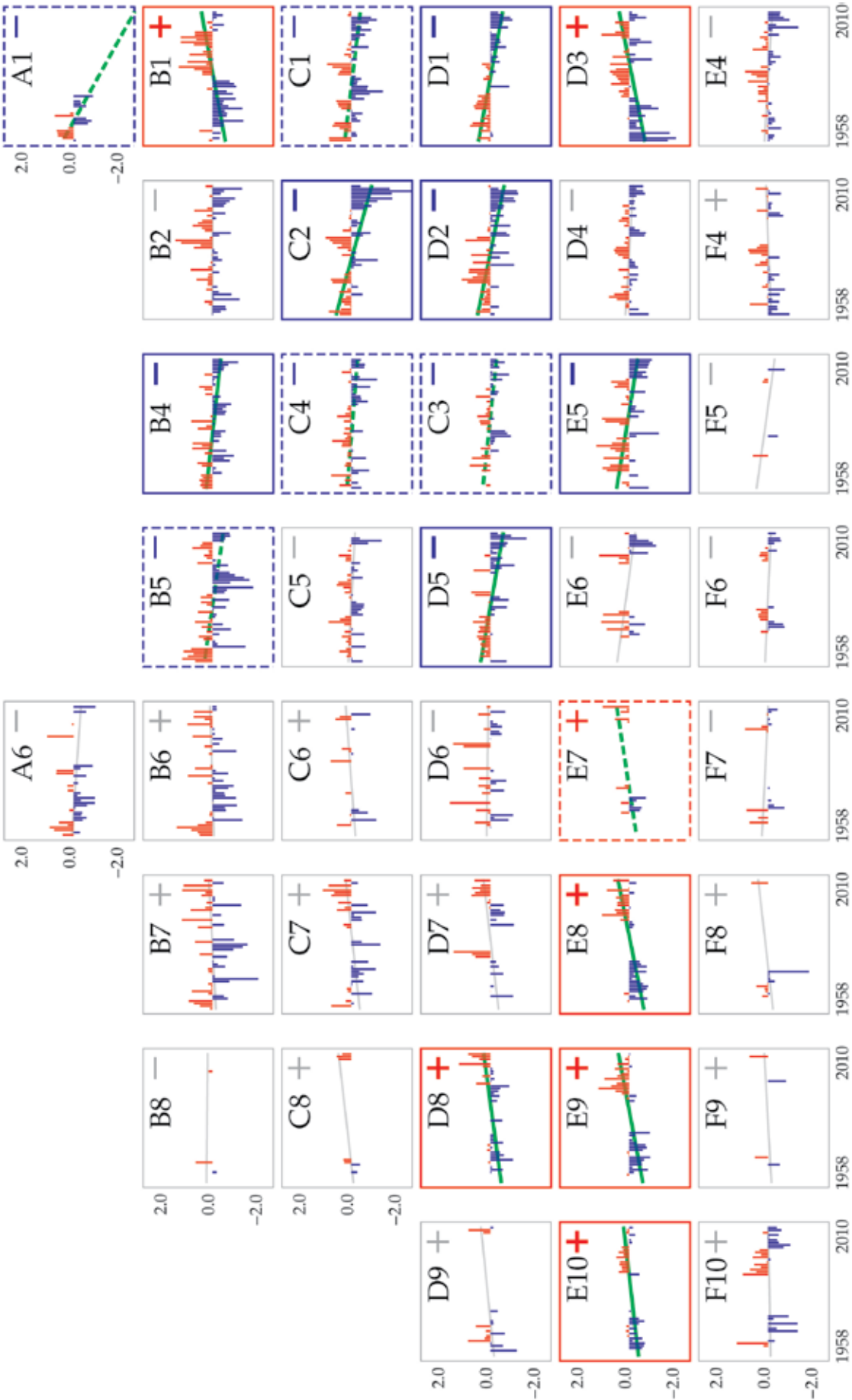
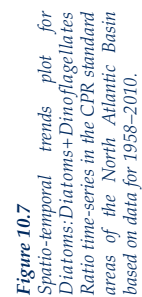


Figure 10.6
Spatio-temporal trends plot for
Total Dinoflagellates time-series
in the CPR standard areas of the
North Atlantic Basin based on
data for 1958–2010.



Wind Speed

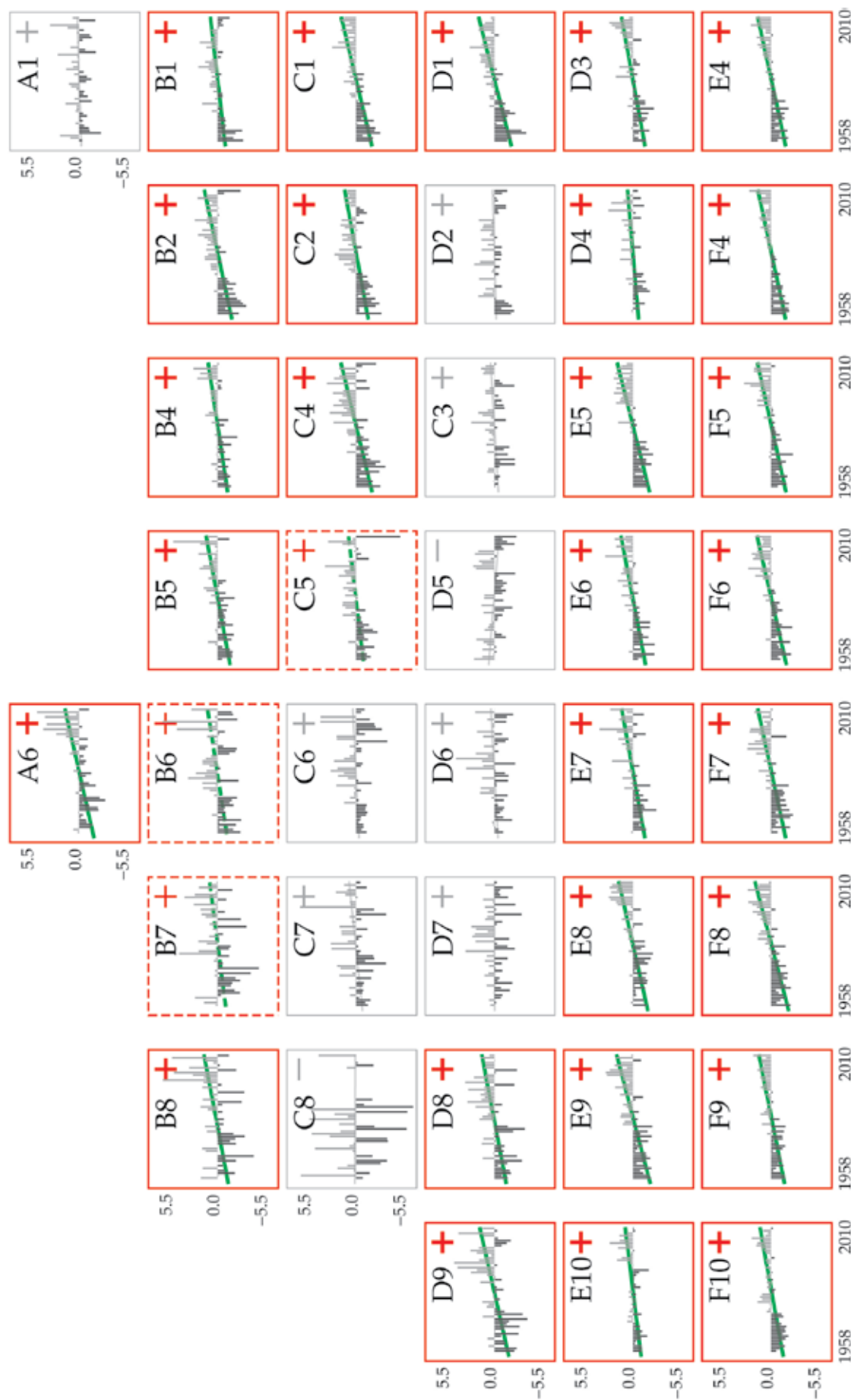


Figure 10.8
Spatio-temporal trends plot for
COADS Wind speed time-series
in the CPR standard areas of the
North Atlantic Basin based on
data for 1958–2010.

Total Tintinnids

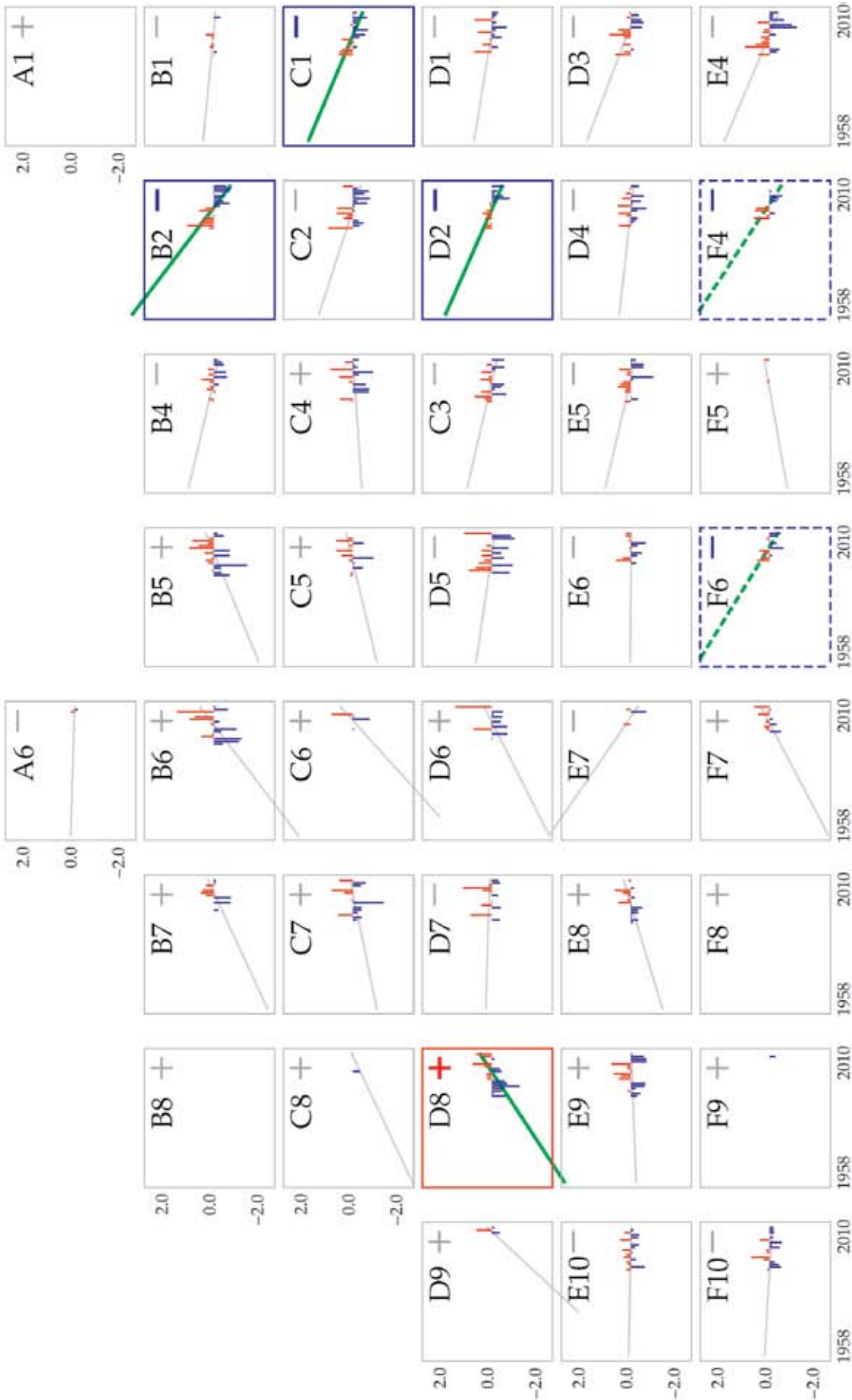
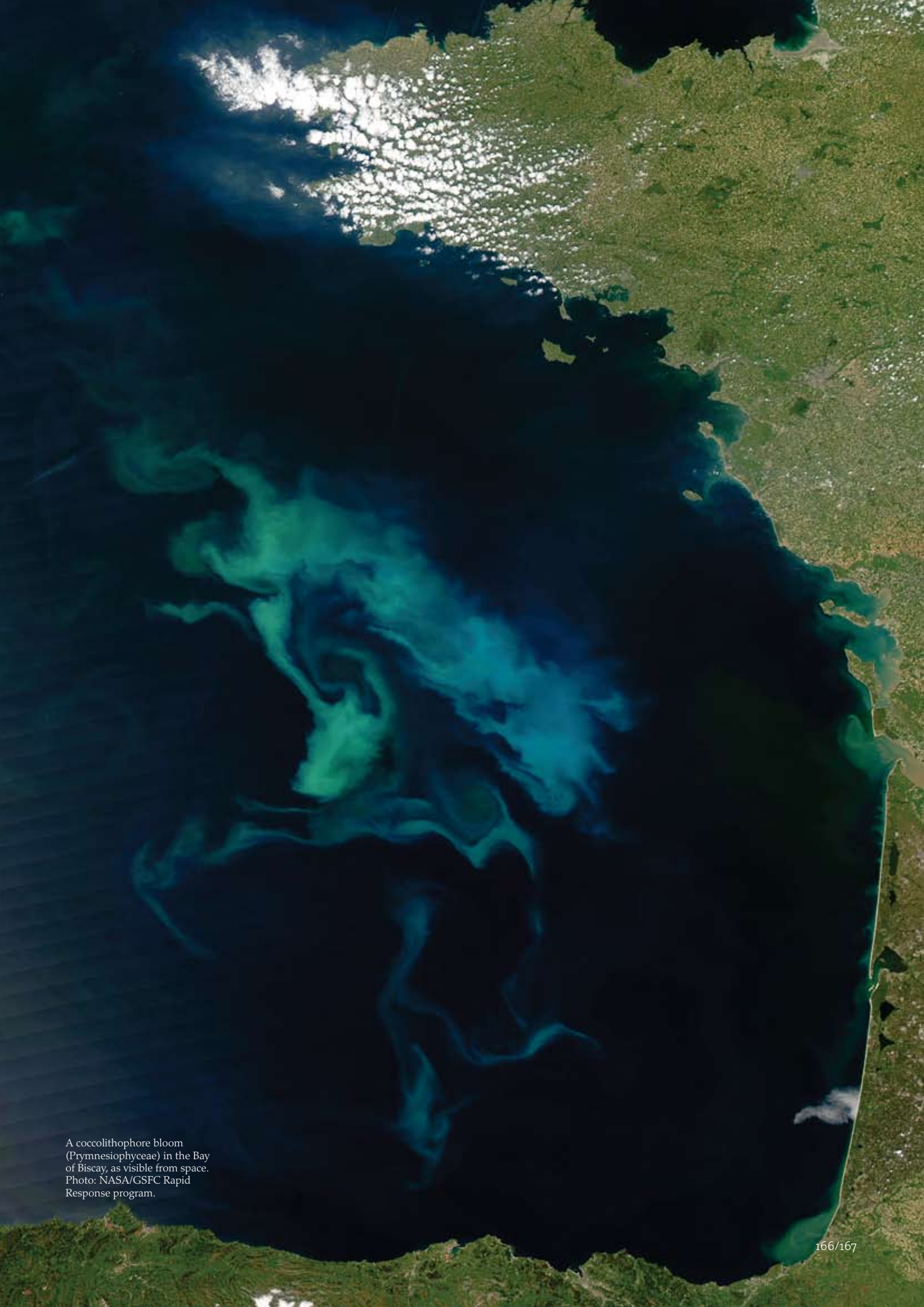


Figure 10.9
Spatio-temporal trends plot for
Total Tintinnids time-series in the
CPR standard areas of the North
Atlantic Basin based on data for
1993–2010.



A coccolithophore bloom (Prymnesiophyceae) in the Bay of Biscay, as visible from space. Photo: NASA/GSFC Rapid Response program.

11. SPATIO-TEMPORAL ATLAS OF THE NORTH ATLANTIC

William K. W. Li, Todd D. O'Brien, and Xosé Anxelu G. Morán

In the foregoing chapters, temporal change was visually indicated in the interannual trend plots with a slope line representing the linear regression of the annual anomalies vs. year. The color and form of this line indicated the significance level of this regression (e.g. a solid green line if $p < 0.01$, a dashed green line if $p < 0.05$, a thin grey line if non-significant, see Section 2.2). Because the process of change cannot be assumed to be linear, the slope is not an inferential predictor. Depending on the length of the observation period, the slope can be expected to be different at the same monitoring site. Thus, the slope is used here as a simple descriptor of the current state (through 2010) of the microbial system in relation to its past state for two starting points in the past (1981 and 2001), representing 10 and 30 years of monitoring. In this section, we map and tabulate this statistic for selected common variables across the 61 monitoring sites and 40 CPR standard areas introduced in the foregoing chapters. For the 10-year trend analysis, we considered only those time-series for which there existed at least 7 years of observations in the period 2001–2010. Similarly, for the 30-year trend analysis, we considered only those time-series for which there existed at least 21 years of observations in the period 1981–2010.

The spatio-temporal summary tables presented in this section list the site names and the regression slopes of select variables from the 61 monitoring sites (Tables 11.1 and 11.3) and the 40 CPR standard areas (Tables 11.2 and 11.4). The cells in these tables are colour-coded according to one of six regression result classes, depending on the sign of its slope (positive or negative) and the strength of the slope's statistical significance (strongly significant, significant, or not significant). The code is: dark red (positive slope, $p < 0.01$); pink (positive slope, $p < 0.05$); light pink (positive slope, $p > 0.05$); light cyan (negative slope, $p > 0.05$); cyan (negative slope, $p < 0.05$); dark blue (negative slope, $p < 0.01$). The same color coding was used in the spatio-temporal maps (Figures 11.2–11.16), with a star symbol used to represent the location and trends of each of the 40 CPR standard area regressions and a circle symbol used to indicate the location and trends of each of the 61 monitoring sites.

The salient patterns that appear from this large-scale consolidation are described as follows. At the shorter time-scale of ten years, the majority (>50%) of the 61 monitoring sites listed in Table 11.1 show decreasing sea surface temperature, increasing wind speed, and chlorophyll *a* concentrations, decreasing total diatom abundance, increasing total dinoflagellate abundance, decreasing diatoms:diatoms+dinoflagellates ratios,

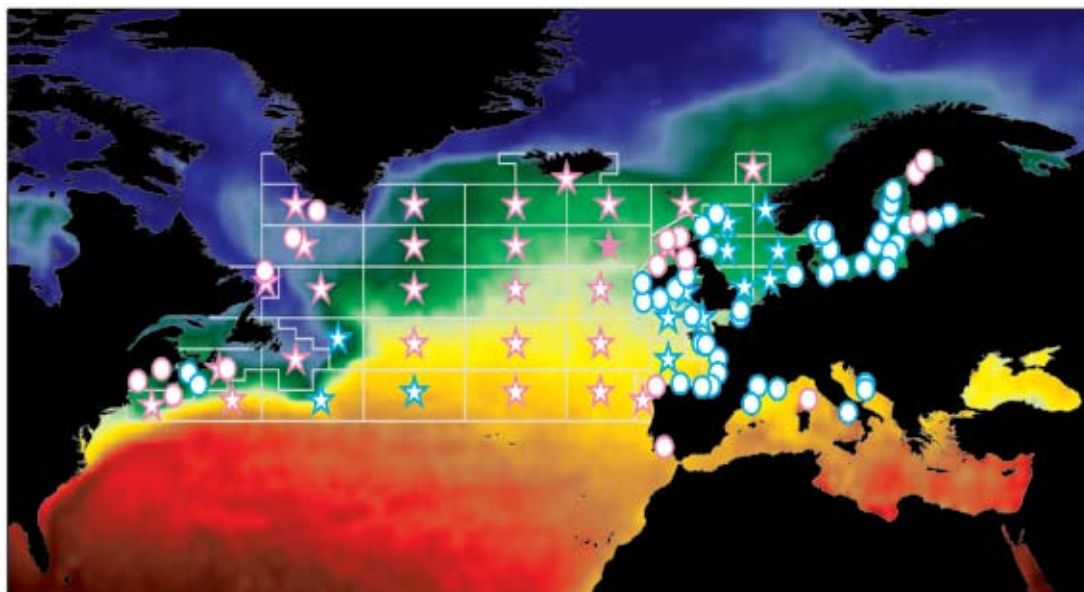


Figure 11.1
Spatio-temporal map of 10-year trends in sea surface temperature plotted on a background of average sea surface temperature (see also Figure 11.2).

increasing picophytoplankton abundance (both picoeukaryotes and *Synechococcus*), and decreasing bacteria abundance. In contrast, many of the 10-year CPR standard area trends (Table 11.2) show an opposite trend, with a majority exhibiting increasing SST, decreasing wind speed, and decreasing phytoplankton colour index (a chlorophyll *a* proxy), diatoms, and dinoflagellates.

The spatial distribution patterns of these trends varied from variable to variable. The combined CPR and monitoring site spatio-temporal map for 10-year sea surface temperature (Figure 11.2) indicated cooling along most of the European coastlines and warming in the central Atlantic basin and along much of the North American coast. A similar east-west distribution of opposite trends is also visible in wind speed (Figure 11.3), with increasing wind speed in many of the eastern regions and decreasing wind speeds in many of the western regions. This east-west trend was not as visibly present in the remaining variables, however. Chlorophyll trends (Figure 11.4), for example, formed small clusters of same-sign trends. Diatom abundance (Figure 11.5) and dinoflagellate abundance (Figure 11.6) featured similar regionalized clusters like the chlorophyll, but varied in correlation direction with chlorophyll (i.e. in some regions, diatoms increased with increasing chlorophyll, whereas in others, they decreased with increasing chlorophyll). The

diatoms:diatoms+dinoflagellates ratio (Figure 11.6) followed this same regional clustering pattern. Although relatively few sites exist for *Synechococcus* and picoeukaryotes, the regionalized trend clustering appears to be present (Figures 11.7 and 11.8).

At the longer time-scale of 30 years, the majority of the monitoring sites listed in Table 11.3 show increasing sea surface temperature, chlorophyll *a* concentrations, and total diatom abundance, but decreasing total dinoflagellate abundance and diatoms:diatoms+dinoflagellates ratio. This same majority pattern was found in the CPR standard areas (Table 11.4), with the exception of an increasing diatoms:diatoms+dinoflagellates ratio. It should be noted that the absence of 30-year trend information for picophytoplankton and bacteria stems from the fact that these smallest size classes have only recently been incorporated into time-series (i.e. they did not meet the minimum of 21 years criteria for the 30-year analysis).

One striking result of the 30-year analysis is found in the sea surface temperature trends. Out of the 101 locations listed in Tables 11.3 and 11.4, only one site indicated cooling. Of the 100 warming locations, 96 had significant trends (nine with $p < 0.05$ and 85 with $p < 0.01$). In the 30-year spatio-temporal map (Figure 11.11), the one cooling site

and three of the four non-significant warming trend sites are found in the Gulf of Maine region. The cooling trends along the European coastline are replaced with strong ($p < 0.01$) warming trends in the 30-year analysis.

Despite losing points from some of the shorter (< 21 year) sites, the regional clustering of like trends (seen in the 10-year maps) is also present in the 30-year maps, in some instances expanding in spatial coverage. Trends seen in the 10-year analysis reverse in some 30-year sites and strengthen in others. The apparent 10-year/30-year trend differences in the large phytoplankton groups (diatoms, dinoflagellates, and their ratio) is difficult to interpret, but may be the result of reduced natural variability in environmental factors as a time-series grows in length. A main finding of the SCOR Global Comparisons of Zooplankton Time-

series working group (WG125) was that 30 years was a rough minimum for looking at longer-term trends, responses to climate forcing, and synchrony between sites (see Batchelder *et al.*, 2012; Mackas *et al.*, 2012). Although the majority of the zooplankton survey sites were in shelf and open waters, a large portion of the phytoplankton and microbial plankton sites (with exception of the CPR data) are located in shallow coastal waters, bays, estuaries, and lagoons. In these environments, local hydrographic forcing (e.g. tides, river run-off, anthropogenic nutrient inputs) are likely to contribute heavily to increasing the variability within these time-series. Likewise, functional groups such as total diatoms or total dinoflagellates can often mask the subtleties or responses given by individual species. Nevertheless, functional groups underlie the functional approach to understanding ecosystem change.

Table 11.1

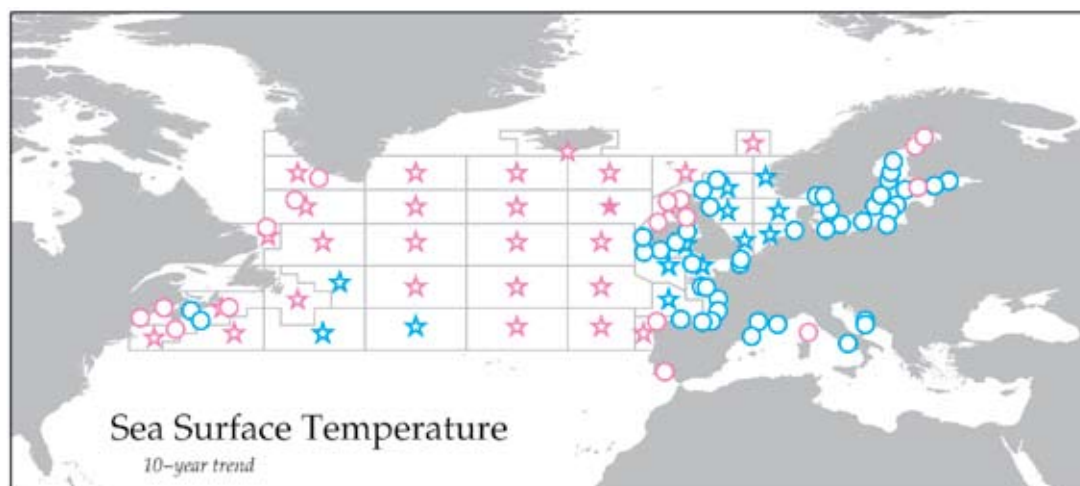
Table of 10-year trends and linear regression slope values listed by monitoring site and variable name. Cell colors indicate slope (blue/cyan = negative, red/pink = positive). Statistical significance is indicated by color and symbol (dark red (+++) /blue (---) = $p < 0.01$, medium pink (++) /cyan (--) = $p < 0.05$). Lightest pink (+) / cyan cells (-) indicate slope of non-significant trend ($p > 0.05$).

Region	Station #	Site Name	Sea Surface Temperature	Wind Speed	Chlorophyll	Total Diatoms	Total Dinoflagellates	Diatoms to Dinoflagellates ratio	Picocaryotes	Synchroscous	Bacteria
Northwest Atlantic Shelf	1	Booth Bay - Maine	0.064 (+)	-0.142 (-)	0.003 (+)					0.025 (+)	-0.012 (-)
	2	Bay of Fundy	0.070 (+)	-0.066 (-)	-0.041 (-)	-0.027 (-)	0.010 (+)	-0.021 (-)			
	3	Bedford Basin	-0.009 (-)	-0.133 (-)	-0.019 (-)				0.038 (+++)	0.087 (+++)	-0.009 (-)
	4	Western Scotian Shelf	0.025 (+)	-0.151 (-)	-0.001 (-)				0.025 (+)	0.010 (+)	0.029 (+++)
	5	Central Scotian Shelf	-0.005 (-)	-0.007 (-)	-0.029 (-)				0.018 (+)	0.096 (+++)	0.020 (+++)
	6	Eastern Scotian Shelf	0.029 (+)	-0.017 (-)	-0.053 (-)				0.004 (+)	0.026 (+)	-0.002 (-)
Labrador Sea	7	Labrador Shelf and Slope	0.020 (+)	-0.098 (-)	0.030 (+)				-0.013 (-)	0.042 (+)	0.022 (+)
	8	Labrador Basin	0.038 (+)	0.626 (+)	0.022 (+)				0.026 (+)	0.011 (+)	-0.004 (-)
	9	Greenland Shelf and Slope	0.092 (+)	0.033 (+)	0.048 (+)				0.011 (+)	-0.004 (-)	-0.013 (-)
Baltic Sea	10	Bothnian Bay F2	0.114 (+)	0.175 (+)	-0.001 (-)	-0.004 (-)	-0.034 (-)	0.054 (+)			
	11	Bothnian Bay BO3	0.032 (+)	-0.006 (-)	-0.006 (-)	-0.098 (-)	-0.039 (-)	-0.027 (-)			
	12	Bothnian Sea US5b	-0.001 (-)	0.080 (+)	-0.012 (-)	-0.102 (-)	-0.076 (-)	0.010 (+)			
	13	Bothnian Sea SR5	-0.019 (-)	-0.067 (-)	0.014 (+)	-0.178 (-)	-0.016 (-)	-0.038 (-)			
	14	Åland Sea F64	-0.037 (-)	0.109 (+)	0.012 (+)	0.120 (+)	0.050 (+)	-0.037 (-)			
	15	Gulf of Finland LL3a	-0.029 (-)	0.086 (+)	-0.006 (-)	-0.025 (-)	-0.122 (-)	0.041 (+)			
	16	Gulf of Finland LL7	-0.032 (-)	-0.073 (-)	-0.009 (-)	-0.072 (-)	0.024 (+)	-0.021 (-)			
	17	Gulf of Finland LL12	0.015 (+)	0.066 (+)	0.012 (+)	-0.111 (-)	-0.048 (-)	0.005 (+)			
	18	Baltic Proper LL17	-0.017 (-)	-0.033 (-)	0.013 (+)	-0.001 (-)	-0.015 (-)	0.011 (+)			
	19	Baltic Proper LL23	-0.046 (-)	-0.005 (-)	0.030 (+)	0.021 (+)	-0.016 (-)	0.016 (+)			
	20	Baltic Proper BY38	-0.046 (-)	0.097 (+++)	0.037 (+)	-0.010 (-)	0.059 (+)	-0.033 (-)			
	21	Baltic Proper BY15	-0.033 (-)	0.044 (+)	0.032 (+++)	0.042 (+)	0.066 (+)	-0.009 (-)			
	22	Gdansk Basin	-0.039 (-)	-0.051 (-)	-0.033 (-)	-0.076 (-)	-0.081 (-)	-0.010 (-)			
	23	Eastern Gotland Basin	-0.038 (-)	0.036 (+)	0.028 (+)	0.013 (+)	0.029 (+)	-0.008 (-)			
	24	Bornholm Basin	-0.045 (-)	0.061 (+)	0.026 (+)	0.044 (+)	0.041 (+)	-0.006 (-)			
	25	Arkona Basin	-0.024 (-)	0.079 (+)	0.019 (+)	0.044 (+)	0.029 (+)	-0.010 (-)			
	26	Mecklenburg Bight	-0.011 (-)	0.025 (+)	0.014 (+)	-0.020 (-)	-0.008 (-)	0.004 (+)			
	27	SMHI Anholt East	-0.015 (-)	0.129 (+)	-0.002 (-)	0.000 (+)	0.037 (+)	-0.004 (-)			
	28	SMHI Släggö	-0.020 (-)	-0.105 (-)	0.007 (+)	0.010 (+)	0.053 (+)	0.011 (+)			
	29	SMHI Å17	-0.022 (-)	-0.066 (-)	0.000 (-)	-0.029 (-)	-0.021 (-)	-0.008 (-)			
North Sea and English Channel	30	Helgoland Roads	-0.034 (-)	0.025 (+)		0.041 (+++)	-0.010 (-)	0.011 (+++)			
	31	Scalloway - Shetland Isles	-0.007 (-)	-0.143 (-)	0.010 (+)	0.068 (+++)	0.026 (+)	0.005 (+)			
	32	Scapa Bay - Orkney	-0.009 (-)	-0.067 (-)	-0.008 (-)	0.031 (+)	0.021 (+)	0.005 (+)			
	33	Stonehaven	-0.027 (-)	0.038 (+)	0.027 (+++)	0.040 (+)	0.075 (+++)	-0.006 (-)			
	34	REPHY Point 1 SRN Boulogne	-0.065 (-)	0.017 (+)	0.016 (+)	0.062 (+++)	0.099 (+++)	0.006 (+)			
	35	REPHY At So	-0.065 (-)	-0.088 (-)	0.001 (+)	0.052 (+)	0.113 (+++)	0.001 (+)			
	36	Plymouth L4	-0.036 (-)	-0.014 (-)	-0.013 (-)	0.029 (+)	0.012 (+)	0.001 (+)			
Northeast Atlantic Shelf	37	Loch Ewe	0.011 (+)	0.036 (+)	0.018 (+)	0.004 (+)	0.047 (+++)	-0.014 (-)			
	38	Loch Maddy	0.017 (+)	-0.129 (-)	0.016 (+)	0.028 (+)	0.040 (+)	-0.022 (-)			
	39	Millport	0.004 (+)	0.166 (+)	0.018 (+)						
	40	Cypris Station - Isle of Man	-0.004 (-)	0.084 (+)	-0.003 (-)	-0.011 (-)	-0.017 (-)	-0.003 (-)			
	41	East Coast Ireland	-0.014 (-)	0.116 (+)		-0.024 (-)	0.040 (+)	-0.006 (-)			
	42	South Coast Ireland	-0.013 (-)	0.180 (+)		-0.009 (-)	0.006 (+)	0.002 (+)			
	43	Southwest Coast Ireland	-0.009 (-)	-0.089 (-)		-0.012 (-)	-0.016 (-)	0.005 (+)			
	44	West Coast Ireland	-0.009 (-)	0.013 (+)		-0.044 (-)	-0.028 (-)	0.009 (-)			
	45	Northwest Coast Ireland	0.004 (+)	0.051 (+)		-0.029 (-)	0.006 (+)	-0.025 (-)			
Bay of Biscay and western Iberian Shelf	46	REPHY Men er Roue	-0.043 (-)	0.046 (+)		0.044 (+)	0.023 (+)	0.006 (+)			
	47	REPHY Ouest Loscolo	-0.045 (-)	0.031 (+)		0.051 (+++)	0.041 (+++)	0.002 (+)			
	48	REPHY Le Comand	-0.035 (-)	0.065 (+)	0.015 (+)	0.016 (+)	0.013 (+)	-0.005 (-)			
	49	REPHY Treyhan Bis	-0.031 (-)	0.001 (+)		0.040 (+)	-0.008 (-)	-0.003 (-)			
	50	AZTI Station D2	-0.029 (-)	0.090 (+)	0.014 (+)	0.059 (+)	0.054 (+)	0.000 (+)			
	51	Nervión River Estuary	-0.026 (-)	0.153 (+)		0.039 (+)	0.051 (+)	0.013 (+)			
	52	RADIALES Gijón/Xixón Station 2	-0.007 (-)	0.079 (+)	0.004 (+)				-0.009 (-)	0.012 (+)	0.012 (+)
	53	RADIALES A Coruña Station 2	0.003 (+)	0.151 (+)	0.009 (+)	-0.003 (-)	-0.007 (-)	0.004 (+)		-0.036 (-)	-0.002 (-)
	54	Guadiana Estuary	0.027 (+)	0.060 (+)	-0.004 (-)	-0.087 (-)					
Mediterranean Sea	55	Bianes Bay	-0.014 (-)	0.017 (+)	-0.009 (-)				0.002 (+)	0.002 (+)	-0.014 (-)
	56	Thau Lagoon	-0.015 (-)	0.118 (+)	-0.034 (-)	0.080 (+++)	0.010 (+)	0.020 (+++)	0.015 (+)	0.053 (+)	
	57	REPHY Lazaret A	-0.009 (-)	0.047 (+)	0.122 (+++)	0.014 (+)	-0.011 (-)	-0.001 (-)			
	58	REPHY Diana Centre	0.028 (+)	0.036 (+)	0.081 (+)	-0.053 (-)	0.037 (+)	-0.016 (-)			
	59	Gulf of Naples LTER-MC	-0.022 (-)	0.134 (+)		0.012 (+)	0.016 (+)	0.002 (+)			
	60	Kaštel Bay	-0.019 (-)	-0.424 (-)							0.110 (+++)
	61	Stonice	-0.030 (-)	-0.159 (-)							0.007 (+)
Percent of Positive Slopes			27%	62%	60%	47%	59%	44%	80%	83%	38%
Number of Positive Slopes			17 of 61	35 of 61	29 of 48	23 of 48	28 of 47	21 of 47	8 of 10	10 of 12	3 of 13

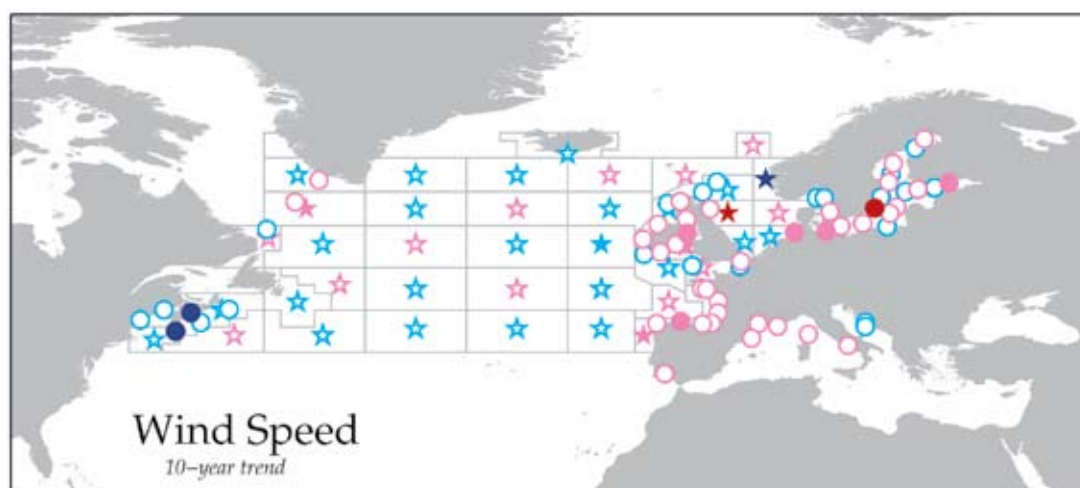
Region	Site Name	Sea Surface Temperature	Wind Speed	Phytoplankton Colour Index	Total Diatoms	Total Dinoflagellates	Diatoms to Dinoflagellates ratio
Western North Atlantic	CPR-F10	0.075 (+)	-0.067 (-)	-0.017 (-)	-0.039 (-)	0.001 (+)	-0.002 (-)
	CPR-E10	0.029 (+)	-0.062 (-)	-0.035 (---)	-0.041 (---)	-0.018 (-)	-0.007 (-)
	CPR-F09	0.026 (+)	0.023 (+)				
	CPR-E09	0.030 (+)	-0.138 (-)	-0.027 (---)	-0.023 (-)	-0.025 (-)	0.005 (+)
	CPR-D09	0.039 (+)	0.025 (+)				
	CPR-F08	-0.002 (-)	-0.060 (-)				
	CPR-E08	-0.014 (-)	0.003 (+)	-0.004 (-)	-0.006 (-)	-0.024 (-)	0.010 (+)
	CPR-D08	0.038 (+)	-0.002 (-)	0.002 (+)	0.026 (+)	0.060 (++)	-0.014 (-)
	CPR-C08	0.048 (+)	0.523 (++)	-0.005 (-)	-0.017 (-)		-0.032 (---)
	CPR-B08	0.087 (+)	-0.081 (-)				
Central North Atlantic	CPR-F07	-0.008 (-)	-0.107 (-)	-0.018 (-)	-0.032 (-)	-0.035 (-)	0.001 (+)
	CPR-E07	0.036 (+)	-0.064 (-)	0.016 (+)	0.006 (+)	0.044 (+)	-0.010 (-)
	CPR-D07	0.022 (+)	0.039 (+)	-0.014 (-)	0.062 (++)	-0.028 (-)	0.006 (+)
	CPR-C07	0.031 (+)	-0.026 (-)	-0.004 (-)	0.034 (+)	-0.053 (-)	-0.007 (-)
	CPR-B07	0.058 (+)	-0.078 (-)	-0.002 (-)	0.054 (+)	0.011 (+)	0.006 (+)
	CPR-F06	0.016 (+)	-0.051 (-)	-0.017 (-)	0.009 (+)	-0.024 (-)	0.005 (+)
	CPR-E06	0.027 (+)	0.011 (+)	0.007 (+)	0.002 (+)	-0.035 (-)	0.001 (+)
	CPR-D06	0.022 (+)	-0.058 (-)	-0.009 (-)	-0.033 (-)	-0.025 (-)	0.007 (+)
	CPR-C06	0.017 (+)	0.121 (+)	0.036 (+)			
	CPR-B06	0.033 (+)	-0.110 (-)	0.006 (+)	0.062 (+)	-0.010 (-)	0.017 (+++)
Eastern North Atlantic	CPR-A06	0.032 (+)	-0.048 (-)	-0.027 (-)	-0.087 (---)	-0.088 (-)	0.014 (+)
	CPR-F05	0.010 (+)	-0.086 (-)	0.000 (+)	-0.031 (-)		0.016 (+)
	CPR-E05	0.011 (+)	-0.019 (-)	-0.016 (-)	-0.021 (-)	-0.078 (---)	0.021 (++)
	CPR-D05	0.028 (+)	-0.214 (---)	0.003 (+)	-0.077 (---)	-0.070 (-)	0.001 (+)
	CPR-C05	0.030 (++)	-0.019 (-)	-0.052 (-)	-0.021 (-)	-0.080 (---)	0.030 (++)
	CPR-B05	0.018 (+)	0.053 (+)	-0.038 (-)	-0.023 (-)	-0.080 (---)	0.010 (+)
	CPR-F04	0.002 (+)	0.080 (++)	-0.016 (---)	-0.031 (-)	-0.007 (-)	0.011 (+)
	CPR-E04	-0.002 (-)	0.057 (+)	-0.015 (-)	-0.023 (-)	-0.021 (-)	0.008 (+)
	CPR-D04	-0.015 (-)	-0.066 (-)	-0.022 (---)	-0.053 (---)	-0.036 (---)	0.003 (+)
	CPR-C04	0.015 (+)	-0.152 (-)	0.002 (+)	0.037 (+++)	-0.006 (-)	0.015 (+)
North Sea	CPR-B04	0.006 (+)	0.058 (+)	-0.027 (---)	-0.017 (-)	-0.050 (---)	0.007 (+)
	CPR-D03	-0.039 (-)	0.091 (+)	-0.023 (---)	-0.033 (---)	-0.082 (---)	0.019 (++)
	CPR-C03	-0.016 (-)	0.164 (++)	-0.033 (---)	-0.025 (-)	-0.008 (-)	0.002 (+)
	CPR-D02	-0.050 (-)	-0.005 (-)	0.004 (+)	0.004 (+)	0.010 (+)	0.002 (+)
	CPR-C02	-0.038 (-)	0.140 (+++)	-0.010 (-)	-0.004 (-)	-0.050 (-)	0.011 (+)
	CPR-B02	-0.023 (-)	-0.095 (-)	0.001 (+)	0.008 (+)	-0.007 (-)	0.011 (+)
	CPR-D01	-0.051 (-)	-0.013 (-)	-0.004 (-)	0.001 (+)	-0.030 (-)	0.011 (++)
	CPR-C01	-0.035 (-)	0.051 (+)	0.003 (+)	-0.009 (-)	0.016 (+)	-0.008 (-)
	CPR-B01	-0.037 (-)	-0.120 (---)	-0.004 (-)	0.061 (+++)	-0.054 (---)	0.033 (+++)
	CPR-A01	0.007 (+)	0.085 (+)				
Percent of Positive Slopes		67%	40%	31%	38%	18%	79%
Number of Positive Slopes		27 of 40	16 of 40	11 of 35	13 of 34	6 of 32	27 of 34

Table 11.2

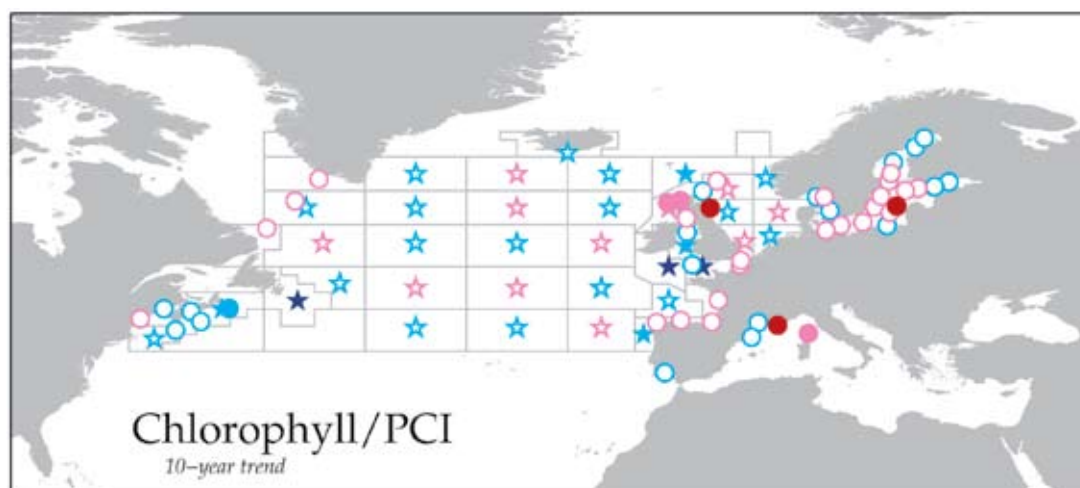
Table of 10-year trends and linear regression slope values listed by CPR standard area and variable name. Cell colors indicate slope (blue/cyan = negative, red/pink = positive). Statistical significance is indicated by color and symbol (dark red (+++) /blue (---) = $p < 0.01$, medium pink (++) /cyan (--) = $p < 0.05$). Lightest pink (+) / cyan cells (-) indicate slope of non-significant trend ($p > 0.05$).

**Figure 11.2**

Spatio-temporal map of 10-year trends in sea surface temperature present within the CPR standard areas (star symbols) and other monitoring sites (circle symbols). Symbol colors indicate slope (blue/cyan = negative, red/pink = positive) and statistical significance (dark red/blue = $p < 0.01$, pink/cyan = $p < 0.05$). Symbols with a white, unfilled, centre indicate slope with a non-significant ($p > 0.05$) trend.

**Figure 11.3**

Spatio-temporal map of 10-year trends in wind speed present within the CPR standard areas (star symbols) and other monitoring sites (circle symbols). Symbol colors indicate slope (blue/cyan = negative, red/pink = positive) and statistical significance (dark red/blue = $p < 0.01$, pink/cyan = $p < 0.05$). Symbols with a white, unfilled, centre indicate slope with a non-significant ($p > 0.05$) trend.

**Figure 11.4**

Spatio-temporal map of 10-year trends in the Phytoplankton Colour Index present within the CPR standard areas (star symbols) and chlorophyll a present within the other monitoring sites (circle symbols). Symbol colors indicate slope (blue/cyan = negative, red/pink = positive) and statistical significance (dark red/blue = $p < 0.01$, pink/cyan = $p < 0.05$). Symbols with a white, unfilled, centre indicate slope with a non-significant ($p > 0.05$) trend.

Figure 11.5

Spatio-temporal map of 10-year trends in total diatom abundance present within the CPR standard areas (star symbols) and other monitoring sites (circle symbols). Symbol colors indicate slope (blue/cyan = negative, red/pink = positive) and statistical significance (dark red/blue = $p < 0.01$, pink/cyan = $p < 0.05$). Symbols with a white, unfilled, centre indicate slope with a non-significant ($p > 0.05$) trend.

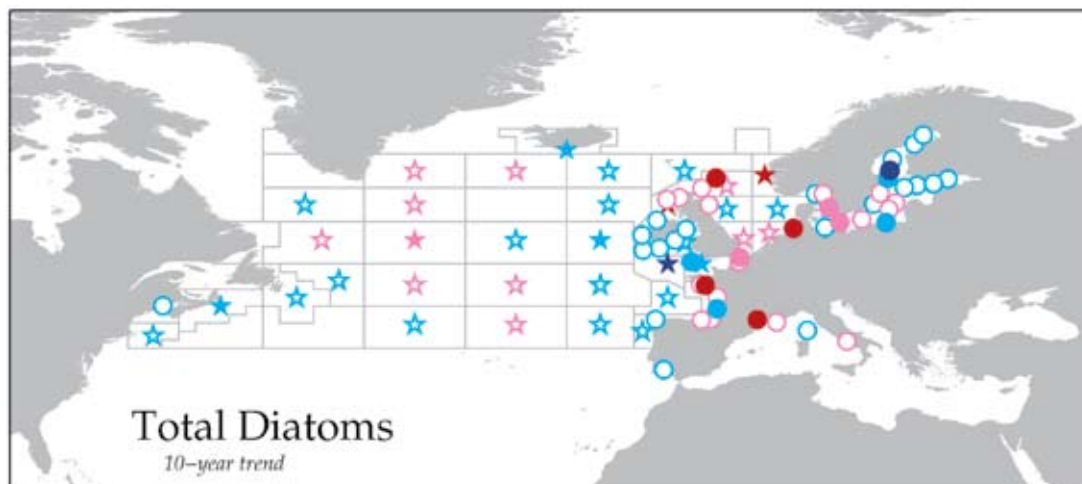


Figure 11.6

Spatio-temporal map of 10-year trends in total dinoflagellate abundance present within the CPR standard areas (star symbols) and other monitoring sites (circle symbols). Symbol colors indicate slope (blue/cyan = negative, red/pink = positive) and statistical significance (dark red/blue = $p < 0.01$, pink/cyan = $p < 0.05$). Symbols with a white, unfilled, centre indicate slope with a non-significant ($p > 0.05$) trend.

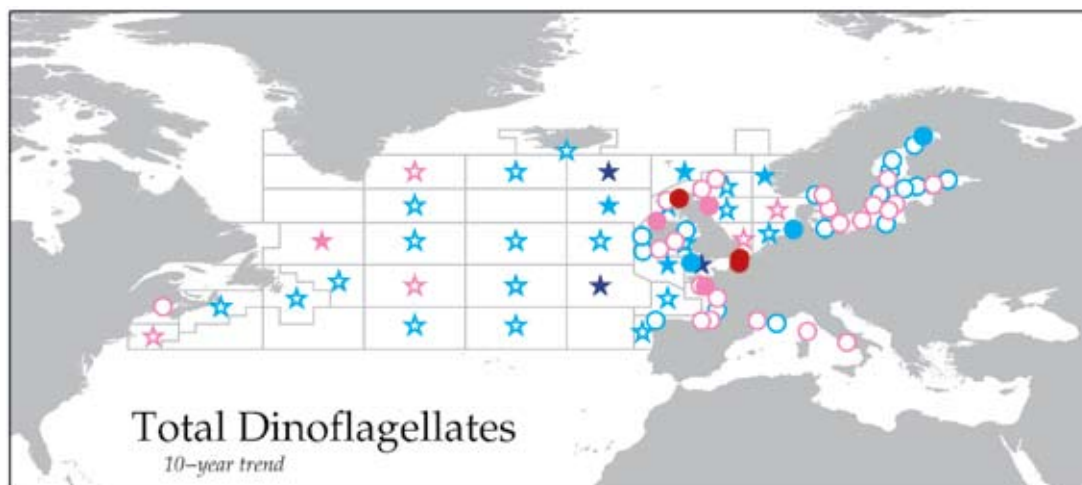
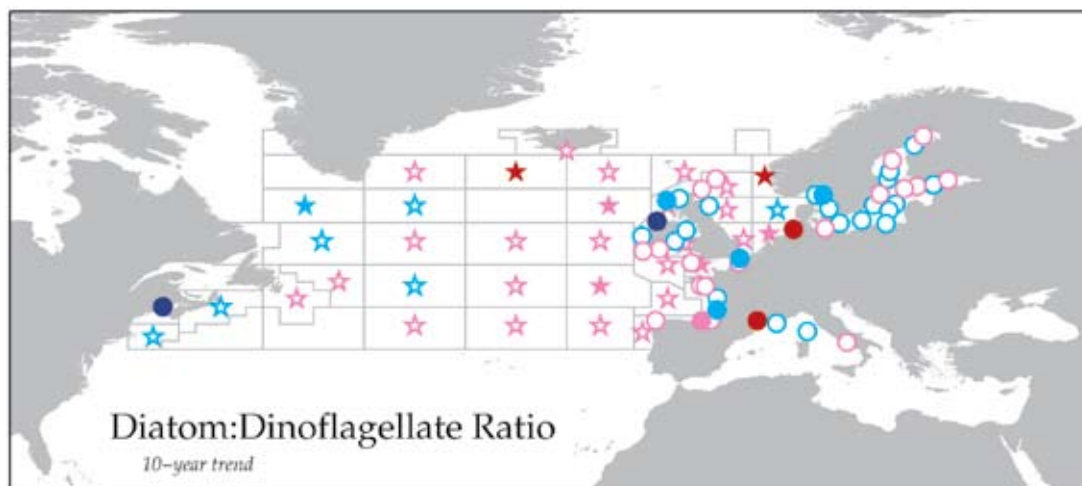


Figure 11.7

Spatio-temporal map of 10-year trends in the diatoms:dinoflagellates ratio present within the CPR standard areas (star symbols) and other monitoring sites (circle symbols). Symbol colors indicate slope (blue/cyan = negative, red/pink = positive) and statistical significance (dark red/blue = $p < 0.01$, pink/cyan = $p < 0.05$). Symbols with a white, unfilled, centre indicate slope with a non-significant ($p > 0.05$) trend.



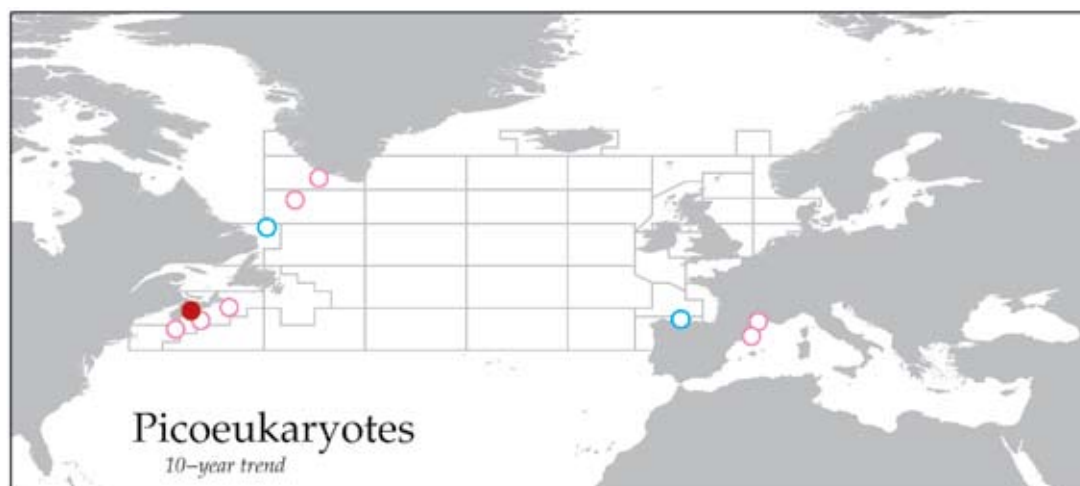


Figure 11.8
Spatio-temporal map of 10-year trends in picoeukaryote abundance present within the phytoplankton monitoring sites. (This variable is not currently available from the CPR programme.) Symbol colors indicate slope (blue/cyan = negative, red/pink = positive) and statistical significance (dark red/blue = $p < 0.01$, pink/cyan = $p < 0.05$). Symbols with a white, unfilled, centre indicate slope with a non-significant ($p > 0.05$) trend.

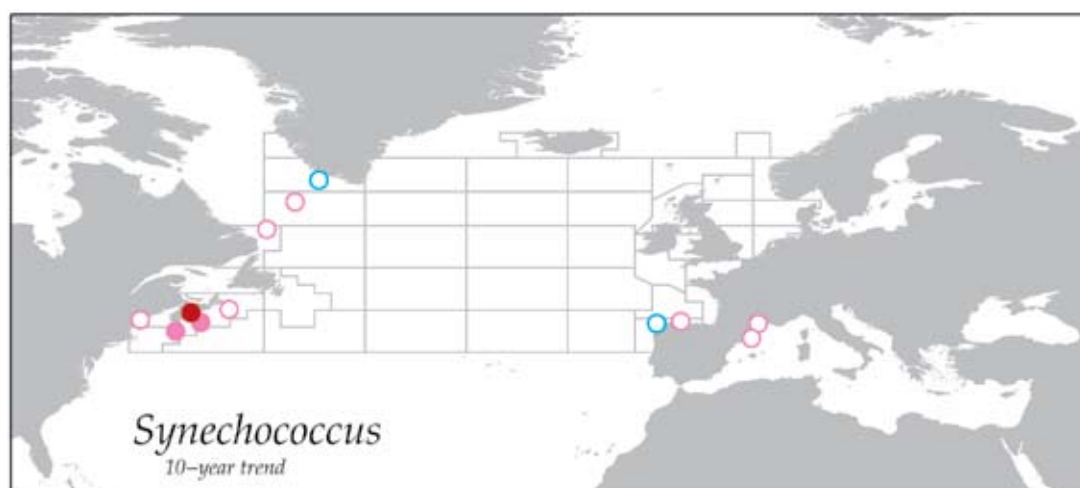


Figure 11.9
Spatio-temporal map of 10-year trends in *Synechococcus* abundance present within the phytoplankton monitoring sites. (This variable is not currently available from the CPR programme.) Symbol colors indicate slope (blue/cyan = negative, red/pink = positive) and statistical significance (dark red/blue = $p < 0.01$, pink/cyan = $p < 0.05$). Symbols with a white, unfilled, centre indicate slope with a non-significant ($p > 0.05$) trend.



Figure 11.10
Spatio-temporal map of 10-year trends in bacteria abundance present within the phytoplankton monitoring sites. (This variable is not currently available from the CPR programme.) Symbol colors indicate slope (blue/cyan = negative, red/pink = positive) and statistical significance (dark red/blue = $p < 0.01$, pink/cyan = $p < 0.05$). Symbols with a white, unfilled, centre indicate slope with a non-significant ($p > 0.05$) trend.

Region	Station #	Site Name	Sea Surface Temperature	Wind Speed	Chlorophyll	Total Diatoms	Total Dinoflagellates	Diatoms to Dinoflagellates ratio	Picoeukaryotes	Synechococcus	Bacteria
Northwest Atlantic Shelf	1	Booth Bay - Maine	0.005 (+)	-0.089 (—)							
	2	Bay of Fundy	-0.004 (-)	-0.063 (—)		0.028 (+++)	0.032 (+++)	-0.003 (-)			
	3	Bedford Basin	0.024 (++)	-0.051 (—)	0.008 (++)						
	4	Western Scotian Shelf	0.016 (++)	-0.032 (—)							
	5	Central Scotian Shelf	0.032 (+++)	0.022 (+++)							
	6	Eastern Scotian Shelf	0.032 (+++)	0.073 (+++)							
Labrador Sea	7	Labrador Shelf and Slope	0.038 (+++)	0.006 (+)							
	8	Labrador Basin	0.054 (+++)	-0.022 (-)							
	9	Greenland Shelf and Slope	0.046 (+++)	-0.025 (-)							
Baltic Sea	10	Bothnian Bay F2	0.039 (++)	-0.028 (-)							
	11	Bothnian Bay BO3	0.041 (+++)	0.033 (++)	0.004 (+)	-0.034 (-)	-0.027 (-)	0.002 (+)			
	12	Bothnian Sea USSb	0.044 (+++)	0.033 (++)	0.005 (+)	-0.026 (-)	-0.026 (-)	0.001 (+)			
	13	Bothnian Sea SR5	0.044 (+++)	0.004 (+)	0.011 (++)	-0.028 (-)	-0.027 (-)	0.002 (+)			
	14	Åland Sea F64	0.045 (+++)	0.045 (+++)	0.013 (+++)	-0.038 (—)	-0.007 (-)	-0.011 (-)			
	15	Gulf of Finland LL3a	0.025 (+++)	0.007 (+)	0.014 (+++)	-0.025 (-)	-0.026 (-)	0.000 (-)			
	16	Gulf of Finland LL7	0.023 (++)	0.016 (+)	0.009 (++)	-0.022 (-)	-0.009 (-)	-0.006 (-)			
	17	Gulf of Finland LL12	0.030 (+++)	0.030 (+++)	0.004 (+)	-0.022 (-)	-0.005 (-)	-0.001 (-)			
	18	Baltic Proper LL17	0.045 (+++)	0.003 (+)	0.005 (+)	-0.008 (-)	-0.008 (-)	0.000 (+)			
	19	Baltic Proper LL23	0.049 (+++)	0.017 (+)	0.008 (++)	-0.003 (-)	-0.005 (-)	-0.002 (-)			
	20	Baltic Proper BY38	0.051 (+++)	0.023 (+++)							
	21	Baltic Proper BY15	0.051 (+++)	0.016 (++)	0.006 (+)	-0.015 (-)	-0.005 (-)	-0.004 (-)			
	22	Gdansk Basin	0.052 (+++)	-0.007 (-)	0.002 (+)						
	23	Eastern Gotland Basin	0.052 (+++)	0.021 (++)	0.013 (+++)	0.004 (+)	0.036 (+++)	-0.007 (-)			
	24	Bornholm Basin	0.051 (+++)	0.005 (+)	0.009 (++)	0.017 (+)	0.046 (+++)	-0.006 (-)			
	25	Arkona Basin	0.056 (+++)	-0.031 (—)	0.005 (++)	0.016 (+)	0.016 (+)	0.031 (++)			
	26	Mecklenburg Bight	0.084 (+++)	-0.046 (—)	0.002 (+)	0.004 (+)	0.030 (++)	-0.002 (-)			
	27	SMHI Anholt East	0.055 (+++)	0.052 (+++)							
	28	SMHI Släggö	0.053 (+++)	0.061 (+++)							
	29	SMHI Å17	0.049 (+++)	0.025 (+)							
North Sea and English Channel	30	Helgoland Roads	0.052 (+++)	-0.020 (-)		0.046 (+++)	0.071 (+++)	-0.008 (—)			
	31	Scalloway - Shetland Isles	0.032 (+++)	-0.028 (-)							
	32	Scapa Bay - Orkney	0.029 (+++)	-0.014 (-)							
	33	Stonehaven	0.039 (+++)	-0.008 (-)							
	34	REPHY Point 1 SRN Boulogne	0.047 (+++)	-0.011 (-)							
	35	REPHY At So	0.041 (+++)	0.002 (+)		0.002 (+)	0.095 (+++)	-0.003 (—)			
	36	Plymouth L4	0.025 (+++)	0.025 (++)							
Northeast Atlantic Shelf	37	Loch Ewe	0.022 (+++)	0.024 (+)							
	38	Loch Maddy	0.019 (+++)	0.001 (+)							
	39	Millport	0.024 (+++)	0.021 (+)							
	40	Cypris Station - Isle of Man	0.034 (+++)	0.003 (+)	0.003 (+)						
	41	East Coast Ireland	0.029 (+++)	-0.025 (-)							
	42	South Coast Ireland	0.023 (+++)	-0.014 (-)							
	43	Southwest Coast Ireland	0.023 (+++)	-0.045 (—)		0.036 (++)	-0.005 (-)	0.010 (+++)			
	44	West Coast Ireland	0.026 (+++)	-0.055 (—)		0.036 (++)	0.010 (+)	0.007 (+)			
	45	Northwest Coast Ireland	0.023 (+++)	-0.027 (-)		0.051 (++)	0.028 (+)	0.002 (+)			
	46	REPHY Men er Roue	0.029 (+++)	-0.039 (—)		-0.008 (-)	-0.012 (-)	0.001 (+)			
Bay of Biscay and western Iberian Shelf	47	REPHY Ouest Loscolo	0.029 (++)	-0.046 (—)		0.053 (++)	0.004 (+)	0.002 (+)			
	48	REPHY Le Cornard	0.029 (+++)	0.008 (+)		0.023 (+++)	0.022 (++)	0.001 (+)			
	49	REPHY Teychan Bis	0.030 (+++)	0.024 (+)							
	50	AZTI Station D2	0.031 (+++)	0.009 (+)	-0.002 (-)						
	51	Nervión River Estuary	0.033 (+++)	0.011 (+)							
	52	RADIALES Gijón/Xixón Station 2	0.035 (+++)	0.015 (+)							
	53	RADIALES A Coruña Station 2	0.027 (+++)	0.032 (+++)							
	54	Guadiana Estuary	0.027 (+++)	0.009 (+)							
	55	Blanes Bay	0.016 (++)	0.022 (+++)							
	56	Thau Lagoon	0.022 (+++)	-0.022 (-)	-0.003 (-)	-0.022 (-)	0.006 (+)	-0.001 (-)			
Mediterranean Sea	57	REPHY Lazaret A	0.025 (+++)	0.008 (+)		0.013 (+++)	-0.027 (—)	0.013 (+++)			
	58	REPHY Diana Centre	0.033 (+++)	0.017 (+)							
	59	Gulf of Naples LTER-MC	0.023 (+++)	0.035 (++)		0.016 (++)					
	60	Kastela Bay	0.011 (+)	0.132 (+++)							
	61	Stončica	0.014 (++)	0.114 (+++)							
Percent of Positive Slopes			98%	62%	89%	53%	48%	48%			
Number of Positive Slopes			60 of 61	38 of 61	17 of 19	14 of 26	12 of 25	12 of 25			

Table 11.3

Table of 30-year trends and linear regression slope values listed by monitoring site and variable name. Cell colors indicate slope (blue/cyan = negative, red/pink = positive). Statistical significance is indicated by color and symbol (dark red (+++) /blue (---) = $p < 0.01$, medium pink (++) /cyan (--) = $p < 0.05$). Lightest pink (+) /cyan (-) indicate slope of non-significant trend ($p > 0.05$).

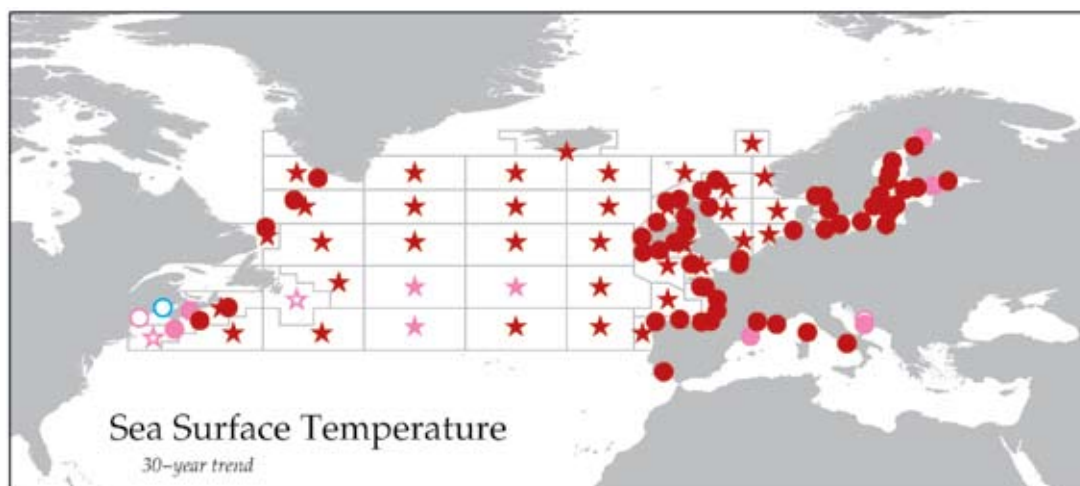
Region	Site Name	Sea Surface Temperature	Wind Speed	Phytoplankton Colour Index	Total Diatoms	Total Dinoflagellates	Diatoms to Dinoflagellates ratio
Western North Atlantic	CPR-F10	0.017 (+)	0.011 (+)				
	CPR-E10	0.028 (+++)	0.027 (++)				
	CPR-F09	0.048 (+++)	0.028 (+++)				
	CPR-E09	0.019 (+)	0.030 (++)				
	CPR-D09	0.023 (+++)	0.019 (+)				
	CPR-F08	0.046 (+++)	0.036 (+++)				
	CPR-E08	0.081 (+++)	0.062 (+++)	0.000 (-)	-0.006 (-)	0.007 (+)	-0.004 (-)
	CPR-D08	0.059 (+++)	0.004 (+)	0.009 (++)	0.016 (+++)	0.033 (+++)	-0.009 (---)
	CPR-C08	0.049 (+++)	-0.048 (-)				
	CPR-B08	0.054 (+++)	0.042 (+)				
Central North Atlantic	CPR-F07	0.021 (++)	0.013 (+)				
	CPR-E07	0.022 (++)	0.020 (+)				
	CPR-D07	0.046 (+++)	-0.026 (-)	0.008 (+)	0.008 (+)	0.004 (+)	-0.003 (-)
	CPR-C07	0.055 (+++)	-0.002 (-)	0.003 (+)	0.011 (+)	0.021 (++)	-0.004 (---)
	CPR-B07	0.058 (+++)	0.002 (+)	0.014 (+++)	0.016 (++)	0.018 (+)	0.000 (+)
	CPR-F06	0.023 (+++)	0.036 (+++)				
	CPR-E06	0.020 (++)	0.022 (++)				
	CPR-D06	0.031 (+++)	-0.009 (-)	0.000 (-)	-0.013 (-)	-0.022 (---)	0.007 (++)
	CPR-C06	0.039 (+++)	-0.030 (-)				
	CPR-B06	0.042 (+++)	-0.004 (-)	0.025 (+++)	0.017 (++)	0.006 (+)	0.003 (+)
	CPR-A06	0.045 (+++)	0.054 (+++)	0.006 (+)	0.006 (+)	-0.001 (-)	0.005 (+)
	CPR-F05	0.022 (+++)	0.041 (+++)				
Eastern North Atlantic	CPR-E05	0.022 (+++)	0.028 (+++)	0.001 (+)	-0.006 (-)	-0.014 (-)	0.002 (+)
	CPR-D05	0.026 (+++)	-0.005 (-)	0.008 (+)	-0.007 (-)	-0.018 (---)	0.002 (+)
	CPR-C05	0.033 (+++)	-0.025 (-)	-0.003 (-)	-0.012 (---)	-0.008 (-)	-0.003 (-)
	CPR-B05	0.035 (+++)	0.036 (++)	0.015 (+++)	0.010 (+)	0.006 (+)	0.000 (+)
	CPR-F04	0.019 (+++)	0.031 (+++)	0.004 (+)	-0.011 (---)	-0.012 (---)	-0.003 (-)
	CPR-E04	0.030 (+++)	0.032 (+++)	0.009 (+++)	-0.001 (-)	-0.018 (---)	0.006 (+++)
	CPR-D04	0.022 (+++)	-0.002 (-)	0.013 (+++)	0.002 (+)	-0.014 (---)	0.002 (+)
	CPR-C04	0.018 (+++)	-0.010 (-)	0.005 (++)	-0.003 (-)	-0.009 (---)	0.006 (+++)
	CPR-B04	0.033 (+++)	0.023 (++)	0.010 (++)	0.003 (+)	-0.009 (-)	0.005 (++)
	CPR-D03	0.026 (+++)	0.032 (+++)	0.007 (++)	-0.007 (-)	-0.012 (-)	0.002 (+)
	CPR-C03	0.030 (+++)	-0.004 (-)	0.009 (+++)	-0.003 (-)	-0.010 (---)	0.005 (+++)
North Sea	CPR-D02	0.056 (+++)	-0.020 (-)	0.007 (+++)	0.010 (++)	-0.016 (---)	0.005 (++)
	CPR-C02	0.045 (+++)	-0.016 (-)	0.002 (+)	-0.002 (-)	-0.037 (---)	0.013 (+++)
	CPR-B02	0.038 (+++)	-0.010 (-)	0.008 (+++)	0.009 (+++)	-0.017 (---)	0.009 (+++)
	CPR-D01	0.057 (+++)	0.013 (+)	0.011 (+++)	0.017 (+++)	-0.016 (---)	0.008 (+++)
	CPR-C01	0.050 (+++)	0.026 (+++)	0.007 (++)	0.010 (+++)	-0.014 (---)	0.007 (+++)
	CPR-B01	0.028 (+++)	-0.018 (-)	0.015 (+++)	0.013 (+++)	-0.001 (-)	0.006 (++)
	CPR-A01	0.041 (+++)	-0.001 (-)				
Percent of Positive Slopes		100%	60%	88%	56%	28%	76%
Number of Positive Slopes		40 of 40	24 of 40	22 of 25	14 of 24	7 of 25	19 of 25

Table 11.4

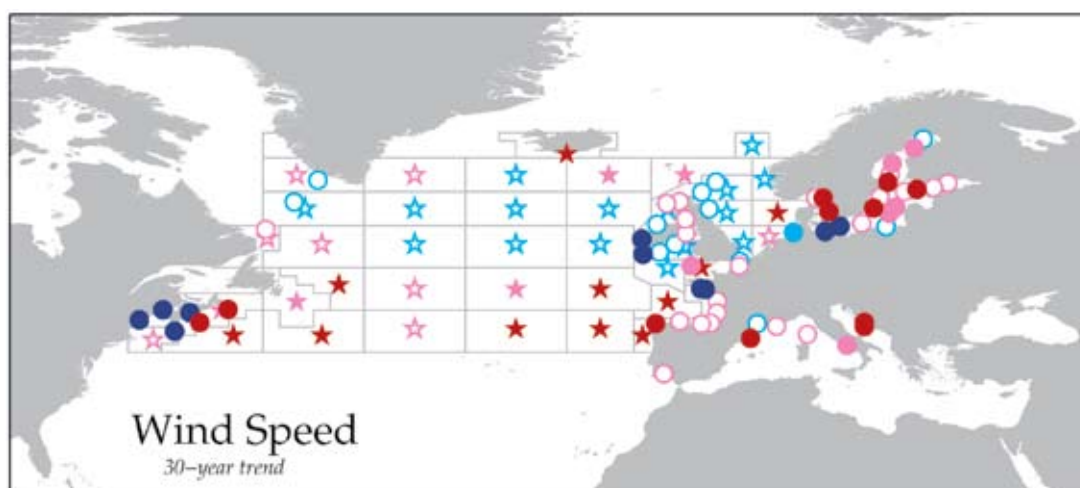
Table of 30-year trends and linear regression slope values listed by CPR standard area and variable name. Cell colors indicate slope (blue/cyan = negative, red/pink = positive). Statistical significance is indicated by color and symbol (dark red (+++) /blue (---) = $p < 0.01$, medium pink (++) /cyan (--) = $p < 0.05$). Lightest pink (+) /cyan cells (-) indicate slope of non-significant trend ($p > 0.05$).

Figure 11.11

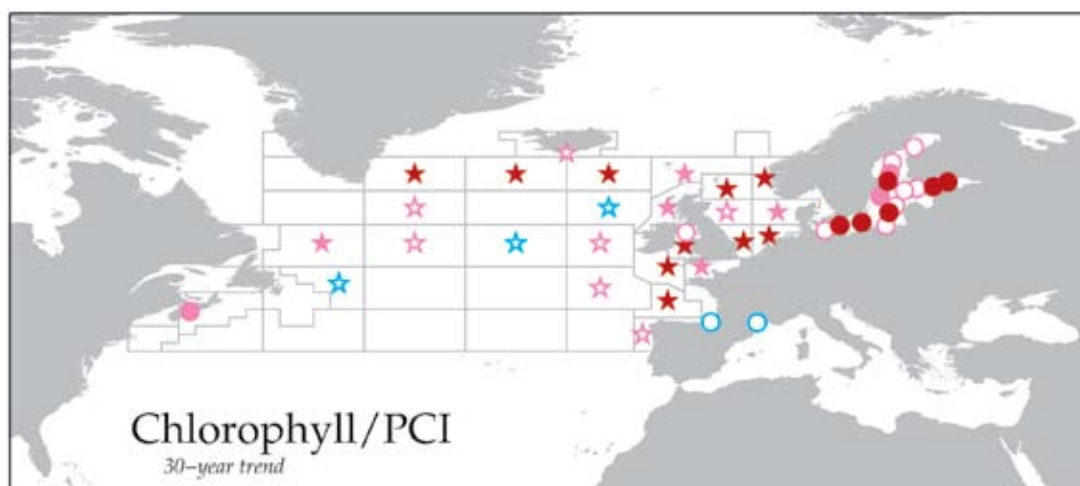
Spatio-temporal map of 30-year trends in sea surface temperature present within the CPR standard areas (star symbols) and other monitoring sites (circle symbols). Symbol colors indicate slope (blue/cyan = negative, red/pink = positive) and statistical significance (dark red/blue = $p < 0.01$, pink/cyan = $p < 0.05$). Symbols with a white, unfilled, centre indicate slope with a non-significant ($p > 0.05$) trend.

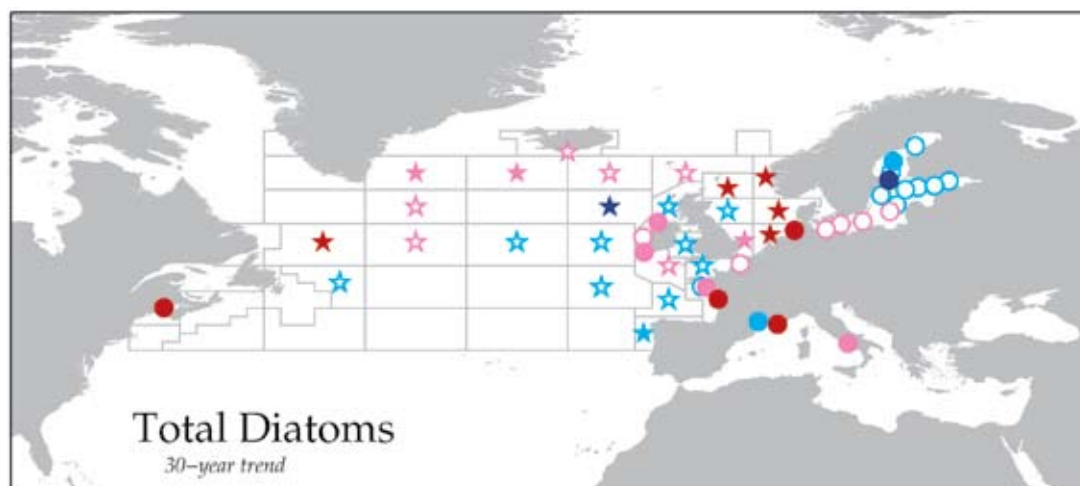
**Figure 11.12**

Spatio-temporal map of 30-year trends in wind speed present within the CPR standard areas (star symbols) and other monitoring sites (circle symbols). Symbol colors indicate slope (blue/cyan = negative, red/pink = positive) and statistical significance (dark red/blue = $p < 0.01$, pink/cyan = $p < 0.05$). Symbols with a white, unfilled, centre indicate slope with a non-significant ($p > 0.05$) trend.

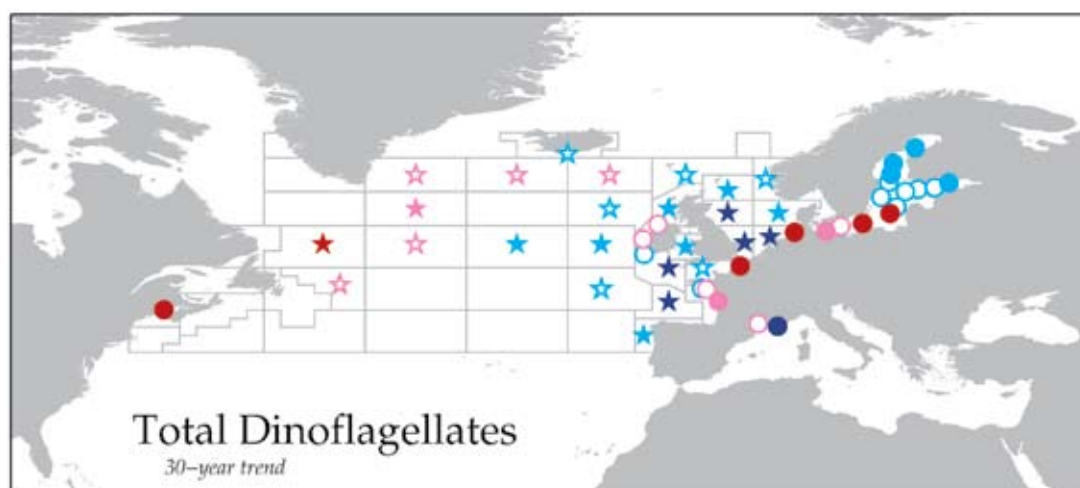
**Figure 11.13**

Spatio-temporal map of 30-year trends in the Phytoplankton Colour Index present within the CPR standard areas (star symbols) and chlorophyll a present within the other monitoring sites (circle symbols). Symbol colors indicate slope (blue/cyan = negative, red/pink = positive) and statistical significance (dark red/blue = $p < 0.01$, pink/cyan = $p < 0.05$). Symbols with a white, unfilled, centre indicate slope with a non-significant ($p > 0.05$) trend.

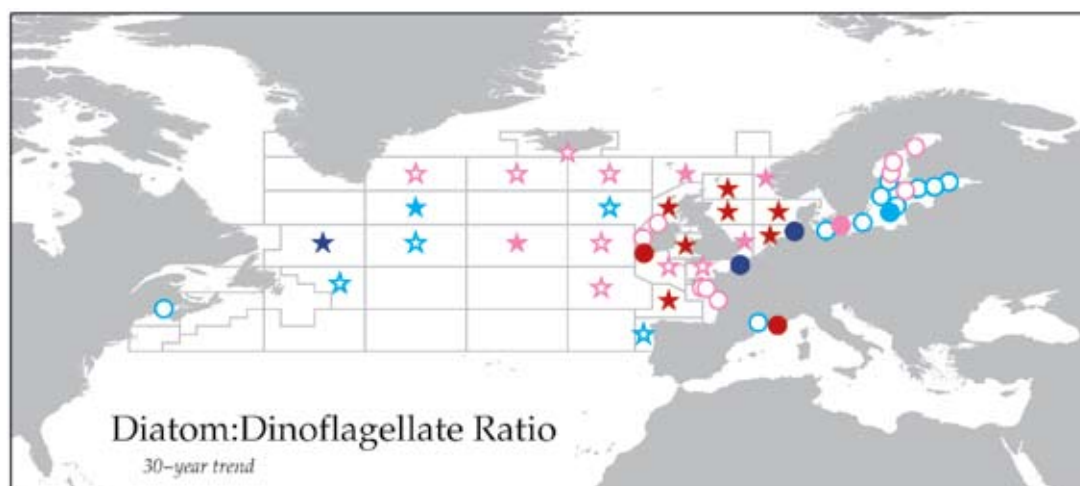



Figure 11.14

Spatio-temporal map of 30-year trends in total diatom abundance present within the CPR standard areas (star symbols) and other monitoring sites (circle symbols). Symbol colors indicate slope (blue/cyan = negative, red/pink = positive) and statistical significance (dark red/blue = $p < 0.01$, pink/cyan = $p < 0.05$). Symbols with a white, unfilled, centre indicate slope with a non-significant ($p > 0.05$) trend.


Figure 11.15

Spatio-temporal map of 30-year trends in total dinoflagellate abundance present within the CPR standard areas (star symbols) and other monitoring sites (circle symbols). Symbol colors indicate slope (blue/cyan = negative, red/pink = positive) and statistical significance (dark red/blue = $p < 0.01$, pink/cyan = $p < 0.05$). Symbols with a white, unfilled, centre indicate slope with a non-significant ($p > 0.05$) trend.


Figure 11.16

Spatio-temporal map of 30-year trends in the diatoms:dinoflagellates ratio present within the CPR standard areas (star symbols) and other monitoring sites (circle symbols). Symbol colors indicate slope (blue/cyan = negative, red/pink = positive) and statistical significance (dark red/blue = $p < 0.01$, pink/cyan = $p < 0.05$). Symbols with a white, unfilled, centre indicate slope with a non-significant ($p > 0.05$) trend.

12. REFERENCES

- Agawin, N. S. R., Duarte, C. M., and Agustí, S. 1998. Growth and abundance of *Synechococcus* sp. in a Mediterranean Bay: Seasonality and relationship with temperature. *Marine Ecology Progress Series*, 170: 45–53.
- Alheit, J. Möllmann, C., Dutz, J., Kornilovs, G., Loewe, P., Mohrholz, V., and Wasmund, N. 2005. Synchronous ecological regime shifts in the central Baltic and the North Sea in the late 1980s. *ICES Journal of Marine Science*, 62: 1205–1215.
- Alonso-Sáez, L., Balagué, V., Sà, E. L., Sánchez, O., González, J. M., Pinhassi, J., Massana, R., *et al.* 2007. Seasonality in bacterial diversity in north-west Mediterranean coastal waters: assessment through clone libraries, fingerprinting and FISH. *FEMS Microbiology Ecology*, 60: 98–112.
- Alonso-Sáez, L., Vázquez-Domínguez, E., Cardelús, C., Pinhassi, J., Sala, M. M., Lekunberri, I., Balagué, V., *et al.* 2008. Factors controlling the year-round variability in carbon flux through bacteria in a coastal marine system. *Ecosystems*, 11: 397–409.
- Alvarez, I., Gomez-Gesteira, M., deCastro, M., and Dias, J. M. 2008. Spatiotemporal evolution of upwelling regime along the western coast of the Iberian Peninsula. *Journal of Geophysical Research–Oceans*, 113: C07020, doi:10.1029/2008JC004744.
- Álvarez-Salgado, X. A., Figueiras, F. G., Pérez, F. F., Groom, S., Nogueira, E., Borges, A. V., Chou, L., *et al.* 2003. The Portugal coastal counter current off NW Spain: new insights on its biogeochemical variability. *Progress in Oceanography*, 56: 281–321.
- Ameryk, A., Podgórska, B., and Witek, Z., 2005. The dependence between bacterial production and environmental conditions in the Gulf of Gdańsk. *Oceanologia*, 47 (1): 27–45.
- Aminot, A., and Rey, F. 2002. Standard procedure for the determination of chlorophyll *a* by spectroscopic methods. *ICES Techniques in Marine Environmental Sciences* No. 28.
- Andersson, A., Hajdu, S., Haecky, P., Kuparinen, J., and Wikner, J. 1996. Succession and growth of phytoplankton in the Gulf of Bothnia (Baltic Sea). *Marine Biology*, 126: 791–801.
- Arístegui, J., Álvarez-Salgado, X. A., Barton, E. D., Figueiras, F. G., Hernández-León, S., Roy, C., and Santos, A. M. P. 2006. Chapter 23. Oceanography and fisheries of the Canary Current/Iberian region of the Eastern North Atlantic (18a, E). *In* The Global Coastal Ocean: Interdisciplinary Regional Studies and Syntheses. The Sea: Ideas and Observations on Progress in the Study of the Seas, pp. 877–931. Ed. by A. R. Robinson and K. Brink. Harvard University Press, Boston.
- Arístegui, J., Barton, E. D., Álvarez-Salgado, X. A., Santos, A. M. P., Figueiras, F. G., Kifani, S., Hernández-León, S., *et al.* 2009. Sub-regional ecosystem variability in the Canary Current upwelling. *Progress in Oceanography*, 83: 33–48.
- Barbosa, A. B., Domingues, R. B., and Galvão, H. M. 2010. Environmental forcing of phytoplankton in a Mediterranean estuary (Guadiana Estuary, southwestern Iberia): a decadal of anthropogenic and climatic influences. *Estuaries and Coasts*, 33: 324–341.
- Batchelder, H. P., Mackas, D. L., and O'Brien, T. D. 2012. Spatial-temporal scales of synchrony in marine zooplankton biomass and abundance patterns: A world-wide comparison. *Progress in Oceanography*, 97–100: 15–30.
- Batten, S., Walne, A. W., Edwards, M., and Groom, S. B. 2003. Phytoplankton biomass from continuous plankton recorder data: an assessment of the phytoplankton colour index. *Journal of Plankton Research*, 25: 697–702.
- Beaugrand, G., Reid, P. C., Ibanez, F., Lindley, J. A., and Edwards, M. 2002. Reorganization of North Atlantic marine copepod biodiversity and climate. *Science*, 296: 1692–1694.

- Beaugrand, G., Edwards, M., Brander, K., Luczaki, C., and Ibenez, F. 2008. Causes and projections of abrupt climate-driven ecosystem shifts in the North Atlantic. *Ecology Letters*, 11: 1157–1168.
- Beaugrand, G., Edwards, M., and Legendre, L. 2010. Marine biodiversity, ecosystem functioning, and carbon cycles. *Proceedings of the National Academy of Sciences of the United States of America*, 107: 10120–10124.
- Bec, B., Collos, Y., Souchu, P., Vaquer, A., Lautier, J., Fiandrino, A., Benau, L., *et al.* 2011. Distribution of picophytoplankton and nanophytoplankton along an anthropogenic eutrophication gradient in French Mediterranean coastal lagoons. *Aquatic Microbial Ecology*, 63: 29–45.
- Becker, G. A., and Pauly, D. 1996. Sea surface temperature changes in the North Sea in relation to decadal North Sea variability. *ICES Journal of Marine Science*, 53: 887–898.
- Behrenfeld, M. J., O'Malle, R. T., Siegel, D. A., McClain, C. R., Sarmiento, J. L., Feldman, G. C., Milligan, A. J., *et al.* 2006. Climate-driven trends in contemporary ocean productivity. *Nature*, 444: 752–755.
- Belin, C. 1998. French phytoplankton monitoring: an exploration of optimum data presentation. *ICES Journal of Marine Science*, 55: 705–710.
- Bergström, S., and Carlsson, B. 1994. River run-off to the Baltic Sea – 1950–1990. *Ambio*, 23: 280–287.
- Boalch, G. T., and Harbour, D. S. 1977. Unusual diatom off the coast of south-west England and its effect on fishing. *Nature*, 269: 687–688.
- Bode, A., and Varela, M. 1998. Primary production and phytoplankton in three Galician Rias Altas (NW Spain): seasonal and spatial variability. *Scientia Marina*, 62: 319–330.
- Bode, A., Casas, B., Fernández, E., Marañón, E., Serret, P., and Varela, M. 1996. Phytoplankton biomass and production in shelf waters off NW Spain: spatial and seasonal variability in relation to upwelling. *Hydrobiologia*, 341: 225–234.
- Bode, A., Hare, J., Li, W. K. W., Morán, X. A. G., and Valdés, L. 2011a. Chlorophyll and primary production in the North Atlantic. *In* ICES status report on climate change in the North Atlantic, pp. 77–102. Ed. by P. C. Reid and L. Valdés. ICES Cooperative Research Report No. 310.
- Bode, A., Anadón, R., Morán, X. A. G., Nogueira, E., Teira, E., and Varela, M. 2011b. Decadal variability in chlorophyll and primary production off NW Spain. *Climate Research*, 48: 293–305.
- Boersma, M., Malzahn, A., Greve, W., and Javidpour, J. 2007. The first occurrence of the ctenophore *Mnemiopsis leidyi* in the North Sea. *Helgoland Marine Research*, 61: 153–155.
- Boras, J. A., Sala, M. M., Vázquez-Dominguez, E., Weinbauer, M. G., and Vaqué, D. 2009. Annual changes of bacterial mortality due to viruses and protists in an oligotrophic coastal environment (NW Mediterranean). *Environmental Microbiology*, 11: 1181–1193.
- Borja, A., Fontán, A., Sáenz, J., and Valencia, V. 2008. Climate, oceanography, and recruitment: the case of the Bay of Biscay anchovy. *Fisheries Oceanography*, 17: 477–493.
- Bralewska, J. M. 1992. Cycling seasonal fluctuations of the phytoplankton biovolume and composition in the Gdansk Basin in 1987–1988. *ICES Document CM 1992/L: 15*. 40 pp.
- Bresnan, E., Fryer, R., Hart, M., and Percy, P. 2005. Correlation between algal presence in water and toxin presence in shellfish. FRS Contract Report 04/05 (http://www.frs-scotland.gov.uk/Delivery/Information_resources/information_resources_view_document.aspx?resourceId=31137anddocumentId=2829).
- Bresnan, E., Hay, S., Hughes, S. L., Fraser, S., Rasmussen, J., Webster, L., and Slesser, G. 2009. Seasonal and interannual variation in the phytoplankton community in the north east of Scotland. *Journal of Sea Research*, 61: 17–25.
- Callies, U., Pluess, A., Kappenberg, J., and Kapitza, H. 2011. Particle tracking in the vicinity of Helgoland, North Sea. *Ocean Dynamics*, 61: 2121–2139.
- Calvo-Díaz, A., and Morán, X. A. G. 2006. Seasonal dynamics of picoplankton in shelf waters of the southern Bay of Biscay. *Aquatic Microbial Ecology*, 42: 159–174.
- Calvo-Díaz, A., Morán, X. A. G., Nogueira, E., Bode, A., and Varela, M. 2004. Picoplankton community structure along the northern Iberian continental margin in late winter–early spring. *Journal of Plankton Research*, 26: 1069–1081.

- Calvo-Díaz, A., Morán, X. A. G., and Suárez, L. A. 2008. Seasonality of picophytoplankton chlorophyll *a* and biomass in the central Cantabrian Sea, southern Bay of Biscay. *Journal of Marine Systems*, 72: 271–281.
- Casas, B., Varela, M., Canle, M., González, N., and Bode, A. 1997. Seasonal variations of nutrients, seston and phytoplankton, and upwelling intensity off La Coruña (NW Spain). *Estuarine, Coastal and Shelf Science*, 44: 767–778.
- Casas, B., Varela, M., and Bode, A. 1999. Seasonal succession of phytoplankton species on the coast of A Coruña (Galicia, northwest Spain). *Boletín del Instituto Español de Oceanografía*, 15(1–4): 413–429.
- Cebrián, J., Duarte, C. M., and Pascual, J. 1996. Marine climate in the NW Mediterranean littoral. *In* Seasonality in the Blanes Bay: a paradigm of the northwest Mediterranean littoral. Ed. by C. M. Duarte. *Publicaciones especiales del Instituto Español de Oceanografía*, 22: 9–21.
- Cerino, F., and Zingone, A., 2006. A survey of cryptomonad diversity and seasonality at a coastal Mediterranean site. *European Journal of Phycology*, 41: 363–378.
- CIESM. 2003. Mediterranean biological time-series. The Mediterranean Science Commission, Monaco. CIESM Workshop Monographs No 22. 141 pp.
- CIESM. 2010. Phytoplankton response to Mediterranean environmental changes. The Mediterranean Science Commission, Monaco. CIESM Workshop Monographs No 40. 120 pp.
- Cloern, J. E., and Jassby, A. D. 2010. Patterns and scales of phytoplankton variability in estuarine–coastal ecosystems: *Estuaries and Coasts*, 33: 230–241.
- Collos, Y., Bec, B., Jauzein, C., Abadie, E., Laugier, T., Lautier, J., Pastoureaud, A., *et al.* 2009. Oligotrophication and emergence of picocyanobacteria and a toxic dinoflagellate in Thau lagoon, southern France. *Journal of Sea Research*, 61: 68–75.
- Cooper, L. H. N. 1967. The physical oceanography of the Celtic Sea. *Oceanography and Marine Biology: An Annual Review*, 5: 99–110.
- Costa, O. G. 1838. *Fauna del Regno di Napoli. Infusori*. Azzolini, Napoli. 24 pp.
- Courties, C., Vaquer, A., Trousselier, M., Lautier, J., Chrétiennot-Dinet, M.-J., Neveux, J., Machado, C., *et al.* 1994. Smallest eukaryotic organism. *Nature*, 370: 255.
- Cusack, C., Chamberlain, T., Devilly, L., Clarke, D., and Silke, J. 2001. Summary of phytoplankton monitoring trends in 2001. *Proceedings of the 2nd Irish Marine Biotoxin Science Workshop*. Marine Institute, Galway, pp. 19–23.
- Cusack, C., Chamberlain, T., Devilly, L., Clarke, D., and Silke, J. 2002. Review of phytoplankton and environmental monitoring 2002. *Proceedings of the 3rd Irish Marine Biotoxin Science Workshop*. Marine Institute, Galway.
- Davidson, K., Miller, P., Wilding, T. A., Shutler, J., Bresnan, E., Kennington, K., and Swan, S. 2009. A large and prolonged bloom of *Karenia mikimotoi* in Scottish waters in 2006. *Harmful Algae*, 8: 349–361.
- deCastro, M., Gómez-Gesteira, M., Álvarez, I., Lorenzo, M., Cabanas, J. M., Prego, R., and Crespo, A. J. C. 2008. Characterization of fall–winter upwelling recurrence along the Galician western coast (NW Spain) from 2000 to 2005: Dependence on atmospheric forcing. *Journal of Marine Systems*, 72: 145–178.
- deCastro, M., Gómez-Gesteira, M., Álvarez, I., and Gesteira, J. 2009. Present warming within the context of cooling–warming cycles observed since 1854 in the Bay of Biscay. *Continental Shelf Research*, 29: 1053–1059.
- Díaz, E., Valencia, V., and Villate, F. 2007. Size fractionated seston abundance and biochemical composition, over the anchovy spawning period in the Basque shelf (Bay of Biscay), during years 2000 and 2001. *Journal of Experimental Marine Biology and Ecology*, 341: 45–59.
- Dolan, J. R., Lemée, R., Gasparini, S., Mousseau, L., and Heyndrickx, C., 2006. Probing diversity in the plankton: using patterns in tintinnids (planktonic marine ciliates) to identify mechanisms. *Hydrobiologia*, 555: 143–157.
- Domingues, R. B., Barbosa, A. B., and Galvão, H. 2005. Nutrients, light and phytoplankton succession in a temperate estuary (the Guadiana, south-western Iberia). *Estuarine Coastal and Shelf Science*, 64: 249–260.

- Domingues, R. B., Anselmo, T. P., Barbosa, A. B., Sommer, U., and Galvão, H. M. 2011a. Light limitation and phytoplankton primary production in the turbid Guadiana estuary. *Estuarine, Coastal and Shelf Science*, 91(4): 526–535.
- Domingues, R. B., Anselmo, T. P., Barbosa, A. B., Sommer, U., and Galvão, H. M. 2011b. Nutrient limitation of phytoplankton in the freshwater tidal zone of a turbid, Mediterranean estuary. *Estuarine, Coastal and Shelf Science*, 91(2): 282–297.
- Domingues, R. B., Barbosa, A. B., Sommer, U., and Galvão, H. M. 2011c. Ammonium, nitrate and phytoplankton interactions in a freshwater tidal estuarine zone: potential effects of cultural eutrophication. *Aquatic Sciences*, 73: 331–343.
- Domingues, R. B., Barbosa, A. B., Sommer, U., and Galvão, H. M. 2012. Environmental drivers of phytoplankton in the Guadiana estuary (SW Iberia): unraveling changes induced after dam construction. *Science of the Total Environment*, 416: 300–313.
- Duarte, C. M., Agustí, S., Kennedy, H., and Vaqué, D. 1999. The Mediterranean climate as a template for the Mediterranean marine ecosystem: the example of the NE Spanish littoral. *Progress in Oceanography*, 44: 245–270.
- Duarte, C. M., Agustí, S., and Vaqué, D. 2004. Controls on planktonic metabolism in the Bay of Blanes, northwestern Mediterranean littoral. *Limnology and Oceanography*, 49: 2162–2170.
- Ducklow, H. W., Doney, S. C., and Steinberg, D. K. 2009. Contributions of long-term research and time-series observations to marine ecology and biogeochemistry. *Annual Review of Marine Science*, 1: 279–302.
- Dyrssen, D. 1993. The Baltic–Kattegat–Skagerrak Estuarine System. *Estuaries*, 16: 448–452.
- Edler, L. (Ed). 1979. Recommendations on methods for marine biological studies in the Baltic Sea. Phytoplankton and chlorophyll. Baltic Marine Biologists Publication, 5: 1–38.
- Edwards, A., Jones, K., Graham, J. M., Griffiths, C. R., MacDougall, N., Patching, J., Richard, J. M., *et al.* 1996. Transient coastal upwelling and water circulation in Bantry Bay, a ria on the southwest coast of Ireland. *Estuarine, Coastal and Shelf Science*, 42: 213–230.
- Edwards, M., and Richardson, A. J. 2004. Impact of climate change on marine pelagic phenology and trophic mismatch. *Nature*, 430: 881–884.
- Edwards, M., Reid, P., and Planque, B. 2001. Long-term and regional variability of phytoplankton biomass in the Northeast Atlantic (1960–1995). *ICES Journal of Marine Science*, 58: 39–49.
- Edwards, M., Beaugrand, G., Reid, P. C., Rowden, A. A., and Jones, M. B. 2002. Ocean climate anomalies and the ecology of the North Sea. *Marine Ecology Progress Series*, 239: 1–10.
- Edwards, M., Johns, D. G., Leterme, S. C., Svendsen, E., and Richardson, A. J. 2006. Regional climate change and harmful algal blooms in the northeast Atlantic. *Limnology and Oceanography*, 51: 820–829.
- Edwards, M., Beaugrand, G., Hays, G. C., Koslow, J. A., and Richardson, A. J. 2010. Multi-decadal oceanic ecological datasets and their application in marine policy and management. *Trends in Ecology and Evolution*, 25: 602–610.
- Elliott, S. A. J. 1991. Monthly distributions of surface to bottom temperatures in the northwest European shelf sea. *Continental Shelf Research*, 11: 453–466.
- Elmgren, R., and Larsson, U. 2001. Eutrophication in the Baltic Sea area: integrated coastal management issues. *In Science and Integrated Coastal Management*, pp. 15–35. Ed. by B. Bodungen and R. Turner. Dahlem University, Berlin.
- Fasham, M. J. R., Holligan, P. M., and Pugh, P. R. 1983. The spatial and temporal development of the spring phytoplankton bloom in the Celtic Sea, April 1979. *Progress in Oceanography*, 12: 87–145.
- Feistel, R., Nausch, G., and Wasmund, N. (Eds). 2008. State and Evolution of the Baltic Sea, 1952–2005. John Wiley and Sons, Hoboken, NJ, USA. 703 pp.
- Fernand, L., Nolan, G. D., Raine, R., Chambers, C. E., Dye, S. R., White, M., and Brown, J. 2006. The Irish coastal current: a seasonal jet-like circulation. *Continental Shelf Research*, 26: 1775–1793.
- Fernández, E., Álvarez, F., Anadón, R., Barquero, S., Bode, A., García, A., García-Soto, C., *et al.* 2004. The spatial distribution of plankton communities in a Slope Water anticyclonic Oceanic eDDY (SWODDY) in the Southern Bay of Biscay. *Journal of the Marine Biological Association of the UK*, 84: 501–517.

- Ferrer, L., Fontán, A., Mader, J., Chust, G., González, M., Valencia, V., Uriarte, A., *et al.* 2009. Low-salinity plumes in the oceanic region of the Basque Country. *Continental Shelf Research*, 29: 970–984.
- Figueiras, F. G., and Niell, F. X. 1987. Distribución estacional y espacial del fitoplancton en la Ria de Pontevedra (NO de España). *Investigación Pesquera*, 51: 293–320.
- Figueiras, F. G., and Pazos, Y. 1991. Microplankton assemblages in the three Rias Baixas (Vigo, Arosa and Muros, Spain) with a sub-surface chlorophyll maximum: their relationships to hydrography. *Marine Ecology Progress Series*, 76: 219–233.
- Fonselius, S. 1995. *Västerhavet och Östersjöns Oceanografi*. SMHIVästra Frölunda. 200 pp.
- Fuhrman, J. A., and Azam, F. 1980. Bacterioplankton secondary production estimates for coastal waters of British Columbia, Antarctica and California. *Applied and Environmental Microbiology*, 39: 1085–1094.
- Garcia-Barcina, J. M., Gonzalez-Oreja, J. A., and De la Sota, A. 2006. Assessing the improvement of the Bilbao estuary water quality in response to pollution abatement measures. *Water Research*, 40: 951–960.
- Garel, E., Nunes, S., Neto, J. M., Fernandes, R., Neves, R., Marques, J. C., and Ferreira, Ó. 2009. The autonomous Simpatico system for real-time continuous water-quality and current velocity monitoring: examples of application in three Portuguese estuaries. *Geo-Marine Letters*, 29(5): 331–341.
- Garmendia, M., Revilla, M., Bald, J., Franco, J., Laza-Martínez, A., Orive, E., Seoane, S., *et al.* 2011. Phytoplankton communities and biomass size structure (fractionated chlorophyll "a"), along trophic gradients of the Basque coast (northern Spain). *Biogeochemistry*, 106: 243–263.
- Gee, K., and Burkard, B. 2010. Cultural ecosystem services in the context of offshore wind farming: A case study from the west coast of Schleswig-Holstein. *Ecological Complexity*, 7: 349–358.
- Goberville, E., Beaugrand, G., Sautour, B., and Treguer, P. 2010. Climate-driven changes in coastal marine systems of western Europe. *Marine Ecology Progress Series*, 408: 129–159.
- Goikoetxea, N., Borja, A., Fontán, Á., González, M., and Valencia, V. 2009. Trends and anomalies in sea-surface temperature, observed over the last 60 years, within the southeastern Bay of Biscay. *Continental Shelf Research*, 29: 1060–1069.
- González, M., Mader, J., Fontán, Á., Uriarte, A., and Ferrer, L. 2008. Análisis de la tendencia de la temperatura superficial del agua del mar en Donostia-San Sebastián a partir del estudio de la serie del Aquarium (1946–2007). *Revista de Investigación Marina*, 4. 7 pp. <http://www.azti.es/rim>.
- González-Pola, C., Lavín, A., and Vargas-Yáñez, M. 2005. Intense warming and salinity modification of intermediate water masses in the southeastern corner of the Bay of Biscay for the period 1992–2003. *Journal of Geophysical Research-Oceans*, 110: C05020, doi:10.1029/2004JC002367.
- Gowen, R. J., Mills, D. K., Trimmer, M., and Nedwell, D. B. 2000. Production and its fate in two coastal regions of the Irish Sea: the influence of anthropogenic nutrients. *Marine Ecology Progress Series*, 208: 51–64.
- Gowen, R. J., Hydes, D. J., Mills, D. K., Stewart, B. M., Brown, J., Gibson, C. E., Shammon, T. M., *et al.* 2002. Assessing trends in nutrient concentrations in coastal shelf seas: a case study in the Irish Sea. *Estuarine, Coastal and Shelf Science*, 54: 927–939.
- Grasshoff, K. (Ed). 1976. *Methods of Seawater Analysis*. Verlag Chemie, Weinheim. 317 pp.
- Greenan, B., Harrison, G., Yashayaev, I., Azetsu-Scott, K., Head, E., Li, W. K. W., and Loder, J. 2010. Physical, chemical, and biological conditions in the Labrador Sea in 2009. *AZMP Bulletin*, 9: 11–19.
- Gromisz, S., and Witek, Z. 2001. Main phytoplankton assemblages in the Gulf of Gdansk and the Pomeranian Bay from 1994 to 1997. *Bulletin of Sea Fisheries Institute*, 2(153): 31–51.
- Groom, S., Martinez-Vicente, V., Fishwick, J., Tilstone, G., Moore, G., Smyth, T., and Harbour, D. 2008. The Western English Channel observatory: Optical characteristics of station L4. *Journal of Marine Systems*, 77: 278–295.
- Guadayol, O., Peters, F., Marrasé, C., Gasol, J. M., Roldán, C., Berdalet, E., Massana, R., *et al.* 2009. Episodic meteorological and nutrient load events as drivers of coastal ecosystem dynamics: a time-series analysis. *Marine Ecology Progress Series*, 381: 139–155.

- Gutiérrez-Rodríguez, A., Latasa, M., Scharek, R., Massana, R., Vila, G., and Gasol, J. M. 2011. Growth and grazing rate dynamics of major phytoplankton groups in an oligotrophic coastal site. *Estuarine Coastal and Shelf Science*, 95: 77–87.
- Hajdu, S., Hällfors, S., Gromisz, S., Skjevik, A.-T., Busch, S., Kownacka, J., Jurgensone, I., *et al.* 2008. Unusual phytoplankton event during winter–spring 2007–2008. HELCOM Indicator Fact Sheets. http://www.helcom.fi/environment2/ifs/ifs2008/en_GB/Phytoplankton_events/.
- Halpern, B. S., Walbridge, S., Selkoe, K. A., Kappel, C. V., Micheli, F., D'Agrosa, C., Bruno, J. F., *et al.* 2008. A global map of human impact of marine ecosystems. *Science*, 319: 948–952.
- Harris, R. P. 2010. The L4 time-series: the first 20 years. *Journal of Plankton Research*, 32: 577–583.
- Harrison, W. G., and Li, W. K. W. 2007. Phytoplankton growth and regulation in the Labrador Sea: Light and nutrient limitation. *Journal of Northwest Atlantic Fishery Science*, 39: 71–82.
- Harrison, W. G., Johnson, C., Head, E., Spry, J., Pauley, K., Maass, H., Kennedy, M., *et al.* 2009. Optical, chemical, and biological oceanographic conditions in the Maritimes Region in 2008. DFO Canadian Science Advisory Secretariat Research Document, 2009/054. 55 pp.
- Harrison, W. G., Børsheim, K. Y., Li, W. K. W., Maillet, G. L., Pepin, P., Sakshaug, E., Skogen, M. D., *et al.* 2012. Phytoplankton production and growth regulation in the sub-arctic North Atlantic: A comparative study of the Labrador Sea–Labrador/Newfoundland Shelves and Barents/Norwegian/Greenland Seas and Shelves. *Progress in Oceanography*. *In press*.
- Hays, G. C., Richardson, A. J., and Robinson, C. 2005. Climate change and marine plankton. *Trends in Ecology and Evolution*, 20: 337–344.
- HELCOM. 2002. Environment of the Baltic Sea area 1994–1998. *Baltic Sea Environment Proceedings* 82 B. 215 pp.
- HELCOM. 2007. Climate change in the Baltic Sea area. HELCOM Thematic Assessment in 2007. *Baltic Sea Environment Proceedings* 111. 49 pp.
- HELCOM. 2009. Eutrophication in the Baltic Sea – An integrated thematic assessment of the effects of nutrient enrichment and eutrophication in the Baltic Sea region. *Baltic Sea Environment Proceedings* 115B. 148 pp.
- HELCOM. 2010. Manual for marine monitoring in the COMBINE programme of HELCOM, Part C. – Internet, updated 2010: http://www.helcom.fi/groups/monas/CombineManual/AnnexesC/en_GB/.
- Hénard, D. 1978. Production primaire d'une lagune méditerranéenne – Etang de Thau (Hérault) – année 1976. Thèse Académie de Montpellier, Université des Sciences et Techniques du Languedoc. 85 pp.
- Hinder, S. L., Manning, J. E., Gravenor, M. B., Edwards, M., Walne, A. W., Burkhill, P. H., and Hays, G. C. 2011. Long-term changes in abundance and distribution of microzooplankton in the NE Atlantic and North Sea. *Journal of Plankton Research*, 34: 83–91.
- Hinder, S. L., Hays, G. C., Edwards, M., Roberts, E. C., Walne, A. W., and Gravenor, M. B. 2012. Changes in marine dinoflagellates and diatom abundance under climate change. *Nature Climate Change*, 12: 1–5.
- Holliday, N. P., Hughes, S. L., Borenäs, K., Feistel, R., Gaillard, F., Lavin, A., Loeng, H., *et al.* 2011. Long-term physical variability in the North Atlantic Ocean, pp. 21–46. *In* ICES status report on climate change in the North Atlantic. Ed. by P. C. Reid and L. Valdés. ICES Cooperative Research Report No. 310.
- Holligan, P. M., Maddock, L., and Dodge, J. D. 1980. The distribution of dinoflagellates around the British Isles in July, 1977: a multivariate analysis. *Journal of the Marine Biological Association of the UK*, 60: 851–867.
- Hughes, S. L., Holliday, N. P., Colbourne, E., Ozhigin, V., Valdimarsson, H., Østerhus, S., and Wiltshire, K. 2009. Comparison of *in situ* time-series of temperature with gridded sea surface temperature datasets in the North Atlantic. *ICES Journal of Marine Science*, 66: 1467–1479.
- Hughes, S. L., Holliday, N. P., and Beszczynska-Möller, A. (Eds). 2011. ICES Report on Ocean Climate 2010. ICES Cooperative Research Report No. 309. 69 pp.

- ICES. 2011. Report of the Working Group on Phytoplankton and Microbial Ecology (WGPM), 21–24 March 2011, Galway, Ireland. ICES Document CM 2011/SSGEF: 04. 32 pp.
- Ji, R., Davis, C. S., Chen, C., Townsend, D. W., Mountain, D. G., and Beardsley, R. C. 2007. Influence of ocean freshening on shelf phytoplankton dynamics. *Geophysical Research Letters*, 34, L24607. doi:10.1029/2007GL032010.
- Johns, D. J., Edwards, M., and Batten, S. 2001. Arctic boreal plankton species in the Northwest Atlantic. *Canadian Journal of Fisheries and Aquatic Sciences*, 58: 2121–2124.
- Johnson, G. C., and Gruber, N. 2007. Decadal water mass variations along 20 degrees W in the Northeastern Atlantic Ocean. *Progress in Oceanography*, 73: 277–295.
- Joyce, L. B. 2005. Observations of *Alexandrium tamarense* (Dinophyceae) vegetative cells and oceanographic parameters in Scapa Flow, Orkney Islands, Scotland. *Journal of the Marine Biological Association of the United Kingdom*, 85(2): 277–282.
- Klais, R., Tamminen, T., Kremp, A., Spilling, K., and Olli, K. 2011. Decadal-scale changes of dinoflagellates and diatoms in the anomalous Baltic Sea spring bloom. *PLoS ONE*, 6, e21567. doi:10.1371/journal.pone.0021567.
- Kraberg, A. C., Carstens, K., Peters, S., Tilly, K., and Wiltshire, K. H. 2011. The diatom *Mediopyxis helysia* at Helgoland Roads: a success story? *Helgoland Marine Research*, doi:10.1007/s10152-011-0277-9.
- Lafuente, J. G., and Ruiz, J. 2007. The Gulf of Cádiz pelagic ecosystem: a review. *Progress in Oceanography*, 74: 228–251.
- Lavin, A., Valdes, L., Sanchez, F., Abaunza, P., Forest, A., Boucher, A., Lazure, P., *et al.* 2006. The Bay of Biscay: The encountering of the ocean and the shelf (18b, E). *In The Sea*, Volume 14, pp. 933–1001. Ed. by A. R. Robinson and K. H. Brink. Harvard University Press, Boston.
- Laza-Martinez, A. 2012. *Urgorri complanatus* gen. et sp. nov. (Cryptophyceae), a red-tide-forming species in brackish waters. *Journal of Phycology*, 48: 423–435.
- Laza-Martinez, A., Seoane, S., Zapata, M., and Orive, E. 2007. Phytoplankton pigment patterns in a temperate estuary: from unialgal cultures to natural assemblages. *Journal of Plankton Research*, 29: 913–929.
- Laza-Martinez, A., Orive, E., and Miguel, I. 2011. Morphological and genetic characterisation of benthic dinoflagellates of the genera *Coolia*, *Ostreopsis* and *Prorocentrum* from the Southeastern Bay of Biscay. *European Journal of Phycology*, 46: 45–65.
- Le Quéré, C., Harrison, S. P., Prentice, I. C., Buitenhuis, E. T., Aumont, O., Bopp, L., Claustre, H., *et al.*, 2005. Ecosystem dynamics based on plankton functional types for global ocean biogeochemistry models. *Global Change Biology*, 11: 2016–2040.
- Lee, A. J., and Ramster, J. W. 1981. Atlas of the seas around the British Isles. Ministry of Agriculture Fisheries and Food, Directorate of Fisheries Research, London. 5 pp.
- Lefebvre, A., Guiselin, N., Barbet, F., and Artigas, F. L. 2011. Long-term hydrological and phytoplankton monitoring (1992–2007) of three potentially eutrophic systems in the eastern English Channel and the Southern Bight of North Sea. *ICES Journal of Marine Science*, 68: 2029–2043.
- Lemos, R. T., and Sansó, B. 2006. Spatio-temporal variability of ocean temperature in the Portugal Current System. *Journal of Geophysical Research–Oceans*, 11: C04010. doi:10.1029/2005JC003051.
- Leterme, S. C., Edwards, M., Seuront, L., Attrill, M. J., Reid, P. C., and John, A. W. G. 2005. Decadal basin-scale changes in diatoms, dinoflagellates, and phytoplankton color across the North Atlantic. *Limnology and Oceanography*, 50: 1244–1253.
- Li, W. K. W., and Dickie, P. M. 2001. Monitoring phytoplankton, bacterioplankton and virioplankton in a coastal inlet (Bedford Basin) by flow cytometry. *Cytometry*, 44: 236–246.
- Li, W. K. W., and Harrison, W. G. 2008. Propagation of an atmospheric climate signal to phytoplankton in a small marine basin. *Limnology and Oceanography*, 53: 1734–1745.
- Li, W. K. W., Harrison, W. G., and Head, E. J. H. 2006. Coherent sign switching in multiyear trends of microbial plankton. *Science*, 311: 1157–1160.

- Li, W. K. W., Lewis, M. R., and Harrison, W. G. 2010. Multiscalarity of the nutrient–chlorophyll relationship in coastal phytoplankton. *Estuaries and Coasts*, 33: 440–447.
- Li, W. K. W., Morán, X. A. G., and O'Brien, T. D. 2011a. Towards an ecological status report for phytoplankton and microbial plankton in the North Atlantic. ICES Document CM/2011/B: 02.
- Li, W. K. W., Andersen, R. A., Gifford, D. J., Incze, L. S., Martin, J. L., Pilska, C. H., Rooney-Varga, J. N., *et al.* 2011b. Planktonic microbes in the Gulf of Maine Area. *PLoS ONE*, 6(6): e20981. doi:10.1371/journal.pone.0020981.
- Licandro, P., Head, E., Gislason, A., Benfield, M. C., Harvey, M., Margonski, P., and Silke, J. 2011. Overview of trends in plankton communities. *In* ICES status report on climate change in the North Atlantic, pp. 103–122. Ed. by P. C. Reid and L. Valdés. ICES Cooperative Research Report No. 310.
- Llope, M., Anadón, R., Viesca, L., Quevedo, M., González-Quirós, R., and Stenseth, N. C. 2006. Hydrography of the southern Bay of Biscay shelf-break region: integrating the multi-scale physical variability over the period 1993–2003. *Journal of Geophysical Research–Oceans*, 111: C09021. doi:10.1029/2005JC002963.
- Llope, M., Anadón, R., Sostres, J. A., and Viesca, L. 2007. Nutrients dynamics in the southern Bay of Biscay (1993–2003): winter supply, stoichiometry, long-term trends, and their effects on the phytoplankton community. *Journal of Geophysical Research*, 112: C07029. doi:10.1029/2006JC003573.
- Loder, J. W., Petrie, B., and Gawarkiewicz, G. 1998. The coastal ocean off Northeastern North America: a large scale view. Coastal segment (1, W). *In* The Sea, Volume 11, pp. 105–133. Ed. by A. R. Robinson and K. H. Brink. Harvard University Press, Boston.
- Longhurst, A. R. 1998. Ecological geography of the sea. Academic Press, San Diego. 398 pp.
- Longhurst, A. R. 2007. Ecological Geography of the Sea, 2nd edition. Academic Press. 560 pp.
- Lucea, A., Duarte, C. M., Agustí, S., and Kennedy, H. 2005. Nutrient dynamics and ecosystem metabolism in the Bay of Blanes (NW Mediterranean). *Biogeochemistry*, 73: 303–323.
- Mackas, D. L., Thomson, R. E., and Galbraith, M. 2001. Changes in the zooplankton community of the British Columbia continental margin, 1985–1999, and their covariation with oceanographic conditions. *Canadian Journal of Fisheries and Aquatic Sciences*, 58: 685–702.
- Mackas, D., Pepin, P., and Verheye, H. 2012. Interannual variability of marine zooplankton and their environments: Within- and between-region comparisons. *Progress in Oceanography*, 97–100: 1–14.
- Mackenzie, B. R., and Schiedek, D. 2007. Daily ocean monitoring since the 1860s shows record warming of northern European seas. *Global Change Biology*, 13: 1335–1347.
- Margalef, R. 1945. Fitoplancton nerítico de la Costa Brava catalana (Sector de Blanes). *Publicación Biología Mediterránea*, 1: 1–48.
- Margalef, R. 1948. Le phytoplancton estival de la “Costa Brava” catalane en 1946. *Hydrobiologia. Acta Hydrobiologia, Limnologica et protistologica*. 1: 15–21.
- Margalef, R. 1964. Fitoplancton de las costas de Blanes (provincia de Gerona, Mediterráneo Occidental), de julio de 1959 a junio de 1963. *Investigación Pesquera*, 26: 131–164.
- Margalef, R., Durán, M., and Saiz, F. 1955. El fitoplancton de la Ria de Vigo de enero de 1953 a marzo de 1954. *Investigación Pesquera*, 2, 85–129.
- Martin, J. L., Wildish, D. J., LeGresley, M. M., and Ringuette, M. M. 1995. Phytoplankton monitoring in the southwestern Bay of Fundy during 1990–1992. *Canadian Manuscript Report of Fisheries and Aquatic Sciences*, 2277. 154 pp.
- Martin, J. L., LeGresley, M. M., Strain, P. M., and Clement, P. 1999. Phytoplankton monitoring in the southwest Bay of Fundy during 1993–96. *Canadian Technical Report of Fisheries and Aquatic Sciences*, 2265. 132 pp.
- Martin, J. L., LeGresley, M. M., and Strain, P. M. 2001. Phytoplankton monitoring in the western isles region of the Bay of Fundy during 1997–98. *Canadian Technical Report of Fisheries and Aquatic Sciences*, 2349. 85 pp.

- Martin, J. L., LeGresley, M. M., and Strain, P. M. 2006. Plankton monitoring in the Western Isles Region of the Bay of Fundy during 1999–2000. Canadian Technical Report of Fisheries and Aquatic Sciences, 2629. 88 pp.
- Martinez, R., Orive, E., Laza, A., and Seoane, S. 2010. Growth response of six strains of *Heterosigma akashiwo* to varying temperature, salinity and irradiance conditions. Journal of Plankton Research, 32: 529–538.
- Massana, R., Balagué, V., Guillou, L., and Pedrós-Alió, C. 2004. Picoeukaryotic diversity in an oligotrophic coastal site studied by molecular and culturing approaches. FEMS Microbiology Ecology, 50: 231–243.
- Mazzocchi, M. G., Dubroca, L., Garcia-Comas, C., Di Capua, I., and Ribera d'Alcalà, M. 2012. Stability and resilience in coastal copepod assemblages: the case of the Mediterranean long-term ecological research at stn MC (LTER-MC). Progress in Oceanography, 97–100: 135–151.
- MCCIP. 2008. Marine Climate Change Impacts Partnership. Annual Report Card 2007–2008. Lowestoft, UK.
- McClain, C. R., Chao, S.-Y., Atkinson, L., Blanton, J., and de Castillo, F. F. 1986. Wind-driven upwelling in the vicinity of Cape Finisterre, Spain. Journal of Geophysical Research–Oceans, 91: 8470–8486.
- McCollin, T., Lichtman, D., Bresnan, E., and Berx, B. 2011. A study of phytoplankton communities along a hydrographic transect on the north east coast of Scotland. Marine Scotland Science report, 04/11. <http://www.scotland.gov.uk/Topics/marine/science/Publications/publicationslatest/Science/MSSR/2011Reports/MSSR0411>.
- McDonald, S. M., Sarno, D., Scanlan, D. J., and Zingone, A. 2007. Genetic diversity of eukaryotic ultraphytoplankton in the Gulf of Naples during an annual cycle. Aquatic Microbial Ecology, 50: 75–89.
- McGinty, N., Power, A. M., and Johnson, M. P. 2011. Variation among northeast Atlantic regions in the responses of zooplankton to climate change: not all areas follow the same path. Journal of Experimental Marine Biology and Ecology, 400: 120–131.
- Mieruch, S., Freund, J. A., Feudel, U., Boersma, M., Janisch, S., and Wiltshire, K. H. 2010. A new method of describing phytoplankton blooms: examples from Helgoland Roads. Journal of Marine Systems, 79: 36–43.
- Mitchell, M. R., Harrison, G., Pauley, K., Gagné, A., Maillet, G., and Strain, P. 2002. Atlantic Zonal Monitoring Program Sampling Protocol. Canadian Technical Report of Hydrography and Ocean Sciences, 223. 23 pp.
- Morán, X. A. G., López-Urrutia, A., Calvo-Díaz, A., and Li, W. K. W. 2010. Increasing importance of small phytoplankton in a warmer ocean. Global Change Biology, 16: 1137–1144.
- Morán, X. A. G., Díaz-Pérez, L., Nogueira, E., and Bode, A. 2011. Coastal bacterioplankton in the southern Bay of Biscay: changes in abundance and cell size at seasonal and interannual scales. ICES Document CM 2011/B: 04. 18 pp.
- Nehring, S. 1995. *Gymnodinium catenatum* Graham (Dinophyceae) in Europe: a growing problem? Journal of Plankton Research, 17: 85–102.
- Nehring, S. 1998. Establishment of thermophilic phytoplankton species in the North Sea: biological indicators of climate change? ICES Journal of Marine Science, 55: 818–823.
- Niemi, A. 1975. Ecology of phytoplankton in the Tvärminne area, SW coast of Finland. II. Primary production and environmental conditions in the archipelago and the sea zone. Acta Botanica Fennica, 105. 74 pp.
- O'Boyle, S. 2002. Summer flora of shelf waters around western Ireland: interactions between physical dynamics and phytoplankton and consequences for potentially harmful algal events. Ph.D. Thesis, National University of Ireland, Galway, Ireland. 309 pp.
- O'Boyle, S., and Raine, R. 2007. The influence of local and regional oceanographic processes on phytoplankton distribution in continental shelf waters off north-western Ireland. Biology and Environment Proceedings of the Royal Irish Academy, 107B: 95–109.
- O'Brien, T. D., Wiebe, P. H., and Hay, S. 2011. ICES Zooplankton Status Report 2008/2009. ICES Cooperative Research Report No. 307. 152 pp.

- Olenina, I., Hajdu, S., Edler, L., Andersson, A., Wasmund, N., Göbel, J., Huttunen, M., *et al.* 2006. Biovolumes and size-classes of phytoplankton in the Baltic Sea. *Baltic Sea Environment Proceedings* No. 106.
- Olsen, Y., Agustí, S., Andersen, T., Duarte, C. M., Gasol, J. M., Gismervik, I., Heiskanen, A-S., *et al.* 2006. A comparative study of responses in planktonic foodweb structure and function in contrasting European coastal waters exposed to experimental nutrient additions. *Limnology and Oceanography*, 51: 488–503.
- Orive, E. 1989. Differences in phytoplankton composition between the Abra of Bilbao and the adjacent shelf waters. *Hidrobiología*, 182: 121–135.
- Orive, E., Laza-Martínez, A., Seoane, S., Alonso, A., Andrade, R., and Miguel, I. 2010. Diversity of *Pseudo-nitzschia* in the Southeastern Bay of Biscay. *Diatom Research*, 25: 125–145.
- Pardo, P. C., Padín, X. A., Gilcoto, M., Farina-Busto, L., and Pérez F. F. 2011. Evolution of upwelling systems coupled to the long-term variability in sea surface temperature and Ekman transport. *Climate Research*, 48: 231–246.
- Pérez, F. F., Padín, X. A., Pazos, Y., Gilcoto, M., Cabanas, M., Pardo, P. C., Doval, M. D., and Farina-Busto, L. 2010. Plankton response to weakening of the Iberian coastal upwelling. *Global Change Biology*, 16: 1258–1267. doi: 10.1111/j.1365-2486.2009.02125.x.
- Pingree, R. D., and Le Cann, B. 1990. Structure, strength and seasonality of the slope currents in the Bay of Biscay region. *Journal of the Marine Biological Association of the UK*, 70: 857–885.
- Pingree, R. D., and Le Cann, B. 1993. Three anticyclonic Slope Water eDDIES (SWODDIES) in the Southern Bay of Biscay in 1990. *Deep Sea Research II*, 39: 1147–1175.
- Pingree, R. D., Holligan, P. M., Mardell, G. T., and Head, R. N. 1976. The influence of physical stability on spring, summer and autumn phytoplankton blooms in the Celtic Sea. *Journal of the Marine Biological Association of the UK*, 56: 845–873.
- Pinhassi, J., Gómez-Consarnau, L., Alonso-Sáez, L., Sala, M. M., Vidal, M., Pedrós-Alió, C., and Gasol, J. M. 2006. Seasonal changes in bacterioplankton nutrient limitation and its effects on bacterial diversity in the NW Mediterranean Sea. *Aquatic Microbial Ecology*, 44: 241–252.
- Porter, K. G., and Feig, Y. S. 1980. The use of DAPI for identifying and counting aquatic microflora. *Limnology and Oceanography*, 25: 943–948.
- Prego, R., Guzmán-Zúñiga, D., Varela, M., de Castro, M., and Gómez-Gesteira, M. 2007. Consequences of winter upwelling events on biogeochemical and phytoplankton patterns in a western Galician ria (NW Iberian peninsula). *Estuarine, Coastal and Shelf Science*, 73: 409–422.
- Puillat, I., Lazure, P., Jégou, A. M., Lampert, L., and Miller, P. I. 2004. Hydrographical variability of the French continental shelf in the Bay of Biscay, during the 1990s. *Continental Shelf Research*, 24: 1143–1163.
- Raabe, T., and Wiltshire, K. H. 2009. Quality control and analyses of the long-term nutrient data from Helgoland Roads, North Sea. *Journal of Sea Research*, 61: 3–16.
- Raine, R., and McMahon, T. 1998. Physical dynamics on the continental shelf off southwestern Ireland and their influence on coastal phytoplankton blooms. *Continental Shelf Research*, 18: 883–914.
- Raine, R., O'Mahony, J., McMahon, T., and Roden, C. 1990. Hydrography and phytoplankton of waters off south-west Ireland. *Estuarine, Coastal and Shelf Science*, 30: 579–592.
- Raine, R., McMahon, T., and Roden, C. M. 1993. A review of the summer phytoplankton distribution in Irish coastal waters, a biogeography related to physical oceanography. *In* *Biogeography of Ireland: past, present and future*. Ed. by M. J. Costello and K. S. Kelly. Occasional Publication of the Irish Biogeographical Society, 2: 99–111.
- Raine, R., McDermott, G., Silke, J., Lyons, K., Nolan, G., and Cusack, C. 2010. A simple short range model for the prediction of harmful algal events in the bays of south-western Ireland. *Journal of Marine Systems*, 83: 150–157.

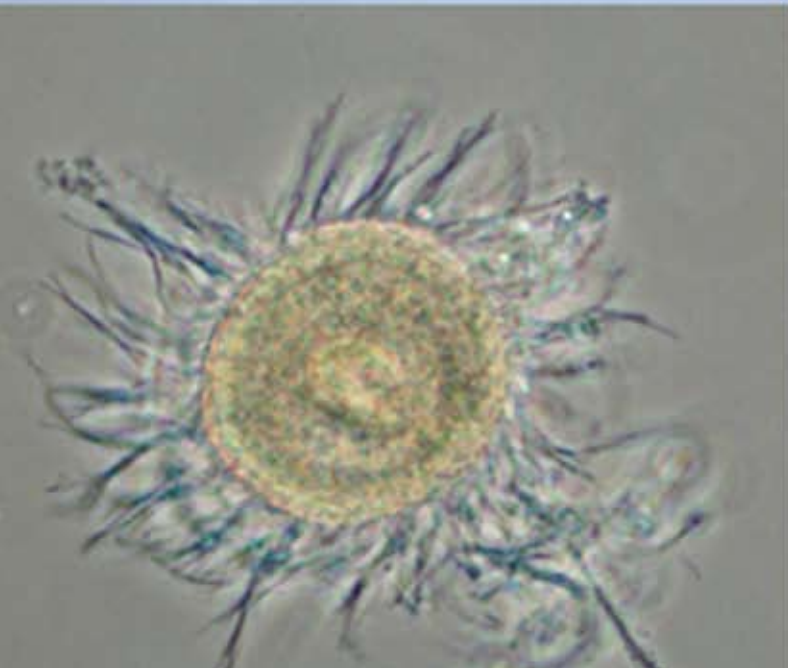
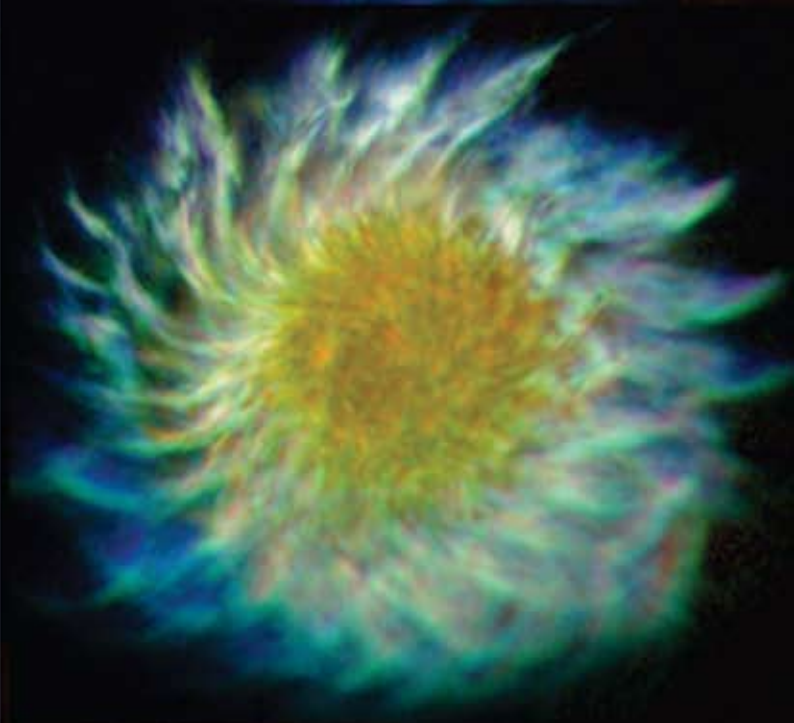
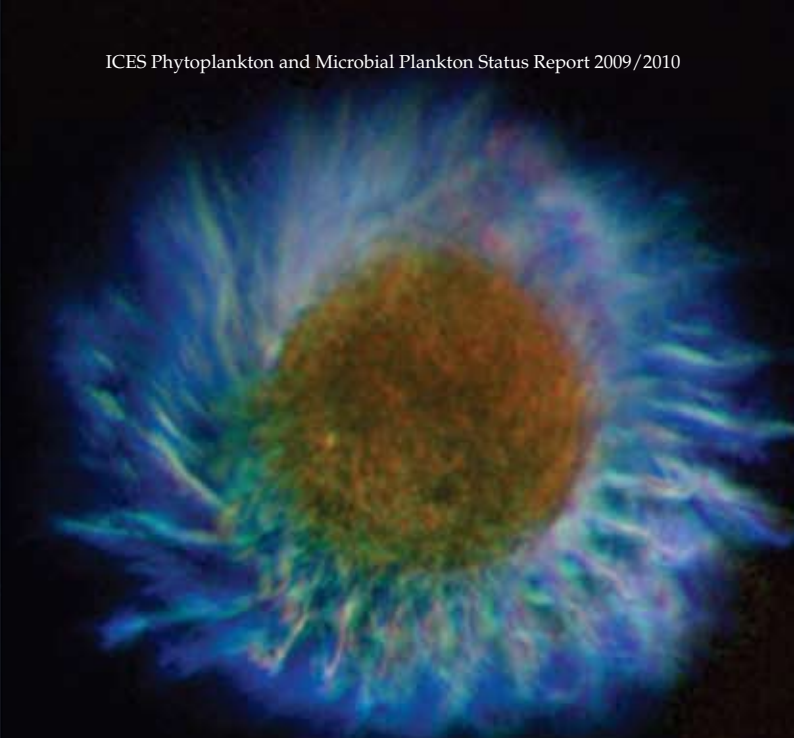
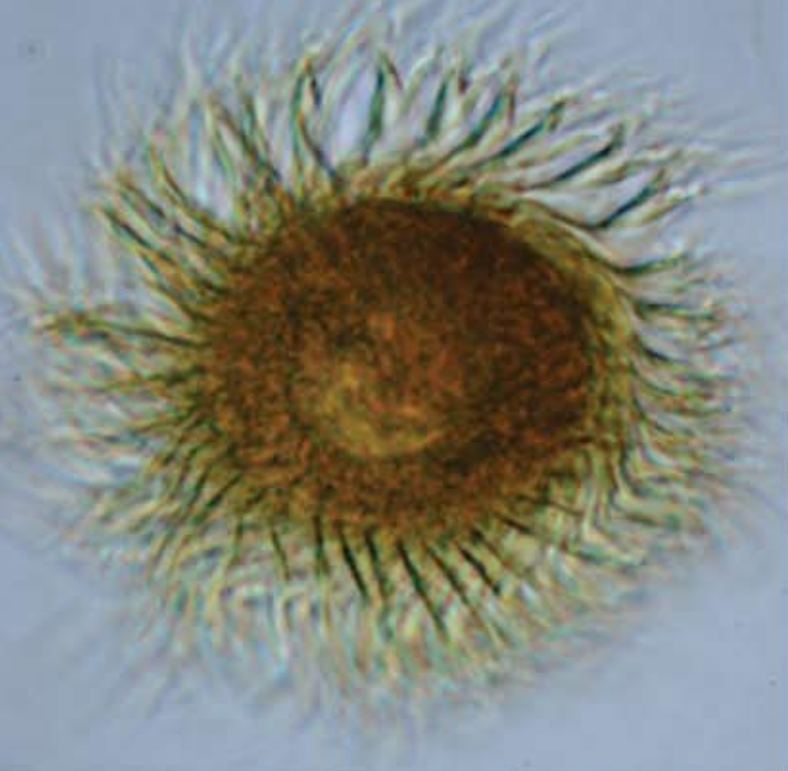
- Raitsos, D. E., Reid, P. C., Lavender, S., Edwards, M., and Richardson, A. J. 2005. Extending the SeaWiFS chlorophyll data set back 50 years in the northeast Atlantic. *Geophysical Research Letters*, 32: 1–4.
- Reid, P. C., and Edwards, M. 2001. Long-term changes in the pelagos, benthos and fisheries of the North Sea. *Marine Biodiversity*, 31: 107–115.
- Reid, P. C., and Valdés, L. (Eds). 2011. ICES status report on climate change in the North Atlantic. ICES Cooperative Research Report No. 310. 262 pp.
- Reid, P. C., de Fatima Borges, M., and Svendsen, E. 2001. A regime shift in the North Sea circa 1988 linked to changes in the North Sea horse mackerel fishery. *Fisheries Research*, 50: 163–171.
- Reid, P. C., Edwards, M., Beaugrand, G., Skogen, M., and Stevens, D. 2003. Periodic changes in the zooplankton of the North Sea during the twentieth century linked to oceanic inflow. *Fisheries Oceanography*, 12: 260–269.
- Reid, P. C., Johns, D. G., Edwards, M., Starr, M., Poulin, M., and Snoeijs, P. 2007. A biological consequence of reducing Arctic ice cover: arrival of the Pacific diatom *Neodenticula seminae* in the North Atlantic for the first time in 800 000 years. *Global Change Biology*, 13: 1910–1921.
- Relvas, P., Barton, E. D., Dubert, J., Oliveira, P. B., Peliz, Á. J., da Silva, J. C., and Santos, A. M. P. 2007. Physical oceanography of the Western Iberia Ecosystem: latest views and challenges. *Progress in Oceanography*, 74: 149–173.
- Relvas, P., Luis, J., and Santos, A. M. P. 2009. Importance of the mesoscale in the decadal changes observed in the northern Canary upwelling system. *Geophysical Research Letters*, 36: L22601.
- Revilla, M., Borja, Á., Chust, G., Fontán, A., Franco, J., González, M., and Valencia, V. 2009. A two-decade record of temperature and chlorophyll “a” in surface waters within the Basque Country (southeastern Bay of Biscay). ICES Document CM 2009/D: 11.
- Revilla, M., Borja, Á., Fontán, A., Franco, J., González, M., and Valencia, V. 2010. A two-decade record of surface chlorophyll “a” and temperature in offshore waters of the Basque country (southeastern Bay of Biscay). *Revista de Investigación Marina*, 17(2): 14–20.
- Ribera d’Alcalà, M., Conversano, F., Corato, F., Licandro, P., Mangoni, O., Marino, D., Mazzocchi, M. G., *et al.* 2004. Seasonal patterns in plankton communities in a pluriannual time-series at a coastal Mediterranean site (Gulf of Naples): an attempt to discern recurrences and trends. *Scientia Marina*, 68 (Suppl.1): 65–83.
- Richardson, A. J., and Schoeman, D. S. 2004. Climate impact on plankton ecosystems in the Northeast Atlantic. *Science*, 305: 1609–1612.
- Rincé, Y., and Paulmier, G. 1986. Données nouvelles sur la distribution de la diatomée marine *Coscinodiscus wailesii* Gran and Angst (Bacillariophyceae). *Phycologia*, 25: 73–79.
- Rocha, C., Galvão, H. M., and Barbosa, A. B. 2002. Role of transient silicon limitation in the development of cyanobacteria blooms in the Guadiana estuary, south-western Iberia. *Marine Ecology Progress Series*, 228: 35–45.
- Rönnberg, C., and Bonsdorff, E. 2004. Baltic Sea eutrophication: area-specific ecological consequences. *Hydrobiologia*, 514: 227–241.
- Rose, J. M., Caron, D. A., Sieracki, M. E., and Poulton, N. J. 2004. Counting heterotrophic nanoplanktonic protists in cultures and in aquatic communities by flow cytometry. *Aquatic Microbial Ecology*, 34: 263–277.
- Santos, F., Gomez Gesteira, M., and de Castro, M. 2011. Coastal and oceanic SST variability along the western Iberian Peninsula. *Continental Shelf Research*, 31: 2012–2017.
- Sarmiento, H., Montoya, J. M., Vázquez-Domínguez, E., Vaqué, D., and Gasol, J. M. 2010. Warming effects on marine microbial foodweb processes: how far can we go when it comes to predictions? *Philosophical Transactions of the Royal Society B: Biological Sciences*, 365: 2137–2149.
- Schauer, M., Balagué, V., Pedrós-Alió, C., and Massana, R. 2003. Seasonal changes in the taxonomic composition of bacterioplankton in a coastal oligotrophic system. *Aquatic Microbial Ecology*, 31: 163–174.
- Schlüter, M., Merico, A., Wiltshire, K. H., Greve, W., and von Storch, H. 2008. A statistical analysis of climate variability and ecosystem response in the German Bight. *Ocean Dynamics*, 58: 169–186.

- SCOR. 1964. Report of the SCOR–UNESCO Working Group 17 on Determination of Photosynthetic Pigments which met on June 4–6, 1964 at UNESCO, Paris. The Group, Sidney, Australia. 24 pp.
- Seoane, S., Laza, A., Urrutxurtu, I., and Orive, E. 2005. Phytoplankton assemblages and their dominant pigments in the Nervion River estuary. *Hydrobiologia*, 549: 1–13.
- Seoane, S., Laza, A., and Orive, E. 2006. Partitioning by size classes of the main phytoplankton marker pigments at the seaward end of a temperate estuary in spring and summer. *Estuarine, Coastal and Shelf Science*, 67: 343–354.
- Seoane, S., Eikrem, W., Arluzea, J., and Orive, E. 2009. Haptophytes of the Nervion River estuary, Northern Spain. *Botanica Marina*, 52: 47–59.
- Sieracki, C. K., Sieracki, M. E., and Yentsch, C. S. 1998. An imaging-in-flow system for automated analysis of marine phytoplankton. *Marine Ecology Progress Series*, 168: 285–296.
- Silke, J., O’Beirn, F., and Cronin, M. 2005. *Karenia mikimotoi*: an exceptional dinoflagellate bloom in western Irish waters – summer 2005. Marine Institute, Galway, Ireland. Marine Environmental Health Services, 21: 1–44.
- Simó, R., Vila-Costa, M., Alonso-Sáez, L., Cardelús, C., Guadayol, Ò., Vázquez-Domínguez, E., and Gasol, J. M. 2009. Annual series of DMSP contribution to S and C fluxes through phytoplankton and bacterioplankton in a NW Mediterranean coastal site. *Aquatic Microbial Ecology*, 57: 43–55.
- Simpson, J. H. 1994. Introduction to the North Sea Project. In *Understanding the North Sea System*, pp. 1–4. Ed. by H. Charnock, K. R. Dyer, J. M. Huthnance, P. S. Liss, J. H. Simpson, and P. B. Tett. The Royal Society, University Press, Cambridge. 222 pp.
- Smetacek, V., von Bondungen, B., Knoppers, B., Peinert, R., Pollehne, F., Stegmann, P., and Zeitzschel, B. 1984. Seasonal stages characterizing the annual cycle of an inshore pelagic system. *Rapports et Procès-Verbaux des Réunions du Conseil International pour l’Exploration de la Mer*, 183: 126–135.
- Smyth, T. J., Tyrrell, T., and Tarrant, B. 2004. Time-series of coccolithophore activity in the Barents Sea, from twenty years of satellite imagery. *Geophysical Research Letters*, 31, L11302. doi:10.1029/2004GL019735.
- Smyth, T. J., Fishwick, J. R., Al-Moosawi, L., Cummings, D. G., Harris, C., Kitidis, V., Rees, A. P., *et al.* 2010. A broad spatio-temporal view of the Western English Channel observatory. *Journal of Plankton Research*, 32: 585–601.
- Šolić, M., Krstulović, N., Marasović, I., Baranović, A., Pucher-Petković, T., and Vučetić, T. 1997. Analysis of time-series of planktonic communities in the Adriatic Sea: distinguishing between natural and man-induced changes. *Oceanologica Acta*, 20: 131–143.
- Šolić, M., Krstulović, N., Bojanić, N., Marasović, I., and Ninčević, Ž. 1998. Seasonal switching between relative importance of bottom-up and top-down control of bacterial and heterotrophic nanoflagellate abundance. *Journal of the Marine Biology Association of the UK*, 78: 755–766.
- Šolić, M., Krstulović, N., Vilibić, I., Kušpilić, G., Šestanović, S., Šantić, D., and Ordulj, M. 2008. The role of water mass dynamics in controlling bacterial abundance and production in the middle Adriatic Sea. *Marine Environmental Research*, 65: 388–404.
- Šolić, M., Krstulović, N., Vilibić, I., Bojanić, N., Kušpilić, G., Šestanović, S., Šantić, D., *et al.* 2009. Variability in the bottom-up and top-down control of bacteria on trophic and temporal scale in the middle Adriatic Sea. *Aquatic Microbial Ecology*, 58: 15–29.
- Šolić, M., Krstulović, N., Kušpilić, G., Ninčević Gladan, Ž., Bojanić, N., Šestanović, S., Šantić, D., *et al.* 2010. Changes in microbial foodweb structure in response to changed environmental trophic status: A case study of the Vranjic Basin (Adriatic Sea). *Marine Environmental Research*, 70: 239–249.
- Song, H., Ji, R., Stock, C., and Wang, Z. 2010. Phenology of phytoplankton blooms in the Nova Scotian Shelf–Gulf of Maine region: remote sensing and modeling analysis. *Journal of Plankton Research*, 32: 1485–1499.
- Song, H., Ji, R., Stock, C., Kearney, K., and Wang, Z. 2011. Interannual variability in phytoplankton blooms and plankton productivity over the Nova Scotian Shelf and in the Gulf of Maine. *Marine Ecology Progress Series*, 426: 105–118.

- Souchu, P., Vaquer, A., Collos, Y., Landrein, S., Deslous-Paoli, J. M., and Bibent, B. 2001. Influence of shellfish farming activities on the biogeochemical composition of the water column in Thau lagoon. *Marine Ecology Progress Series*, 218: 141–152.
- Sournia, A. 1978. *Phytoplankton Manual*. Paris, IOC–UNESCO. (Monographs on Oceanographic Methodology 4.6).
- Southwood, T. R. E. 1988. Tactics, strategies and templets. *Oikos*, 52: 3–18.
- Strain, P. M., and Clement, P. M. 1996. Nutrient and dissolved oxygen concentrations in the Letang Inlet, New Brunswick, in the summer of 1994. *Canadian Data Report of Fisheries and Aquatic Sciences*, 1004. 33 pp.
- Suikkanen, S., Laamanen, M., and Huttunen, M. 2007. Long-term changes in summer phytoplankton communities of the open northern Baltic Sea. *Estuarine Coastal and Shelf Science*, 71: 580–592.
- Tamminen, T., and Andersen, T. 2007. Seasonal phytoplankton nutrient limitation patterns as revealed by bioassays over Baltic Sea gradients of salinity and eutrophication. *Marine Ecology Progress Series*, 340: 121–138.
- Therriault, J.-C., Petrie, B., Pepin, P., Gagnon, J., Gregory, D., Helbig, J., Hernan, A., *et al.* 1998. Proposal for a northwest Atlantic zonal monitoring program. *Canadian Technical Report of Hydrography and Ocean Sciences*, 194. 57 pp.
- Tian, T., Su, J., Floser, G., Wiltshire, K. H., and Wirtz, K. 2011. Factors controlling the onset of spring blooms in the German Bight 2002–2005: light, wind and stratification. *Continental Shelf Research*, 31: 1140–1148.
- Touzet, N., Raine, R., and Franco, J. M. 2007. Characterization of nontoxic and toxin-producing strains of *Alexandrium minutum* (Dinophyceae) in Irish coastal waters. *Applied and Environmental Microbiology*, 73: 3333–3342.
- Townsend, D. W., Thomas, A. C., Mayer, L. M., Thomas, M. A., and Quinlan, J. A. 2006. Oceanography of the Northwest Atlantic Shelf (1, W). *In* *The Sea*, Volume 14, pp. 119–168. Ed. by A. R. Robinson and K. Brink. Harvard University Press, Boston.
- Tunin-Ley, A., Ibañez, F., Labat, J.-P., Zingone, A., and Lemée, R., 2009. Phytoplankton biodiversity and NW Mediterranean Sea warming: changes in the dinoflagellate genus *Ceratium* in the 20th century. *Marine Ecology Progress Series*, 541: 101–112.
- Unrein, F., Massana, R., Alonso-Sáez, L., and Gasol, J. M. 2007. Significant year-round effect of small mixotrophic flagellates on bacterioplankton in an oligotrophic coastal system. *Limnology and Oceanography*, 52: 456–459.
- Urrutxurtu, I. 2004. Seasonal succession of tintinnids in the Nervión River estuary, Basque Country, Spain. *Journal of Plankton Research*, 26: 307–314.
- Utermöhl, H. 1958. Zur vervollkommenung der quantitativen Phytoplankton Methodik. *Mitteilungen der Internationalen Vereinigung für theoretische und angewandte Limnologie*, 9: 1–38.
- Valderama, J. C. 1981. The simultaneous analysis of total nitrogen in natural waters. *Marine Chemistry*, 10: 109–122.
- Valencia, V., and Franco, J. 2004. Main characteristics of the water masses. *In* *Oceanography and Marine Environment of the Basque Country*, pp. 197–232. Ed. by Á. Borja and M. Collins. Elsevier, Amsterdam.
- Vaquer, A., Troussellier, M., Courties, C., and Bibent, B. 1996. Standing stock and dynamics of picophytoplankton in the Thau lagoon (northwest Mediterranean coast). *Limnology and Oceanography*, 41: 1821–1828.
- Varela, M., and Prego, R. 2003. Hydrography and phytoplankton in an isolated and non-pristine ria area: the A Coruña Harbour (NW Spain). *Acta Oecologica*, 24: 113–124.
- Varela, M., Bode, A., Alvarez, M., Prego, R., Canle, M., Casas, B., Lorenzo, J., *et al.* 1996. Sistema pelágico. *In* *Seguimiento de la contaminación producida por el accidente del buque “Aegean Sea”*, pp. 15–63. Ed. by J. Ros. Ministerio de Medio Ambiente. Madrid.
- Varela, M., Prego, R., Belzunce, M. J., and Martín-Salas, F. 2001. Inshore–offshore differences in seasonal variations of phytoplankton assemblages: the case of a Galician Ria Alta (A Coruña Ria) and its adjacent shelf (NW Spain). *Continental Shelf Research*, 21: 1815–1838.

- Varela, M., Prego, R., Pazos, Y., and Moroño, A. 2005. Influence of upwelling and river run-off interaction of phytoplankton assemblages in a Middle Galician Ria and comparison with northern and southern rias (NW Iberian Peninsula). *Estuarine, Coastal and Shelf Science*, 64: 721–737.
- Varela, M., Bode, A., Lorenzo, J., Alvarez-Ossorio, M. T., Miranda, A., Patrocinio, T., Anadón, R., *et al.* 2006. The effect of the 'Prestige' oil spill on the plankton in the N-NW Spanish coast. *Marine Pollution Bulletin*, 53: 272–286.
- Varela, M., Prego, R., and Pazos, Y. 2008. Spatial and temporal variability of phytoplankton biomass, primary production and community structure in the Pontevedra Ria (NW Iberian Penin): oceanographic periods and possible response to environmental changes. *Marine Biology*, 154: 483–499.
- Varela, M., Álvarez-Ossorio, M. T., Bode, A., Prego, R., Bernárdez, P., and García Soto, C. 2010. The effects of a winter upwelling on biogeochemical and planktonic components in an area close to the Galician Upwelling Core: The Sound of Corcubión (NW Spain). *Journal of Sea Research*, 64: 260–272.
- Varela, M., Lorenzo, J., Mene, L., Anadón, R., Bode, A., and Viesca, L. 2012. Fitoplancton. *In* Cambio climático y oceanográfico en el Atlántico del norte de España, pp. 177–198. Ed. by A. Bode, A. Lavin, and L. Valdes. Instituto Español de Oceanografía, Madrid.
- Veldhuis, M. J. W., Cucci, T. L., and Sieracki, M. E. 1997. Cellular DNA content of marine phytoplankton using two new fluorochromes: taxonomic and ecological implications. *Journal of Phycology*, 33: 527–541.
- Verity, P. G. 1987. Abundance, community composition, size distribution, and production rates of tintinnids in Narragansett Bay, Rhode Island. *Estuarine, Coastal and Shelf Science*, 24: 671–690.
- Vezzulli, L., Pruzzo, C., and Fabiano, M. 2004. Response of the bacterial community to in-situ bioremediation of organic-rich sediments. *Marine Pollution Bulletin*, 49: 740–751.
- Vezzulli, L., Brettar, I., Pezzati, E., Reid, P. C., Colwell, R. R., Hofle, M. G., and Pruzzo, C. 2011. Long-term effects of ocean warming on the prokaryotic community: evidence from the vibrios. *ISME Journal*, 6: 21–30.
- Vila-Reixach, G., Gasol, J. M., Cardelús, C., and Vidal, M. 2012. Seasonal dynamics and net production of dissolved organic carbon in an oligotrophic coastal environment. *Marine Ecology Progress Series*, 456: 7–19.
- Warner, A. J., and Hays, G. C. 1994. Sampling by the Continuous Plankton Recorder survey. *Progress in Oceanography*, 34: 237–256.
- Wasmund, N., and Siegel, H. 2008. Chapter 15. Phytoplankton. *In* State and Evolution of the Baltic Sea, 1952–2005. A Detailed 50-Year Survey of Meteorology and Climate, Physics, Chemistry, Biology, and Marine Environment, pp. 441–481. Ed. by R. Feistel, G. Nausch, and N. Wasmund. John Wiley and Sons, Hoboken, NJ, USA. 712 pp.
- Wasmund, N., and Uhlig, S. 2003. Phytoplankton trends in the Baltic Sea. *ICES Journal of Marine Science*, 60: 177–186.
- Wasmund, N., Nausch, G., and Matthäus, W. 1998. Phytoplankton spring blooms in the southern Baltic Sea – spatio-temporal development and long-term trends. *Journal of Plankton Research*, 20: 1099–1117.
- Wasmund, N., Tuimala, J., Suikkanen, S., Vandepitte, L., and Kraberg, A. 2011. Long-term trends in phytoplankton composition in the western and central Baltic Sea. *Journal of Marine Systems*, 87: 145–159.
- Widdicombe, C. E., Eloire, D., Harbour, D., Harris, R. P., and Somerfield, P. J. 2010. Long-term phytoplankton community dynamics in the Western English Channel. *Journal of Plankton Research*, 32: 643–655.
- Wildish, D. J., Martin, J. L., Wilson, A. J., and DeCoste, A. M. 1988. Environmental monitoring of the Bay of Fundy salmon mariculture industry during 1986 and 1987. *Canadian Technical Report of Fisheries and Aquatic Sciences*, 1648. 44 pp.
- Wildish, D. J., Martin, J. L., Wilson, A. J., and Ringuette, M. 1990. Environmental monitoring of the Bay of Fundy salmonid mariculture industry during 1988–89. *Canadian Technical Reports of Fisheries and Aquatic Sciences*, 1760. 123 pp.
- Wiltshire, K. H., and Dürselen, C-D. 2004. Revision and quality analyses of the Helgoland Reede long-term phytoplankton data archive. *Helgoland Marine Research*, 58: 252–268.

- Wiltshire, K. H., and Manly, B. F. J. 2004. The warming trend at Helgoland Roads, North Sea: phytoplankton response. *Helgoland Marine Research*, 58: 269–273.
- Wiltshire, K. H., Malzahn, A. M., Wirtz, K., Greve, W., Janisch, S., Mangelsdorf, P., Manly, B. F. J., *et al.* 2008. Resilience of North Sea phytoplankton spring bloom dynamics: an analysis of long-term data at Helgoland Roads. *Limnology and Oceanography*, 53: 1294–1302.
- Wiltshire, K. H., Kraberg, A., Bartsch, I., Boersma, M., Franke, H. D., Freund, J., Gebühr, C., *et al.* 2010. Helgoland roads: 45 years of change in the North Sea. *Estuaries and Coasts*, 33: 295–310.
- Wooster, W. S., Bakun, A., and McLain, D. R. 1976. The seasonal upwelling cycle along the eastern boundary of the North Atlantic. *Journal of Marine Research*, 24(2): 131–141.
- Zingone, A., and Sarno, D. 2001. "Recurrent patterns in coastal phytoplankton from the Gulf of Naples." *Archivio di Oceanografia e Limnologia*, 22: 113–118.
- Zingone, A., Casotti, R., Ribera d'Alcalà, M., Scardi, M., and Marino, D. 1995. "St. Martin's Summer": the case of an autumn phytoplankton bloom in the Gulf of Naples (Mediterranean Sea). *Journal of Plankton Research*, 17: 575–593.
- Zingone, A., Sarno, D., and Forlani, G. 1999. Seasonal dynamics of *Micromonas pusilla* (Prasinophyceae) and its viruses in the Gulf of Naples (Mediterranean Sea). *Journal of Plankton Research*, 21: 2143–2159.
- Zingone, A., Licandro, P., and Sarno, D. 2003. Revising paradigms and myths of phytoplankton ecology using biological time-series. *In* *Mediterranean Biological Time-Series*, pp. 109–114. Ed. by F. Briand. Monaco, CIESM Workshop Monographs, 22.
- Zingone, A., Dubroca, L., Iudicone, D., Margiotta, F., Corato, F., Ribera d'Alcalà, M., Saggiomo, V., *et al.* 2010. Coastal phytoplankton do not rest in winter. *Estuaries and Coasts*, 33: 342–361.



13. LIST OF CONTRIBUTORS

Associated Investigator	Country and Associated Institution
Eric Abadie (Eric.Abadie@ifremer.fr)	French Research Institute for Exploration of the Sea (IFREMER): France
Silvia G. Acinas (sacinas@icm.csic.es)	Institut de Ciències del Mar: Spain
Anetta Ameryk (anetta@mir.gdynia.pl)	National Marine Fisheries Research Institute: Poland
Ana B. Barbosa (abarbosa@ualg.pt)	University of Algarve, Centre of Marine and Environmental Research: Portugal
Béatrice Bec (Beatrice.Bec@univ-montp2.fr)	Université Montpellier: France
Antonio Bode (antonio.bode@co.ieo.es)	Instituto Español de Oceanografía: Spain
Ángel Borja (n/a)	Spain
Eileen Bresnan (eileen.bresnan@scotland.gsi.gov.uk)	Marine Scotland: Scotland
Eva Calvo (ecalvo@icm.csic.es)	Institut de Ciències del Mar: Spain
Yves Collos (yves.collos@univ-montp2.fr)	Université Montpellier: France
Caroline Cusack (Caroline.Cusack@marine.ie)	Marine Institute: Ireland
Alejandro de la Sota (n/a)	Spain
Rita V. Domingues (rbdomingues@ualg.pt)	Centre of Marine and Environmental Research: Portugal
Martin Edwards (maed@sahfos.ac.uk)	Sir Alister Hardy Foundation for Ocean Science: UK
Almudena Fontán (n/a)	Spain
Javier Franco (n/a)	Spain
Helena M. Galvão (hgalvao@ualg.pt)	Centre of Marine and Environmental Research: Portugal
Josep M. Gasol (pepgasol@icm.csic.es)	Institut de Ciències del Mar: Spain
Śławomira Gromisz (grosz@mir.gdynia.pl)	National Marine Fisheries Research Institute: Poland
Marie Johansen (marie.johansen@smhi.se)	Swedish Meteorological and Hydrological Institute: Sweden
Kevin Kennington (Kevin.Kennington@gov.im)	Department of Environment, Food, and Agriculture: Isle of Man
Janina Kownacka (janko@mir.gdynia.pl)	National Marine Fisheries Research Institute: Poland
Alexandra Kraberg (Alexandra.Kraberg@awi.de)	Biologische Anstalt Helgoland: Germany
Nada Krstulović (krstulovic@izor.hr)	Institute of Oceanography and Fisheries: Croatia
Aitor Laza-Martínez (n/a)	Spain
Alain Lefebvre (n/a)	French Research Institute for Exploration of the Sea (IFREMER): France
Murielle LeGresley (Murielle.LeGresley@dfo-mpo.gc.ca)	Saint Andrews Biological Station: Canada
Sirpa Lehtinen (sirpa.lehtinen@environment.fi)	Finnish Environment Institute SYKE: Finland
William Li (Bill.Li@dfo-mpo.gc.ca)	Bedford Institute of Oceanography: Canada
Celia Marrasé (celia@icm.csic.es)	Institut de Ciències del Mar: Spain
Jennifer Martin (Jennifer.Martin@dfo-mpo.gc.ca)	Saint Andrews Biological Station: Canada
Ramon Massana (ramonm@icm.csic.es)	Institut de Ciències del Mar: Spain
Danièle Maurer (n/a)	French Research Institute for Exploration of the Sea (IFREMER): France
Xosé Anxelu G. Morán (xelu.moran@gi.ieo.es)	Instituto Español de Oceanografía: Spain
Günther Nausch (guenther.nausch@io-warnemuende.de)	Leibniz Institute for Baltic Sea Research: Germany
Todd D. O'Brien (Todd.O'Brien@noaa.gov)	National Oceanic and Atmospheric Administration: USA
Emma Orive (emma.orive@ehu.es)	Universidad del País Vasco: Spain
Marianna Pastuszek (marianna@mir.gdynia.pl)	National Marine Fisheries Research Institute: Poland
Carlos Pedrós-Alió (cpedros@icm.csic.es)	Institut de Ciències del Mar: Spain
Carles Pelejero (pelejero@icrea.cat)	ICREA and Institut de Ciències del Mar: Spain
Francesc Peters (cesc@icm.csic.es)	Institut de Ciències del Mar: Spain
Nicole Poulton (npoulton@bigelow.org)	Bigelow Laboratory for Ocean Sciences: USA
Marta Revilla (mrevilla@pas.azti.es)	AZTI-Tecnalia: Spain
Myriam Perrière Rumèbe (n/a)	French Research Institute for Exploration of the Sea (IFREMER): France

M. Montserrat Sala (msala@icm.csic.es)	Institut de Ciències del Mar: Spain
Danijela Šantić (segvic@izor.hr)	Institute of Oceanography and Fisheries: Croatia
Diana Sarno (diana@szn.it)	Stazione Zoologica Anton Dohrn: Italy
Renate Scharek (rscharek@gi.ieo.es)	Instituto Español de Oceanografía: Spain
Sergio Seoane (n/a)	Spain
Stefanija Šestanović (sesta@izor.hr)	Institute of Oceanography and Fisheries: Croatia
Michael Sieracki (msieracki@bigelow.org)	Bigelow Laboratory for Ocean Sciences: USA
Joe Silke (joe.silke@marine.ie)	Marine Institute: Ireland
Rafel Simó (rsimo@icm.csic.es)	Institut de Ciències del Mar: Spain
Tim Smyth (tjsm@pml.ac.uk)	Plymouth Marine Laboratory: UK
Mladen Šolić (solic@izor.hr)	Institute of Oceanography and Fisheries: Croatia
Dominique Soudant (Dominique.Soudant@ifremer.fr)	French Research Institute for Exploration of the Sea (IFREMER): France
Rowena Stern (rost@sahfos.ac.uk)	Sir Alister Hardy Foundation for Ocean Science: UK
Glen Tarran (gat@pml.ac.uk)	Plymouth Marine Laboratory: UK
Victoriano Valencia (n/a)	Spain
Dolors Vaqué (dolors@icm.csic.es)	Institut de Ciències del Mar: Spain
Manuel Varela (n/a)	Spain
Norbert Wasmund (norbert.wasmund@io-warnemuende.de)	Leibniz Institute for Baltic Sea Research: Germany
Claire Widdicombe (clst@pml.ac.uk)	Plymouth Marine Laboratory: UK
Karen Wiltshire (Karen.Wiltshire@awi.de)	Biologische Anstalt Helgoland: Germany
Mariusz Zalewski (mariusz@mir.gdynia.pl)	National Marine Fisheries Research Institute: Poland



ICES

International Council for
the Exploration of the Sea

CIEM

Conseil International pour
l'Exploration de la Mer